

INFORMATION TO USERS

This manuscript has been reproduced from the microfilm master. UMI films the text directly from the original or copy submitted. Thus, some thesis and dissertation copies are in typewriter face, while others may be from any type of computer printer.

The quality of this reproduction is dependent upon the quality of the copy submitted. Broken or indistinct print, colored or poor quality illustrations and photographs, print bleedthrough, substandard margins, and improper alignment can adversely affect reproduction.

In the unlikely event that the author did not send UMI a complete manuscript and there are missing pages, these will be noted. Also, if unauthorized copyright material had to be removed, a note will indicate the deletion.

Oversize materials (e.g., maps, drawings, charts) are reproduced by sectioning the original, beginning at the upper left-hand corner and continuing from left to right in equal sections with small overlaps. Each original is also photographed in one exposure and is included in reduced form at the back of the book.

Photographs included in the original manuscript have been reproduced xerographically in this copy. Higher quality 6" x 9" black and white photographic prints are available for any photographs or illustrations appearing in this copy for an additional charge. Contact UMI directly to order.

UMI

A Bell & Howell Information Company
300 North Zeeb Road, Ann Arbor MI 48106-1346 USA
313/761-4700 800/521-0600

University of Alberta

Estimation for Tunnel Lining Loads

by

Hak Joon Kim



A thesis submitted to the Faculty of Graduate Studies and Research in partial
fulfillment of the requirements for the degree of Doctor of Philosophy

in

Geotechnical Engineering

Department of Civil and Environmental Engineering

Edmonton, Alberta

Fall 1997



National Library
of Canada

Acquisitions and
Bibliographic Services

395 Wellington Street
Ottawa ON K1A 0N4
Canada

Bibliothèque nationale
du Canada

Acquisitions et
services bibliographiques

395, rue Wellington
Ottawa ON K1A 0N4
Canada

Your file Votre référence

Our file Notre référence

The author has granted a non-exclusive licence allowing the National Library of Canada to reproduce, loan, distribute or sell copies of this thesis in microform, paper or electronic formats.

The author retains ownership of the copyright in this thesis. Neither the thesis nor substantial extracts from it may be printed or otherwise reproduced without the author's permission.

L'auteur a accordé une licence non exclusive permettant à la Bibliothèque nationale du Canada de reproduire, prêter, distribuer ou vendre des copies de cette thèse sous la forme de microfiche/film, de reproduction sur papier ou sur format électronique.

L'auteur conserve la propriété du droit d'auteur qui protège cette thèse. Ni la thèse ni des extraits substantiels de celle-ci ne doivent être imprimés ou autrement reproduits sans son autorisation.

0-612-23005-8

University of Alberta

Library Release Form

Name of Author: Hak Joon Kim

Title of Thesis: Estimation for Tunnel Lining Loads

Degree: Doctor of Philosophy

Year this Degree Granted: 1997

Permission is hereby granted to the University of Alberta Library to reproduce single copies of this thesis and to lend or sell such copies for private, scholarly, or scientific research purposes only.

The author reserves all other publication and other rights in association with the copyright in the thesis, and except as hereinbefore provided, neither the thesis nor any substantial portion thereof may be printed or otherwise reproduced in any material form whatever without the author's prior written permission.

Hak Joon Kim

Apt. No.1310 - 101 Dong

Jeon-Won Mansion, Hyndai Jutek

Taejeon Dong, Buk-Ku

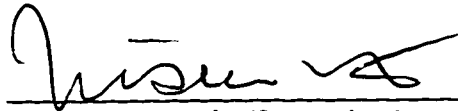
Taegu, Korea, 702-260

Date: Oct. 1, 1997

University of Alberta

Faculty of Graduate Studies and Research

The undersigned certify that they have read, and recommend to the Faculty of Graduate Studies and Research for acceptance, a thesis entitled Estimation for Tunnel Lining Loads submitted by Hak Joon Kim in partial fulfillment of the requirements for the degree of Doctor of Philosophy in Geotechnical Engineering.



Dr. Z. Eisenstein (Supervisor)



Dr. D. M. Cruden



Dr. D. Chan



Dr. D. M. Rogowsky



Dr. K. Barron



Dr. G. R. Martin (External Examiner)

Date: Sep. 24, 1997

ABSTRACT

Prediction of lining loads due to tunnelling is one of the major issues to be addressed in the design of a tunnel. The objective of this study is to investigate rational and realistic design loads on tunnel linings. Factors influencing the lining load are summarized and discussed. The instruments for measuring the lining loads are reviewed and discussed because field measurements are often necessary to verify the design methods.

Tunnel construction in the City of Edmonton has been very active for storm and sanitary purposes. Since the early 1970's, the city has also been developing an underground Light Rail Transit system. The load measurements obtained from these tunnels are compared with the results from the existing design methods. However, none of the existing methods are totally satisfactory. Therefore, there is some room for improvement in the prediction of lining loads.

The convergence-confinement method is reviewed and applied to a case history of a tunnel in Edmonton. The convergence curves are obtained from 2-D finite element analyses using three different material models and theoretical equations. The limitation of the convergence-confinement method is discussed by comparing these curves with the field measurements. Three-dimensional finite element analyses are performed to gain a better understanding of stress and displacement behaviour near the tunnel face.

An improved design method is proposed based on the review of existing design methods and the performance of numerical analyses. A specific method or combination of two different methods is suggested for the estimation of lining loads for different conditions of tunnelling. A method to determine the stress reduction factor is described.

Typical values of dimensionless load factors nD/H for tunnels in Edmonton are obtained from parametric analyses. Finally, the loads calculated using the proposed method are compared with field measurements collected from various tunnels in terms of soil types and construction methods to verify the method. The proposed method gives a reasonable approximation of the lining loads.

The proposed method is recommended as an approximate guideline for the design of tunnels, but the results should be confirmed by field measurements due to the uncertainties of the ground and lining properties and the construction procedures. This is the reason that in-situ monitoring should be an integral part of the design procedure.

ACKNOWLEDGMENTS

This research was conducted at the University of Alberta under the supervision of Dr. Z. Eisenstein. His guidance and assistance are greatly appreciated.

My thanks are extended to the members of my examining committee who provided interesting comments during the final oral examination. I also would like to thank Dr. Geoffrey Martin, who is my external examiner from University of Southern California for his valuable comments.

The work reported herein has improved from discussions with my fellow graduate students. Special thanks go to Amin Touhidi, Xingran Wang, Sam Proskin, Ali Pak, and Ziyaeifar Mansour, for their friendship and encouragement during my studies. I thank also Kenneth Shen for the friendship shown to me during my stay in Edmonton.

Material for parts of this research was obtained through personal correspondence with several individuals and companies. Some of them must be singled out for their great help, including Dr. Paulo Branco Jr., Mr. Mark Valeriote, Mr. Jim Cassie, and Mr. Brad Griffith.

My heartfelt thanks go to my Canadian family Mr. and Mrs. Welwood and their children, for being my family away from home.

I give my special thanks to Dr. Jae Young Lee and other professors at the Kyung-Pook National University in Korea who were always concerned about my study.

Financial assistance came from a variety of sources including the National Science and Engineering Research Council of Canada operating grants to Dr. Z. Eisenstein, the Department of Civil Engineering of the University of Alberta, and the City of Edmonton.

In closing, a very heartfelt thanks must go to all members of my family. I wish to thank my parents for their continuing love and support. My daughter, Eugenia, made the busiest moments a lot happier. Finally, I wish to express my sincere gratitude to my wife, Ji-Sook Yeom. Without her, this work would have been much more difficult to complete.

TABLE OF CONTENTS

| | |
|--|----|
| 1. INTRODUCTION | 1 |
| 1.1 General | 1 |
| 1.2 Scope and Organization of the Thesis..... | 1 |
| 2. METHODS FOR PREDICTING LINING LOADS..... | 4 |
| 2.1 Introduction | 4 |
| 2.2 Ground Response to Tunnelling..... | 5 |
| 2.3 Factors Influencing the Load on the Liner | 6 |
| 2.3.1 Geology | 7 |
| 2.3.2 Relative Rigidity of the Lining with Respect to the Surrounding Ground | 8 |
| 2.3.3 Construction Procedure..... | 9 |
| 2.3.4 Diameter and Depth of the Tunnel..... | 10 |
| 2.3.5 Groundwater Conditions | 10 |
| 2.3.6 The Ratio of the Tunnel Radius and Lining Thickness | 11 |
| 2.3.7 The Length of the Period Which the Cavity Left Unsupported | 11 |
| 2.3.8 The Support Delay and Excavation Round Lengths | 12 |
| 2.3.9 Natural Stress Field..... | 12 |
| 2.3.10 The Passage of Time | 13 |
| 2.3.11 Lining Contact with the Ground | 13 |
| 2.3.12 Influence of External Conditions | 14 |
| 2.4 Classification of Methods | 15 |
| 2.4.1 General | 15 |
| 2.4.2 Empirical and Semi-Empirical Methods..... | 15 |
| 2.4.2.1 Earth Pressure Theories | 15 |
| 2.4.2.2 Terzaghi's Arching Theory | 16 |
| 2.4.2.3 Empirical Techniques | 16 |
| 2.4.3 Ring and Plate Models | 17 |
| 2.4.3.1 Uniform Stress Field Solutions | 17 |

| | |
|---|--------|
| 2.4.3.2 Non-uniform Stress Field Solutions | 18 |
| 2.4.4 Ring and Spring Models | 19 |
| 2.4.5 Numerical Methods..... | 20 |
| 2.5 Summary and Conclusions..... | 21 |
| 3. TUNNEL LOAD MEASUREMENTS | 29 |
| 3.1 Introduction | 29 |
| 3.2 Method of Tunnel Load Measurements | 29 |
| 3.2.1 Pressure Cells..... | 29 |
| 3.2.2 Flat Jack Tests..... | 30 |
| 3.2.3 Lagging Deflection | 32 |
| 3.2.4 Rod or Tape Extensometers | 33 |
| 3.2.5 Strain Gauges | 35 |
| 3.2.5.1 Electrical Resistance Strain Gauges..... | 36 |
| 3.2.5.2 Vibrating Wire Strain Gauges..... | 38 |
| 3.2.6 Load Cells | 39 |
| 3.3 Processing of measurements | 41 |
| 3.3.1 Steel Ribs | 41 |
| 3.3.2 Concrete Linings..... | 44 |
| 3.4 Summary and Conclusions..... | 45 |
| 4. COMPARISON OF LINING LOADS FROM MEASUREMENTS AND EXISTING DESIGN METHODS..... | 60 |
| 4.1 Introduction | 60 |
| 4.2 Tunnels in Edmonton | 60 |
| 4.2.1 Northeast Line..... | 61 |
| 4.2.2 LRT - South Extension | 62 |
| 4.2.3 SLRT-Phase II | 63 |
| 4.2.4 Whitemud Creek Tunnel..... | 65 |
| 4.2.5 170th Street Tunnel..... | 65 |

| | |
|--|-----|
| 4.2.6 Experimental Tunnel..... | 66 |
| 4.2.7 The Tunnel on the Banks of North Saskatchewan River | 68 |
| 4.3 Existing Design Methods Used for Comparison with Field Measurements | 69 |
| 4.4 Comparison of Field Measurements with the Existing Theories | 71 |
| 4.5 Conclusions versus Existing Theories | 72 |
| 4.6 Prediction of Lining Loads Using Correction Factors | 76 |
| 4.6.1 Effect of Delay in Liner Placement..... | 76 |
| 4.6.2 Comparison with Case Study Data | 78 |
| 4.6.3 Discussion of Results..... | 81 |
| 4.6.4 Recalculation of the Lining Loads..... | 83 |
| 4.6.5 Application of the Method to Edmonton Tunnels | 84 |
| 4.7 Application of Stress Reduction Factors to the Existing Design Methods | 86 |
| 4.8 Summary and Conclusions..... | 87 |
| 5. GROUND-SUPPORT INTERACTION DURING EXCAVATION | 119 |
| 5.1 Introduction | 119 |
| 5.2 The Convergence-Confinement Method | 119 |
| 5.2.1 Review of Convergence-Confinement Method | 120 |
| 5.2.2 Comments on the Convergence-Confinement Method..... | 126 |
| 5.3 Two-Dimensional Finite Element Analyses | 127 |
| 5.3.1 General | 127 |
| 5.3.2 Simulation of Excavation..... | 127 |
| 5.3.3 Material Model..... | 129 |
| 5.3.4 Analysis of Experimental Tunnel | 132 |
| 5.3.5 Evaluation of 2-D FEM Combined with CCM..... | 135 |
| 5.4 Displacements before Liner Installation | 137 |
| 5.5 Limitations of 2-D FEM combined with CCM..... | 140 |
| 5.6 Summary and Conclusions..... | 141 |
| 6. THREE-DIMENSIONAL RESPONSE OF GROUND | 159 |

| | |
|--|-----|
| 6.1 Introduction | 159 |
| 6.2 Three-Dimensional Arching around an Advancing Tunnel | 160 |
| 6.3 Review of Three-Dimensional Modelling by the FEM | 160 |
| 6.4 Three-Dimensional Finite Element Analyses | 165 |
| 6.4.1 Description of the Analyses | 165 |
| 6.4.2 Displacements | 167 |
| 6.4.3 Stresses..... | 170 |
| 6.4.4 Convergence Curves | 173 |
| 6.4.5 Comparison of the Equilibrium Points from 2-D and 3-D analyses | 176 |
| 6.5 Summary and Conclusions..... | 178 |
| 7. DEVELOPMENT AND VALIDATION OF SUGGESTED METHODS..... | 201 |
| 7.1 Introduction | 201 |
| 7.2 Estimates of Stress Reduction Factors | 201 |
| 7.3 Suggested Methods for the Prediction of Lining Loads..... | 205 |
| 7.3.1 A Depth to Centerline to Diameter Ratio up to Three | 206 |
| 7.3.2 A Tunnel Depth to Diameter Ratio Greater than Three | 207 |
| 7.3.2.1 No Face Control..... | 207 |
| 7.3.2.2 Positive Face Control with Compressed Air or Fluids | 214 |
| 7.3.2.3 Positive Face Control Using Jet-Grouted Piles..... | 215 |
| 7.4 Verification of the Proposed Method Using Case Histories | 216 |
| 7.4.1 Tunnels in Edmonton..... | 216 |
| 7.4.2 Tunnels Located other than Edmonton | 221 |
| 7.5 Comments on the Estimates of the Stress Reduction Factors | 223 |
| 7.6 Summary and Conclusions..... | 223 |
| 8. CONCLUSIONS..... | 252 |
| REFERENCES | 257 |
| APPENDIX..... | 271 |

List of Tables

| Table | Page |
|-------|---|
| 2.1 | Ultimate Distortion of Tunnels, $\Delta R/R$, for Design Verification24 |
| 3.1 | Strain Gauges - Types and Features.....48 |
| 3.2 | Load Cells - Types and Features49 |
| 3.3 | Calculated and Measured Loads in the Combined Shotcrete-Rib Lining50 |
| 4.1 | Calculation of Dimensionless Radial Displacements based on the Results of Parametric 3-D Finite Element Analyses.....90 |
| 4.2 | Primary Liner Loads in Edmonton Tunnels.....91 |
| 4.3 | Comparisons of Predicted and Measured Average Thrust Coefficients92 |
| 4.4 | Comparisons of Predicted and Measured Average Thrust Coefficients Using Delay Length L_d'93 |
| 7.1 | Coefficients of the Adopted U and K Relations.....226 |
| 7.2 | Stress Reduction Factors Calculated Using Eisenstein and Negro's Method for $K_o=0.6$227 |
| 7.3 | Stress Reduction Factors Calculated Using Eisenstein and Negro's Method for $K_o=0.8$228 |
| 7.4 | Stress Reduction Factors Calculated Using Eisenstein and Negro's Method for $K_o=1.0$229 |
| 7.5 | Parameters used for the Estimation of nD/H for Tunnels in Edmonton230 |
| 7.6 | Calculated Values of nD/H for Tunnels in Edmonton (a) Small Diameter Tunnel ($D<4m$) (b) Large Diameter Tunnel ($D\geq 4m$).....231 |
| 7.7 | Recommended Geotechnical Design Parameters.....232 |
| 7.8 | Initial Support for the Edmonton SLRT-Phase II Tunnels233 |
| 7.9 | Summary of Instrumented Ribs for the SLRT-Phase II Tunnels234 |
| 7.10 | Summary of Primary Liner Loads for the SLRT-Phase II Tunnels235 |
| 7.11 | Stress Reduction Factors Suggested for the Proposed Design Method236 |

List of Figures

| Figure | Page |
|--------|---|
| 2.1 | (a) Distribution of Radial Displacements along the Longitudinal Direction of Tunnel |
| | (b) Convergence-Confinement Curves.....25 |
| 2.2 | Lining Load at Tunnel Springline for Different Compressibility Ratios.....26 |
| 2.3 | (a) Displacements Recorded 0.3 m above the Crown of the Tunnel during the Instantaneous Advances and Stationary of the Face |
| | (b) Development of the Mean Ring Thrust with Time in a Steel Lining in the Kielder Experimental Tunnel.....27 |
| 2.4 | Sequences of Analysis |
| | (a) Without Simulation of Construction (Over Loading Condition) |
| | (b) With Simulation of Construction (Excavation Loading Condition).....28 |
| 3.1 | Layout of LNEC Flat Jack Test51 |
| 3.2 | (a) University of Alberta Deflectometer |
| | (b) Laboratory Arrangement for Calibrated Laggings52 |
| 3.3 | (a) Possible Layout of Measuring Points for the Monitoring of the Lining Deformation |
| | (b) Processing of the Measurements to obtain the Deformed Shape of the Lining53 |
| 3.4 | Types of Electrical Resistance Strain Gauges |
| | (a) Bonded Wire Resistance Strain Gauge |
| | (b) Bonded Foil Resistance Strain Gauge |
| | (c) Unbonded Wire Resistance Strain Gauge.....54 |
| 3.5 | Schematic of Electrical Resistance Load Cell.....55 |
| 3.6 | (a) Location of Strain Gauges on Cross-Section of a Steel Rib |
| | (b) Calculation of Axial Stresses and Bending Stresses56 |
| 3.7 | Induced Moments due to Jacking Load from Mole57 |

| | | |
|------|---|-----|
| 3.8 | (a) Simplified Load Distribution around a Steel Rib with Four Joints | |
| | (b) Equilibrium Equations at a Joint for a Unit Length of Ribs Spacing | 58 |
| 3.9 | (a) Location of Strain Gauges on Cross-Section of a Concrete Lining | |
| | (b) Calculation of Axial Stresses..... | 59 |
| 4.1 | Location of Strain Gauges in Northeast Line Tunnel | 94 |
| 4.2 | Load Cell Location in LRT - South Extension | 95 |
| 4.3 | Load Cell Location of Section B2 of SLRT - Phase II Tunnel | 96 |
| 4.4 | Details of the 170th Street Tunnel Test Section..... | 97 |
| 4.5 | Instrumented Steel Rib of Test Section 1 of Experimental Tunnel | 98 |
| 4.6 | Details of Lining Instruments of Test Section 2 of Experimental Tunnel | 99 |
| 4.7 | Details of Lining Instruments of Test Section 3 of Experimental Tunnel | 100 |
| 4.8 | Calculation of Lining Loads using a Peck et al.'s Method | 101 |
| 4.9 | Calculation of Lining Loads using a Muir Wood's Method | 102 |
| 4.10 | Calculation of Lining Loads using a Einstein and Schwartz Method | 103 |
| 4.11 | Calculation of Lining Loads using a Eisenstein and Negro's Method..... | 104 |
| 4.12 | Comparison of the Dimensionless Factor (n) with Depth in Edmonton Tunnels..... | 105 |
| 4.13 | Measured and Calculated Percent of Overburden in Edmonton Tunnels | 106 |
| 4.14 | Measured and Calculated n for the Linings in Edmonton Tunnels..... | 107 |
| 4.15 | Tunnel Convergence as Function of Tunnel Face..... | 108 |
| 4.16 | Convergence-Confinement Curves for Yielding Ground with Support Delay | 109 |
| 4.17 | Support Delay Correction Factor | 110 |
| 4.18 | Definition of Support Delay Length | |
| | (a) Finite Element Sequence | |
| | (b) Actual Tunnelling Sequence..... | 111 |
| 4.19 | Tunnelling Sequences used in the Finite Element Analyses..... | 112 |
| 4.20 | Upper Bound of Lining Load for Tunnels with Large Support Delay | 113 |
| 4.21 | Measured and Calculated Lining Loads in Edmonton Tunnels Using Schwartz and Einstein's Method..... | 114 |

| | | |
|------|---|-----|
| 4.22 | Measured and Calculated Lining Loads in Edmonton Tunnels Using Schwartz and Einstein's Method ($\lambda_d=0.2$) | 115 |
| 4.23 | Measured and Calculated Percent of Overburden in Edmonton Tunnels Using Reduced Unit Weight | 116 |
| 4.24 | Measured and Calculated n for the Linings in Edmonton Tunnels Using Reduced Unit Weight..... | 117 |
| 4.25 | Measured and Calculated Lining Loads for Edmonton Tunnels Using Reduced Unit Weight and Arbitrary 50 % Stress Reduction for Muir Wood's Method..... | 118 |
| 5.1 | (a) Concept of Convergence-Confinement Method (b) Elastic and Plastic Material Behaviour..... | 143 |
| 5.2 | (a) Short Term and Long Term Convergence Curves (b) Three Different Types of Convergence Curves..... | 144 |
| 5.3 | (a) Effect of Gravity on the Convergence Curve (b) Convergence Curves for the Excavation and Core..... | 145 |
| 5.4 | (a) Creep of Concrete Liner (b) Creep of Ground | 146 |
| 5.5 | (a) Radial Stress and Displacement Distribution along the Crown (b) Ground Response at the Crown..... | 147 |
| 5.6 | The Reduction of 3-D Problem Due to the Tunnel Face to a Problem of Plane Deformation | 148 |
| 5.7 | Illustration of Hyperbolic Model | 149 |
| 5.8 | Two-Dimensional Meshes of the Experimental Tunnel | 150 |
| 5.9 | (a) Contributing Areas for Uniform Stresses (b) Calculation of Equivalent Loads for Initial Stresses | 151 |
| 5.10 | Ground Reaction Curves for the Experimental Tunnel in Section 3 (Elastic Model)..... | 152 |
| 5.11 | Ground Reaction Curves for the Experimental Tunnel in Section 3 (Hyperbolic Model)..... | 153 |

| | | |
|------|---|-----|
| 5.12 | Ground Reaction Curves for the Experimental Tunnel in Section 3 (Elastic-Plastic Model)..... | 154 |
| 5.13 | Ground Reaction Curves for the Experimental Tunnel in Section 3 (Theoretical Equation) | 155 |
| 5.14 | Ground Reaction Curves for the Crown of the Experimental Tunnel in Section 3..... | 156 |
| 5.15 | Ground Reaction Curves for the Springline of the Experimental Tunnel in Section 3..... | 157 |
| 5.16 | Ground Reaction Curves for the Floor of the Experimental Tunnel in Section 3..... | 158 |
| 6.1 | Three-Dimensional Arching near the Face of an Advancing Tunnel | 181 |
| 6.2 | Transversal Section of the 3-D Mesh of the Experimental Tunnel..... | 182 |
| 6.3 | Longitudinal Cross Section of the 3-D Mesh of the Experimental Tunnel..... | 183 |
| 6.4 | Radial Displacement Distribution at the Crown, Springline, and Floor along the Longitudinal Direction (No Liner Installed) | 184 |
| 6.5 | Radial Displacement Distribution at the Springline along the Longitudinal Direction (No Liner Installed)..... | 185 |
| 6.6 | Radial Displacement Distribution at the Springline along the Longitudinal Direction (Liner Installed 1D away from the Face) | 186 |
| 6.7 | Radial Stress Distribution at the Springline along the Longitudinal Tunnel Direction (No Liner Installed)..... | 187 |
| 6.8 | Radial Stress Distribution at the Springline along the Longitudinal Tunnel Direction (Liner Installed 1D away from the Tunnel Face)..... | 188 |
| 6.9 | Radial Stress Distribution at the Springline along the Longitudinal Tunnel Direction for Step 8 and 11 | 189 |
| 6.10 | Comparison of Convergence Curves of Springline for Slices 5 and 6 without Liner..... | 190 |
| 6.11 | Comparison of Convergence Curves of Slice 5 for 2-D and 3-D Analyses.... | 191 |
| 6.12 | Convergence Curves for Slice 5 from 3-D Analyses with Liner Installation . | 192 |
| 6.13 | Comparison of Convergence Curves of Slices 5 and 6 with Liner | |

| | | |
|------|---|-----|
| | Installation..... | 193 |
| 6.14 | (a) Location of Points B and C with Respect to the Face and the Leading Edge of Liner | |
| | (b) Location of Tunnel Face at the Time of Liner Installation in Slice 5 and Slice 6..... | 194 |
| 6.15 | Comparison of Convergence Curves of Slice 5 with and without Liner | 195 |
| 6.16 | Calculation of Confinement Curve for Linear Elastic Support Properties..... | 196 |
| 6.17 | Final Equilibrium Stresses and Displacements on the Liner of Crown from the 2-D and 3-D Analyses | 197 |
| 6.18 | Final Equilibrium Stresses and Displacements on the Liner of Springline from the 2-D and 3-D Analyses (Slice 5)..... | 198 |
| 6.19 | Final Equilibrium Stresses and Displacements on the Liner of Floor from the 2-D and 3-D Analyses | 199 |
| 6.20 | Final Equilibrium Stresses and Displacements on the Liner of Springline from the 2-D and 3-D Analyses (Slice 6)..... | 200 |
| 7.1 | Stress Reduction Factors for Different Tunnel Depths ($\phi=30$, $K_0=1.0$)..... | 237 |
| 7.2 | Variation of n with Flexibility Ratio ($K_0=1.0$)..... | 238 |
| 7.3 | Variation of n with Compressibility Ratio ($K_0=1.0$) | 239 |
| 7.4 | Simplified Representation of Rock Loading of Tunnel | 240 |
| 7.5 | Comparison of Vertical Support Pressures in Relation to Tunnel Width according to Terzaghi Derived Formulae with Actual Case Histories in Edmonton..... | 241 |
| 7.6 | Comparison between n Values according to Terzaghi Derived Formulae and Actual Case Histories in Edmonton | 242 |
| 7.7 | Comparison of the Dimensionless Factor (n) with Tunnel Depth and Diameter for Tunnels in Edmonton..... | 243 |
| 7.8 | Comparison of the Dimensionless Factor (n) with H/D in Edmonton Tunnels..... | 244 |
| 7.9 | Comparison of Predicted n Calculated using the Proposed Method with Measured n for Tunnels in Edmonton (From Eq. 7.1)..... | 245 |

| | | |
|------|---|-----|
| 7.10 | Comparison of Predicted n Calculated using the Proposed Method with Measured n for Tunnels in Edmonton (From Table 7.6) | 246 |
| 7.11 | Plan View of Tunnel Sections with the Location of the Instrumented Ribs | 247 |
| 7.12 | Simplified Geologic Cross Section | 248 |
| 7.13 | A Cross Section in Rib No. 138 of the SLRT-Phase II Tunnels..... | 249 |
| 7.14 | Comparison of Predicted n Calculated using the Proposed Method with Measured n for the SLRT-Phase II Tunnels..... | 250 |
| 7.15 | Comparison of Predicted n Calculated using the Proposed Method with Measured n for the Tunnels Located other than Edmonton | 251 |

List of Symbols

| | |
|-----------------------|---|
| A_1 | Average cross-sectional area of the support per unit length of tunnel |
| C | Compressibility ratio |
| c | Cohesion of soil |
| C_u | Undrained Shear Strength |
| D | External diameter of a tunnel |
| E | Elastic modulus for the ground |
| E_1 | Elastic modulus for the support |
| E_t | Initial tangent modulus for the ground |
| F | Flexibility ratio |
| H | Tunnel depth from the ground surface to the tunnel springline |
| I_1 | Moment of inertia of the cross-section per unit length along the axis of the tunnel |
| K_o | Coefficient of earth pressure at rest |
| L_d | Distance between the tunnel face and the mid-point of the leading support section |
| M_{max} | Maximum bending moments |
| n | Dimensionless factor ($=P/\gamma D$) |
| P | Radial stress |
| P_a | Tunnel air pressure above atmospheric |
| P_o | In-situ radial stress |
| R | External radius of a tunnel |
| R_f | Failure ratio |
| t | Thickness of the lining |
| T_c, T_s, T_i | Lining load at the crown, springline, and invert |
| U_f | Final ground displacement |
| U_i | Ground displacement that occurs before the liner installation |
| U_l | Liner displacement |
| U_o^e | Final elastic displacement of an unlined tunnel |
| U_o' | Pre-support ground movements due to the void between the lining and ground |
| X | Distance from the face to the leading edge of the lining |

| | |
|----------------------------|--|
| Z | Tunnel depth from the ground surface to the tunnel crown |
| α | Stress reduction factor |
| ν | Poisson's ratio for the ground |
| ν_1 | Poisson's ratio for the support |
| γ | Unit weight of the ground |
| γ_{red} | Reduced unit weight of the soil caused by stress release around a tunnel |
| λ_d | Support delay factor |
| λ_y | Yield factor |
| ϕ_a | Adjusted friction angle |
| ϕ_e | Equivalent friction angle |
| σ_1, σ_3 | Major and minor in-situ principal stresses |

1. Introduction

1.1 General

Prediction of lining loads due to tunnelling is one of the major issues to be addressed in the design of a tunnel. However, the problem is not easily solved due to uncertainties and variations of the ground conditions, the redistribution of the in-situ stresses related to the ground deformation before and after lining installation, and the differences in construction procedures. Therefore, most tunnels are often built too conservatively, i.e., more support is used than is necessary.

It is a well-known fact that tunnel lining seldom carries the full total load of the soil or rock located above the tunnel crown. In practice, various lining thicknesses have been used for similar ground conditions. It has been recognized that such variations reflect the absence of consistent design principles. The objective of this study is to investigate rational and realistic design loads on tunnel linings, especially on the primary linings.

1.2 Scope and Organization of the Thesis

There are many existing lining design methods available. The response of the ground and support during excavation should be fully understood to review the problem of the existing design methods. Two or three dimensional finite element analyses can be used for this purpose.

An improved design method is proposed based on the review of the existing design methods. The best way to evaluate the validity of the method is to compare the calculated loads with the field measurements. Therefore, loads calculated using the proposed method are compared with field measurements from the case histories collected from many different areas to verify the method.

Chapter 2 presents discussions on the soil response to tunnelling, factors influencing the load on the liner, and available design methods to estimate the lining loads. It is very important to understand factors influencing the lining load to predict the load reliably. The existing design methods are classified based on the calculation

procedure on which a particular method is developed. The validity of the design methods is discussed briefly based on literature reviews.

Field measurements are often necessary to verify the design methods or assumptions and improve models of ground behaviour. Therefore, the instruments for measuring the lining loads are reviewed in Chapter 3. The methods for the processing of measurements are also presented for two different lining systems. Finally, certain instruments are recommended for the measurement of lining loads for specific conditions.

The validity of the existing design methods is reviewed in Chapter 4 by comparing the loads calculated using the methods with the field measurements obtained from several tunnels in Edmonton. Conclusions concerning the existing design methods are presented based on the comparison. The use of correction factors for the existing design methods is also discussed in this chapter.

The design of a tunnel liner is a ground and structural problem. Ground-support interaction is a consequence of the resistance with which the liner reacts against the movement of the surrounding ground into the excavated opening. The convergence-confinement method (CCM) is one approach to the analysis of ground-support interaction. In Chapter 5, the convergence-confinement method is reviewed and applied for a case history of a tunnel in Edmonton. The convergence curves are obtained from two-dimensional finite element analyses using three different material models and theoretical equations. The limitation of the CCM is also discussed by comparing these curves with the actual field measurements obtained from a tunnel in Edmonton.

Three-dimensional finite element analyses are performed in Chapter 6 in order to have a better understanding of stress and displacement behaviour near the tunnel face. The influence of the construction sequences in ground-support interaction is investigated using the 3-D analyses. The possible causes of the differences in the final equilibrium stresses and displacements on the liner between the 2-D and 3-D analyses are presented. The difficulties involved in the 3-D analyses are also discussed in this chapter.

An improved design method is proposed in Chapter 7 based on the review of the existing design methods and numerical analyses. A method to determine the stress reduction factors is described in detail. In addition, a specific method or combination of

two different methods is suggested to use for each type of tunnelling for the estimation of lining loads. Finally, the results from the proposed method are compared with field measurements of the case histories collected from many different areas to verify the method.

Chapter 8 presents a brief summary of this research and the main conclusions.

2. Methods for Predicting Lining Loads

2.1 Introduction

The lining is designed to support the weight of the overburden and a horizontal pressure equal to some fraction of it. The primary lining is usually designed to resist all transient loads developed during construction activities as well as the short-term ground loads. The secondary lining is used to ensure a safe support of the tunnel for the any other additional loading resulting from future changes in the overall physical conditions and the possible increased long-term ground loads. If the gravitational stress gradient from crown to invert is not considered and no deformation of the soil occurs before, during and after lining installation, the lining loads, T , acting on the lining are expressed as follows;

$$P = \frac{1}{2} \gamma H \{ (1 + K_o) + (1 - K_o) \cos 2\theta \} \text{ and } T = PR \quad (2-1)$$

Therefore,

$$T_s = \gamma H R$$

$$T_{c,i} = \gamma H K_o R \quad (2-2)$$

where P = radial pressure

γ = unit weight of soil

H = tunnel depth from the ground surface to the tunnel springline

θ = measured angle from the crown to a certain point clockwise

R = external radius of the lining

K_o = coefficient of earth pressure at rest

T_s = lining load at the springline

$T_{c,i}$ = lining load at the crown and invert.

However, tunnel linings seldom carry the full total load of the overburden. The soil above the tunnel is only partly supported by the liner. What occurs in all tunnels is that in-situ stresses are redistributed around the opening due to the inherent shear strength and continuity of the ground. This transfer of pressure from a yielding mass of soil onto adjoining stationary parts is called the arching effect. The lining theoretically has to support only those stresses not arched to the adjacent ground.

The prediction of lining loads for the lining design has always been the goal of tunnel engineers. Peck (1969) recommended four separate steps for tunnel design procedures: adequate ring loads, anticipate distortions due to bending, proper consideration to the possibility of buckling and allowance for any significant external conditions not included in previous steps. Due to the redistribution of the in-situ stresses after excavation, the use of flexible primary lining and joints and stress raisers in the lining, the need to accommodate a large bending moment is not an important issue. Furthermore, buckling failures are rare if the soil or filling of the annular space is in continuous contact with the lining. Therefore, the lining load is a very important concern for tunnel design. However, problems exist because of the uncertainties and variations in the ground conditions, the redistribution of the in-situ ground stresses related to the ground deformations before and after lining installation, and construction procedures such as the length of the period during which the excavation is left unsupported. This chapter presents discussions on the soil response to tunnelling, factors influencing the load on the liner and available design methods to estimate the lining loads.

2.2 Ground Response to Tunnelling

The tunnelling operation changes the original in-situ stress field significantly. Understanding these stress changes is very important in the development of any design theory for tunnels. The ground response to tunnelling is shown in Figure 2.1 (a), which shows the longitudinal distribution of the radial displacements that occur in response to the tunnel excavation. The curve represents the displacements that have occurred when the tunnel face was advanced to point A. U_i is the ground displacement that occurs before the liner installation, whereas U_f is the final ground displacement that would have occurred if no liner had been applied. If the liner is installed at point B with good contact with the ground just prior to the progress of the tunnel face, the liner should resist the additional ground displacement, U_a , and ground-liner interaction will begin. The displacement of liner, U_l , is usually smaller than U_a due to the greater stiffness of the liner than that of the ground.

The stress changes and the displacements of tunnels are closely related to each other and can be expressed as the convergence-confinement concept, which considers ground-liner interaction. In Figure 2.1 (b), the ground response of excavation in longitudinal direction shown in Figure 2.1 (a) is replotted in the form of the ground and the liner reaction curves. The ground reaction curve shows the radial stress versus radial displacement in response to the insertion of the excavated stress free boundary in the original in-situ stress field. The support reaction curve represents the response of the liner installed to control these deformations, which results in pressure build up within the liner until an equilibrium point is reached. The liner is installed in contact with the surrounding ground immediately after the radial displacement, U_i . The radial stress is gradually increased on the liner due to the advance of the tunnel face and the time-dependent ground displacements. The equilibrium between the ground and the liner is given by the intersection of the two curves. The stress acting on a liner, P_i , shows the maximum possible pressure on a liner installed with the displacement of U_i if the liner had been incompressible. In the case of a compressible liner, ground-liner interaction occurs, which results in the additional ground and liner displacements up to U_l and the reduction of the stress from the P_i to the P_l . The shape of the ground reaction curve is a function of the stress-strain-time and shear strength properties of the ground mass. The shape and slope of the support reaction curve are functions of the stress-strain properties and dimensions of the liner. The convergence-confinement method will be described in detail in Chapter 5.

2.3 Factors Influencing the Load on the Liner

Tunnel linings seldom carry the full load of the overburden due to the arching effect of the ground as mentioned previously. Many factors contribute to the difference of loads on the linings of many different tunnels. It is very important to understand the influence of these factors on the tunnel lining to predict the loads on the liner more reliably. The factors influencing the load on the liner are reviewed in this section.

2.3.1 Geology

Geology is probably the single most important factor of tunnel construction. It is uncommon for any two tunnels to be constructed in similar conditions. The geology very often varies along the tunnel section in horizontal and vertical directions. Whittaker and Frith (1990) described the importance of geology in detail. It is well-known that support needs decrease rapidly as the strength of the ground increases. In fact, many tunnels in Sweden and Norway have been built without the lining due to the high strength of the ground. If linings were installed in such tunnels, the lining loads would have been close to zero. For rock tunnels, Terzaghi (1946) divided the condition of rocks into several groups: intact, stratified, moderately jointed, blocky and seamy, crushed, squeezing, and swelling. He also provided the approximate values of the rock loads on the roof of linings to be anticipated for each group. The classification clearly showed the increase of lining loads with the decrease of rock strength even though the classification system was too general and did not allow a quantitative evaluation of the rock mass. Barton et al. (1974) and Bieniawski (1976, 1984) presented rock classification systems, which provided estimates of the appropriate support requirements for excavations.

Ward and Pender (1981) discussed the behaviour of a tunnel in different soft ground conditions and their comments related to the lining loads are summarized below. Tunnels in dense sandy or gravelly materials with slight cohesion and proper drainage behave in a similar fashion to tunnels in hard ground or non-swelling rocks having much smaller lining load than those in clays and silts. The lining loads in till stabilize quickly after installation of the lining with the loads depending on the stiffness of the lining, but much less than that corresponding to the overburden pressure. Tunnels in heavily overconsolidated swelling clays have lining loads almost equivalent to the full overburden pressure even though the lining loads may only correspond to about 50 % of the overburden pressure in the first year after construction. For tunnels in lightly overconsolidated silty clays, the lining loads tend to increase with time. The lining loads are dependent on the stiffness of the lining but less than that corresponding to the overburden pressure.

In summary, geology has a major role in reducing the lining loads in certain tunnelling projects. However, the lining loads are dependent not only on the properties of the ground but also on the stiffness of the lining as mentioned above. This concept can be explained as the relative stiffness method as described below.

2.3.2 Relative Rigidity of the Lining with Respect to the Surrounding Ground

The load on the lining is dependent on the stiffness of the lining relative to that of the ground. The stiffer the support is relative to the ground, the greater the support load is, a process which can be explained by the convergence-confinement method as shown in Figure 2.1 (b). There is a need to account for both the stress-strain properties of the ground and liner because a lining that may be stiff with respect to a soft clay may behave as a flexible lining in a very stiff clay as Peck et al. (1972) described. The compressibility ratio, C , is a measure of the relative stiffness of the ground-support system under a uniform or symmetric loading condition and is defined by Einstein and Schwartz (1979) as follows:

$$C = \frac{ER(1 - \nu_l^2)}{E_l A_l (1 - \nu^2)} \quad (2.3)$$

where E , ν and E_l , ν_l = the elastic constants for the ground and support

A_l = the average cross-sectional area of the support per unit length of tunnel (A_l equals to the thickness (t) of the lining for a liner with a uniform thickness along the tunnel)

R = the tunnel radius.

The effect of the relative stiffness between the ground and the liner in terms of the compressibility on normalized lining load, T/PR , is shown in Figure 2.2. The loads are calculated based on the equation presented by Einstein and Schwarz for the no-slip boundary condition at the ground-support interface. The in-situ stress ratio, K_0 , does not affect the result very much because the loads are obtained for the springline. The curves show that the normalized lining load decreases rapidly as the compressibility ratio increases up to 10 and does not change much after the ratio exceeds 20. Eisenstein et al.

(1979) observed that the lining load on the rib and lagging system was smaller than that of the segmented lining due to the smaller stiffness of the lining even though the ground properties were the same for both cases.

2.3.3 Construction Procedure

The preservation of the ground strength is important to minimize lining loads. Lane (1975) stated that the lining loads increased for the blasted U.S tunnels due to the damage of the ground during the excavation rather than inherently low ground strength. Plichon (1980) also noticed that the excavation with explosives would certainly have more negative effects on the stability of the opening than excavation by tunnel machine from observations of Belladonne tunnel. Therefore, the lining load can be reduced by using a tunnel boring machine. The use of the Sequential Excavation Method, derived from the New Austrian Tunnelling Method, can minimize the disturbance of the ground even more. The damage of the ground due to the use of explosives can be reduced if careful measures are taken as mentioned by Hoek (1982).

Szechy (1966) presented approximate formulae to calculate the jacking capacity required to move the shield forward. The jack loads are transferred to the lining through a ram load distribution ring. The induced jacking stresses should be checked against the failure stress of the segment in the longitudinal direction. The jacking pressures from the advancing shield can cause the change of the lining loads. Corbett (1984) showed the effect of the jacking pressures on the loads of wood laggings due to the eccentricity of the jacking forces against the lining. Rossler (1995) investigated the mechanics of the ground response to the action of the grippers of a double-shield tunnel boring machine using 3-D finite element analyses. The gripper pressures and the orientation of gripper pads influence the development of tunnel wall overstressing, which can cause variation of the lining loads. El-Nahhas(1980) observed that more loads tended to be taken by the lining of the Whitemud Creek tunnel compared to those of other tunnels in Edmonton because the use of unshielded drilling machines allowed the installation of the primary lining very close to the face.

2.3.4 Diameter and Depth of the Tunnel

An important principle of tunnelling is that construction difficulty and support costs increase sharply as the diameter of tunnel increases due to the existence of a fractured and jointed ground mass as pointed out by Lane (1975) and Hoek and Brown (1980). The load on the lining will be increased if the ground is loosened due to the existence of such a weak zone. For the good ground, the calculated stresses at the boundaries of the excavation are independent of the tunnel diameter according to the elasticity theory. However, the equation (2.2) shows that the load on the lining increases proportionally as the tunnel diameter increases.

The proximity of the ground surface can affect the behaviour of the lining. Peck et al. (1972) performed finite element analyses to determine the effect of the ground surface on the behaviour of the lining for the in-situ stress ratios of 0.5 and 2. The normalized lining loads, T/PR , increased for the in-situ stress ratio of 0.5 but decreased for the in-situ stress ratio of 2 as the dimensionless depth of the tunnel, H/D , increased. However, the normalized lining loads were almost constant when the dimensionless depth of the tunnel was about 1.5 for both cases, a condition which can be considered as a deep tunnel. Ranken (1978) also concluded that the effect of the free surface on the lining loads is negligible for the H/D ratio greater than 1.5 from the two-dimensional, plane strain finite element analyses. However, Ranken observed that the effect of gravitational stress gradient from crown to invert was not negligible even for the H/D ratio greater than 5.

2.3.5 Groundwater Conditions

The groundwater table is usually lowered during the construction of the tunnel to increase the stability of the unsupported tunnel walls including the face and to prevent flooding in the work space. The groundwater table starts to increase after the installation of the tunnel lining. Two different types of linings exist related to the handling of water. The tunnel lining can be either completely watertight or allow some controlled leakage. O'Rourke (1984) stated that the effects of water pressure on the linings in the ground depend on the relative permeability of the lining with respect to that of the surrounding

ground. Lining with complete watertight measures can be expected to have more loads than that with controlled leakage due to the development of the almost full hydrostatic pressure.

2.3.6 The Ratio of the Tunnel Radius and Lining Thickness

The effect of the compressibility ratio on the lining load was described above. However, the influence of each of the individual parameters has been obscured by grouping the ground mass and liner parameters together in the form of the compressibility ratio. Ranken (1978) studied the variation of the lining load with the change of the tunnel radius-to-lining thickness ratio, R/t , for a deep tunnel using the analytical solutions derived by him. The normalized average lining load, T/PR , showed significant decrease with the increase of the ratio of R/t if the modulus ratio, E/E_1 , is greater than 0.0001 and smaller than 1. Therefore, the lining load can be reduced by reducing the liner thickness in a specific ground strength, E , and a tunnel radius. However, the reduction of the liner thickness to decrease the lining loads should be done carefully because the reduction of the liner thickness results in the increase of the circumferential stress in the liner due to the decrease of the cross sectional area of the liner. Too great of a reduction of the lining thickness can yield compressive stresses in excess of the compressive strength of the liner.

2.3.7 The Length of the Period Which the Cavity is Left Unsupported

Ward (1978) observed that the radial displacements occurred without the advance of the tunnel face due to rock yielding with time as shown in Figure 2.3 (a). The radial displacement is plotted against the normalized distance from the face. The displacement of 7.5 mm, which was shown as a vertical line in the figure, occurred without the advance of the face even though the total measured displacement was only about 12 mm. Therefore, the loads on the lining can increase even though the face does not advance or is located far away from a reference point.

Ward also noticed that the displacement was small after the advance of the face when the face had been stationary only for a short time because the ground had yielded

little and was stiff compared to a face that had been stationary for a long time. In other words, the displacement of the ground is less if the construction of the tunnel is progressed quickly. Therefore, the loads on the lining can vary depending on the rate of the tunnel construction.

2.3.8 The Support Delay and Excavation Round Lengths

The distribution of the lining loads along a tunnel built by incremental excavation is not homogeneous. The lining loads generally decrease as the support delay length, the distance between the tunnel face and the leading edge of the lining, increases because the lining will resist less displacement as shown in Figure 2.1 (a). Ward (1978) demonstrated the effect of lining installation at different positions in relation to the face on the lining loads in the Kielder experimental tunnel. The three linings were butt-welded together and were installed 0.3 m behind the face after the face had been advanced 2.1 m, up to A, by a road header as shown in Figure 2.3 (b). When the face was advanced 2.7 m, up to B, the load in ring 3 was more than twice that in ring 1 due to the shorter support delay length. Pelli et al. (1986) also investigated the effects of the excavation round and the support delay lengths using 3-D finite element analyses. The shorter excavation round length showed higher stresses and more homogeneous stress distribution on the lining than those of the longer excavation round length. They also observed that the leading edge of the lining was most highly stressed.

2.3.9 Natural Stress Field

For certain areas, the in-situ stress can be higher than the value obtained from the multiplication of the unit weight of the soil and the depth of the tunnel. Therefore, it is important to estimate the in-situ stress of the ground as accurately as possible because the load on the lining is closely related to the in-situ stress. O'Rourke (1984) suggested that plastic behaviour may lead to substantial inward displacements before the ground can mobilize enough shear strength to reduce lining loads in tunnels excavated under conditions of high in-situ stress especially in ground of relatively low strength. In such a case, the displacement of the ground causes an increase of the load on the lining because

the ground cannot be stabilized by itself. Furthermore, the in-situ stress ratio should be considered carefully for the estimation of the lining load. The lining load is always likely to be considerably smaller than that corresponding to the overburden pressure. However, Peck (1969) presented several examples where the lining loads were higher than those corresponding to the overburden pressures due to the high in-situ stress ratios.

2.3.10 The Passage of Time

Peck (1969) stated that the lining load may increase at a decreasing rate depending on the nature of the soil due to the passage of time. Peck showed the increase of the lining loads for tunnels in London clay, a process which was roughly proportional to the logarithm of time. The increase of the lining load was very obvious for swelling clays and soft plastic clays but quite small for non-plastic soils especially for sandy soils. In other words, the increase of the lining load mainly occurs in materials that have significant time-dependent behaviour. Field measurements on the primary lining in two tunnels in Edmonton (Eisenstein and Thomson, 1978; Thomson and El-Nahhas, 1980) showed that the lining loads stabilized within two weeks for the tunnel in glacial till and within three months for the tunnel in clay shale. The increase of the loads on the permanent lining can be also observed as time passes either due to creep or deterioration of the initial lining.

2.3.11 Lining Contact with the Ground

The excavated diameter of the tunnel is usually bigger than the outer diameter of the lining to accommodate the support or to have clearance space for the advance of the TBM shield. The voids left behind the lining are filled with some kind of grout or can be closed by the expansion of the lining. In many cases, the voids are left open even though these gaps do not form a continuous annular space as observed by El-Nahhas (1980) through the inspection holes. If the ground has sufficient stand up time and the gap is small, the lining will be in contact with the ground as the tunnel face advances, without the development of local instability or global ground collapse. In this case, the loads on the lining may be even smaller than those from the existing theories due to the stress

redistribution around the opening. However, either local instability or global ground collapse may occur, a process which can cause a large increase of loads on the lining, if the gap is sufficiently large.

2.3.12 Influence of External Conditions

The design of a single tunnel unaffected by external influences has only been considered so far. The most significant modification of the condition is the construction of a parallel tunnel. The load on the lining of the first tunnel usually increases after construction of an adjacent second tunnel because the loads previously carried by the removed material are transferred to the surrounding ground and the existing lining of the first tunnel. Therefore, it is a common tunnelling practice to delay placement of the cast-in-place concrete lining in the first tunnel until the second tunnel heading has passed to reduce bending stresses. Peck (1969) observed that the loads on the test tunnel of Garrison Dam increased from about 15 % of full overburden pressure to almost 100 % after the seven parallel tunnels had been driven. The stress interaction effect is negligible when the two tunnels are 3-4 diameters apart from centre to centre for the hydrostatic stress field according to King et al. (1972). Ghaboussi and Ranken (1977), Ghaboussi et al. (1983), and Srivastava et al. (1988) investigated the interaction between or among adjacent tunnels using a series of finite element analyses.

The existence of an adjacent building or fill placed over a tunnel in soft compressible soils can cause large increases in loads on a tunnel lining. For a concrete lining, the lining loads can be affected due to the shrinkage and temperature change of the lining and the grouting pressure acting between the lining and ground. Paul et al. (1983) summarized the possible causes of additional loads on the precast segmented lining such as the handling stresses prior to installation, the pressures due to expansion of the lining to fill the void between the lining and ground, and nonuniform loads and distortions due to the incomplete grouting or misalignment of segments.

2.4 Classification of Methods

2.4.1 General

The lining loads can be calculated using many existing lining design methods which may be divided into four groups: empirical and semi-empirical methods, ring and plate models, ring and spring models, and numerical models. The classification is based on the calculation procedure on which a particular method is developed. O'Rourke (1984) stated that valid design methods must be capable of representing loads and deformations in accordance with the geologic and construction conditions and of correctly accounting for the ground-lining interaction. To verify the validity of the existing design methods with these criteria, the lining design methods are briefly reviewed in the following sections with the emphasis on the lining loads.

2.4.2 Empirical and Semi-Empirical Methods

These methods are based on the in-situ observations or measurements of completed tunnel supports or simply based on past experiences. These methods usually include an unknown, but normally a wide, margin of safety. Earth pressure theories, Terzaghi's arching theory, and empirical techniques belong to these methods.

2.4.2.1 Earth Pressure Theories

These methods normally provide hypothetical or empirical pressure distribution on the lining, from which the internal lining load can be determined using known solutions from structure analyses. An example of these methods is the analysis proposed by Hewett and Johannesson (1922). They derived formulas for the normal forces and bending moments in the tunnel lining due to these pressure distributions based on the assumption that the lining is a continuous rigid elastic structure. Methods based on the earth pressure theories, including the Hewett-Johannesson method, have major drawbacks. First, they do not consider the redistribution of soil stresses occurring before the lining installation. Second, the ground-lining interaction is neglected with the assumption that the earth pressure loads are independent of the ground displacements.

2.4.2.2 Terzaghi's Arching Theory

Terzaghi (1943) discussed the arching above a trap door covered with sand. According to the theory, the amount of arching is approximated by the transfer of load by shear across imaginary vertical planes drawn from the sides of the trap door to the surface of the material. Terzaghi (1946) extended the arching concept to the determination of loads on tunnel liners in crushed rock and sand. The assumption of imaginary vertical shear planes reaching to the ground surface with full shear strength mobilization equivalents to a near collapse condition. Therefore, the theory would provide ground loads either above or below the actual load depending on the magnitude of the displacements occurring in the field for a case of good ground control as noted by Negro (1988).

2.4.2.3 Empirical Techniques

The lining of a soil tunnel generally deforms by a small percentage of its initial diameter, generally less than 0.5 %, as discussed by Peck et al. (1972). Therefore, a flexible circular lining is designed for a uniform full overburden pressure at the springline, plus an imposed distortion, which is measured from field observations in similar soil conditions and construction procedures, as a percentage change in the lining radius. This design approach is based on the concept of the ideal lining that is very rigid in uniform compression and very flexible upon bending. The lining must be designed to withstand the bending moments induced by the estimated diameter changes. The recommended lining distortion ratios for different soil types are presented by Schmidt (1984) based on field observations as shown in Table 2.1. The maximum bending moments resulting from these imposed lining distortions can be calculated using the elastic beam theory (Morgan, 1961):

$$M_{\max} = 3EI \frac{\Delta R}{R^2}$$

where EI and ΔR are the flexural stiffness and the distortion of the lining respectively. Two problems are apparent in the underlying assumptions of the empirical approach.

First, the consideration of full overburden may be too conservative especially for deep tunnels as mentioned by Schmidt (op. cit.). Second, the assumption of uniform ring compression due to the use of a flexible lining is in conflict with the need to account for moments generated by the imposed distortion. In spite of these drawbacks, Negro (1988) suggested that the method is very useful for a preliminary dimensioning of a lining.

2.4.3 Ring and Plate Models

In these models, the ground is represented by a plate and the lining of a circular opening is represented by a continuous ring. Solutions developed by these models are based on continuum mechanics in the closed form style. These solutions are divided into two groups according to whether the in-situ stress field is uniform or non-uniform. The existing solutions are generally derived based on the following assumptions:

- a) The problem is reduced to plain strain with ground strain parallel to the longitudinal tunnel axis being taken as zero.
- b) A linear elastic model is mainly used for both the lining and ground except a convergence-confinement method.
- c) The plate has an infinite extent. This is not a restrictive assumption for tunnels with the cover to diameter ratio greater than 1.5 as shown in section 2.3.4.
- d) The gravitational stress gradient from crown to invert is not considered. Therefore, these models can be applied only to ideally deep tunnels in which the increase of in-situ stress with depth from crown to invert is negligible.
- e) Lining distortion and compression are resisted or relieved by reactions from the ground.
- f) Radial ground pressure on the lining is the same as the in-situ stress prior to the excavation of a tunnel or some fraction of it.
- g) The in-situ stress ratio of horizontal to vertical is given by the value K_0 .

2.4.3.1 Uniform Stress Field Solutions

These solutions are collectively included in the so called convergence-confinement method (CCM). The ground reaction and the support reaction can be

evaluated independently by assuming an ideally deep tunnel with the in-situ stress ratio, K_0 , to be unity. The CCM requires an understanding of the behaviour of the ground to determine the soil convergence related to the applied confining pressure and the liner behaviour to find the confining pressure acting on the lining in terms of deformation. The method is explained in detail in Chapter 5. The major limitation of this approach, especially for a shallow tunnel, is the assumption of a uniform stress field. In such a stress field, the bending moments developing in the lining of a shallow tunnel cannot be estimated. Prediction of the radial displacement before the liner installation is also a major problem when using the method in practice.

2.4.3.2 Non-uniform Stress Field Solutions

This group includes solutions for the non-uniform stress field, which is caused by the in-situ stress ratio, K_0 , other than unity or the action of gravity. Most of these solutions have been reviewed in detail by a number of authors (Craig and Muirwood, 1978; Negro, 1988; Whittaker and Frith, 1990). Most of the solutions are derived by assuming that the lining is installed in close contact with the surrounding ground prior to any displacement development. In recognition of this unlikely situation in reality, some authors suggested using correction factors to account for the ground stress release caused by the delayed installation of the lining (e.g. Muir Wood, 1975; Schwartz and Einstein, 1980).

Several solutions consider an over loading condition in which the opening and support are in existence prior to the application of the stress field (e.g. Burns and Richard, 1964; Peck et al., 1972; Dar and Bates, 1974). This loading condition, which is shown in Figure 2.4 (a), implies that the opening is excavated and supported before the stress field is applied to the plate and represents the case of a backfilled culvert or delayed surcharge conditions applied to an existing tunnel. Most of the other solutions consider an excavation loading condition where the opening is excavated and supported after the stress field is applied to the plate as shown in Figure 2.4 (b) (e.g. Morgan, 1961; Muir Wood, 1975; Curtis, 1976). This loading condition approximately represents a real tunnel situation. Mohraz et al. (1975) studied the effect of the loading condition on the liner

thrust. The lining load for the over loading condition is higher than that for the excavation loading condition.

The majority of the solutions consider both full slip and no slip conditions at the interface between the liner and ground. These solutions also generally assume the lining to be a thin membrane whose behaviour is approximated by the thin shell theory, which is not as rigorously correct as the thick liner solutions. However, Ranken (1978) showed that both approaches give essentially the same results provided the ratio of the lining thickness to mean lining radius is smaller than 0.1. The major limitations of this approach are the assumption of the linear elastic behaviour of the ground and the inability to consider the ground stress relaxation taking place before the installation of a lining. These methods are also strictly valid only for deep tunnels because they are derived based on the assumptions of the infinite plate disregarding the gravitational stress gradient from crown to invert.

2.4.4 Ring and Spring Models

In these models, the ground is represented by a spring with a plane strain condition. The soil stiffness is related to the stiffness of the spring members. The lining of a circular opening is represented by a continuous ring or a segmented ring depending on whether the ring embedment provided by the springs is continuous or discrete. In the continuous condition, in which the number of springs is infinite, the solution can be obtained analytically by treating the lining as an elastically embedded shell. In the discrete condition, in which the number of springs is a finite, the solution is obtained numerically, especially using computer programs for a frame analysis.

Most models use radial springs only, a condition which is equivalent to a tangential slip case at the ground-lining interface. The assumption of radial spring only normally leads to a safer estimate of the lining moments and thrusts because the exclusion of tangential springs makes the ground less stiff. The comparison of the lining moments and thrusts for the ring and plate and the ring and spring models are given by Duddeck and Erdmann (1985). The ring and spring models can be divided into two groups depending on the loading conditions of the ground. The first group assumes a

localized concentration of gravity loading in the crown region, a condition which is associated with loosened ground loads. The second group assumes that the lining is installed before any ground stress redistribution occurs, a condition which the loads are distributed all around the lining.

In the ring and spring models, the loads may be applied in any direction to the lining and may be given any distribution around the lining, which is the main advantage of the method. The major limitations of the models, which are very similar to those of the ring and plate models, are the assumption of the linear elastic behaviour of the ground and the inability to consider the ground stress relaxation taking place before the installation of a lining. The model also ignores the variation of shear stress in response to normal loads on radial planes.

2.4.5 Numerical Methods

These are methods that make use of procedures such as finite element analyses for the prediction of lining behaviour. In these methods, the lining and ground are both treated as a continuum, which differs from the numerical solutions adopted in the discrete ring and spring models. The major advantage of the numerical methods is the fact that the lining loads and ground displacements can be obtained simultaneously. These methods also have several other advantages over simple closed form solutions, including the ability to allow any opening shapes, presence of the surface boundary, geologic discontinuities, non-linear material behaviour and variation of material properties in space and time.

The numerical methods are divided into two groups: two-dimensional and three-dimensional analyses. The two-dimensional finite element analyses are described in detail in Chapter 5. The main disadvantage of the 2-D analyses is related to the difficulty in determining the relationship between the position of liner installation and the amount of ground displacement occurring before the installation of a liner. The detailed description of the three-dimensional finite element analyses is presented in Chapter 6. The responses of the ground and lining around an advancing tunnel can be modelled properly only by 3-D analyses due to the three-dimensional nature of the problem. However, 3-D analysis is

not an easy task to perform because of the difficulties involved in the preparation of the input data and the handling of the output data.

Numerically derived methods can be included in this group. In these methods, parametric studies for influencing variables, covering ranges of values, are performed using numerical analyses such as the finite element method. The results are generalized to be used for the evaluation of lining loads and displacements for other tunnels that comply within the original conditions. Negro (1988) developed such a design method based on the 2-D and 3-D finite element analyses for shallow tunnels. However, it is very difficult to consider the wide ranges of the material properties for the ground and lining, the geometry and depth of a tunnel, and in-situ stress ratio for the development of a method using parametric analyses.

2.5 Summary and Conclusions

The ground response to tunnelling was reviewed using the concept of the convergence-confinement method. Factors influencing the lining load were also summarized and discussed in this chapter. The lining load would be close to zero if the strength of the ground is very high. Therefore, the most important factor of a tunnel construction is geology. The lining load is also influenced by many other factors, which mainly affect the ground displacement that takes place before and after the installation of the lining. The lining load can be either decreased or increased with the displacement of the ground depending on the stress-strain properties of the ground. The passage of time also affects the lining load. Therefore, it is important to verify whether the measured loads are stabilized or continuously increasing, especially when dealing with materials showing time-dependent behaviour. The location of the load measurement with respect to the tunnel face at the time of installation of instruments should be indicated because the load is not the same along the longitudinal direction of the tunnel due to the effect of the face. Lining design methods should consider all of these factors somehow to predict the lining load reliably.

Available design methods were divided into four groups based on the calculation procedure on which a particular method was developed. The empirical and semi-

empirical methods have major drawbacks regarding the applicability of their basic assumptions to the actual behaviour of the lining and ground. However, the empirical techniques can be used for a preliminary dimensioning of a lining in spite of some drawbacks.

In ring and plate models, the convergence-confinement method is good for qualitative discussions of some of the parameters involved in the design of linings. However, the bending moments developing in the lining, which is especially important for a shallow tunnel, cannot be estimated. Prediction of the radial displacement before the liner installation is also a major problem when using the method in practice. The non-uniform stress field solutions are strictly valid only for deep tunnels in homogeneous, isotropic, and elastic ground due to the assumptions applied to them. Most of these solutions were derived without consideration of the ground stress relaxation taking place before the installation of a lining. The ring and spring models also have very similar limitations to those of the ring and plate models. These methods can give better results if correction factors are used to account for the ground stress release caused by the delayed installation of the lining.

The numerical methods are not required to include many assumptions, which other models are. Therefore, the use of the numerical methods, especially finite element analyses, as a tool for tunnel design seems very promising. However, their reliability is governed by their ability to model the stress-strain behaviour of the ground and lining, including the actual tunnelling procedures as close as possible. The main disadvantage of the 2-D analyses is related to the difficulty in determining the amount of ground displacement occurring before the installation of a liner. The comparison of the results of finite element analyses with actual field measurements will help introduce more refinement into these analyses, and consequently improve their reliability.

The responses of the ground and lining around an advancing tunnel can be modelled properly only by 3-D analyses due to the three-dimensional nature of the problem. However, 3-D analysis is not an easy task to perform because of the difficulties involved in the preparation of the input data and the handling of the output data as discussed in Chapter 6. Numerically derived methods also have a limitation because it is

very difficult to consider the wide ranges of the material properties for the ground and lining, the geometry and depth of a tunnel, and in-situ stress ratio for the development of a method using parametric analyses.

There are several basic requirements of a good design method. First, the design method should be simple to use. Duddeck and Erdmann (1985) reviewed the progress of the development of design models. They concluded that the available design methods are simple enough for practical applications. In other words, if a design method is very complex or time consuming to apply, the method will not be widely used by practical engineers. Second, the design method should consider the stress release occurring before the installation of a liner in some way. Third, the method should take into account the plastic behaviour of the ground as well as that of elastic ground.

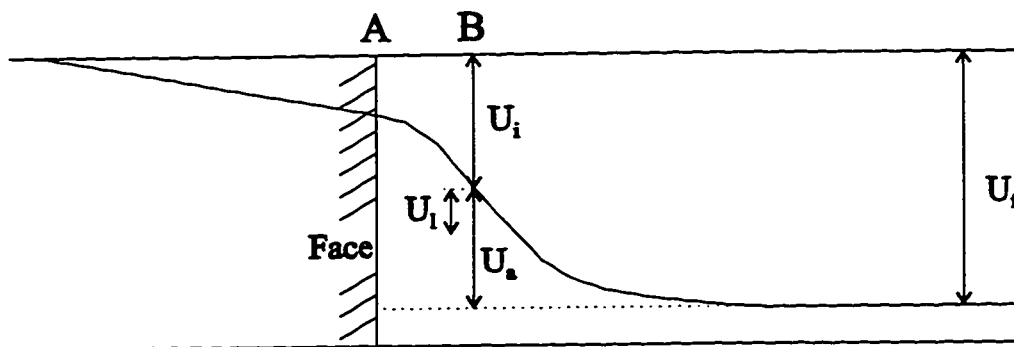
The instruments for measuring the lining loads are reviewed and discussed in the following chapter because field measurements are often necessary to verify the design methods. The validity of the existing design methods is reviewed in Chapter 4 by comparing the results from the methods with the field measurements obtained from several tunnels in Edmonton.

Table 2.1 Ultimate Distortion of Tunnels, $\Delta R/R$, for Design Verification
(Modified after Schmidt, 1984)

| Soil Type | Ultimate Distortion Range, $\Delta R/R$ |
|--|--|
| Stiff to hard clays, overload factor < 2.5 - 3 | 0.15 - 0.40 % |
| Soft clays or silts, overload factor > 2.5 - 3 | 0.25 - 0.75 % |
| Dense or cohesive sands, most residual soils | 0.05 - 0.25 % |
| Loose sands | 0.10 - 0.35 % |

- Notes: (1) Add 0.1 - 0.3 % for tunnels in compressed air, depending on air pressure.
(2) Add appropriate distortion for external effects such as passing a parallel tunnel.
(3) Values assume reasonable care in construction, and standard excavation and lining methods.
(4) Overload Factor=in-situ stress at the tunnel axis/undrained shear strength of the soil

(a)



(b)

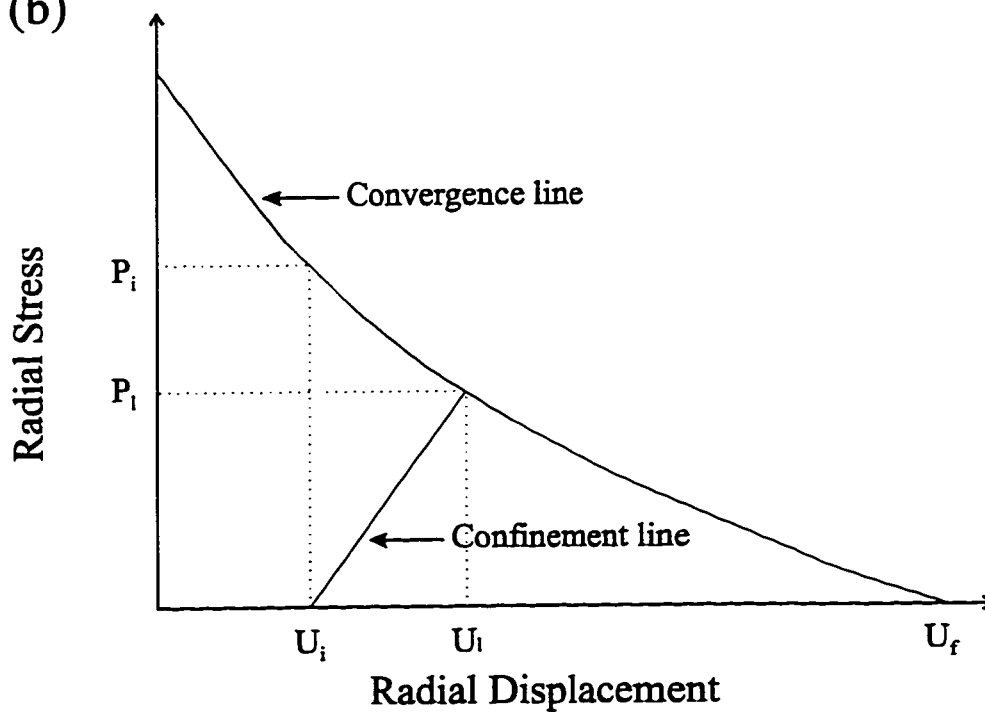


Fig. 2.1 a) Distribution of Radial Displacements along the Longitudinal Direction of Tunnel
b) Convergence-Confinement Curves

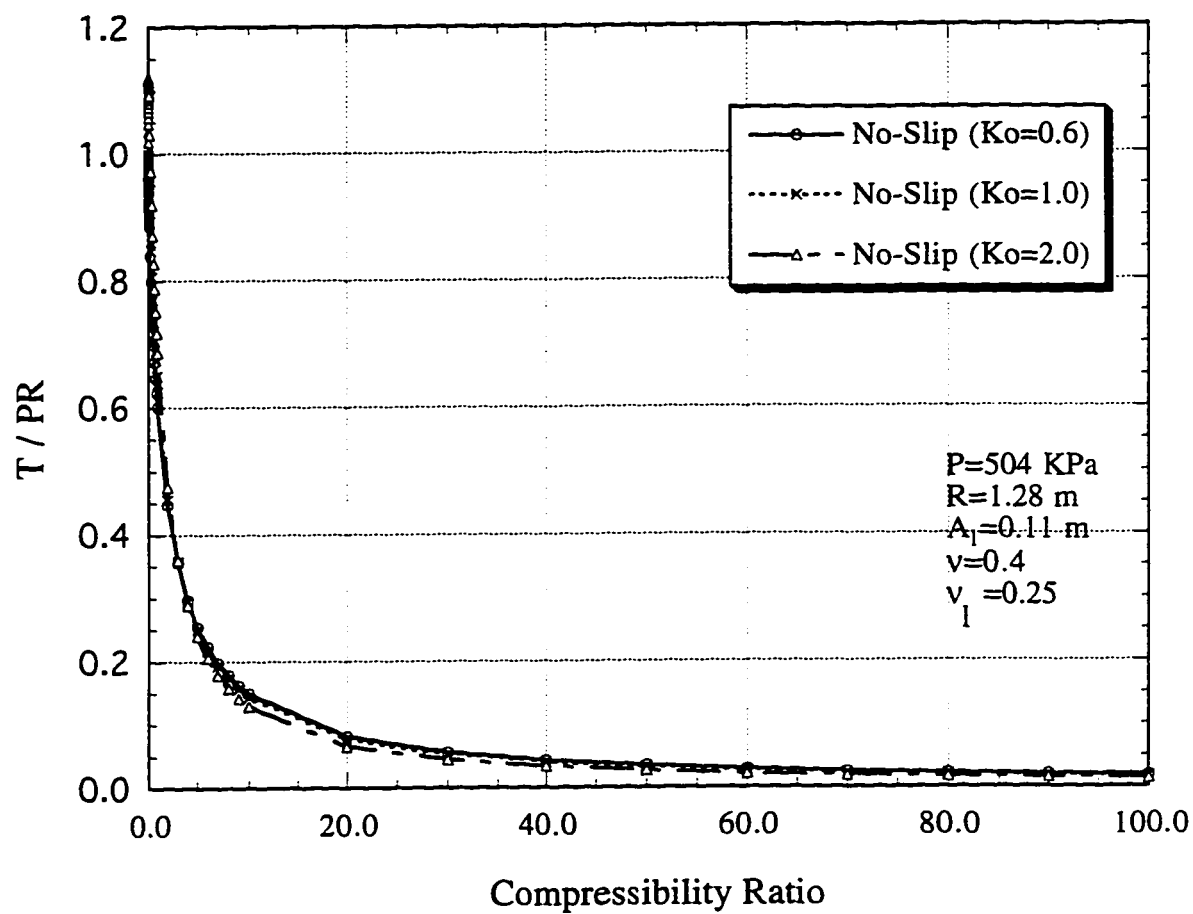


Figure 2.2 Lining Load at Tunnel Springline for Different Compressibility Ratios

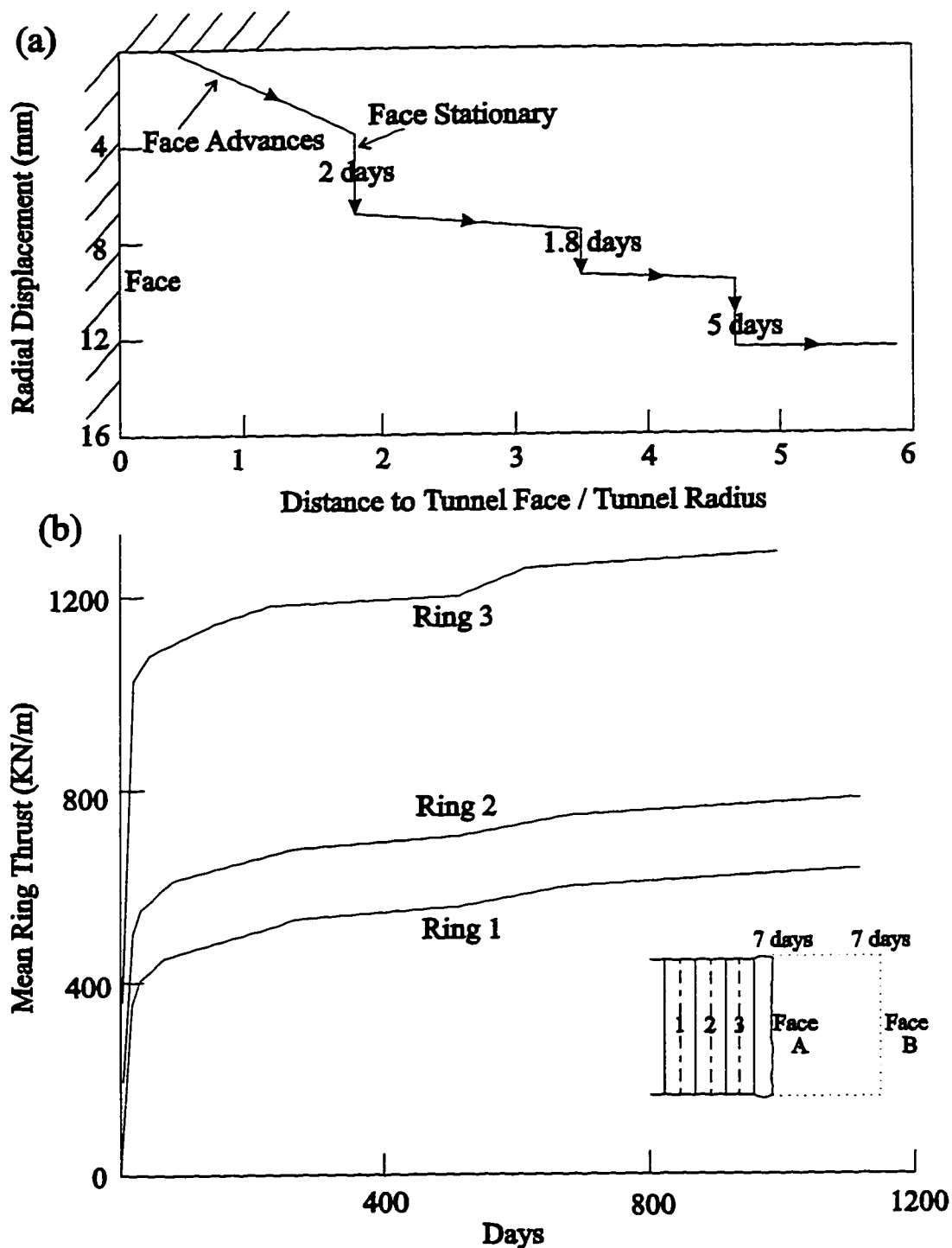
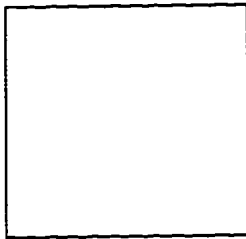


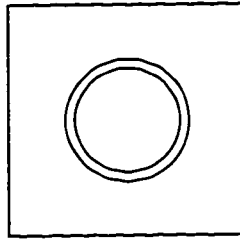
Fig. 2.3 (a) Displacements Recorded 0.3 m above the Crown of the Tunnel during the Instantaneous Advances and Stationary of the Face
 (b) Development of the Mean Ring Thrust with Time in a Steel Lining in the Kielder Experimental Tunnel
 (Modified after Ward, 1978)

(a)

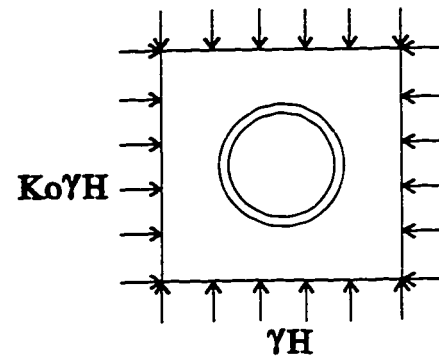
Step 1: Unstressed
Region of Analysis



Step 2: Install
Tunnel and liner

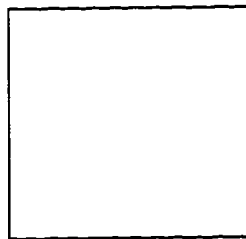


Step 3: Apply
Stresses

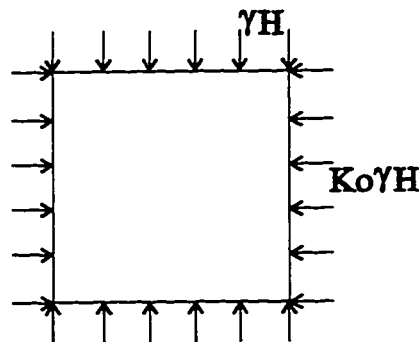


(b)

Step 1: Unstressed
Region of Analysis



Step 2: Apply
Stresses (in-situ)



Step 3: Install
Tunnel and Liner

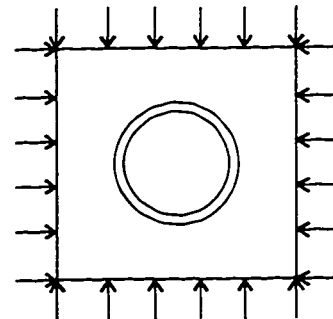


Figure 2.4 Sequence of Analysis

(a) Without Simulation of Construction (Over Loading Condition)

(b) With Simulation of Construction (Excavation Loading Condition)

(Modified after Ranken, 1978)

3. Tunnel Load Measurements

3.1 Introduction

Prediction of lining loads due to tunnelling is one of the major issues to be addressed in the design of a tunnel. The existing design methods do not consider some of the details of construction and the variation of geology along the tunnel section in longitudinal and vertical directions. Therefore, field measurements are often necessary to verify the design methods or assumptions and improve models of ground behaviour. The results can be used in the design of upcoming tunnel sections for the same tunnel project or for future tunnels working in similar material with the similar construction methods.

The lining stress or load can be measured directly or indirectly using pressure cells, flat jack tests, lagging deflection, rod extensometers, strain gauges, or load cells. The magnitude and distribution of stresses acting on the lining can be obtained from the measurement. In this chapter, the instruments for measuring the lining load are reviewed and discussed in detail.

3.2 Method of Tunnel Load Measurements

3.2.1 Pressure Cells

Earth pressures acting on a tunnel lining can be measured directly using pressure cells. There are two basic types of pressure cells: embedment earth pressure cells and contact earth pressure cells (Dunnicliff, 1988). The embedment earth pressure cell is installed for the measurement of total pressure at a point within a soil mass and is mainly used in an earth dam or fill overlying a culvert. The contact earth pressure cell, which is also called a boundary cell, is used for the measurement of total pressure at the face of a structural element. The contact pressure cell has been used to measure radial soil pressure acting on a tunnel lining, i.e., soil-lining contact pressure.

The deflection of the cell is sensed by an electrical resistance strain gauge transducer bonded directly on the interior face of the cell, a vibrating-wire transducer or liquid. Thomas and Ward (1969) preferred using the vibrating-wire strain gauge for the measurement of pressures in the clay core of an earthfill dam because of its long-term stability, robustness and freedom from electrical troubles when read over long distances.

Uff (1970) showed that measurements at the outer face, which were obtained at the side close to the soil, had significant errors caused by uneven loading based on a point load test across the diaphragm of a contact pressure cell. Therefore, for a contact pressure cell, Dunnicliff (1988) suggested measuring pressures from both faces of the pressure cell based on Uff's test results, placing more reliance on measurements at the inner face.

The contact pressure cell should be designed to have similar stiffness and wall roughness as the structure, a condition which is not easy to fulfill. Even in cases in which these requirements are met, the local variation of soil contact pressures on the lining caused by ground irregularity, construction method, and overexcavation can create a large variation in measured pressures. Therefore, pressure cell measurements generally show large scatter that is difficult to interpret. Tattersall et al. (1955) measured radial earth pressures on the three linings of Ashford Common Tunnel in London Clay by using vibrating-wire and hydraulic pressure cells. However, there was a considerable scatter in the pressure values measured in each lining. More reliable results were obtained using vibration-wire load cells, which measured hoop thrusts in segments. Difficulties in obtaining reliable results from a contact pressure cell have been also reported by Delory et al. (1979), Ward and Pender (1981), and Thomson and El-Nahhas (1980). Cording et al. (1975) suggested using strain gauge instrumentation on the lining with the measurements of deflection and deformation of the lining rather than using pressure cells because of the long and unsuccessful history of using pressure cells.

3.2.2 Flat Jack Tests

The interpretation of concrete lining instrumentation is very difficult due to stress independent strains such as shrinkage and temperature changes and time-dependent creep deformations. For a NATM tunnel, these problems are obvious because the shotcrete is loaded at an early age. During this period, the curing shotcrete exhibits a complex mechanical behaviour that changes with the age. A flat jack test can eliminate several problems described above.

The flat jack test was originally used in the field of rock mechanics for the determination of the deformability and in-situ stress in rock masses (Rocha, 1968).

Kuwajima (1991) used the flat jack test in the shotcrete lining of the SLRT-South Tunnel in Edmonton to obtain the stress on the lining. Kuwajima originally attempted to apply the flat jack test using the method suggested by Rocha et al. (1966) at the Laboratorio Nacional de Engenharia Civil (LNEC) in Portugal. Figure 3.1 shows the typical LNEC test arrangement, which has three steps for the determination of the stress. First, the distances between the base points A'-A', B'-B', A''-A'', and B''-B'' are measured using a 0.2 m long extensometer with a 0.001 mm sensitivity dial gauge. Second, the rock is cut between the bases using a sawing machine and a circular disk saw having a 0.6 m diameter and 5 mm thick diamond-edge, with the monitoring of the displacements between base points. Third, a flat jack is pressurized in the slot until the initial displacements are restored. The pressure measured is related to the average normal stress acting on the slot plane before the cutting operation.

Kuwajima experienced three problems in applying the conventional LNEC procedure directly to the SLRT-South Tunnel project. First, the dimensions and shape of the slot were not appropriate for the tunnel lining. The shotcrete lining thickness was 0.18 m close to the steel ribs and 0.14 m mid way between the ribs. The spacing between steel ribs also varied. In other words, the shotcrete lining had a slight curvature in the longitudinal direction. This caused incompatibility of the shape between the slot and the jack because the slot was curved at the shotcrete surface while the jack had a straight edge. Therefore, smaller flat jacks were used for a better match to these curvatures. Second, vibrating wire strain gauges were used for the measurement of displacements because the extensometer was inconvenient and inaccurate to use for the tunnel lining. Third, the depth of the slot was minimized due to the limitation of the lining thickness. However, to keep the pressure transmission efficiency from the jack to the testing material, which decreases as the depth to radius ratio of the slot decreases, the cutting radius was also reduced. Correction factors were obtained from laboratory tests due to the deficient transmission of the pressures from the flat jack to the testing material.

The agreement between imposed and measured pressures in the laboratory tests was within 20 %. However, the accuracy of the tests should be less in the field because the surface of the lining was very irregular even with the application of an electric

concrete grinder and had curvatures in the longitudinal direction. Eisenstein and Kuwajima (1990) also stated that extrapolations of results, which had deviations of between 30 % and 40 %, were necessary for the data interpretation to estimate lining loads. Therefore, even though the mini flat jack test can be an economical and fast procedure for evaluating the stresses in tunnel linings, more case histories should be collected before the method is used with confidence.

3.2.3 Lagging Deflection

Steel ribs and wood laggings have been widely used as a primary lining system. Deflections occurring at the centre of regular wood laggings can be used to back calculate lagging loads if certain assumptions are made. The magnitude and distribution of pressures acting on the laggings must be available to obtain the lagging loads. Kovari et al. (1977) developed an integrated measuring technique to determine the lagging pressure and load from lagging deflection measurements. Branco (1981) used twelve pieces of steel laggings combined with three weldable electric strain gauges attached to the face of each steel lagging to evaluate the lagging pressures. Corbett (1984) observed that the previous methods required a large number of measurements per lagging. Therefore, Corbett presented a method based on Kovari et al.'s concept but in a simpler form by measuring only one deflection point with the assumption of a uniform pressure distribution. Under this assumption, the distributed load can be directly related to the lagging deflections using simple statics principles. To measure deflections with sufficient accuracy, the University of Alberta Deflectometer was designed and built.

The deflectometer was designed to obtain deflections by measuring a central reference point between two points placed near the ends of a wood lagging as shown in Figure 3.2 (a). The accuracy of the deflectometer was user dependent but close to ± 0.2 mm for an experienced operator. Recorded measurements were reduced into equivalent pressures using equations derived from simple statics principles. Calibration of a wood lagging was obtained by placing two equal point loads on the lagging while simulating simple supports at the ends as shown in Figure 3.2 (b). The deflectometer was used to measure the deflection under increasing load. Corbett used correction factors because the

measuring end points were not placed exactly at the end of the beam. Full derivation of the equations are presented by Corbett (1984). Steel laggings were also used to validate loads obtained from the wood laggings because steel is a much more predictable and consistent material than wood. To avoid complications involving stiffness variations, a steel cross-section was designed to have a similar flexural rigidity (EI) to that of a wood lagging.

Corbett used a total of 78 calibrated wood laggings and 27 simulated steel laggings to measure pressures on the linings. The pressures obtained by the wood laggings were comparable to those from the steel laggings but were generally underestimated due to the shoving forces from the mole. Even though Corbett considered the method reliable, several problems are obvious for using the method to calculate the lagging pressures. First, the contact surface between the lagging and soil is usually irregular, having voids in a certain portion behind the lagging. Second, laggings installed even side by side in a longitudinal or vertical direction can have different lagging pressures depending on the degree of the contact with the soil, which very much relies on the construction procedures. Third, the pressures on the lagging often do not show a uniform pressure distribution as assumed for the calculation of the lagging pressures. Fourth, the material properties of wood laggings, which are used for the calculation of the lagging pressures, can vary considerably. Actually, the field measurements obtained by Corbett showed considerable variations. Therefore, even though the monitoring of wood laggings for the measurement of lagging pressures can be done easy and economical ways, the method should be applied with caution.

3.2.4 Rod or Tape Extensometers

A extensometer is used to measure the change of the distance between two reference points on the linings. Displacement measurements are generally more reliable and straightforward than load measurements. Dunnicliff (1971) and Cording et al. (1975) discussed many different types of extensometers in detail. The portable extensometers are generally used for measuring lining deformations. Cording et al. (op. cit.) suggested that an accuracy of ± 0.25 mm is required to measure diametrical liner deformations in the

range of less than 0.5 %. The rod extensometers are more easily damaged and generally limited to spans of about 3 m. The tape extensometers are more versatile and can be used for distances up to about 9 m. The extensometer consists of a dial gauge and a spring. The spring attached to the dial gauge is used to create a constant tension in the tape, eliminating the sagging effects. The accuracy of the tape extensometer varies depending on the spring tension force used in the tape. El-Nahhas (1977) suggested taking the average of the three corresponding readings of the dial gauge after a constant tension is applied and released three times using the spring. Temperature corrections should be applied because both types of extensometers are temperature sensitive.

Tattersall et al. (1955) used rod extensometers for pressure tunnels in London Clay to measure the distance between the five pairs of diametrically opposite segments. The displacement measurements of the lining can be used for numerical analyses as a displacement boundary to back analyse the lining pressure. Szechy (1966) showed rod extensometers in a radial arrangement 60° apart. If pressure, P , is distributed uniformly over a circle of diameter, D , and of unit length, the pressure can be determined using the following equation:

$$P = \frac{E\delta}{D(1 + \nu)}$$

However, the above equation often cannot be used because lining deformations around a tunnel are seldom uniform. Figure 3.3 (a) shows one of the possible layouts of the reference points for monitoring the lining deformation. The location of reference points after the starting of the lining deformation can be obtained from the displacement measurements using the law of cosines and simple trigonometry as shown in Figure 3.3 (b). The line AB is used as a reference with a fixed coordinate point A. The displacement vectors for the points of B, I, J, and K are found by comparing the obtained coordinate points to the original corresponding points taken just after the expansion of the lining. The deformed lining shape can be obtained by connecting those points as smoothly as possible. The greater the number of reference points used, the better the definition of the deformed lining shape.

The above results show only the relative displacement among reference points. It is desirable to measure the absolute movements in space of the reference points on the lining using surveying techniques with a bench mark located far from the excavation. However, the measurement of the absolute movements often can not be done because this may disturb construction operations.

Eisenstein et al. (1977) measured displacements between six points fixed inside three sets of ribs. The average observed displacement vectors were drawn, assuming that the horizontal movements were symmetrical about the vertical centerline and vice-versa. A finite element analysis was performed in terms of imposed displacement boundary to find out the pressure on the lining. Several other assumptions such as a soil material model, in-situ stress ratio, and full contact between the lining and soil were necessary to obtain the relationship between the horizontal displacement and the change of horizontal stress. Therefore, the use of the lining displacement for the prediction of lining pressure is only an approximate solution, which was also mentioned by the authors. Even the rigid body motion of the lining cannot be detected without measurements of the absolute movement of the reference points.

In conclusion, the measurement of lining displacement using the rod or tape extensometers can be an effective tool for checking the stability of an excavation. If the rate of lining displacement does not show any sign of equilibrium, immediate strengthening of the lining is needed to avoid a possible tunnel collapse. However, the prediction of the lining pressure from the lining displacement should not be made on a regular basis and should be combined with other lining instrumentation such as strain gauges or load cells.

3.2.5 Strain Gauges

Strain gauges conveniently measure strains across the lining thickness over a known length. Strain data can be converted into both normal loads and bending moments in the lining. Strain measurements are widely used in the instrumentation program of a tunnel project because they are usually very simple and reliable. Strain gauges can be installed within the lining, especially for concrete lining or attached to the surface of the

lining for steel ribs or precast segmented linings. Among many different types of strain gauges, electrical resistance and vibrating wire strain gauges are the most commonly used for the tunnel lining. Therefore, only these two types of strain gauges are briefly discussed in this section. Cording et al. (1975) described the other types of strain gauges in detail, which are summarized in Table 3.1. Dunnicliff (1988) also reviewed strain gauges comprehensively.

3.2.5.1 Electrical Resistance Strain Gauges

The principle of operation of the electrical resistance strain gauge is based on the fact that the electrical resistance of a wire is proportional to its length. Therefore, measurements of the wire resistance can be used to determine the strains in a tunnel lining if the wire is attached to the lining. The relationship between resistance change, ΔR , and length change, ΔL , is expressed by the gauge factor, GF, as follows:

$$\frac{\Delta R}{R} = \frac{\Delta L}{L} \times GF.$$

The gauge factor varies depending on the types of electrical resistance strain gauges used. There are five types of electrical resistance strain gauges: bonded wire, bonded foil, unbonded wire, semiconductor, and weldable.

The bonded wire resistance strain gauge is fabricated with a thin copper-nickel or nickel-chromium wire, whereas the bonded foil resistance strain gauge is composed of a thin metal foil such as constantan or nichrome. These bonded strain gauges are bonded to a thin elastic mounting of paper, plastic, or epoxy, which in turn is bonded to the tunnel lining being monitored. Figure 3.4 (a) and (b) show typical wire resistance and foil resistance strain gauges respectively. The bonded foil gauge is usually preferred for short gauge lengths. Cording et al. (op. cit.) stated that bonded gauges are generally difficult to use under field conditions because they need very careful handling and skill in preparing the measurement surface and bonding the gauge in place. They are also very sensitive to moisture and difficult to waterproof under field conditions.

The unbonded wire resistance strain gauge is composed of a fine wire looped around two sets of electrically insulated posts, which are attached to the structure being

monitored. The gauge is shown in Figure 3.4 (c). The unbonded wire strain gauge is not commonly used because it is less robust than the bonded gauge. However, the Carlson unbonded wire strain gauge transducer is frequently used in embedment strain gauges and has proven reliability and longevity (Dunnicliff, op.cit.). The Carlson strain transducer has two coils of highly elastic carbon-steel wire each looped around two posts. These two coils are arranged so that one coil contracts while the other expands when strain occurs. The change in resistance ratio of the two coils is a measure of strain.

The semiconductor resistance strain gauge uses semiconductor crystals of silicon or germanium. The crystals undergo a change in resistance proportional to the strain. This type of gauge is much more sensitive than other types due to gauge factors of 50-200, which are very high. The disadvantages of the gauge are the necessity of relatively complicated techniques for correction of errors induced by temperature change and the limited range of capacity for monitoring strains, which is about 100 microstrain. The weldable resistance strain gauge is composed of a resistance element, such as a bonded foil gauge or a strain filament encased in a small tube, which is permanently attached to a thin stainless steel mounting flange. The mounting flange is later welded to the steel lining being monitored.

Experiences with the use of the resistance strain gauges in tunnel lining are reported by Eisenstein et al. (1977), DeLory et al. (1979). Dunnicliff (1988) stated that the longevity of electrical resistance strain gauges is mainly dependent on methods of gauge installation, sealing, and protection, rather than on inherent properties of the gauges themselves. However, bonded strain gauges are not generally recommended for long term field measurements of tunnel linings mainly because of the difficulties related to the waterproofing. DeLory et al. (op. cit.) reported problems using the electrical resistance strain gauges welded to the steel ribs of the temporary lining partly due to the high humidity and dirt conditions in a tunnel. Electrical resistance strain gauges are also vulnerable to lead wire and zero drift problems.

3.2.5.2 Vibrating Wire Strain Gauges

Vibrating wire strain gauges have been used successfully for performance measurements in tunnels. The principle of operation for the vibrating wire strain gauges is explained in detail by the Norwegian Geotechnical Institute (1962) and Cording et al. (op. cit.). Experiences with the use of the vibrating wire strain gauges in tunnel lining are reported by Ward and Chaplin (1957), Ward and Thomas (1965), Curtis et al. (1976), Eisenstein et al. (1979), Harris and Papanicolas (1983), and Matheson and Rupprecht (1984). The vibrating wire strain gauge operates based on the fact that the natural frequency of a tensioned vibrating wire varies with the square root of the tension in the wire as follows:

$$f = \frac{1}{2L} \sqrt{\frac{T}{m}} = \frac{1}{2L} \sqrt{\frac{AE\varepsilon}{m}}$$

where f = frequency of vibration

L = effective length of the wire

T = tension in the wire

m = mass per unit length of the wire

A = cross-sectional area of the wire

E = Young's modulus for the wire

ε = strain.

If the initial frequency of the wire vibration, f_0 , is known and a frequency, f , is measured later, then the change in strain can be obtained as follows:

$$(f^2 - f_0^2) = K^2 \Delta\varepsilon$$

$$\text{where } K = \frac{1}{2L} \sqrt{\frac{AE}{m}}$$

The calibration factor, K , can be verified by calibration tests. Therefore, a change in the frequency of the vibrating wire can be used to measure the strain of the lining to which the gauge is attached.

The vibrating wire strain gauge consists of a steel wire that is stretched between two posts or brackets attached to the lining being monitored. Cording et al. (op. cit.) suggested that the tension of wire should be kept below 15 to 25 % of the yield strength

to ensure the linear elastic behaviour of the wire. The gauge has typical operating frequency limits of between 200 and 1500 Hz. The initial tension must be set correctly, depending on whether the lining is expected to be in compression or tension, within the operating limits. The vibrating wire gauge can be surface mounted either through welding or bolting or embedded in the concrete. Cording et al. suggested installing vibrating strain gauges on the both sides of the neutral axis of the lining to prevent inaccuracy of strain measurements if the lining is subjected to bending.

There are several advantages of the vibrating wire gauge. First, the resistance changes in the lead wires, which existed in the electrical strain gauges, do not affect the frequency of the wire. Second, the strain gauge can be successfully used in dusty and humid environments such as tunnels. Third, the gauge can be installed easily and later recovered for future use after reconditioning. The relatively large size of the gauge and difficulties measuring the dynamic nature of loading such as that which results from the mole reaction are disadvantages of the vibrating wire gauge. However, in general, the vibrating wire strain gauge can be used very effectively, especially for long-term strain measurements in the tunnel lining.

3.2.6 Load Cells

Load cells consist of a solid-circular steel column or a thick wall steel tube. Short segments of the lining can be replaced with load cells to measure strain if the lining is a relatively simple structure such as steel ribs and lagging. The load cells must be aligned carefully to minimize eccentricity. Load cells, which are equipped with strain gauges, are calibrated before use in the laboratory to obtain the relationship between applied load and gauge reading.

There are several types of load cells: electrical resistance, vibrating wire, mechanical, and photoelastic. The classification is based on the type of a strain gauge attached to the load cell. The properties of each type of the load cell are controlled by the strain gauge attached to it. Dunnicliff (1988) summarized the properties of each type of load cell as shown in Table 3.2. Only electrical resistance and vibrating wire load cells

are briefly discussed in this section because they are the most commonly used for the tunnel lining.

Most electrical resistance load cells have electrical strain gauges bonded to the outer periphery of the cylinder at its midsection as shown in Figure 3.5. The gauges are oriented to measure both tangential and axial strains. Since electrical resistance strain gauges are very sensitive to moisture, the strain gauges should be protected by an outer protective steel cover, sealed at the ends with O-rings, and filled with a waterproofing compound. Electrical resistance load cells are not generally recommended for long-term field measurements of tunnel linings due to the high humidity and dirt conditions in a tunnel. A severe amount of measurement drift was also experienced by the current author in several bonded strain gauges mounted on load cells installed in the HUB Mall section of SLRT in Edmonton.

Most vibrating wire load cells have three or more vibrating wire transducers, which are arranged similarly to the electrical resistance load cell as shown in Figure 3.5. Experiences with the use of the vibrating wire load cells in tunnel lining are reported by Cooling and Ward (1953), Tattersall et al. (1955), Curtis et al. (1976), Eisenstein et al. (1979). Cording et al. (1975) recommended the vibrating wire load cells for long term measurements under adverse conditions because of the superior long-term stability of the vibrating wire gauge. Barratt and Tyler (1976) used the vibrating wire load cells successfully for long-term performance measurements in a tunnel. Lead wire damage is not a problem with the vibrating wire load cells as mentioned before.

There are several sources of inaccuracy in load cells. Load cells are usually designed for axial loads only, which can be achieved by providing spherical seats for the structural members. To compensate for eccentric loading and obtain average strains, electrical resistance and vibrating wire load cells must be gauged at several intervals around the periphery of the cylinder as shown in Figure 3.5. End effects of load cells can cause errors if load cells have the small ratios of length to diameter (l/d). It has been widely known in compression tests of rocks that the strength of rocks decreases as the ratio of the length to diameter increases. Paterson (1978) discussed the subject in detail. The main reason for the l/d dependence is the nonuniform stress field by boundary effects

at the contact with the platens. It is generally recommended that the ratio of length to diameter should not be less than 2:1 or, preferably, 2.5:1. However, since most load cells have spherical seats to measure only axial loads as mentioned above, the end effects are not much of a problem. Dunnicliff (op. cit.) suggested that the ratio of one appears to be free from significant end effects.

Cording et al. (op. cit.) suggested that the load cell capacity should be equal to at least the yield strength of the rib times the cross-sectional area of the rib. The size of the load-bearing member should be selected to maintain its elastic limit, at least twice the working capacity. However, load cells with too much capacity reduce sensitivity as experienced by Corbett (1984).

3.3 Processing of measurements

The available field instruments for the monitoring of lining stress or load were reviewed in the previous sections. Among these instruments, strain gauges and load cells were considered the most reliable for measuring the lining load. Therefore, strain gauges and load cells are described in more detail in this section, especially for the location of the instruments on the lining and processing of measurements. The lining load is commonly measured in steel ribs or concrete linings, including precast segmented liners and shotcrete.

3.3.1 Steel Ribs

The lining load produces axial load in the steel ribs and bending about the x-axis of the cross-section as shown in Figure 3.6 (a). The axial load is obtained from axial strain measurements. Two strain gauges, numbers 1 and 2, are located on opposite sides of the rib web at the neutral axis to minimize the influence of bending strains as shown in the figure. The axial strain, which is obtained by averaging the two strain measurements, is converted to an axial load by multiplying the strain by the cross-sectional area and elastic modulus of the rib.

Bending moments in ribs can be obtained from strain measurements of strain gauges located at several distances from the neutral axis. If two strain gauges such as

numbers 8 and 11 are used, axial loads and bending moments can be found, assuming a linear distribution of strain across the lining thickness as shown in Figure 3.6 (b). However, bending moments may not be easily determined due to variations in rib blocking and the distribution of applied load. Therefore, Cording et al. (1975) suggested that strain gauges should be placed at several points on the rib and on adjacent ribs to measure the variations and pattern of bending. Eisenstein et al. (1977) used 10 strain gauges, numbered 1 to 10, for each cross-section instrumented as shown in Figure 3.6 (a). However, the measured strains were mainly due to axial load with very minor bending moment about the x-axis.

Cording et al. (op. cit.) recommended that strain gauges should be installed at a distance of at least 3 times the rib depth from joints and flanges of ribs to avoid non-representative strain patterns at the gauge locations. Several ribs in a row, usually three or four consecutive ones, should be instrumented to allow for variation in the load due to variations in geology and support installation details. The strain gauges also need a robust cover for mechanical protection during handling and erection of the lining. However, Eisenstein et al. (op. cit.) had several gauges malfunction as a result of damage to the leads rather than to the gauges themselves in spite of their being protected using steel channels.

For geotechnical engineering research purposes, the loads due to earth pressure are a major concern. However, stresses in the ribs due to the installation procedure such as outward expansion of the steel ribs by the radially directed hydraulic rams and forces resulting from the longitudinal reaction of the mole may be significant. Eisenstein et al. (op. cit.) observed that the loads in the ribs due to the installation procedure were not large. However, the reaction from the mole taken by the ribs and lagging adjacent to the machine was large, particularly when the longitudinally directed rams were used selectively to steer the machine. The magnitude of the applied forces was unknown. Szechy (1966) presented an approximate solution to calculate the jacking capacity required to move the mole forward under ideal conditions. However, the actual effect of mole reaction on the lining load is very difficult to predict. Figure 3.7 shows the induced moments in the rib due to mole reaction. The magnitude and eccentricity of the force, F ,

are unknown. Furthermore, certain parts of the rib have more loads than other parts due to selective use of rams for steering the mole and variability of lagging lengths. Therefore, the effect of mole reaction on the lining load cannot be calculated reliably.

In order to isolate the effects of the loads other than soil loads, differential strains can be used rather than absolute strains. Doing so will eliminate the effects of the strains imposed by the longitudinal forces. Therefore, linings should be instrumented in the early stages of the tunnelling to measure strains just before and after the advance of the mole. As the mole progresses away from the instrumented section, the influence of the longitudinal loads decrease and the loads due to earth pressure become more important. If longitudinal stresses resulting from mole reaction are measured directly, Dunnicliff (1988) suggested using resistance gauges rather than vibrating wire strain gauges due to the dynamic nature of the loading.

Load cells can be installed between the ends of the steel rib sections. Both ends of load cells are welded to the end plates, which in turn are placed between end plates of the steel ribs and tightened with bolts and nuts. A factor of safety of load cell against yielding can be checked by assuming full overburden at the springline and uniform pressure acting around the lining. The maximum normal load in the load cell can be calculated using the following equation and compared to compressive yield strength of the steel cell to get the factor of safety:

$$\text{Normal load} = \text{soil unit weight} \times \text{depth of springline} \times \text{rib spacing} \times \text{lining radius}.$$

The loads measured at the joints of the steel ribs in a rib and lagging system represent the combined stress acting along the ribs and adjoining pieces of lagging. There are many possible stress distributions that yield the same set of loads as measured by load cells. For example, stress distribution around a deep tunnel is commonly assumed to be symmetric to the vertical and horizontal axes with a horizontal stress equal to some fraction of vertical stress as shown in Figure 3.8 (a). This assumption of stress distribution is valid only when load cells installed in both upper and lower joints measure similar loads. The relationship between measured loads at the joints and the stresses acting on the lining is derived using equilibrium equations as given in Figure 3.8 (b). If rib spacing is other than a unit length, the right side of the final equation in the figure

should be divided by the rib spacing to obtain the final stresses acting on the lining. Other relationships can be derived based on different assumptions of the stress distribution around a tunnel (e.g. Branco, 1981).

A combined lining system is often used for the initial support of the ground. For example, steel ribs in soft ground tunnels may include shotcrete linings. In the rib and lagging system, all the radial loads carried by the lagging are assumed to be transmitted to the ribs as mentioned before. However, the loads in a combined lining system of the rib and shotcrete are shared by the rib and shotcrete separately. It has been suggested that the load share between shotcrete and steel ribs in terms of thrust, T , can be expressed as the ratio between the product of Young's modulus versus the area (EA) of each of these structural elements:

$$\frac{T_{\text{rib}}}{T_{\text{shotcrete}}} = \frac{(EA)_{\text{rib}}}{(EA)_{\text{shotcrete}}}$$

The results shown in Table 3.3 encourage the use of this ratio as a simplified way to predict the load share between the shotcrete and rib in NATM tunnels. In other words, if lining loads are measured only in either shotcrete or steel ribs, an average lining load can be obtained by adding the loads in the rib and shotcrete using the above equation and dividing the total loads by the combined length of the rib and shotcrete.

A more rigorous solution can be obtained for estimating the load share between the shotcrete and rib using a procedure recommended by Hoek and Brown(1980). However, Eisenstein et al.(1991) and Kuwajima (1991) showed that the relative differences between these two evaluations were smaller than 5% and suggested the use of ratio $(EA)_{\text{rib}} / (EA)_{\text{shotcrete}}$ due to its simplicity. They also suggested the use of the above ratio for K values other than 1 based on several case histories even though the above equation implicitly assumes an insitu stress ratio $K=1$.

3.3.2 Concrete Linings

Strain gauges can be installed on the surface of concrete linings such as precast concrete segmental, cast-in-place concrete, and shotcrete linings or can be embedded in the concrete as shown in Figure 3.9 (a). Strain measurements in concrete are difficult

because measured strains can include strains due to creep, shrinkage, and temperature changes of concrete linings. Cording et al. (1975) described methods for estimating these strains which are not related to soil loads.

Another problem with using strain gauges in the concrete lining is the variation of the modulus of elasticity of the concrete, which is especially obvious in cast-in-place and shotcrete linings. Cording et al. (op. cit.) suggested determining the modulus of elasticity from test cylinders with embedded strain gauges cast with the lining and cured under similar conditions. Whenever a set of lining strains is measured, a test cylinder is also loaded in a testing machine to determine the modulus of elasticity. However, the suggested method can be very inconvenient. Alternatively, the variation of the modulus of elasticity of the lining with age can be estimated by means of an extensive series of laboratory tests as Kuwajima (1991) did for the shotcrete lining.

If two strain gauges are installed on the surface and inside of concrete linings as shown in Figure 3.9 (a), axial stresses can be found assuming a linear distribution of strain across the lining thickness as shown in Figure 3.9 (b). The axial stresses can be multiplied by the thickness of a lining and divided by the radius of the lining to estimate stress distribution around a tunnel.

Load cells also have been widely used in concrete linings, especially precast concrete segmented linings. The relationship between applied load and gauge reading is obtained in the laboratory before load cells are installed in the lining. The measured loads provide an overall average measurement of normal forces in the lining. A pair of load cells are usually placed between segments in the springline to measure hoop thrust. Total load per ring is obtained by adding the loads from these two cells. Stress distribution around a tunnel can be approximated by dividing the total load by the radius and the longitudinal length of the segmented lining.

3.4 Summary and Conclusions

The instruments for measuring the lining load are reviewed in this chapter. Pressure cells are not generally recommended for measuring lining loads because of the long and unsuccessful history of attempting to do so. Flat jack tests can be an economical

and fast procedure to evaluate the stresses in concrete linings. However, more case histories should be collected to improve the accuracy of the method. Lagging deflection can be used for estimating lining loads in a rib and lagging support system. Again, the method should be applied with caution because the amount of lagging deflection varies depending on several factors as explained in Section 3.2.3. The use of rod or tape extensometers for estimating lining loads requires several assumptions, which make the method only an approximate solution.

It was shown that strain gauges and load cells are the most effective and reliable ways for measuring lining loads. If measurements from both strain gauges and load cells are obtained in combined lining systems, the lining loads shared between two different lining types should be considered when calculating an average lining load. The pattern of strain throughout the lining may be highly variable and difficult to convert into stress without certain assumptions of the stress distribution. Therefore, a large number of strain gauges are generally required to examine the overall behaviour of the lining because a strain gauge provides reliable measurement of strain at only one point in the lining. On the other hand, one or two load cells provide an overall average measurement of normal loads in the lining. Therefore, using load cells is more cost effective than using strain gauges. However, the assumption of stress distribution around a tunnel should be well approximated to calculate reliably the average radial stresses acting on the lining.

The loads due to other than earth pressure may affect the measurements of lining loads. Special care should be taken for the measurements of strain gauges in the ribs and precast concrete segmented linings because stresses due to the installation procedure such as outward expansion of the linings by the radially directed rams may affect the readings. Measurements from load cells are not much affected by the expansion of the linings because the load cells are generally activated after the pressure in the expansion jacks is released. The forces resulting from the longitudinal reaction of the mole may be significant for the measurements of lining loads. In order to isolate the effects of the loads from the mole, differential strains can be used rather than absolute strains. In concrete linings, high lining strains may develop locally as a result of creep, shrinkage, and

temperature changes. Therefore, strain measurements in concrete linings should be corrected to consider these factors.

Long-term load measurements in a tunnel are important to check the stability of a tunnel because lining loads generally increase as time passes. Therefore, considering the high humidity and dirt conditions in a tunnel, the vibrating wire strain gauges or load cells are recommended for the load measurements in a tunnel. The geology and construction sequence, including the location of the tunnel face with respect to the instrumented lining, should be recorded in detail because they are closely related to the variation of the lining load. Several ribs in a row, usually three or four consecutive ones, should be instrumented to allow for variation in the load due to variations in geology and support installation details. In the following chapter, measured lining loads from case histories are presented and compared with the lining loads from existing theories.

Table 3.1 Strain Gauges - Types and Features (Modified after Cording et al., 1975)

| Type | Strain Sensitivity, Microstrains | Gage Length, (cm) | Typical Range, Microstrains | Advantages | Limitations and Precautions | Reliability |
|---|----------------------------------|-------------------|------------------------------|--|---|-------------|
| Bonded Electrical Resistance Gauge | 2 - 4 | 0.02 - 15.24 | 20,000 - 50,000 | Small Size, low cost. Temperature compensation available. | Errors due to lead wire and circuit resistance changes unless compensated. Long term stability may be poor due to cement creep. Meticulous Installation procedure. Difficult to waterproof. | Poor - Fair |
| Vibrating Wire Gauge | 1 - 2 | 10.16 - 35.56 | 600 - 7,000 | Not as affected by lead wire resistance changes. Easy to install, factory waterproofing. Long experience record. Robust, reusable. | Small range. Temperature correction required. | Good |
| Encapsulated, unbonded, Electrical Resistance | | | | | | |
| a) Ailtech Weldable Gauge | 2 - 4 | 2.54 - 15.24 | 20,000 | Factory waterproofing. Welded surface mount, temperature compensation available. | Errors due to lead wire and circuit resistance changes unless compensated. | Fair - Good |
| b) Carlson Gauge | 4 | 20.32 - 50.80 | 700 tension 1400 compression | Factory waterproofing, easy to install. Long experience record. | Errors due to lead wire and circuit resistance changes unless compensated. Small range. Temperature correction required. | Good |
| Mechanical Gauge | 5 - 10 | 5.08 - 203.2 | 10,000 - 50,000 | Simple, low cost, waterproofing not required. | Requires skill in reading. Cannot be read remotely. | Excellent |

Table 3.2 Load Cells - Types and Features (Modified after Dunnicliff, 1988)

| Type of Load Cell | Advantages | Limitations | Approximate Accuracy |
|-----------------------|---|---|---|
| Electrical Resistance | Remote readout Readout can be automated | Low electrical output Lead wire effects Errors owing to moisture and electrical connections are possible Need for lightning protection should be evaluated | $\pm 2 - 5 \%$ * |
| Vibrating Wire | Remote readout Lead wire effects minimal Readout can be automated Single-gauge versions available for in-line use in tension | Special manufacturing techniques required to minimize zero drift Need for lightning protection should be evaluated | Single-gauge versions for in-line use in tension, better than $\pm 2 \%$ Multigauge versions for general use, $\pm 2 - 5 \%$ * |
| Mechanical | Robust and reliable | Requires access to cell | $\pm 2 - 10 \%$ * |
| Photoelastic | Robust and reliable | Requires access to cell Limited capacity Requires skill to read Most users prefer more direct numerical reading | $\pm 2 - 5 \%$ |

* These are accuracies of the load cells when used with adequately designed and installed mounting arrangements. However, because of misalignment of load, off-centre loading, and end effects, system accuracy is often no better than $\pm 5-10 \%$, and may be significantly worse if mounting arrangements are inadequate.

Table 3.3 Calculated and Measured Loads in the Combined Shotcrete-Rib Lining

| Reference | (EA)rib/(EA)shotcrete | | Insitu stress ratio (K) | Method of measurements |
|---|-----------------------|------------|-------------------------|---|
| | Measured | Calculated | | |
| Aydan et al. (1988)-3D FEM simulation | 78% | 88% | K=complex | from 3D FEM simulation |
| Eisenstein and Kuwajima(1990)-Tunnel in Soft rock | 11% | 10% | K=2 | Load cells for the steel ribs Flat jack for the shotcrete |
| Kuwajima(1991)-Till | 16% 20% | 18% 18% | K=0.8 | Vibrating wire strain gages for the shotcrete. Resistance strain gages for the steel ribs |

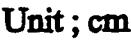


Figure 3.1 Layout of LNEC Flat Jack Test (Modified after Rocha et al., 1966)

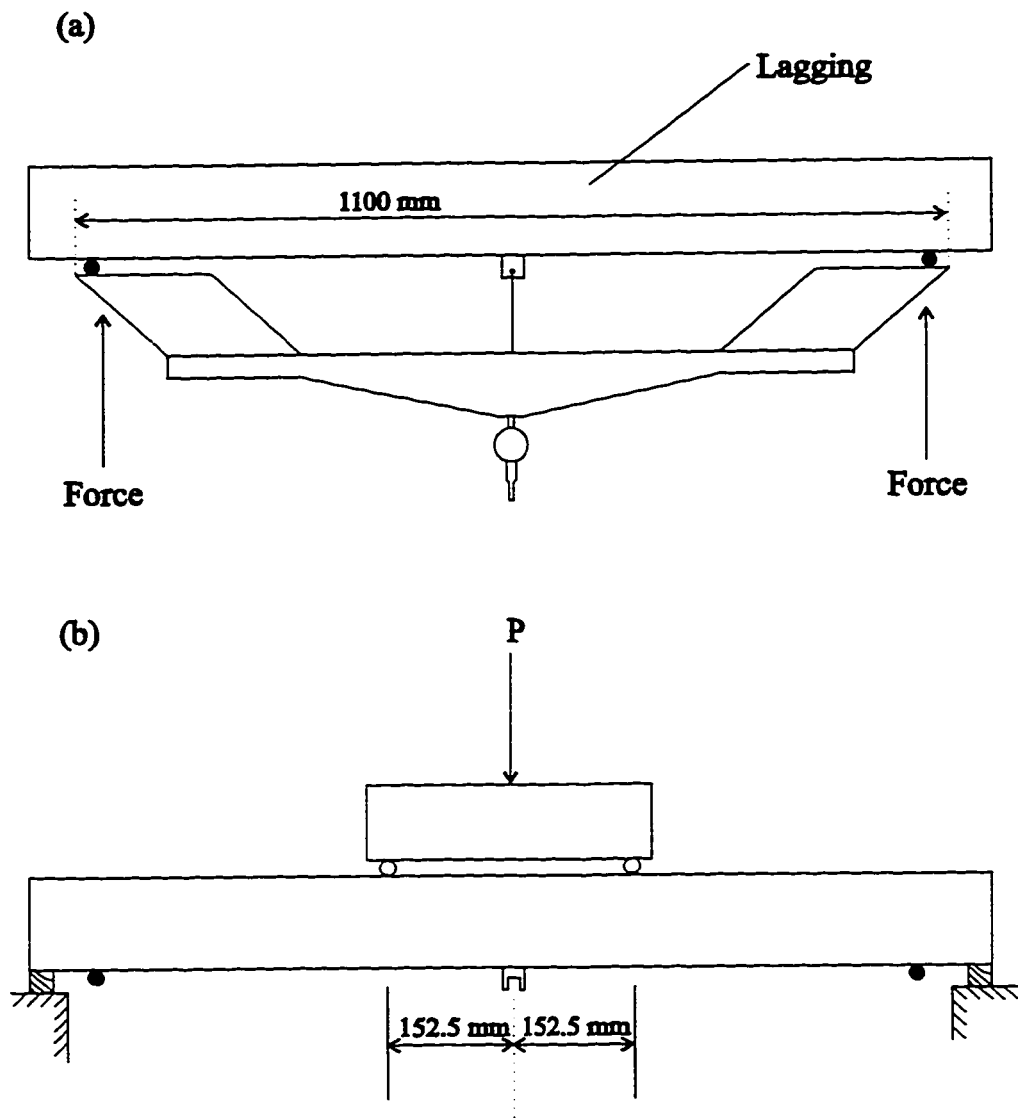
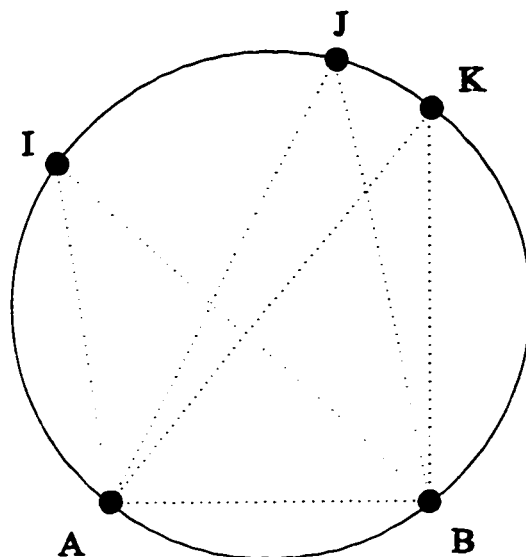
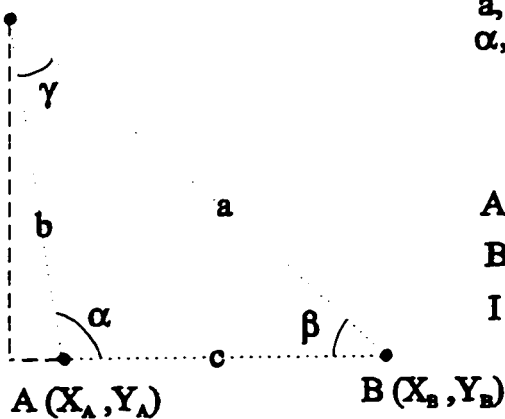


Figure 3.2 (a) University of Alberta Deflectometer
(b) Laboratory Arrangement for Calibrated Laggings
(Modified after Corbett, 1984)

(a)



(b)

I (X_I, Y_I)

a, b, c; measurement from extensometers
 α, β, γ ; obtained using the following equations

$$a^2 = b^2 + c^2 - 2bc \cos \alpha$$

$$b^2 = a^2 + c^2 - 2ac \cos \beta$$

$$c^2 = a^2 + b^2 - 2ab \cos \gamma$$

A (X_A, Y_A) ; Assign arbitrary coordinate points

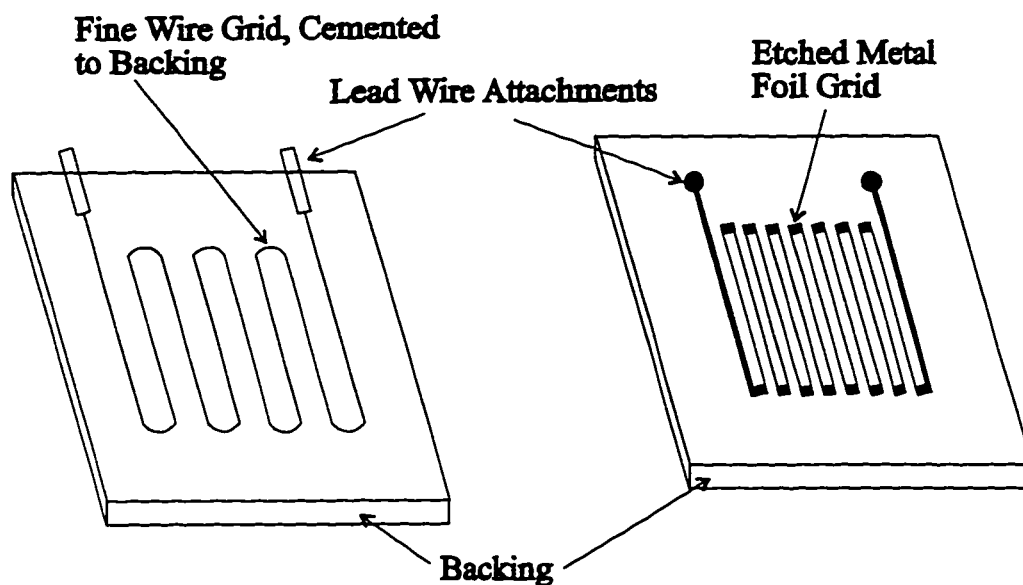
B (X_B, Y_B) ; X_B = X_A + c, Y_B = Y_A

I (X_I, Y_I) ; X_I = X_A - (cos(180- α)*b)
 Y_I = Y_A + (sin(180- α)*b)

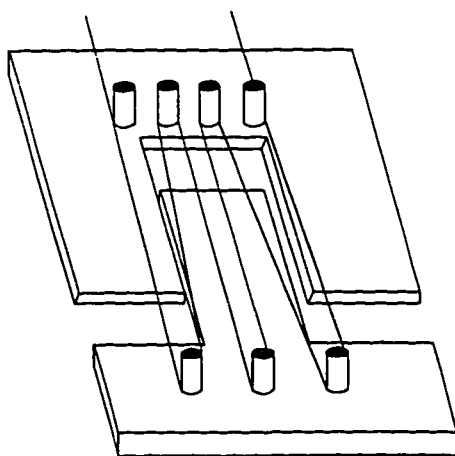
J (X_J, Y_J) and K (X_K, Y_K) can be obtained
 using $\triangle ABJ$ and $\triangle ABK$ respectively.

Figure 3.3 (a) Possible Layout of Measuring Points for the Monitoring of the Lining Deformation

(b) Processing of the Measurements to obtain the Deformed Shape of the Lining



(a) Bonded Wire Resistance Strain Gauge (b) Bonded Foil Resistance Strain Gauge



(c) Unbonded Wire Resistance Strain Gauge

Figure 3.4 Types of Electrical Resistance Strain Gauges
(Modified after Cording et al., 1975 and Dunnicliff, 1988)

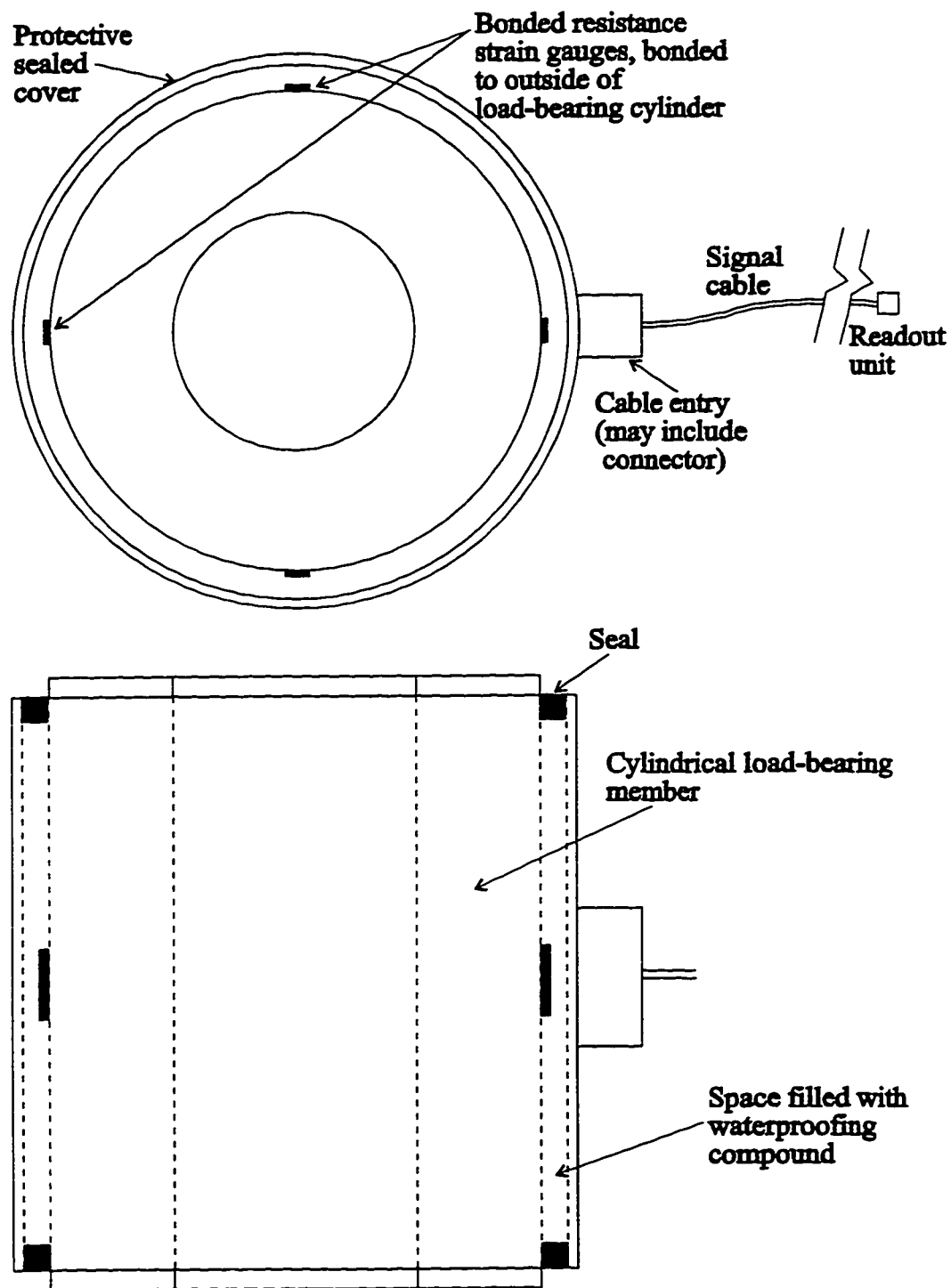


**Figure 3.5 Schematic of Electrical Resistance Load cell
(Modified after Dunicliff, 1988)**

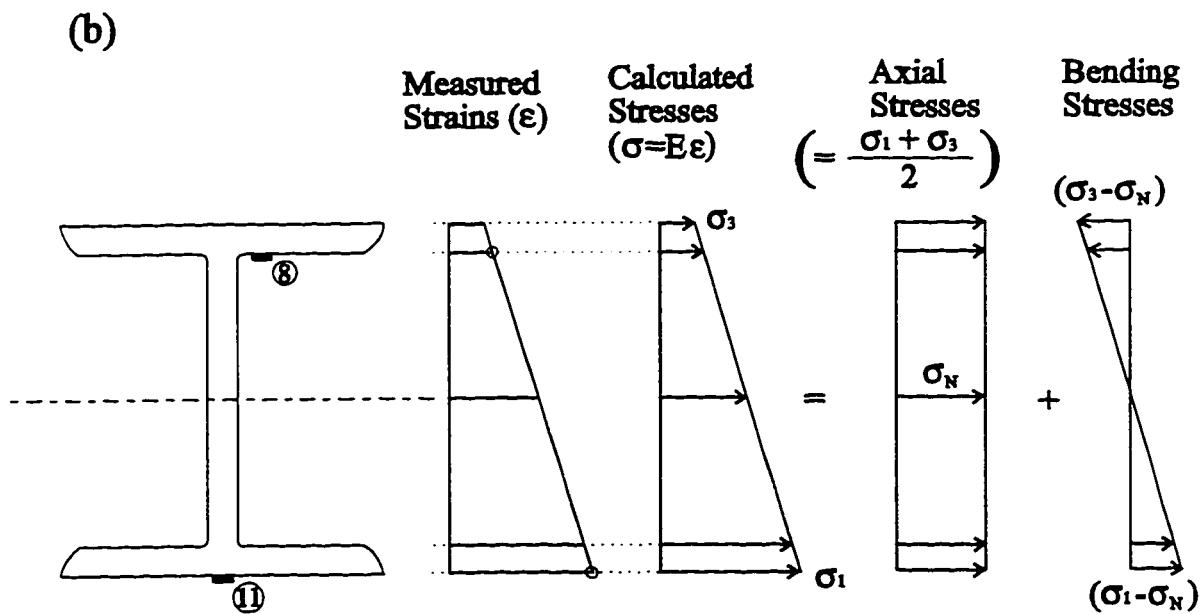
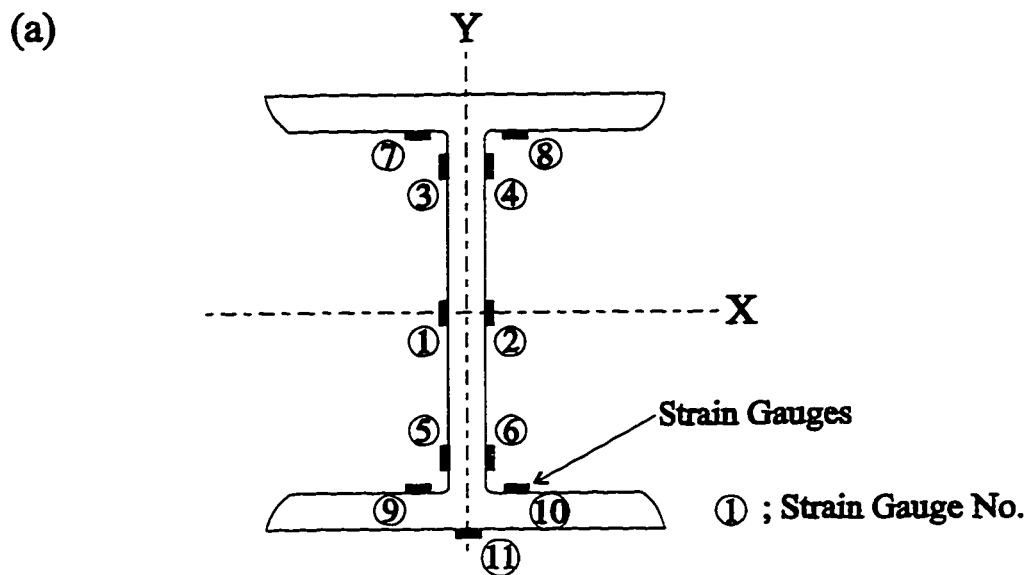


Figure 3.6 (a) Location of Strain Gauges on Cross-Section of a Steel Rib
(b) Calculation of Axial Stresses and Bending Stresses

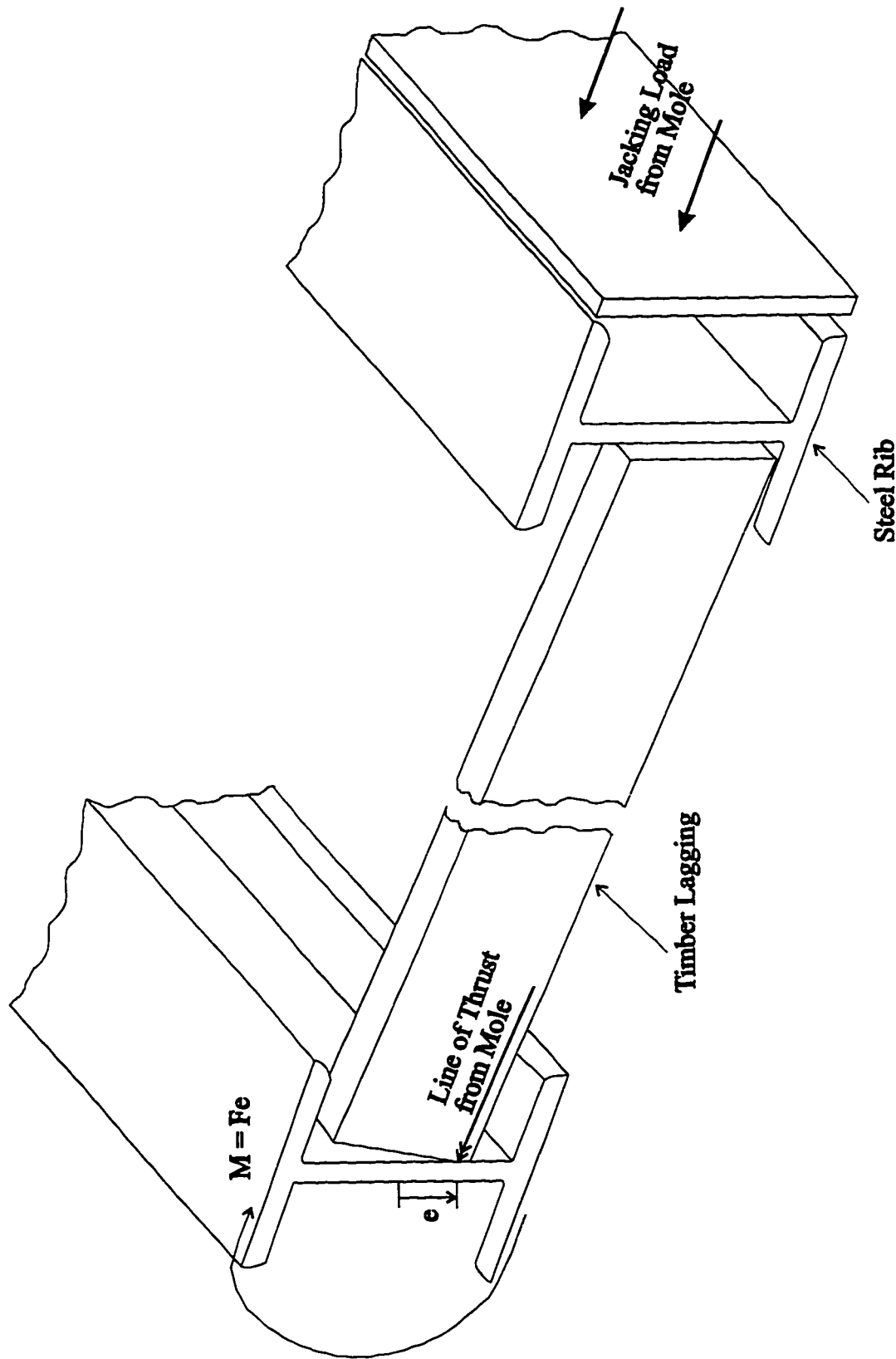
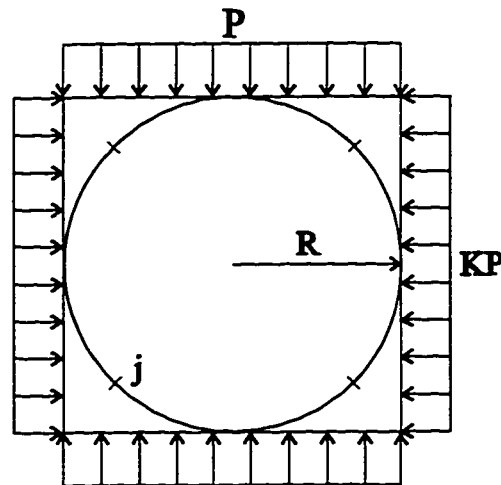
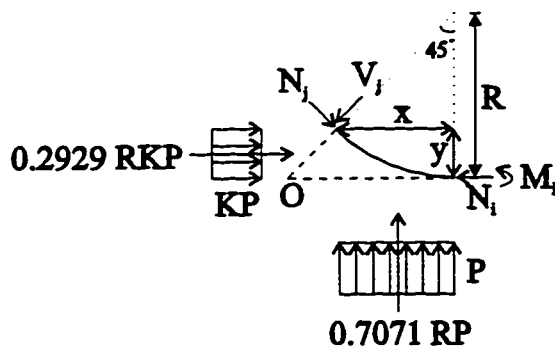


Figure 3.7 Induced Moments due to Jacking Load from Mole

(a)



(b)



Assumptions:

- Symmetry with respect to the vertical axis ($V_1 = 0$)
- Joints do not carry bending moments ($M_1 = 0$)

$$x = R \sin 45 = 0.7071R$$

$$y = R - R \cos 45 = 0.2929R$$

$$M_1 = 1/4 P(K-1)R^2$$

$$+\sum M_o = -0.2929 RKP \frac{0.2929R}{2} - 0.4142 R N_j + 1/4 P(K-1)R^2 + 0.7071 RP(0.6465R) = 0$$

$$0.2071 RKP - 0.25PR + 0.4571 RP = 0.4142 N_j$$

$$N_j = 0.5 RKP + 0.5 PR = 0.5 PR(1+K)$$

$$\therefore P = \frac{2N_j}{R(1+K)}$$

Figure 3.8 (a) Simplified Load Distribution around a Steel Rib with Four Joints

(b) Equilibrium Equations at a Joint for a Unit Length of Ribs Spacing

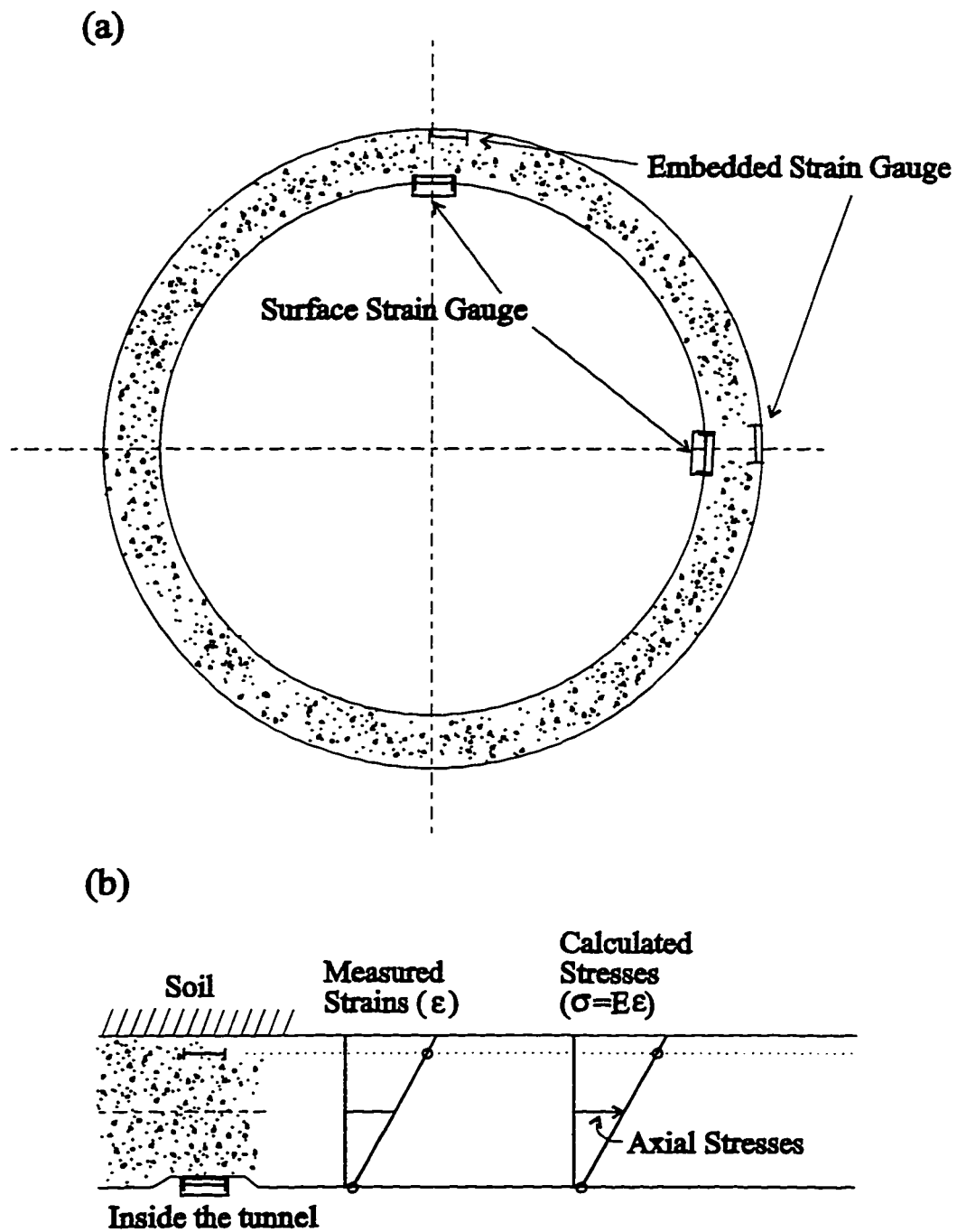


Figure 3.9 (a) Location of Strain Gauges on Cross-Section of a Concrete Lining
(b) Calculation of Axial Stresses

4. Comparison of Lining Loads from Measurements and Existing Design Methods

4.1 Introduction

Methods for predicting and measuring lining loads were reviewed in the previous two chapters. Many factors contribute to the differences in the lining loads of many different tunnels as explained before. Therefore, it is very important to understand the influence of these factors on the tunnel lining to predict the loads on the liner more reliably. In other words, lining design methods should try to take into account all of these factors to predict the lining load reliably. The validity of the existing design methods, three from ring and plate models and one from numerically derived methods, is reviewed in this chapter by comparing the loads calculated using the methods with the field measurements obtained from several tunnels in Edmonton. The use of correction factors for the existing design methods is also discussed in this chapter.

4.2 Tunnels in Edmonton

Tunnel construction in the City of Edmonton has been very active, especially for storm and sanitary purposes. A total length of 2294 km of sewer systems was built prior to 1971 (Beaulieu, 1972). Tunnelling activity has been continuous since then, as a result of the growth of the city. The city has been developing a Light Rail Transit (LRT) system since the early seventies. The development of the system has been in stages, the first of which is termed the Northeast Line, connecting the city centre with northeast suburbs. The line is located underground in the city centre, but emerges on the surface to utilize the existing CNR right-of-way for the rest of its length (Eisenstein and Thomson, 1978). This section includes two underground stations, Central and Churchill.

The second stage is termed the South Extension and connects the Central station with the Canadian Pacific Railway right-of-way, south of 100th avenue, parallel to 109th street (Branco, 1981). The two stages have a total length of 10.3 km, with eight stations. 1.5 km, including four stations, runs underground through the city centre (Sorensen, 1986).

The third stage, which is 1.8 km long, is termed the SLRT-Phase II tunnels and connects the North Saskatchewan River bank to Corona station (Tweedie et al., 1989).

The fourth stage connects the portal on the North Saskatchewan River bank to the University station. The geology, construction methods, lining system and load measurements of these LRT tunnels and several sewer tunnels are reviewed in the following sections.

4.2.1 Northeast Line

The line is located underground within the downtown core, emerging on the surface to utilize the existing CNR right-of-way for the rest of its length. The tunnel line has a curved geometry and passes under an intensively developed area. Therefore, this portion of the line had to be designed as two parallel tunnels, one for each rail line. The circular tunnels are approximately 250 m long and 6.1 m in diameter and are separated by about 11 m centre to centre. The tunnels are located within a dense, jointed till sequence. The tunnels were advanced using a shielded mechanical mole manufactured by Lovat Tunnelling Equipment Inc., Toronto. The project, including a detailed description of the configuration of the shielded mole, is described in detail by Eisenstein et al. (1977) and Eisenstein and Thomson (1978).

The primary support system is composed of steel ribs at 1.22 m centers and timber laggings while the permanent lining was cast-in-place reinforced concrete. The steel rib was assembled from four segments connected at joints. Every steel rib was expanded twice against the soil by a hydraulically operated rib expander. The first phase of activation took place as soon as the rib left the shield while the second phase of activation was carried out at the same time as the first activation of the next rib. The timber lagging struts were placed on the inner flange of the rib sections to complete the ring between the ribs.

The loads in the ribs were measured by means of electric resistance strain gauges installed on the ribs. Ten electric resistance type strain gauges were placed on each cross section instrumented as shown in Figure 4.1 (a). The strains measured were converted to stresses and then to loads. Readings were continued until the concrete for the permanent lining began to be placed. The gauges were installed at four locations per rib on three consecutive ribs, which were called Ribs A, B and C, as shown in Figure 4.1 (b). The

uniform radial soil pressure on the lining was 169 KPa, which is equivalent to 79% of overburden pressure.

4.2.2 LRT - South Extension

The tunnel connects the Central Station with the Canadian Pacific Railway right-of-way parallel to 109th street. The tunnel was excavated with a tunnel boring machine (TBM) built by Lovat Tunnel Equipment Inc., Ontario. The tunnel is located within till and has an excavated diameter of 6.2 m. The tunnel is described in detail by Branco (1981) and Eisenstein et al. (1982).

The initial support system for the tunnel is composed of steel ribs at 1.22 m centers and 10 x 15 cm wooden laggings placed between the webs of successive ribs. The steel ribs were expanded immediately after these were exposed to the soil with the help of the rib expansion ring. The permanent lining consists of 0.30 to 0.38 m thick cast-in-place reinforced concrete.

Twelve pieces of steel lagging, eight load cells, tape extensometers, and eyebolts were used to study the interaction between the steel ribs and wooden lagging. The twelve pieces of hollow steel lagging were designed to have the same bending stiffness as the wooden lagging. Two load cells designed to measure only axial loads were installed on each of four steel rib rings. The structural members of the load cells were a solid cylinder of cold rolled steel. Two vibrating wire strain gauges were welded to the cylinder in diametrically opposite directions so that strains could be averaged. After the joint expansion, the load cells were placed between the end plates of the steel ribs. The eight load cells were installed as shown in Figure 4.2. Branco (1981) recommended using the load cell readings taken when the shield tail was 36.4 m away, which was about 14 days after installation of the load cells. This distance was considered to be great enough to avoid mole jacking effects. However, the load cell readings showed a continuous increase after the above period. Therefore, maximum load cell readings were taken as the lining loads of the tunnel for this study. Stress distributions around the steel ribs were obtained by combining loads measured in the upper and lower joints of rings 1 and 2, rings 2 and 3, and rings 3 and 4. The average ring stresses on the steel ribs were 52.09, 60.86, and

64.38 KPa respectively. These stresses are equivalent to 21 %, 25 % and 26 % of the overburden pressure. The average ring stresses on the steel lagging were 15.89, 17.02 and 30.25 KPa, which are equivalent to 6 %, 7 % and 12 % of the overburden pressure.

4.2.3 SLRT - Phase II

The Edmonton South Light Rail Transit (SLRT) - Phase II tunnels extend from the North Portal on the North Saskatchewan River Valley slope to Corona Station. The project is described in detail by Tweedie et al. (1989) and Phelps and Brandt (1989). The tunnels, which are 1.8 km long, typically have an excavated diameter of 6.3 m. A tunnel boring machine (TBM), built by Lovat Tunnel Equipment Inc., Ontario, was used to excavate about 800 m of tunnel between the North Portal and the Crossover Cavity, which includes instrumented Sections B2 and A1. The northbound and southbound tunnels between the Crossover Cavity and Corona Station include Section C2. The tail track section south of the Crossover Cavity was completed using the Sequential Excavation Method (SEM). The tunnels in Sections B2 and C2 are located within a thick layer of glacial till while Section A1 is located in postglacial sand.

The primary support system for the SEM tunnel (Section C2) is composed of shotcrete placed in two layers: the first layer, 40 mm thick was applied immediately after excavation, followed by the placement of wire mesh and steel ribs at 1.0 m centers, followed by an additional 110 mm of shotcrete. The initial support system for the TBM tunnel (Sections B2 and A1) is composed of steel ribs at 1.0 m centers and wooden lagging. The permanent support was formed by 0.25 m thick cast-in-place concrete.

Tunnel instrumentation included load cells, pressure cells, and vibrating wire and resistance strain gauges. Four load cells were installed between rib segments on two adjacent ribs at Section B2 as shown on Figure 4.3. The loads stabilized at between 200 and 230 KN soon after installation and increased to the range of 255 to 420 KN after the southward advance of the adjacent SEM tailtrack tunnel. The average soil pressures on the liner (PL) are estimated from the assumption that the pressures on the lagging are finally transmitted to the steel ribs. The average soil pressure on the primary liner is 105 KPa, which is approximately 32% of the overburden pressure.

Tunnel instrumentation in Section C2 included pressure cells installed between the soil and the primary shotcrete liner, embedded vibrating wire and resistance strain gauges installed within the primary shotcrete liner to measure strains, and miniature flat jacks in the completed primary shotcrete liner. The soil pressure of 30 Kpa as measured by pressure cells is approximately 15% of the estimated vertical overburden pressure. Tweedie et al. (1989) reported the difficulties interpreting the results of the vibrating wire strain gauges due to the substantial amount of temperature change and early age creep of the concrete measured soon after shotcreting. The corrected strain readings were microstrains of 180 and 260. The equivalent liner loads are in the order of 400 KN/m, which is about 65% of overburden pressure. Liner stresses measured by the flat jack tests were 1200 KPa at two tunnel diameters back from the face. For the measured liner thickness of 200 mm, this latter pressure is equivalent to a soil pressure on the liner of about 37% of the overburden.

The three methods of measurement in Section C2 show a relatively wide spread in the liner load estimates. The pressure cell readings have been considered unreliable because the pressure cells are too small and too sensitive to installation details to measure a representative load on the lining as mentioned in the previous chapter. Difficulties in interpreting the vibrating wire strain gauges were referred to above. Therefore, Tweedie et al. (1989) considered the flat jack tests the most direct measure of the liner stress.

It has been suggested that the load share between shotcrete and steel ribs in terms of thrust can be expressed as the ratio between the product of Young's modulus versus the area (EA) of each of these structural elements as explained in the previous chapter. Since the ratio of $(EA)_{rib}$ and $(EA)_{shotcrete}$ in Section C2 is 0.173, the soil pressure on the primary liner is 89 KPa, which is approximately 44% of the estimated vertical overburden pressure.

Tunnelling in Section A1 was closely monitored due to the potential for ground settlement in the sand. Jet-grouted piles were used prior to tunnelling to enhance face stability during the tunnelling operation. The soil pressure on the primary rib from the load cell measurement was 46 KPa. The percentage of overburden pressure carried by the lining is approximately 13%.

4.2.4 Whitemud Creek Tunnel

The Whitemud Creek Tunnel is about 2.1 km long with an excavated diameter of, typically, 6.05 m. The tunnel is an extension of a storm system to an outfall in the North Saskatchewan River. The tunnel was bored through Upper Cretaceous clay shale by two moles. The first mole advanced to the west from the eastern shaft while the second advanced to the east from the western construction shaft.

The primary lining consisted of segmented steel ribs at 1.5 m centers and 5 cm x 20 cm spruce laggings, which were placed outside the ribs in an overlapping pattern. This type of lagging has the advantages of being simple to place and providing protection for the tunnel crews. The plain concrete secondary lining was placed about 4 months after completion of the moling operation (El-Nahhas, 1977, Thomson and El-Nahhas, 1980).

A test section consisted of points established on three successive ribs to monitor diameter and chord changes. Deformation measurements were continued for more than four months until the permanent concrete lining was placed. The elevation of the tunnel invert was established relative to an arbitrary datum to calculate the absolute movements of the ribs. The transfer of load to the rib system appears to be time-dependent, but the transfer was complete in about 3 months. The stresses in the steel ribs were calculated using finite-element analysis. A set of analyses was performed using the deformed shapes of the ribs as an imposed boundary condition for the inside surface of the ribs. The maximum soil pressure on the lining was 140 KPa, which corresponded to 14% of the overburden pressure.

4.2.5 170 th Street Tunnel

This tunnel was constructed to connect the sewer network under a new city subdivision to the existing main sewer interceptor. The mole used was fully shielded and similar to that used in the Northeast Line (Eisenstein and Thomson, 1978). The tunnel was bored through till and had a diameter of 2.56 m. The initial lining consisted of steel ribs at 1.5 m centers with 5 cm x 20 cm timber lagging placed between the webs of successive ribs. The plain concrete permanent lining was placed 10 days after completion

of the moling of the tunnel. The mole was fully shielded, and the rib and lagging system was assembled within the tailpiece of the mole. The mole was advanced by jacking against the web of the steel ribs. When the mole had advanced sufficiently that the rib emerged from the tailpiece, it was expanded outwards using hydraulic jacks (El-Nahhas, 1977, Thomson and El-Nahhas, 1980).

Tunnel instrumentation included horizontal and vertical diameters and level changes of the invert in three successive steel ribs, two pressure cells on the lagging, and lagging deflection points. Measurements were continued for two months until the permanent concrete lining was placed. The deflection of the lagging in the tunnel was measured between two pins set in the face of the lagging. The layout of the lagging test section is shown in Figure 4.4. Only 4 pieces out of 9 pieces of lagging could be used for measurements due to damage to the rest of the lagging. L3 and L5, both in the crown, had a maximum deflection of 3.8 mm, which corresponds to a pressure of 240 KPa, while the deflections of L6 and L8, both in the springline, correspond to a pressure of 112 KPa and 160 KPa respectively. The average soil pressure on the lining was 188 KPa, which is equivalent to 45% of the overburden pressure. However, the loads carried by the steel ribs were not measured.

Two pressure cells, 12 cm in diameter by 1.25 cm thick, were installed in the lagging. The maximum pressures recorded by these pressure cells were 12 KPa and 6 KPa respectively. These pressures correspond to 2.9% and 1.4% of the overburden pressure. The pressure cells were considered to be of little value, and their use was not recommended by Thomson and El-Nahhas (1980).

4.2.6 Experimental Tunnel

In Edmonton, a new tunnel construction method was introduced on an experimental basis using a precast segmented concrete lining in 1978. This was the first time that precast concrete segments were used to line a tunnel in the overconsolidated soils of the Prairies (El-Nahhas, 1980). The tunnel is used as a main storm sewer for a freeway. The tunnel was bored through till and has an excavated diameter of 2.56 m. The mole used in excavating the tunnel was built by Lovat Tunnel Equipment Inc., Ontario.

The tunnel is described in detail by Eisenstein et al. (1979), El-Nahhas (1980), and Eisenstein et al. (1981).

The conventional two-phase support system (Section 1) and the precast segmented lining (Section 2 and 3) were used in two separate parts of the tunnel. The conventional lining system is a two-phase lining: an initial and a final lining. The primary lining is composed of segmented steel ribs at 1.5 m centers and 5 x 20 cm timber lagging placed between the webs of successive ribs. The secondary lining is cast-in-place plain concrete, 20 cm thick. The rib and lagging system was assembled within the shield of the mole. The rib was expanded using hydraulic jacks when it emerged from the shield. Each metre of the precast concrete lining consists of four segments 11 cm thick. Each segment has a longitudinal stress raiser and two lifting recesses. All segments are provided with a light reinforcement mesh located at their centre line to prevent cracking of the concrete. These segments were assembled in the shield behind the mole and were expanded radially to the excavated surface of the soil as soon as the shield advanced beyond them.

In Test Section 1, four weldable vibrating wire strain gauges were installed on the top segment of a steel rib as shown in Figure 4.5. The development of normal forces and bending moments was obtained assuming a linear distribution of strain across the lining thickness. The maximum normal force corresponds to an average soil pressure on the lining of 103 KPa, which is equivalent to 18% of the overburden pressure.

A set of concrete segments was cast for Test Section 2. These segments had two embedded vibrating wire strain gauges, two surface vibrating wire strain gauges, two load cells, two eye-bolts, and eight inspection holes. Details of this test section are shown in Figure 4.6. Stresses at the springline and crown sections were obtained from the measured strains using an average value of Young's modulus of 25,100 MPa. Their ultimate values are 2.9 MPa at the springline and 1.7 MPa at the crown, representing 39% of the overburden pressure. The ultimate liner thrust measured by the load cells was 138 KN/ring, which is equivalent to 21% of the overburden pressure.

In Test Section 3, five sets of special concrete rings were made. One of the load cells in ring No. 4 malfunctioned before the ring expanded. These segments have special recesses to accommodate two vibrating wire load cells to be positioned at one of the

lower longitudinal joints of each ring as shown in Figure 4.7. Each ring has twelve inspection holes and eye-bolts. Ultimate thrusts of 170, 250, 180 and 155 KN/ring were measured in ring No. 1, No. 2, No. 3 and No. 5 respectively. These loads are equivalent to 29, 43, 31 and 27 % of the overburden pressure. El-Nahhas (1980) disregarded the results of ring No. 2 because the insertion of additional steel plates under the load cells caused a significant prestress in this ring. Therefore, excluding the results from ring No. 2, the ultimate load measured in the ring varies between 155 and 180 KN/ring.

4.2.7 The Tunnel on the Banks of North Saskatchewan River

The tunnel is 1670 m long with an excavated diameter of 3.2 m. The tunnel was bored through till (Section 1 and 2) and sand (Section 4) by a Tunnel Boring Machine (TBM). The TBM used in this project was a Lovatt M126-series No 4800 with a maximum of 485 horsepower (Corbett, 1984). The tunnel is used to convey storm water to the North Saskatchewan River.

The primary lining consists of segmented steel ribs at 1.22 m centers and timber lagging. The three steel segments required to make the complete circle were erected within the shield. Steel sets were expanded using radially positioned rams. The expansion spaces were maintained by inserting 10 cm long "I" section steel spacers. The dimension of the lagging was 8 cm x 13 cm in the crown area and 5 cm x 25 cm below springline respectively.

Tunnel instrumentation included the measurements of the deflections at the laggings using a deflectometer and measurements of loads using 16 load cells. The deflectometer was designed such that deflections between two measuring points placed near the ends of the lagging boards and a central reference point could be measured. Steel laggings were used to validate loads obtained from the wood laggings because steel is a much more predictable and consistent material than wood. A steel cross section with a similar flexural rigidity (EI) to that of the wood lagging was used to avoid complications involving stiffness variations.

In Test Section 1, four load cells, 18 wood laggings, and 9 simulated steel laggings were used. Four load cells, 30 calibrated wood laggings, and 9 simulated steel

laggings were used for Test Section 2. Test Section 4 consisted of 4 load cells, 30 calibrated wood laggings and 9 simulated steel laggings. Overburden depth varied near Section 4 because of the presence of a recently constructed embankment. The average lagging pressures in Test Section 1, 2 and 4 were 7.54, 7.03 and 179.43 KPa respectively, which are equivalent to 3 %, 2 % and 62 % of the overburden pressure. The average ring stresses on the steel rib from the load cell measurements in Test Section 1, 2 and 4 were 26.90, 14.20 and 259.85 KPa respectively, which are equivalent to 9 %, 5 % and 74 % of the overburden pressure.

4.3 Existing Design Methods used for Comparison with Field Measurements

There are many existing lining design methods available which were reviewed briefly in chapter 2. Three methods from ring and plate models, i.e., Peck et al.'s, Muir Wood's, and Einstein and Schwartz's, and one from numerically derived methods, i.e., Eisenstein and Negro's, are compared with the actual load measurements in this study. The three methods from ring and plate models were chosen because these methods have been widely used by practical engineers due to their simplicity. The four methods used for comparison are summarized in this section with the emphasis on the lining loads.

Closed-form solutions for the interaction of an elastic medium with a buried cylinder were derived by Burns and Richard (1964) and Hoeg (1968). Peck et al. (1972) modified them to calculate the internal forces and deformation of a deeply buried tunnel lining even though these analyses were originally developed to study the behaviour of culverts. They assumed that the condition of full slippage was more appropriate for the behaviour of soft-ground tunnel liners than that of no slippage due to the existence of high shear stresses at the interface between the liner and the medium. The equations for the thrust are given in Figure 4.8.

A similar attempt to analyze the behaviour of a tunnel lining, using the Airy stress function, was given by Morgan (1961). His analysis was based on the assumption that the lining deformed into an elliptical mode in elastic ground, neglecting shear stresses between extrados and ground. Muir Wood (1975) recognized a basic error in Morgan's paper in terms of the assumption that plane strain leads to plane stress. He corrected and

extended the analysis for bending moments and deformation of the lining. The tangential ground stress was included, but that part of the radial deformation which was due to the tangential stresses was not considered. Since Muir Wood did not give an equation for loads on the lining, Morgan's equations were used for the calculation of thrust considering Muir Wood's correction parameters. The equations for the thrust are given in Figure 4.9. With regard to the application of the design method for the calculation of bending moment, Muir Wood suggested a 50 % reduction of the initial vertical and horizontal ground load due to the stress relaxation process which takes place between tunnelling and erection of the support. In the present study, thrusts on the lining were obtained using 50 % of initial ground loads for comparison with the actual measurements.

Einstein and Schwartz (1979) derived relative stiffness solutions for excavation unloading conditions from the original work of Burns and Richard (1964). The ground mass was considered to be an infinite, elastic, homogeneous, isotropic medium. The tunnel support was regarded as an elastic thick-walled shell in which both flexural and circumferential deformations are considered. They also included the full-slip or no-slip boundary conditions at the ground support interface for their revised relative stiffness solutions. Only full-slip boundary conditions were used for the calculation of lining loads in this study because the results from the two different assumption were almost the same. The equations for the axial thrust are shown in Figure 4.10.

Eisenstein and Negro (1985 and 1990) and Negro (1988) developed a comprehensive design method for shallow tunnels based on ground reaction curves calculated for a variety of ground and geometrical conditions. The design method assumes the ground behaviour to be non-linear and time-independent and the tunnel to be shallow, single and circular and considers factors such as the three-dimensional stress release due to excavation, softening of the ground around the opening and the ground-lining interaction.

Parametric 3-D finite element analyses were performed, assuming a linear elastic material model, to investigate the influence of factors affecting the tunnel convergence. Negro (op. cit.) presented relationships between the radial displacements of the tunnel wall and the location of lining activation behind the tunnel face based on the analyses as

shown in Table 4.1. The variation of the in-situ tangent modulus with depth was considered for the calculation of radial displacements by using calculated in situ principal stresses. Ground reaction curves were obtained by parametric 2-D finite element analyses, assuming a hyperbolic elastic material model for distinct points around the tunnel perimeter and for varying ground and geometric conditions. The results of the generalization process for ground reaction curves were presented through equations and charts. Stress reduction factors can be found combining the radial displacements calculated using Table 4.1 and these ground reaction curves.

Thrust forces on the lining were obtained using Hartmann's solution (Hartmann, 1970). The general procedure for using the method is shown in Figure 4.11 with the equations for the thrust using Hartmann's solution. The effects of the delayed lining installation, represented by the stress relaxation and ground stiffness degradation, were accounted for through the use of a reduced unit weight of the soil and a reduced ground stiffness obtained using calculation sheets. A full range of charts and diagrams facilitating the use of this method in a variety of geometric and geotechnical conditions was presented by Negro (1988).

4.4 Comparison of Field Measurements with the Existing Theories

Soil pressures on tunnel linings can be expressed either in terms of the percentage of overburden pressure or in the form of:

$$P=n\gamma D$$

where

P = the applied pressure

n = a dimensionless factor

γ = unit weight of soil

D = tunnel diameter.

A summary of the loads carried by the primary support system on Edmonton tunnels is shown in Table 4.2. The pressure carried by the primary lining ranged from 5% to 79% of the overburden pressure with an average of 33%. The dimensionless factor (n) is plotted as a function of the ratio of springline depth to tunnel diameter in Figure 4.12. The figure

indicates that "n" increases as the ratio of tunnel depth to tunnel diameter increases. The dimensionless factor, n, varies from 0.21 to 4.08, with an average of 1.65.

Four different design methods, those of Peck et al., Muir Wood, Einstein and Schwartz, and Eisenstein and Negro, were compared with the actual load measurements in this study. In all applications of the methods, no attempts were made to best fit the observed lining performances. These tests were not back-analyses of case histories, as it was assumed that all parameters and variables governing the tunnel response would represent the most probable conditions found in each case. For supports, Young's modulus of 200000 MPa, 25100 MPa, and 10000 MPa were used for rib and lagging, segmented lining, and shotcretes respectively. For the ground, Young's modulus of 150 MPa, 100 MPa, and 250 MPa were used for till, sand, and claystone respectively.

The measured and calculated percentage of overburden pressures and dimensionless factors (n) for the primary lining in Edmonton tunnels are shown in Figures 4.13 and 4.14 respectively. The figures clearly show that Peck's method overestimates the lining load consistently except in the Northeast Line (A).

Einstein and Schwartz's method also overestimates the lining load except in two tunnels, Northeast Line (A) and Section 4 on the Banks of North Saskatchewan River (M). Muir Wood suggested taking only 50 % of the overburden pressure, taking into account some pre-decompression of the ground around the tunnel opening before the lining was placed. Muir Wood's method still overestimates the liner load by an average of 37 % but underestimates in Northeast Line (A) and Section 4 on the Banks of North Saskatchewan River (M).

Eisenstein and Negro's method gives the closest estimates, an average of 28 % more than the actual lining loads measured. However, this method underestimates the lining loads in 5 tunnels. The following section describes the possible causes of these discrepancies between the measurements and predictions.

4.5 Conclusions versus Existing Theories

Lining loads calculated from four different design methods were compared with actual load measurements in the previous section. Peck's method consistently gave much

higher lining loads than those from measurements as expected. This can be explained by using a radial displacement curve along the longitudinal direction of a tunnel as shown in Figure 4.15. If the lining is installed in contact with the ground at point B, the lining will resist only U_a . In other words, the lining does not have to support full overburden pressure because radial displacements cause a certain amount of stress reduction around a tunnel. However, lining loads from Peck's method was calculated based on the assumption of an overpressure loading condition, which implies that the tunnel opening has been excavated and supported even before the full overburden pressure is applied. This loading condition is suitable for backfilled culverts but not tunnels. Therefore, Peck's method consistently overestimates the lining loads.

Einstein and Schwartz's method also generally overestimated the lining loads even though the method gave a better approximation than Peck's method. Their method assumes an excavation unloading condition, which indicates that the tunnel opening is excavated and supported after the full overburden pressure is applied. Therefore, stress redistribution induced by the opening was considered in their method. However, the opening is simultaneously excavated and supported in one step. In other words, lining loads from Einstein and Schwartz's method were calculated based on the full overburden pressure without consideration of the stress reduction occurring prior to lining installation.

Muir Wood suggested taking only 50 % of the overburden pressure, taking into consideration some stress reduction of the ground around a tunnel opening before the lining was placed. Muir Wood's method gave a better approximation than the previous two methods, with an average of 37 % overestimation of the lining load. Actually, the stress reduction factor of 50 % worked reasonably well for soils in Edmonton but can be misleading for certain geologic materials. Various stress reduction factors have been suggested by various authors, as will be discussed in detail later in this chapter.

The common problems with the above three methods are that they make assumptions about only concerning linear elastic ground, and there is uncertainty about the determination of the stress reduction factor. Eisenstein and Negro's method not only considered non-linear ground behaviour but also was capable of calculating the stress

reduction factor as mentioned in the previous section. Therefore, the method gave the closest estimates of the actual lining loads.

Lining loads in several tunnels could not be predicted reliably, possibly due to the lack of accuracy of the field measurements themselves. The lining loads measured in the Northeast Line (A) were higher than those predicted, as shown in Figure 4.13. Eisenstein et al. (1977) considered the strain gauge readings from Rib C as representative after examining all data in three ribs. This was because Ribs A and B showed the influence of the longitudinal load due to the reaction of the mole, a condition which was not obvious in Rib C. The lining loads were measured from August 27 to October 22 for almost 2 months. During the period between September 2 and 29, the compressive forces in all of the ribs were decreasing. The causes of the reduction of loads were not clear. The authors suggested calculating the load by multiplying the values obtained, excluding the data obtained during the period between September 2 and 29, by 1.15. This multiplier is the average increment for segments C1 and C3 for the period September 2-29, and these two segments were considered to be the most reliable by the authors based on an examination of individual strain gauge data. The lining load in Section C was considered to be higher than was actually measured due to the use of multiplier. However, the method of data analysis could not be justified because the causes of the load reduction during the period were not clear. If the load reduction during the period September 2-29 is included, the average soil on rib C is 134 KPa, which is equivalent to 63 % of overburden. In either case, the load on the lining is still higher than those of other tunnels. This could be related to the relatively low ratio of tunnel depth to tunnel diameter, which is only 1.7.

The lining loads of Section A1 of SLRT-Phase II (E) were much less than those predicted. Since the tunnel was driven through postglacial sand, jet-grouted piles were used prior to tunnelling to enhance face stability during the tunnelling operation. The low lining loads may be a result of the fillcreting operations used in the tunnel. In other words, higher soil strength should have been used for the calculation of the lining loads considering the use of jet-grouted piles.

The Whitemud Creek tunnel (F) showed much lower lining loads than those predicted. The tunnel was excavated through clay shale using unshielded drilling

machines, whereas the other tunnels were driven through till or sand using shielded moles. The high strength of the clay shale allowed more arching of soil pressure around the tunnel and thus lower lining loads. Furthermore, the use of unshielded drilling machines may have caused more stress releases on the ground than those of other tunnels, a condition which resulted in lower lining loads.

The load measured in the Banks of the North Saskatchewan River tunnel varied from less than 10 % overburden in Sections 1 (K) and 2 (L) to 74 % overburden in Section 4 (M). As Corbett (1984) pointed out, the lining loads measured from the load cells installed in Sections 1 and 2 proved to be less than 10 % of the design load, which might have caused errors in measurements. The original cross section was therefore halved in area to increase the sensitivity of the load cells in Section 4. The lining loads in Section 4 were higher than those from Muir Wood's and Eisenstein and Negro's methods. The high lining loads could be related to poor ground conditions, i.e. sand, coupled with increased overburden at the section due to the recent construction of an embankment on the ground surface. In fact, observed settlement in Section 4 was much greater than those of other sections due to poor ground conditions. The load increase caused by an embankment simulates the overpressure loading condition, which was assumed in Peck's method. This may be the reason that Peck's method gave a better approximation of lining loads for Section 4 than for other tunnels.

Eisenstein and Negro's method gave the closest estimates of actual lining loads as shown in Figures 4.13 and 4.14. However, this method underestimated the lining loads in 5 tunnels, i.e. tunnels A, D, G, I and M, even though the differences were not that great for tunnels D and I. Negro (1988) provided a full range of charts and diagrams facilitating the usage of this method for the most typical ranges of in situ stress ratios ($K_0=0.6$ to 1.0), cover to diameter ratios ($Z/D=1.5$ to 6), strength parameters ($\phi=0$ to 40° and $C_u/\gamma D=0.3125$ to 2.5) and distance from face to the location of support activation to diameter ratios ($X/D=0$ to 2). In the case of tunnels A and D, cover to diameter ratios are 1.17 and 1.04 respectively. Therefore, the ratio of 1.5 was used for the calculation of the lining loads. The increase of the ratio from 1.04 to 1.5 for the calculation of lining loads in tunnel D could increase the stiffness of soil (E_s) and consequently decrease the load

calculated. The possible causes of the load discrepancy between measurement and calculation for tunnels A and M were described already. In the case of tunnels G and I, cover to diameter ratios are 7.31 and 10.05 respectively. The ratio of 6 was used for the calculation of the loads for both tunnels. The small load discrepancy between measurement and calculation may be caused by the fact that the method was mainly developed for shallow tunnels. In other words, the method should be used carefully for tunnels which have different ranges of ratios and material parameters than those given above because the method was developed based on the parametric finite element analyses within these ranges.

Because most of the available design methods did not consider non-linear ground behaviour and stress reduction factors, Schwartz and Einstein (1980) suggested using correction factors to take into account these problems. The proposed method is described in detail and applied to the tunnels in Edmonton in the following section. The main purpose of this exercise is to verify the applicability of the method, especially for the tunnels in Edmonton.

4.6 Prediction of Lining Loads using Correction Factors

4.6.1 Effect of Delay in Liner Placement

Einstein and Schwartz (1979) presented closed form solutions for the estimation of loads on the liner, solutions which depend mainly on the relative support stiffness and in-situ stress ratio. The solutions were described in the previous section. Schwartz and Einstein (1980; a and b) included the decrease of support loads with the delay of the support construction behind the face and the increase of support loads due to development of ground yielding with the original closed form solutions in the form of a support delay factor λ_d and a yield factor λ_y respectively. The support delay factor can be expressed as:

$$\frac{P_s'}{P_s} = \frac{U_o^e - U_i}{U_o^e} = \lambda_d. \quad (4.1)$$

P_s is the support load obtained from the plane strain relative stiffness solution and P_s' is the reduced support load due to the effect of support delay as shown in Figure 4.16. U_o^e

and U_i are also shown in the figure. The support delay factor was obtained from axisymmetric finite element analyses for $K_o=1$ in-situ conditions and from plane strain finite element analyses by using the core modulus reduction scheme for $K_o \neq 1$ conditions respectively. These studies all assumed linearly elastic behaviour for the ground. The delay length L_d is defined as the distance between the tunnel face and the mid-point of the leading support section. Based on the results from the axisymmetric and plane strain parametric studies, λ_d depended mainly on the support delay length, only slightly on the relative support stiffness and not at all on the lateral in-situ stress ratio for tunnels in elastic ground masses. Figure 4.17 shows the relationship between λ_d and the normalized support delay length determined from the results of the axisymmetric finite element analyses using values for L_d/R of 0.25, 0.75, and 1.25. The relationship can be expressed as follows:

$$\lambda_d = 0.98 - 0.57(L_d/R). \quad (4.2)$$

Schwartz and Einstein suggested not using Eq. 4.2 for cases in which L_d/R is less than 0.15 or more than about 1.5.

The equilibrium support pressure in a yielding ground should satisfy the equation:

$$f_g(P_s) - f_s(P_s) - f_d(\lambda_d) = 0. \quad (4.3)$$

The terms in the equation are shown in Figure 4.16. The ground characteristic curve, $f_g(P_s)$, is the functional relationship between the radial ground displacement and the internal pressure for a tunnel in a yielding ground under plane strain conditions. The value can be obtained from any of the standard axisymmetric plasticity solutions for the tunnelling problem (e.g., Deere et al., 1969). Schwartz and Einstein (op. cit.) found the value using a Mohr-Coulomb yield criterion with zero total volume change in the yield zone. $f_s(P_s)$ is the support characteristic curve, which is expressed as follows for a linearly elastic support:

$$f_s(P_s) = \frac{P_s R^2 (1 - \nu_s^2)}{E_s A_s}. \quad (4.4)$$

$f_d(\lambda_d)$ is the offset of the support characteristic curve equivalent to the support delay, which can be expressed as:

$$f_d(\lambda_d) = \frac{PR(1+\nu)}{E}(1-\lambda_d). \quad (4.5)$$

If there is no support delay, λ_d is 1 and $f_d(\lambda_d)$ equals 0.

The yield factor λ_y is mainly a function of the strength of the ground and is indirectly dependent on the support delay and the relative support stiffness. To calculate λ_y , Eq. 4.3 must be solved twice. First, P_s^* is calculated for the yielding ground case using the correct ground strength properties. Second, P_s' is obtained for the elastic case using artificially high ground strength properties. For example, unconfined compressive strength can be assumed to be twice that of in-situ ground stress at the tunnel centerline to calculate P_s' . The ground yield factor λ_y is then equal to the ratio P_s^* / P_s' . The final thrust T can be expressed as:

$$T = \lambda_d \lambda_y T_1 \quad (4.6)$$

in which T_1 is the thrust calculated from the original closed form solutions. The yield factor λ_y should be less than about 2 for values of an in-situ stress ratio much different from unity according to the parameter study of finite element analyses. The in-situ stress ratio has to be close to unity in order to apply the method for a very high value of λ_y .

4.6.2 Comparison with Case Study Data

Schwartz and Einstein (1980; a) applied the procedure to five tunnel projects in order to verify the accuracy of the proposed method. These case histories are described briefly in this section.

The Garrison Dam outlet tunnels include eight 370 m long circular tunnels ranging from 7.9 m to 10.7 m in diameter, which were excavated by using a conventional full-face drill and blast technique through the heavily consolidated clay shale. The tunnels lie at depths of 30-55 m below the original ground surface. Blocked steel sets and lagging with crown bars were used as temporary support, followed by a cast-in-place concrete liner up to 0.9 m thick. Strains in the steel sets were obtained using Whittemore strain gauges at the crown, invert and two springlines of the tunnels. The support loads were measured approximately 2 to 3 months after excavation. Lane (1960) and Burke (1960) described the tunnels in detail.

The Kielder Experimental tunnel was constructed to investigate the performance of various support systems in the Carboniferous rocks. The test section considered here was excavated by a road-header type excavator through strongly jointed mudstone and supported by a 12.7 mm thick and 0.7 m long segmented steel liner. The gap between the liner and the ground averaged 108 mm in thickness and was filled with grout before the next round of advance. The 3.3 m diameter experimental tunnel lies at depths ranging from 75 to 100 m. A group of three rings was instrumented with twin-wire vibrating-wire strain gauges. These gauges were located to obtain the circumferential thrusts at eight different locations around the periphery of each ring. The average support load measured at the middle ring after 8 months was taken for comparison with the predicted support load. The project was well documented by Ward et al. (1976) and Ward (1978).

The Thunder Bay Sewer tunnel was constructed using a full faced tunnel boring machine with a shield and supported by unbolted precast concrete segmented rings, which are 1 m long and 0.11 m thick. The machine was advanced after the support was erected within the tailpiece of the TBM, and a clay grout was injected into the 4.5 cm thick tailpiece void. The 2.38 m diameter tunnel lies at a depth of about 10.5 m below the ground surface in silty clay deposits. The radial support pressure was measured using a set of 12 total pressure cells. These cells were all located on one ring. The average pressure acting on the liner during the first month after construction was used for comparison with the predicted support load. Belshaw and Palmer (1978) presented a detailed description of the tunnelling conditions and the instrumentation.

The Tyne Sewer tunnel was hand excavated without a shield. The bolted precast concrete segments, which were 0.61 m long, were erected tight up to the tunnel face because of the absence of a shield. The 3.2 m diameter tunnel lies at a depth of 12.1 m below the ground surface in stiff stony clay and laminated clay. The radial support pressure was obtained using a set of 6 total pressure cells on each of the two instrumented rings. The radial pressure on the lining increased rapidly over time, reaching a stable maximum value 7-8 days after erection. The tunnelling conditions and the measurement program were given in detail by Attewell and El-Naga (1977).

The Victoria Line tunnels were machine-excavated using a full-face digger shield through London clay. The tunnels lie at depths of about 26.1 m with a 4.0 m diameter for the cast iron section and 27.9 m with a 4.28 m diameter for the precast concrete length. Tunnel linings were expanded as soon as they cleared the tail of the shield. The support segments were unbolted and 0.61 m long in both cases. The loads on the lining in the two tunnel sections were measured using sets of vibrating wire strain gauges spaced equally around the circumference. A significant increase in the tunnel support loads was observed over time due to swelling of the London clay upon unloading. The short-term loads up to a few weeks after construction were compared with the predicted support loads. Ward and Thomas (1965) gave details on the measured support loads.

The above method was compared with field measurements of the case histories and gave errors in the predicted support loads that ranged between the extremes of -68 % (underestimated) and 62 % (conservative), with an average error of 32 %, as shown in Table 4.3. Schwartz and Einstein (1980) reported several problems when applying the method suggested above. The support delay length L_d for the Kielder Experimental tunnel was 4.0 m. Since the tunnel radius was 1.65 m, the normalized delay length L_d/R of 2.4 exceeded the upper limits of about 1.5. This means that if the ground were elastic, all of the radial displacements would take place before the support was installed and the support loads would be zero. In this case, the yield factor λ_y does not have any meaning according to Eq. 4.6, and the above method cannot be used to predict the support load. The authors found the upper bound support load from the equilibrium point between the convergence and confinement curves assuming that the support curve offset is U_o^c . The support load was calculated from the combination of the relative stiffness solution and Eq. 4.3.

Another problem was to calculate the support delay length L_d for the tunnel constructed by a TBM with a shield such as that of the Thunder Bay Sewer tunnel. The support delay length was taken from the tail of the rigid TBM rather than from the face of the tunnel to the midpoint of the second ring behind the TBM because the tail void could be grouted after clearing the TBM tailpiece. However, the measured settlements indicated that the grouting procedure was not effectively filling the tail void between the support

and the ground. Therefore, the pre-support ground movements, U_o' , were added to the calculation of support delay. Eq. 4.2 for the support delay correction factor could be modified as:

$$\lambda_d = 0.98 - 0.57 (L_d / R) - U_o' / U_o^c. \quad 0 \leq \lambda_d \leq 1 \quad (4.7)$$

Since the Thunder Bay tunnel was very similar to the Kielder Experimental tunnel in that the round length is large compared to the tunnel diameter, the ratio L_d/R exceeded the upper limits of λ_d . This problem became even worse when a U_o' of 4.5 cm was added. Therefore, the above method could not be used, and only an upper bound estimate for the support load could be determined using the method mentioned for the Kielder tunnel. In the case of the Victoria Line tunnels, two components of U_o' were considered. The first components were the ground movement behind the cutting bead at the leading edge of the digger shield. The approximate values of this void were between 1.27 and 1.59 cm. The second components of U_o' were considered as negative displacements caused by the expansion of the lining during erection. The authors presented equations for the negative displacement due to jacking pressure. The second components of U_o' were subtracted from the first components to get the total values for U_o' .

4.6.3 Discussion of Results

Schwartz and Einstein (1980) compared the actual and simulated tunnelling sequences as shown in Figure 4.18. Excavation and support occur at one step in a finite element analysis even though the excavation and support construction do not take place simultaneously in the actual tunnelling sequence. Therefore, the authors considered a delay length L_d for actual tunnelling sequences as the delay length L_d in the finite element analyses. This is true if the liner is installed before excavation in the finite element sequence. Hutchinson (1982) observed that L_d' , the distance from the old face before excavation to the centre of the closest liner segment, should be considered as the delay length for the actual tunnelling sequences based on the axisymmetric finite element analyses and case histories. The author suggested that the line for Eq. 4.2 in Figure 4.17 should be translated as shown with the new equation as follows:

$$\lambda_d = 0.70 - 0.57(L_d'/R) . \quad (4.8)$$

Hutchinson suggested using Eq. 4.8 with a delay length L_d' based on the assumption that the excavation and lining installation might not be done at the same time in the finite element analyses of Schwartz and Einstein. However, if Hutchinson's assumption is valid, Eq. 4.2 should have been used with L_d' .

There is an actual reason that Eq. 4.8 should be used with L_d' rather than applying Eq. 4.2 with L_d , which was not recognized by Hutchinson. Hutchinson performed axisymmetric finite element analyses and compared the results with those from the analyses of Schwartz and Einstein as shown in Figure 4.17. The results are plotted as LC1 and LC1'. However, the comparison was not done correctly for the point, LC1', obtained from the delay length of L_d because the round length and the length of support that Hutchinson adopted for the analyses were 1R.

The differences in two tunnelling sequences applied for the finite element analyses are presented in Figure 4.19. It is a well-known fact that the load distribution along one segment of lining is not uniform. The load at the leading edge of the lining is higher than that of the following edge because the stress near the excavation front is less released (See Figure 4.15). Therefore, the load should be taken at the centre of the liner segment to get the average value. A L_d of 1.5R was used for both tunnelling sequences in the finite element analyses as shown in Figure 4.19. However, the distance L_d' , which is from the old face before excavation to the centre of the liner segment to be installed in the next round, as shown in Figure 4.19, actually determines the amount of stress release before liner installation. After one round of simultaneous excavation and support for both cases, the distance L_d' for Hutchinson's case is 0.5R, which is shorter than the 1R of Schwartz and Einstein's case. This is the reason that the load from Hutchinson's analyses gave a higher value than that of Schwartz and Einstein's for the case compared with a L_d such as LC1' as shown in Figure 4.17. In other words, a different λ_d can be obtained for the same delay length of L_d depending on the round length if Eq. 4.2 is applied with a L_d as suggested by Schwartz and Einstein, which is a major problem with the method.

λ_d calculated from Eq. 4.2 and Eq. 4.8 using L_d and L_d' respectively are the same only if a round length of 0.5R is used for a certain tunnelling sequence because the round

length or the length of the support ring used for the finite element analyses of Schwarz and Einstein was $0.5R$. This is the reason that Eq. 4.8 can be obtained if $(L_d' + 0.5R)$ is substituted for L_d in Eq. 4.2. The problem can be eliminated if Eq. 4.8 is used with L_d' because the distance actually determines the load on the lining in the finite element analyses and in the actual tunnelling sequence. In other words, the same lining loads can always be obtained for the same delay length of L_d' regardless of the round length. Therefore, Eq. 4.8, which is obtained from finite element analyses using the distance L_d' , should be applied with the delay length L_d' from the actual tunnelling sequence. This is the reason that LC1 matches well with the line from Eq. 4.8 along with a L_d' of $0.5R$, while LC1' does not agree with the line from Eq. 4.2 combined with L_d of $1.5R$. Eq. 4.8 is not applicable for values of L_d'/R greater than about 1.

4.6.4 Recalculation of the Lining Loads

Lining loads of case histories calculated by Schwartz and Einstein were recalculated using Eq. 4.8 and delay length L_d' as shown in Table 4.4. There is another advantage to using L_d' over L_d . A group of three rings, each ring being 0.7 m long, were installed at a distance of 0.3 m from the leading edge of the lining to the face in the Kielder Experimental tunnel. The face was then advanced 2.7 m after the rings were butt-welded together and grouted. Therefore, the method suggested by Schwartz and Einstein could not be used for the tunnel because the delay length L_d was 4 m with the normalized delay length L_d/R of 2.4, which exceeded the upper limits of L_d/R of about 1.5. The long delay length L_d/R was caused by the long round length of $1.64R$. However, the method could be applied without any problem if L_d' is used since L_d' was 1.3 m with a L_d'/R of 0.79, which is less than the upper limits of L_d'/R of about 1.

Another modification is applied during the recalculation of the lining loads due to the existence of the pre-support ground movements, U_o' . Eq. 4.7 should be used to calculate λ_d for the Thunder Bay tunnel because of U_o' . However, a U_o' of 4.5 cm exceeded the elastic radial displacement of the unlined tunnel, which is about 2.4 cm. Schwartz and Einstein suggested finding an upper bound support load from the equilibrium point between the convergence and confinement curves assuming that the

support curve offset is U_o^c . The support load was calculated from the combination of the relative stiffness solution and Eq. 4.3. However, the predicted load gave only an upper bound support load. Therefore, λ_d of 0.2 is arbitrarily assumed for the calculation of the load based on the finite element analyses of Hutchinson (1982), which showed that some thrust would be obtained even at large values of support delay in an elastic analysis.

An additional difficulty occurred using the method due to the consideration of negative displacement caused by the expansion of the lining during erection for the case of the Victoria Line tunnels. The authors presented equations for the negative displacement due to jacking pressure assuming that the liner was fully in contact with the soil before the liner was expanded. However, many field measurements in other tunnels showed that the liner might not be fully contacted even after the expansion of the liner (e.g. Eisenstein et al., 1979). Therefore, U_o' is assumed to be one half of the void between the soil and the cutting bead at the leading edge of the digger shield considering the expansion of the liner. Table 4.4 shows that the results give errors in the predicted support loads ranging between the extremes of -52 % (underestimated) and 59 % (conservative), with an average error of 24 %, which is about a 10 % better approximation than that of Schwartz and Einstein.

4.6.5 Application of the Method to Edmonton Tunnels

Schwartz and Einstein's method was applied to Edmonton tunnels to verify the accuracy of the proposed method. One major problem arose when applying the method to Edmonton tunnels. If support delay lengths are taken from the face of the tunnels, all of the normalized delay lengths, L_d/R or L_d'/R , exceeded the upper limits of 1.5 or 1. On the other hand, if support delay lengths are taken from the tail of the TBM with consideration of U_o' due to the existence of voids between the soil and the mole, the normalized delay lengths are within the limits. However, the voids often exceeded U_o^c , which made λ_d meaningless according to Eq. 4.7. This indicates that, if the ground were elastic, all of the radial ground displacements would occur before the support was installed and the lining loads would therefore be zero. The yield factor, λ_y , is no longer defined if λ_d equals to

zero according to Eq. 4.6. Therefore, upper bound lining loads were calculated for Edmonton tunnels using the procedure suggested by the authors.

Schwartz and Einstein (op. cit.) found the upper bound support load from the equilibrium point between the convergence and confinement curves assuming that the support curve offset is U_o^c as shown in Figure 4.20. In other words, the equilibrium pressure P_s^* is considered as a lining load of a certain tunnel because the equilibrium pressure P_s^{\wedge} cannot be determined analytically. P_s^* is an upper bound for P_s^{\wedge} . Eq. 4.3 can still be used to directly calculate P_s^* for $K=1$ conditions, assuming λ_d equals to zero. If the in-situ stress ratio is other than 1, the following equation can be used:

$$[T^*]_{K \neq 1} = [T^*]_{K=1} \frac{[T]_{K \neq 1}}{[T]_{K=1}} \quad (4.9)$$

The values $[T]_{K \neq 1}$ and $[T]_{K=1}$ can be calculated directly from the closed form solutions presented by Einstein and Schwartz (1979), and $[T^*]_{K=1}$, which equals $P_s^* R$, can be obtained from Eq. 4.3. The detailed derivation of Eq. 4.9 was given by the authors.

The upper bound lining loads calculated for Edmonton tunnels using the procedure described above are shown in Figure 4.21. Most of lining loads were underestimated even though the method was supposed to give upper bound lining loads. A possible cause of the underestimation of lining loads may be related to the fact that the actual ground displacements can be smaller than U_o^c even though there is a bigger gap between the soil and TBM than U_o^c . In other words, the method has a major problem due to the difficulties for estimating U_o^c . If the ground displacements were smaller than U_o^c , P_s^* would have been higher than those calculated values according to Figure 4.20.

A λ_d of 0.2 is arbitrarily assumed to calculate lining loads based on Eq. 4.6 as done for the Thunder Bay tunnel. The results are shown in Figure 4.22. The lining loads were slightly better approximated than in the previous case but still underestimated in eight tunnels. The most probable cause could be again related to the improper estimation of λ_d because the lining loads are a direct function of λ_d according to Eq. 4.6. Furthermore, λ_y is also dependent on the λ_d .

In conclusion, the proposed method of Schwartz and Einstein gave reasonable results for tunnels with short delay lengths. However, the method cannot be used reliably

for tunnels either with long delay lengths or with voids between the soil and TBM due to the difficulties in finding U_o' and therefore λ_d . Since most of the tunnels in Edmonton, especially those studied in this chapter, were built using TBM with the clearance voids, Schwartz and Einstein's method is not suitable for estimating lining loads for these tunnels.

4.7 Application of Stress Reduction Factors to the Existing Design Methods

Negro (1988) developed a procedure to estimate the amount of tunnel closure at the section where the support is activated from three-dimensional finite element parametric analyses as mentioned in the previous section. Part of these displacements occur ahead of the tunnel face, followed by another part between the face and the point of activation of the support. An estimation of the distance (X) from the face to the location of support activation enables the dimensionless radial displacements (U) for the crown, springline and floor to be established using Table 4.1. Stress reduction factors can be found combining the radial displacements calculated using the table and ground reaction curves obtained by parametric 2-D finite element analyses. Estimates of stress reduction factors are discussed in detail in Sec. 7.2.

Eisenstein and Negro (1985) suggested that the stress reduction factor found using their method could be used coupled with any analytical solution for calculation of thrust forces and bending moments. For example, Muir Wood presented a closed form solution, recommending a 50 % reduction of the full overburden pressures to account for face and heading effects occurring prior to lining installation. The 50 % stress reduction is an arbitrary value, and various suggestions have been given by others, e.g. about a 33 % stress reduction as suggested by Panet (1973). Einstein and Schwartz (1980) also suggested that the stress reduction factor could be between 15 % and 100 % according to simple analytical and numerical techniques and case study data.

The results from Eisenstein and Negro's method showed that the amount of stress release at lining activation for Edmonton tunnels ranged from 43 % to 66 %, with an average of 59 %. This value compares favorably with Muir Wood's arbitrary reduction by 50 % of the overburden stresses suggested for lining design. This is probably because the

soil in Edmonton is generally strong enough for an excavation without special measures. In other words, the soil in Edmonton is stiff enough to stand unsupported without failure during the time needed for a lining installation in a typical tunnelling procedure. These findings indicate that, for a quick lining-ground interaction analysis, it may be adequate to assume a 50 % reduction for the ground overburden stresses, provided the tunnels are excavated in geologically stable ground or with good ground control.

Instead of applying this rather arbitrary reduction, the reduced unit weight of soil found from Eisenstein and Negro's method was used for each tunnel to reevaluate the lining load from the analytical methods. The results are shown in Figures 4.23 and 4.24. The results encourage the use of the reduced unit weight considering that the stress release occurred before lining installation. The lining loads calculated based on Muir Wood's method using the reduced unit weight of soil found from Eisenstein and Negro's method were compared with those calculated using Muir Wood's arbitrary reduction by 50 % of the overburden stresses as shown in Figure 4.25. The figures clearly show that the actual lining loads were better approximated by using the reduced unit weight. However, the method might work for the tunnels in Edmonton because the soil is stiff but might not work for the tunnels in soft clays due to the development of plastic zones. This may be the reason that the results were not satisfactory for Tunnel M, which had poor ground conditions. In other words, the stress reduction factors can be used reliably only for stable ground due to the assumption of linear elastic ground and an unlined opening for the findings of these values. The use of stress reduction factors, coupled with other analytical solutions, for the prediction of lining loads is further discussed in detail in Chapter 7.

4.8 Summary and Conclusions

The validity of the existing design methods was reviewed in this chapter by comparing the results from the methods with the field measurements obtained from several tunnels in Edmonton. A design method for the prediction of lining loads should include the decrease of lining loads due to the stress release before lining installation and the increase of lining loads due to development of ground yielding. However, Peck et al.

and Einstein and Schwartz did not include these two factors in their design methods. Only Muir Wood included the stress reduction factor, but the stress reduction of 50 % was rather arbitrary.

Eisenstein and Negro's method considered the stress reduction factor more reliably. The yield factor was also considered in their method by using a hyperbolic elastic material model. Therefore, the method gave the closest estimates of actual lining loads. However, the method had some limitations for its full use in terms of ranges of in-situ stress ratios, cover to diameter ratios, and distance from face to the location of support activation to diameter ratios. Furthermore, the method is valid only for stable ground due to the assumption of linear elastic ground and an unlined opening for the determination of the stress release factor. Therefore, the method should be used carefully if a tunnel has either cover to diameter ratios other than those in the range covered by Negro such as tunnels A and G or poor ground conditions such as Tunnel M.

Schwartz and Einstein included both factors in their original closed form solutions in the form of a support delay factor λ_d and a yield factor λ_y respectively. The proposed method of Schwartz and Einstein gave reasonable results for tunnels with short delay lengths. However, the method cannot be used reliably for tunnels either with long delay lengths or with voids between the soil and TBM due to the difficulties finding U_o' and therefore λ_d .

The stress reduction factor found using Eisenstein and Negro's method can be used coupled with any analytical solution for calculation of lining loads. However, the stress reduction factor obtained using their method is only valid for stable ground. Negro (1988) observed that the proposed method for the prediction of stress reduction factors gave reasonable results in tunnels built using the NATM regardless of the soil type provided the face is stable. For TBM and shield tunnels, to use the method reliably according to case studies done by Negro, the support should be activated at distances from the face smaller than 1 to 1.2 D, especially in soft soils.

The validity of the existing design methods has been reviewed in this chapter by comparing the loads calculated using the methods with the field measurements obtained from several tunnels in Edmonton and other areas. In conclusion, none of the above

methods are totally satisfactory for the estimation of lining loads even though certain methods can give reasonable results under specific conditions. Therefore, there is some room for improvement in the prediction of lining loads. An improved design method will be proposed in Chapter 7 based on the review of existing design methods in this chapter and performance of numerical analyses in the following two chapters.

Table 4.1 Calculation of Dimensionless Radial Displacements, U, based on the Results of Parametric 3-D Finite Element Analyses (Modified after Negro, 1988)

| X / D | Crown | | Springline | | Floor | |
|-------|-------|-------|------------|-------|-------|-------|
| | a | b | a | b | a | b |
| 0 | 0.375 | 0.147 | 0.210 | 0.033 | 0.226 | 0.137 |
| 0.25 | 0.783 | 0.380 | 0.390 | 0.014 | 0.575 | 0.350 |
| 0.50 | 0.923 | 0.453 | 0.460 | 0.016 | 0.681 | 0.433 |
| 1.00 | 1.059 | 0.537 | 0.560 | 0.048 | 0.774 | 0.520 |
| 2.00 | 1.144 | 0.590 | 0.590 | 0.054 | 0.788 | 0.530 |

Notes: - Crown and Floor: $U = a - bK$

- Springline: $U = a - b / K$

- X = Distance from the face to the location of support activation

- D = Tunnel Diameter

- U = Dimensionless displacements = $(U_r * E_{ti}) / (D * \sigma_{ro})$

- K = In-situ stress ratio

- U_r = Radial displacement of tunnel wall

- E_{ti} = In-situ tangent modulus of soil

- σ_{ro} = In -situ radial stress

Table 4.2 Primary Liner Loads in Edmonton Tunnels

| Tunnel | Method | Ground | Depth* (H) | Dia.* (D) | H/D | Pv (KPa) | PL (KPa) | PL/Pv x 100 (%) | h (m) | n=h/D | Method of Measurements |
|--------------------------------|--------|------------|---------------|--------------|------|-------------|-------------|--------------------|-----------|-----------|---------------------------|
| A. Northeast Line | TBM | Till | 10.2 | 6.1 | 1.7 | 214 | 169 | 79 | 8.05 | 1.3 | (e) |
| B. LRT-South Extension | TBM | Till | 11.8 | 6.2 | 1.9 | 248 | 52-64 | 21-26 | 2.48-3.07 | 0.40-0.49 | (a) |
| SLRT-Phase II | | | | | | | | | | | |
| C. (Section B2) | TBM | Till | 15.8 | 6.3 | 2.5 | 332 | 105 | 32 | 5.0 | 0.79 | (a) |
| D. (Section C2) | SEM | Till | 9.7 | 6.3 | 1.5 | 204 | 89.37 | 44 | 4.3 | 0.68 | (b) |
| E. (Section A1) | TBM | Sand | 17.2 | 6.3 | 2.7 | 361 | 46 | 13 | 2.19 | 0.35 | (a) |
| F. Whitemud Creek | TBM | Clay Shale | 47.2 | 6.05 | 7.8 | 991 | 140 | 14 | 6.67 | 1.10 | (c) |
| G. 170th Street | TBM | Till | 20 | 2.56 | 7.8 | 420 | 188 | 45 | 8.95 | 3.50 | (d) |
| Experimental Tunnel | | | | | | | | | | | |
| H. (Section 1) | TBM | Till | 27 | 2.56 | 10.5 | 567 | 103 | 18 | 4.9 | 1.92 | (e) |
| I. (Section 2) | TBM | Till | 27 | 2.56 | 10.5 | 567 | 219.6 | 39 | 10.46 | 4.08 | (f) |
| J. (Section 3) | TBM | Till | 24 | 2.56 | 9.4 | 504 | 135-156 | 27-31 | 6.40-7.44 | 2.50-2.9 | (a) |
| Banks of North Saska. River | | | | | | | | | | | |
| K. (Section 1) | TBM | Till | 13.7 | 3.2 | 4.3 | 288 | 26.9 | 9 | 1.28 | 0.40 | (a) |
| L. (Section 2) | TBM | Till | 13.7 | 3.2 | 4.3 | 288 | 14.2 | 5 | 0.68 | 0.21 | (a) |
| M. (Section 4) | TBM | Sand | 16.7 | 3.2 | 5.2 | 351 | 259.85 | 74 | 12.37 | 3.87 | (a) |

* units in meters

Notes: (a) From load cells

(b) From flat jack tests in the shotcrete liner

(c) From the deformation of the ribs

(d) From lagging deflection

(e) From the measurements of strains in the rib

(f) From the measurements of strains in the precast segmented liner

Table 4.3 Comparisons of Predicted and Measured Average Thrust Coefficients
(Modified after Schwartz and Einstein, 1980)

| Case | $(T/PR)_{Basic}$ | L_d/R | U_o' | λ_d | λ_y | $(T/PR)_{Predic.}$ | $(T/PR)_{Mea.}$ | Error (%) |
|---------------------|------------------|---------|-----------|-------------|-------------|--------------------|-----------------|-----------|
| Garrison, 4A | 0.41 | 1 | 0 | 0.41 | 1.24 | 0.208 | 0.132 | 58 |
| Garrison, 4B1 | 0.03 | 1 | 0 | 0.41 | 4.95 | 0.061 | 0.052 | 17 |
| Garrison, 4B2 | 0.033 | 1 | 0 | 0.41 | 4.66 | 0.063 | 0.039 | 62 |
| Garrison, 2B, F | 0.106 | 1.33 | 0 | 0.22 | 4.33 | 0.101 | 0.078 | 29 |
| Garrison, 2E | 0.123 | 1.17 | 0 | 0.31 | 2.95 | 0.112 | 0.132 | -15 |
| Garrison, 5A - E | 0.14 | 1 | 0 | 0.41 | 2.21 | 0.127 | 0.115 | 10 |
| Kielder Exp. | 0.464 | 2.4 | 0 | 0 | - | 0.227 | 0.162 | 40 |
| Thunder Bay | 0.714 | 1.26 | 0-4.5 | 0.011 | 43.8 | 0.482 | 0.422 | 14 |
| Tyne, Site 1 & 2 | 0.724 | 0.57 | 0 | 0.66 | 1 | 0.478 | 0.387 | 24 |
| Victoria, Concrete | 1.23 | 0.43 | 0.79-1.11 | 0.24 | 1.18 | 0.324 | 0.359 | -10 |
| Victoria, Cast Iron | 1.2 | 0.46 | 0.95-1.27 | 0.07 | 2.29 | 0.16 | 0.49 | -68 |

Table 4.4 Comparisons of Predicted and Measured Average Thrust Coefficients Using
Delay Length L_d'

| Case | $(T/PR)_{Basic}$ | L_d'/R | U_o' (cm) | λ_d | λ_y | $(T/PR)_{Predic.}$ | $(T/PR)_{Mca.}$ | Error (%) |
|---------------------|------------------|----------|-------------|-------------|-------------|--------------------|-----------------|-----------|
| Garrison, 4A | 0.41 | 0.67 | 0 | 0.32 | 1.49 | 0.195 | 0.132 | 48 |
| Garrison, 4B1 | 0.03 | 0.67 | 0 | 0.32 | 6.23 | 0.060 | 0.052 | 15 |
| Garrison, 4B2 | 0.033 | 0.67 | 0 | 0.32 | 5.86 | 0.062 | 0.039 | 59 |
| Garrison, 2B, F | 0.106 | 0.88 | 0 | 0.2 | 4.74 | 0.100 | 0.078 | 28 |
| Garrison, 2E | 0.123 | 0.77 | 0 | 0.26 | 3.48 | 0.111 | 0.132 | -16 |
| Garrison, 5A - E | 0.14 | 0.67 | 0 | 0.32 | 2.7 | 0.121 | 0.115 | 5 |
| Kielder Exp. | 0.464 | 0.79 | 0 | 0.25 | 1.47 | 0.171 | 0.162 | 6 |
| Thunder Bay | 0.714 | 0.42 | 4.5 | 0.2 | 3.22 | 0.460 | 0.422 | 9 |
| Tyne, Site 1 & 2 | 0.724 | 0.19 | 0 | 0.59 | 1 | 0.427 | 0.387 | 10 |
| Victoria, Concrete | 1.23 | 0.14 | 0.72 | 0.24 | 1.07 | 0.316 | 0.359 | -12 |
| Victoria, Cast Iron | 1.2 | 0.16 | 0.72 | 0.17 | 1.14 | 0.233 | 0.49 | -52 |

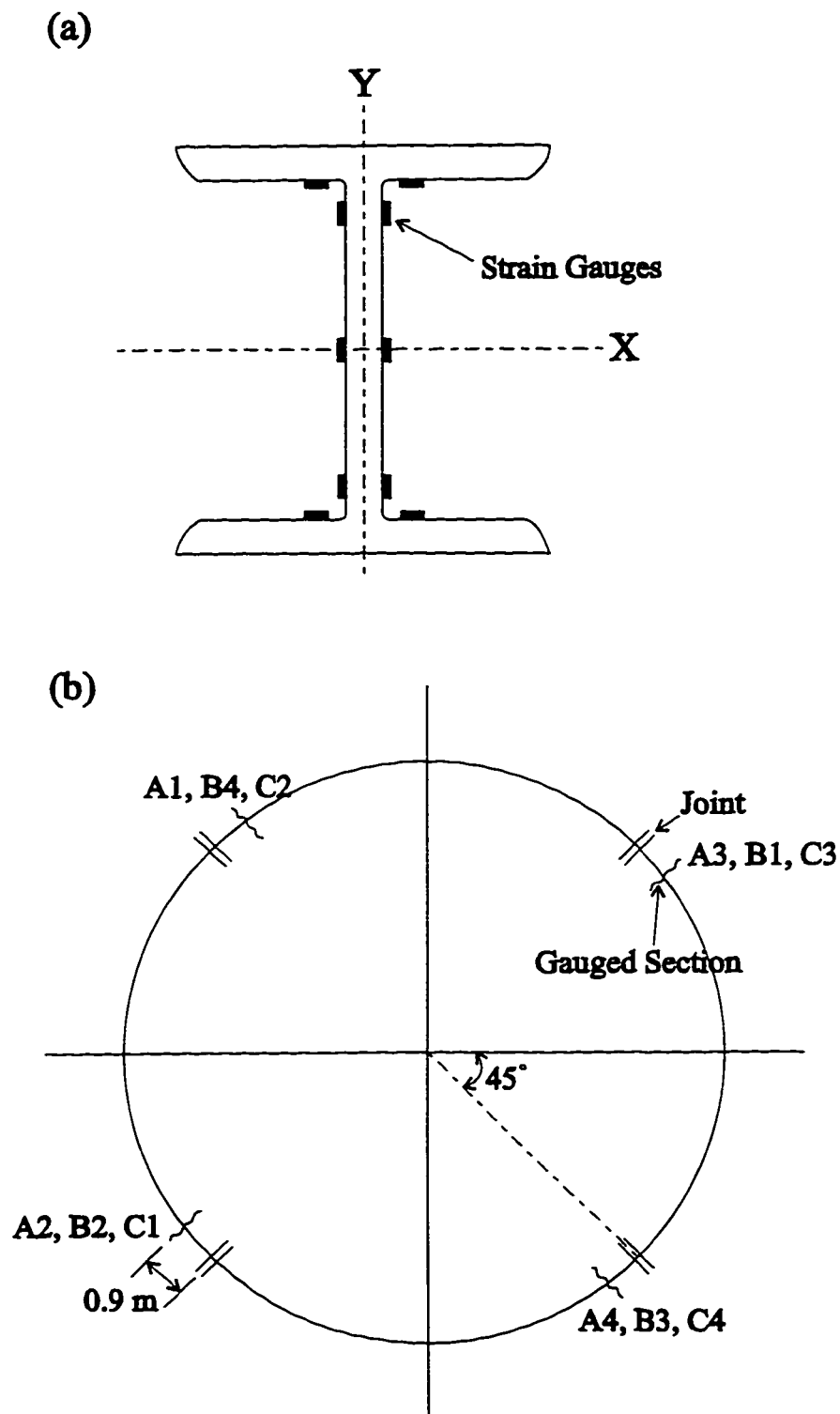


Figure 4.1 Location of Strain Gauges in Northeast Line Tunnel
(Modified after Eisenstein et al., 1977)

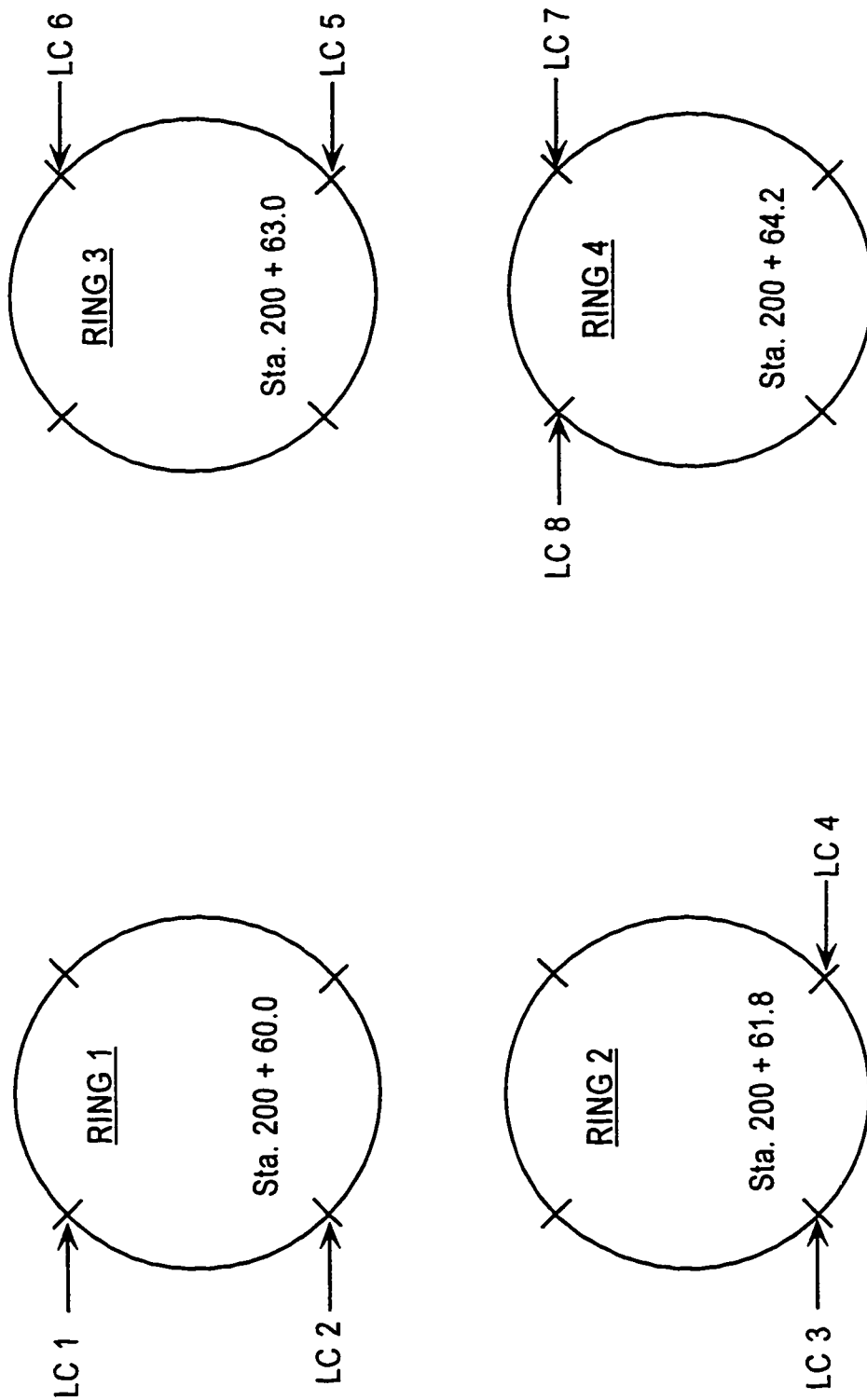


Figure 4.2 Load Cell Location in LRT - South Extension
(Modified after Branco, 1981)

South Bound Tunnel

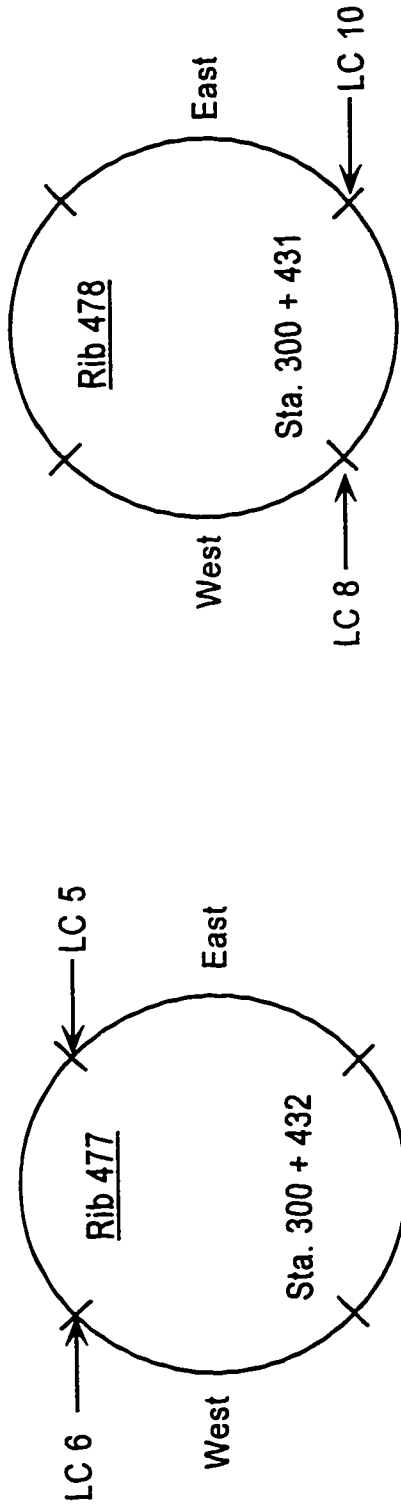


Figure 4.3 Load Cell Location of Section B2 of SLRT - Phase II Tunnel
(Modified after Tweedie et al., 1989)

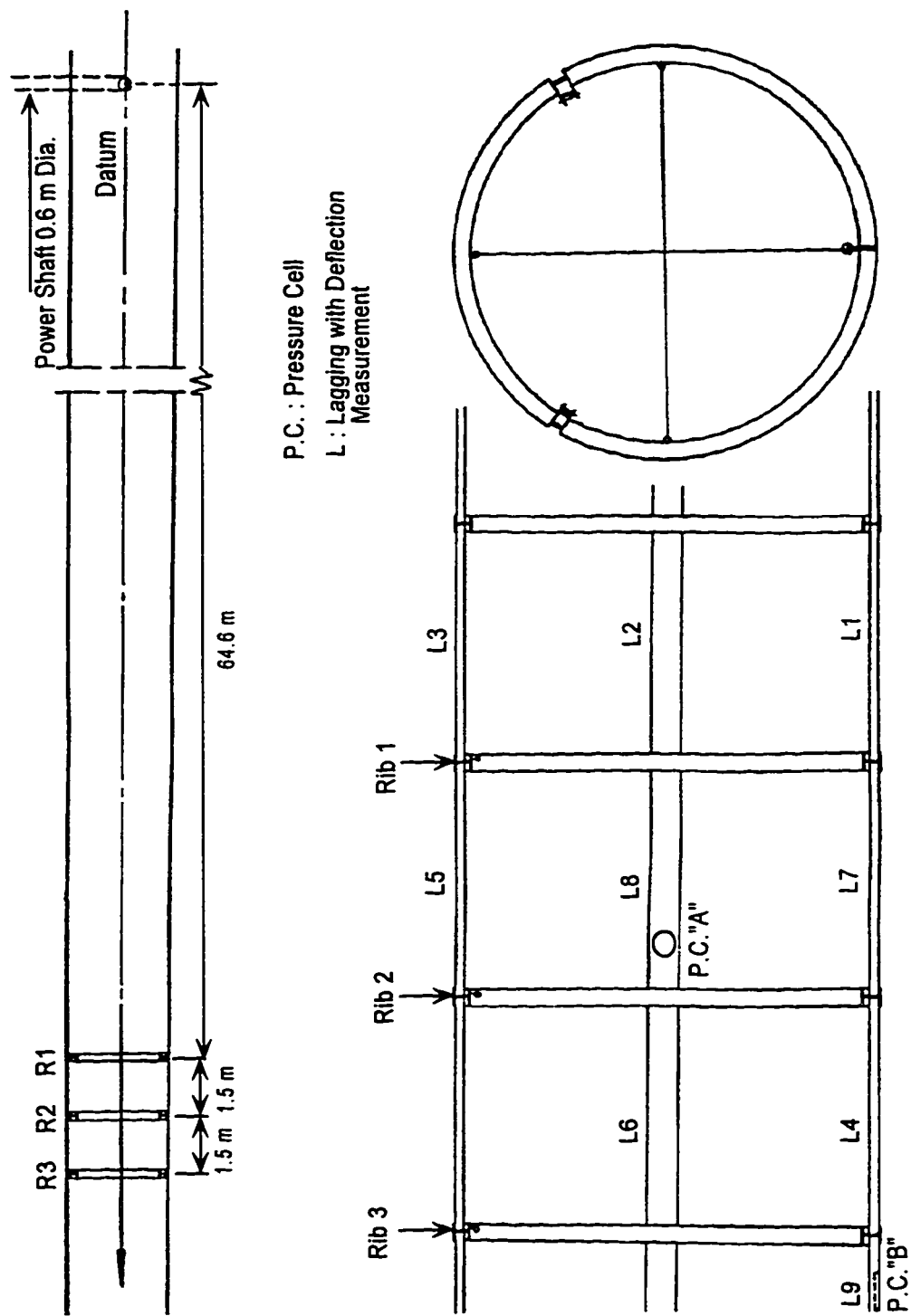


Figure 4.4 Details of the 170th Street Tunnel Test Section
(Modified after Thomson and El-Nahhas, 1980)

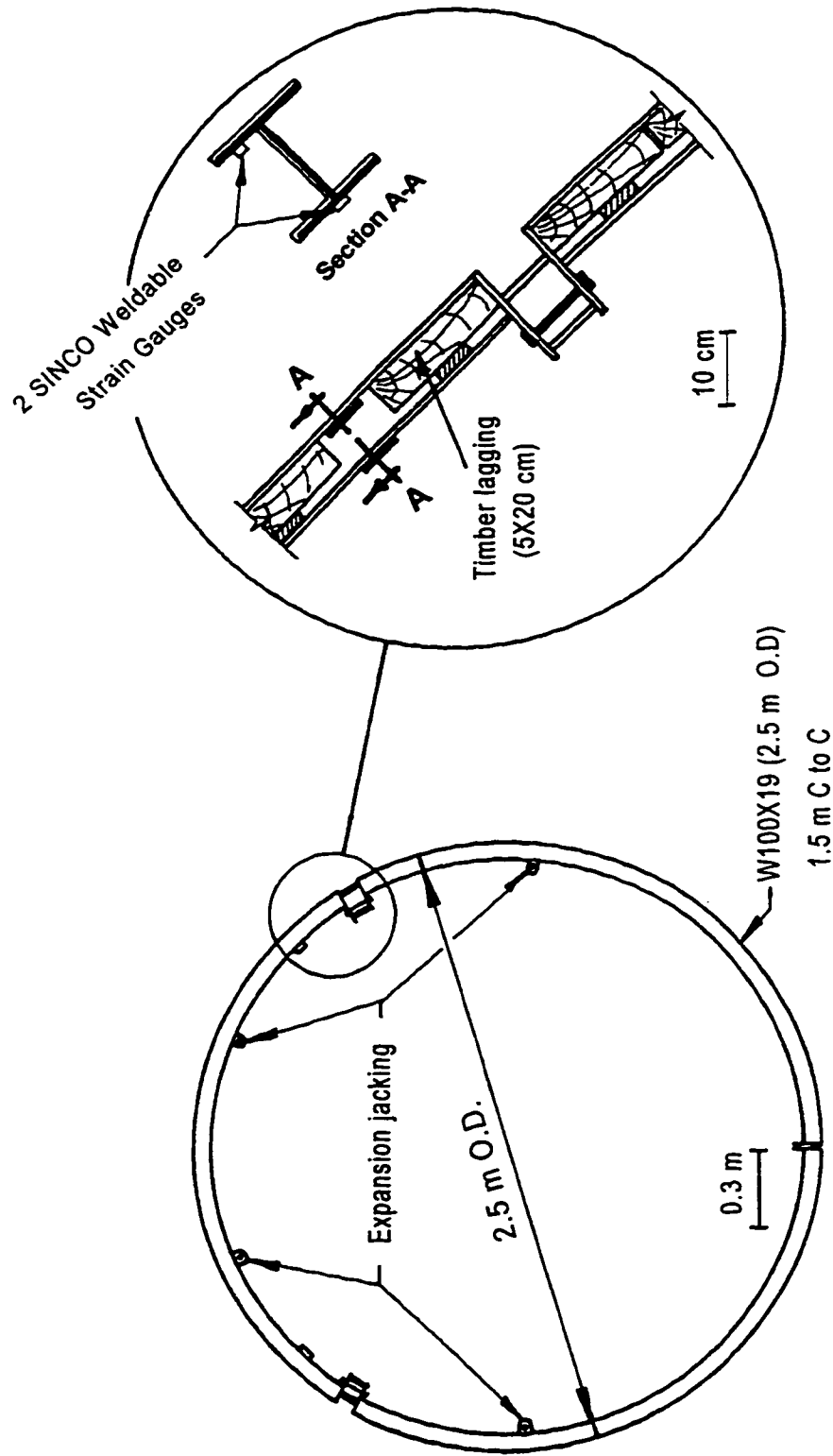


Figure 4.5 Instrumented Steel Rib of Test Section 1 of Experimental Tunnel
(Modified after Eisenstein et al., 1979)

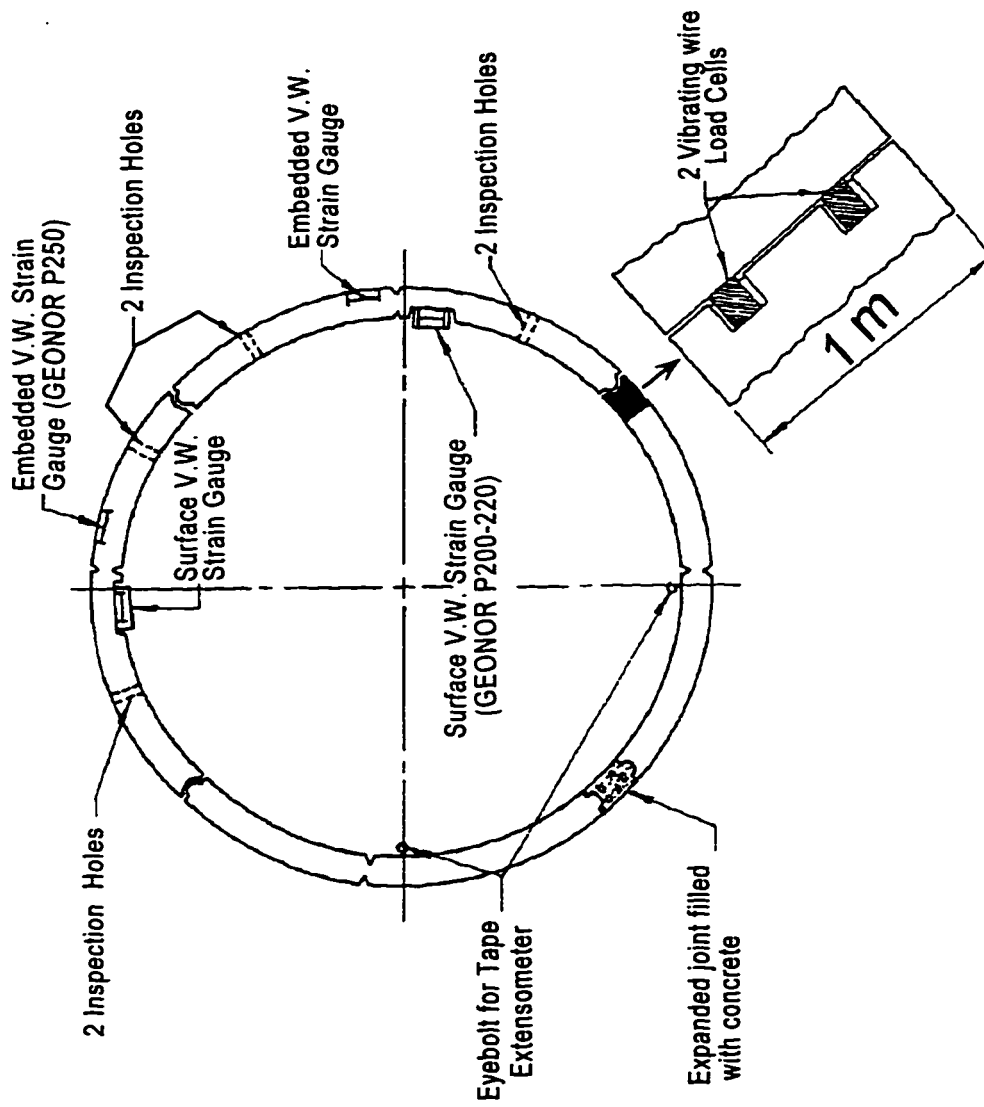


Figure 4.6 Details of Lining Instruments of Test Section 2 of Experimental Tunnel
(Modified after Eisenstein et al., 1979)

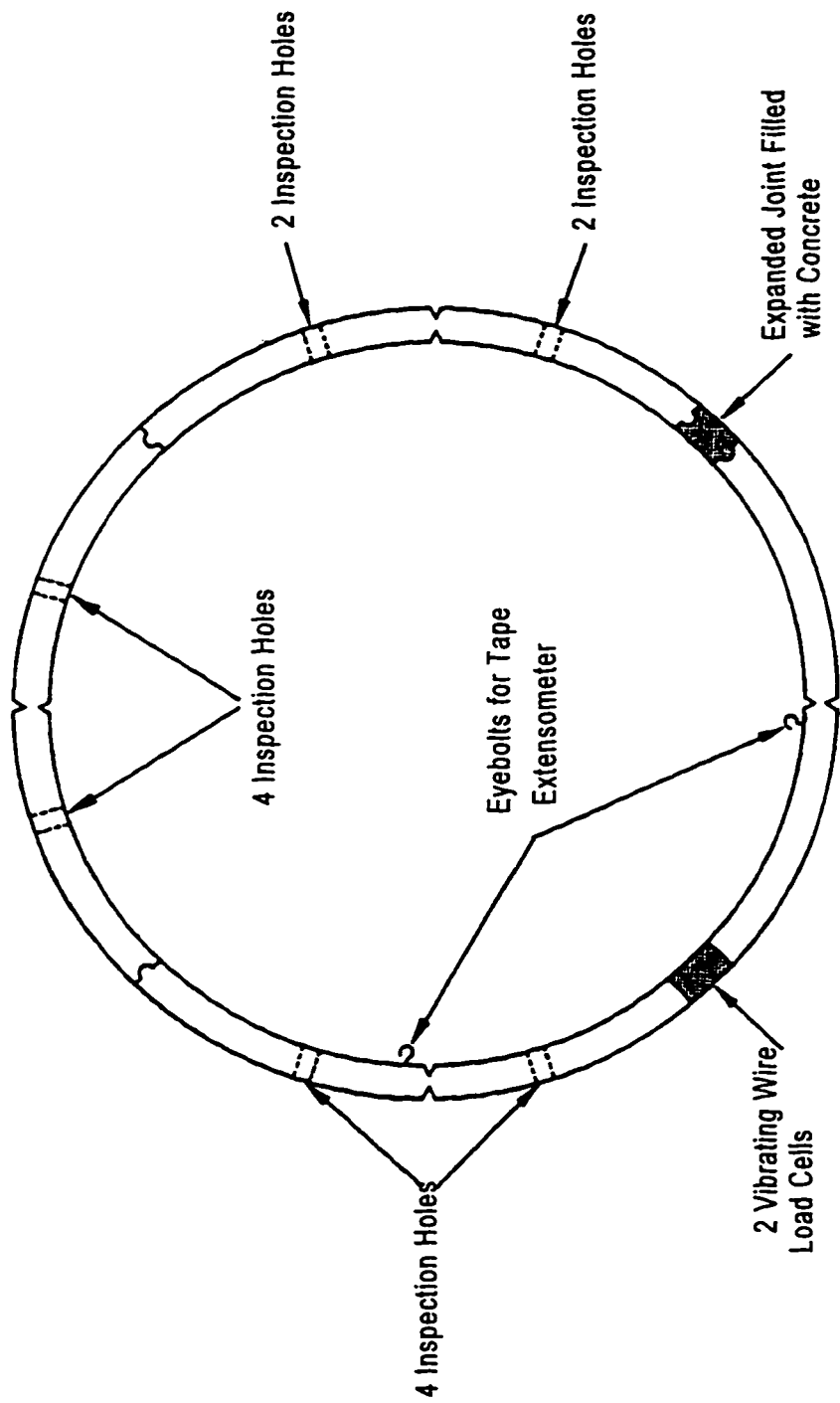


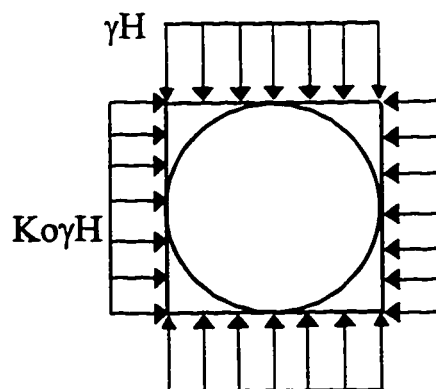
Figure 4.7 Details of Lining Instruments of Test Section 3 of Experimental Tunnel
(Modified after El-Nahhas, 1980)

For Crown and Invert:

$$T = \frac{1}{2}[(1 + K_o)b_1 - \frac{1}{3}(1 - K_o)b_2] \gamma H R$$

For Springline:

$$T = \frac{1}{2}[(1 + K_o)b_1 + \frac{1}{3}(1 - K_o)b_2] \gamma H R$$



where $C = \frac{\frac{E}{(1 + \nu)(1 - 2\nu)}}{\frac{E_1 t}{(1 - \nu_1^2)R}}$

$$F = \frac{\frac{E}{(1 + \nu)}}{\frac{6E_1 I_1}{(1 - \nu_1^2)R^3}}$$

$$b_1 = 1 - a_1$$

$$b_2 = 1 + 3a_2 - 4a_3$$

$$a_1 = \frac{(1 - 2\nu)(C - 1)}{(1 - 2\nu)C + 1}$$

$$a_2 = \frac{2F + 1 - 2\nu}{2F + 5 - 6\nu}$$

$$a_3 = \frac{2F - 1}{2F + 5 - 6\nu}$$

K_o = coefficient of earth pressure at rest

I_1 = moment of inertia of the cross-section per unit length along the axis of the tunnel

ν_1 = poisson's ratio of the lining

ν = poisson's ratio of the ground

E_1 = modulus of elasticity of the lining

E = modulus of elasticity of the ground

R = radius of the lining

t = thickness of the lining

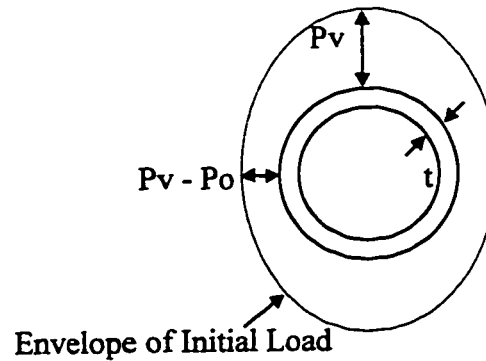
Figure 4.8 Calculation of Lining Loads using a Peck et al.'s Method

For Crown:

$$T = \frac{P_o R}{3} + \frac{4}{3} \lambda U_o R + \frac{P_{av} R}{(1 + R_c)}$$

For Springline:

$$T = \frac{2P_o R}{3} + \frac{2}{3} \lambda U_o R + \frac{P_{av} R}{(1 + R_c)}$$



where

$$\lambda U_o \frac{R}{3} = \frac{E P_o R^4 \eta^2}{18 E_1 I_1 (1 + \nu)(5 - 6\nu) + 6 R^3 E \eta^3}$$

$$R_c = \frac{R E (1 - \nu_1^2)}{\eta t E_1 (1 + \nu)}$$

$$P_o = P_v - P_h$$

U_o = maximum value of radial movement of ground at the tunnel wall

η = ratio of radius of lining centroid to that of extrados

λ = coefficient of ground reaction

E_1 = Young's modulus for lining (replaced by $E_1 / (1 - \nu_1^2)$ where lining continuous along tunnel)

$$P_{av} = (P_v + P_h) / 2$$

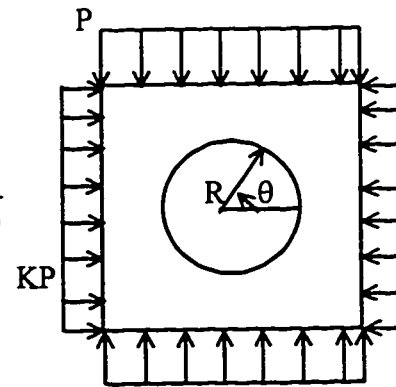
R_c = compressibility of the tunnel in relation to that of the ground

Figure 4.9 Calculation of Lining Loads using a Muir Wood's Method

For the Full-Slip Case:

$$\frac{T}{PR} = \frac{1}{2}(1 + K_o)(1 - a_o) + (1 - K_o)(1 - 2a_2)\cos 2\theta$$

$$a_o = \frac{CF(1 - \nu)}{C + F + CF(1 - \nu)} \quad a_2 = \frac{(F + 6)(1 - \nu)}{2F(1 - \nu) + 6(5 - 6\nu)}$$



For the No-Slip Case:

$$\frac{T}{PR} = \frac{1}{2}(1 + K_o)(1 - a_o) + \frac{1}{2}(1 - K_o)(1 + 2a_2)\cos 2\theta$$

$$a_o = \frac{CF(1 - \nu)}{C + F + CF(1 - \nu)} \quad \beta = \frac{(6 + F)C(1 - \nu) + 2F\nu}{3F + 3C + 2CF(1 - \nu)}$$

$$b_2 = \frac{C(1 - \nu)}{2[C(1 - \nu) + 4\nu - 6\beta - 3\beta C(1 - \nu)]} \quad a_2 = \beta b_2$$

$$C = \frac{ER(1 - \nu_1^2)}{E_1 A_1 (1 - \nu^2)} \quad F = \frac{ER^3(1 - \nu_1^2)}{E_1 I_1 (1 - \nu^2)}$$

where

C = compressibility ratio

F = flexibility ratio

A_1 = average cross-sectional area of the support per unit tunnel length

P = vertical ground stress at the centre line of tunnel

θ = measured angle from the springline to a certain point anticlockwise

Figure 4.10 Calculation of Lining Loads using a Einstein and Schwartz Method

(A) Use a Series of Dimensionless Graphs* and a Table developed from a Combination of the FEM and the Convergence-Confinement Concept to find Radial Displacements and Stress Reduction Factors. (* See Negro, 1988)

(B) Analytical Closed Form Solution for Ground-Lining Interaction (Hartmann, 1970) - Stress Reduction Factors are considered through the Use of a Reduced Unit Weight of the Soil and a Reduced Ground Stiffness when applying the following equation.

$$T = \frac{(1+K)(\alpha+\beta)}{2(1+\alpha+\beta)} \gamma HR + \frac{\alpha(1+K)}{4(1+\alpha)} \gamma R^2 \cos \phi - \frac{(1-K)(3-4\nu)(\alpha+3\beta+12\alpha\beta)}{2(1+\alpha(3-2\nu)+3\beta(5-6\nu+4\alpha(3-4\nu)))} \gamma HR \cos(2\phi) - \frac{(1-K)(3-4\nu)(\alpha+4\beta+36\alpha\beta)}{4(1+\alpha(5-4\nu)+8\beta(7-8\nu+9\alpha(3-4\nu)))} \gamma R^2 \cos(3\phi)$$

where

$$\alpha = \frac{E_1 A_1 (1+\nu)}{ER(1-\nu)^2}$$

$$\beta = \frac{E_1 I_1 (1+\nu)}{ER^3(1-\nu)^2}$$

ϕ = measured angle from the invert to a certain point anticlockwise

Z_0 = depth to springline

Figure 4.11 Calculation of Lining loads using a Eisenstein and Negro's Method

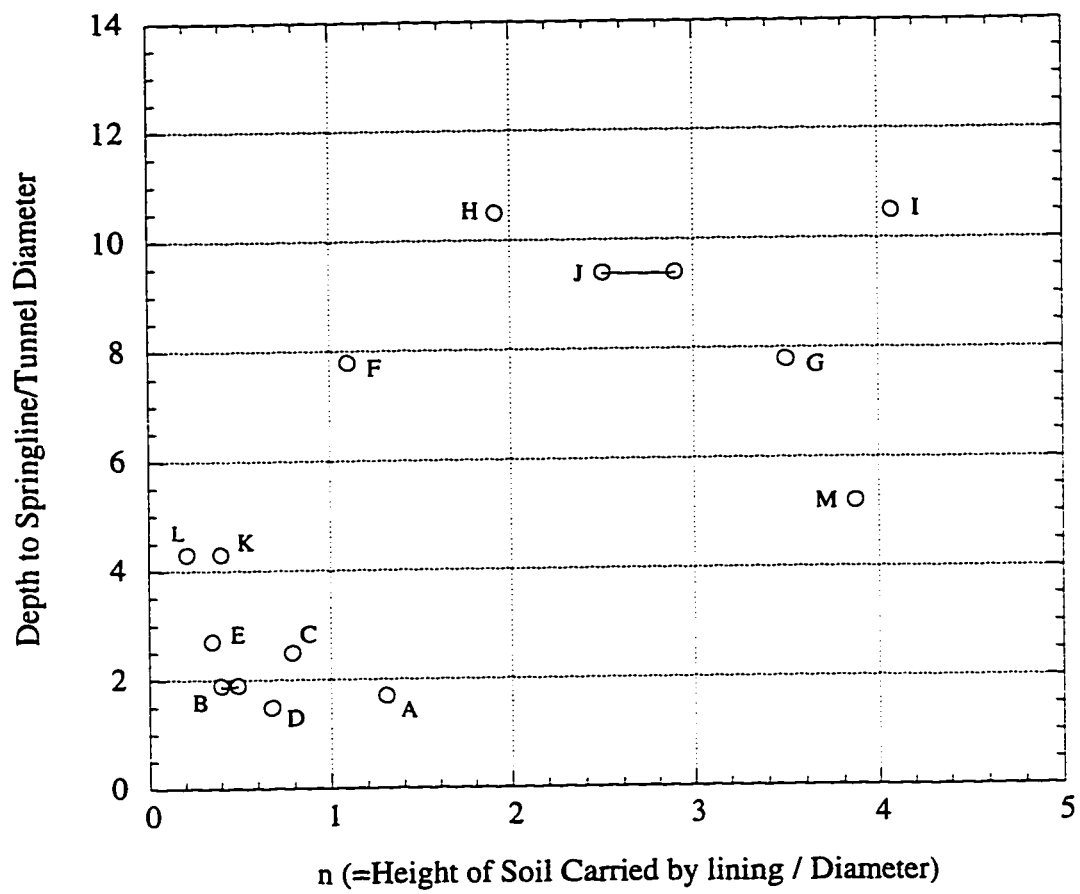


Figure 4.12 Comparison of the Dimensionless Factor (n) with Depth in Edmonton Tunnels

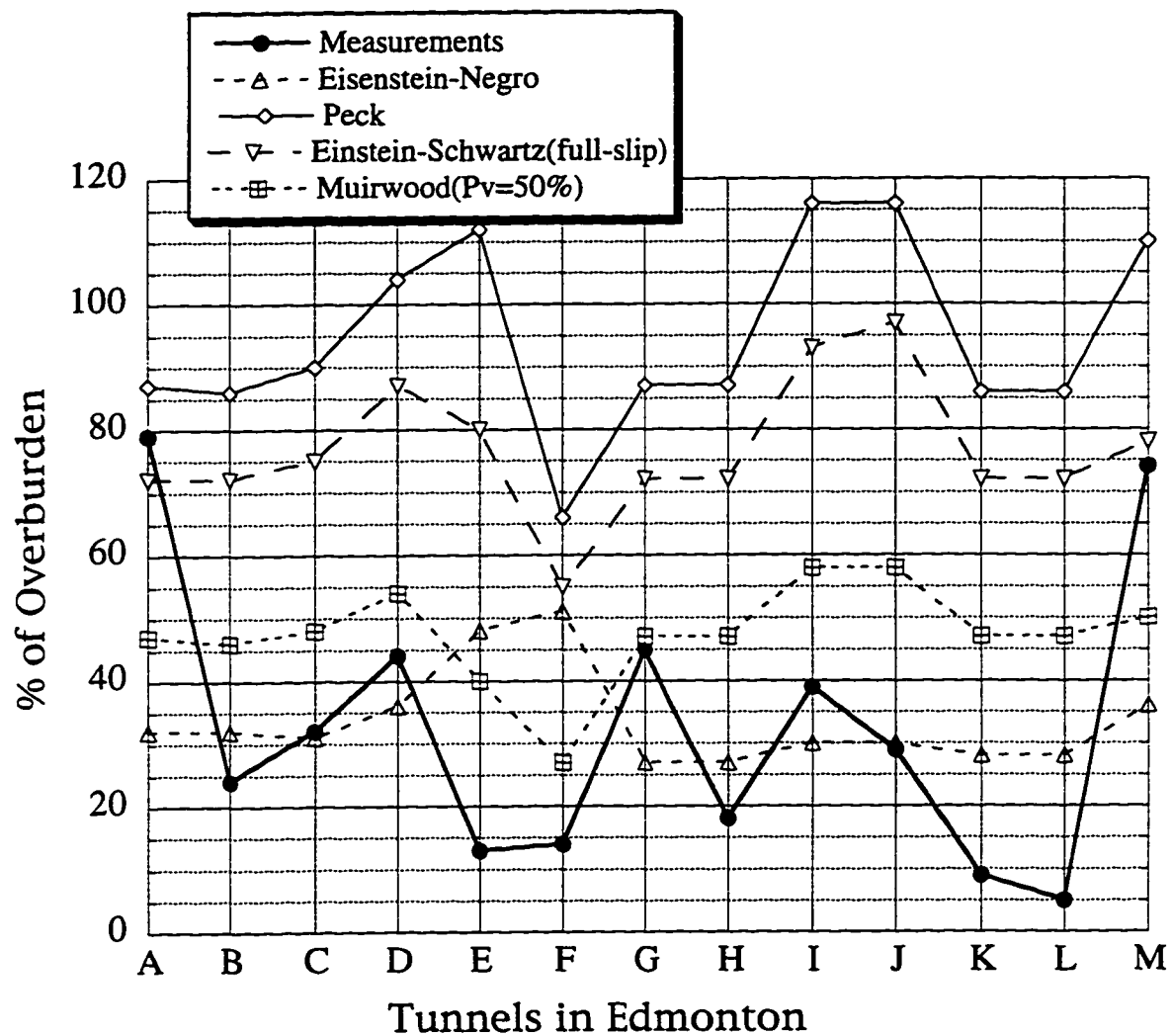


Figure 4.13 Measured and Calculated Percent of Overburden in Edmonton Tunnels

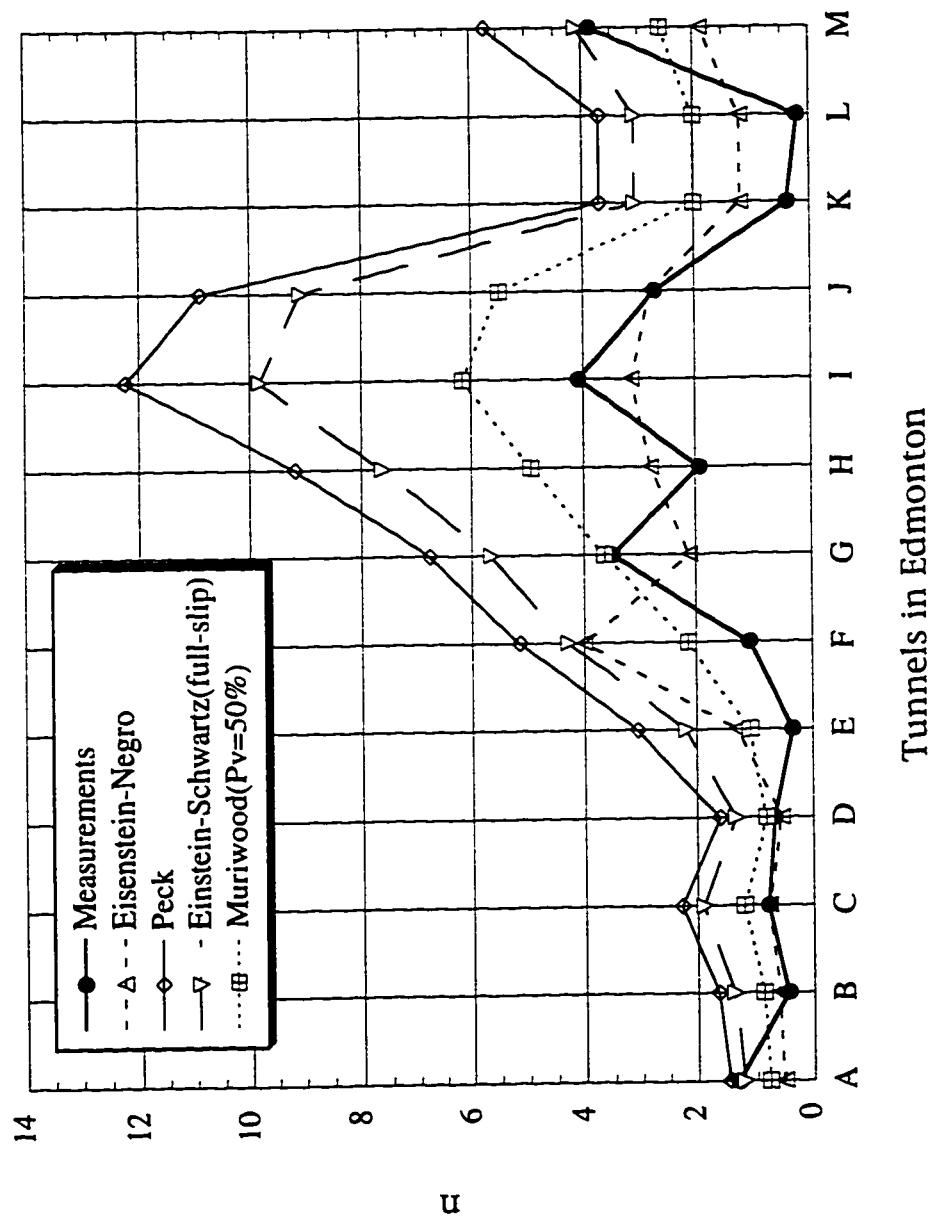


Figure 4.14 Measured and Calculated n for the Linings in Edmonton Tunnels

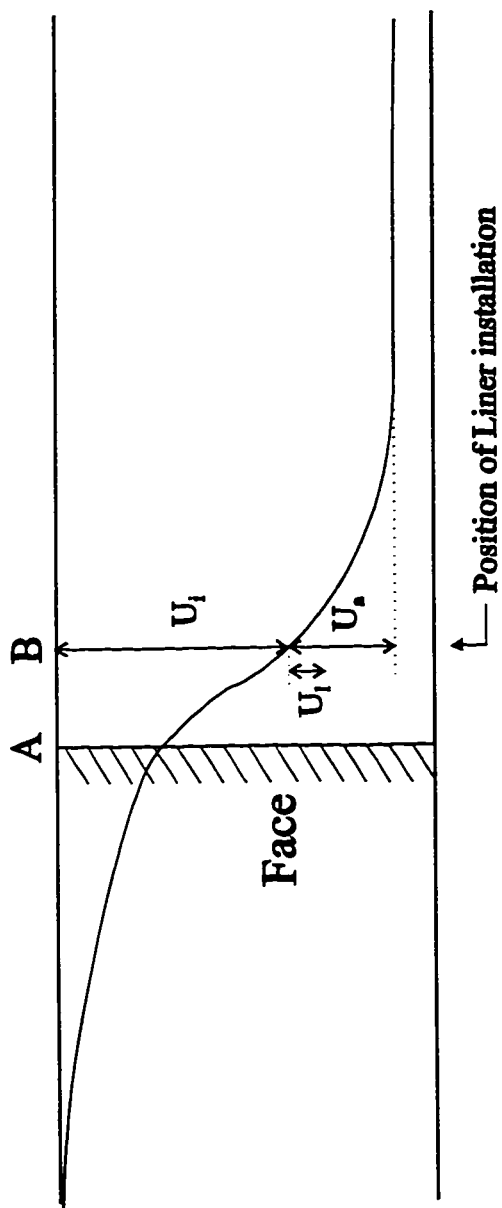
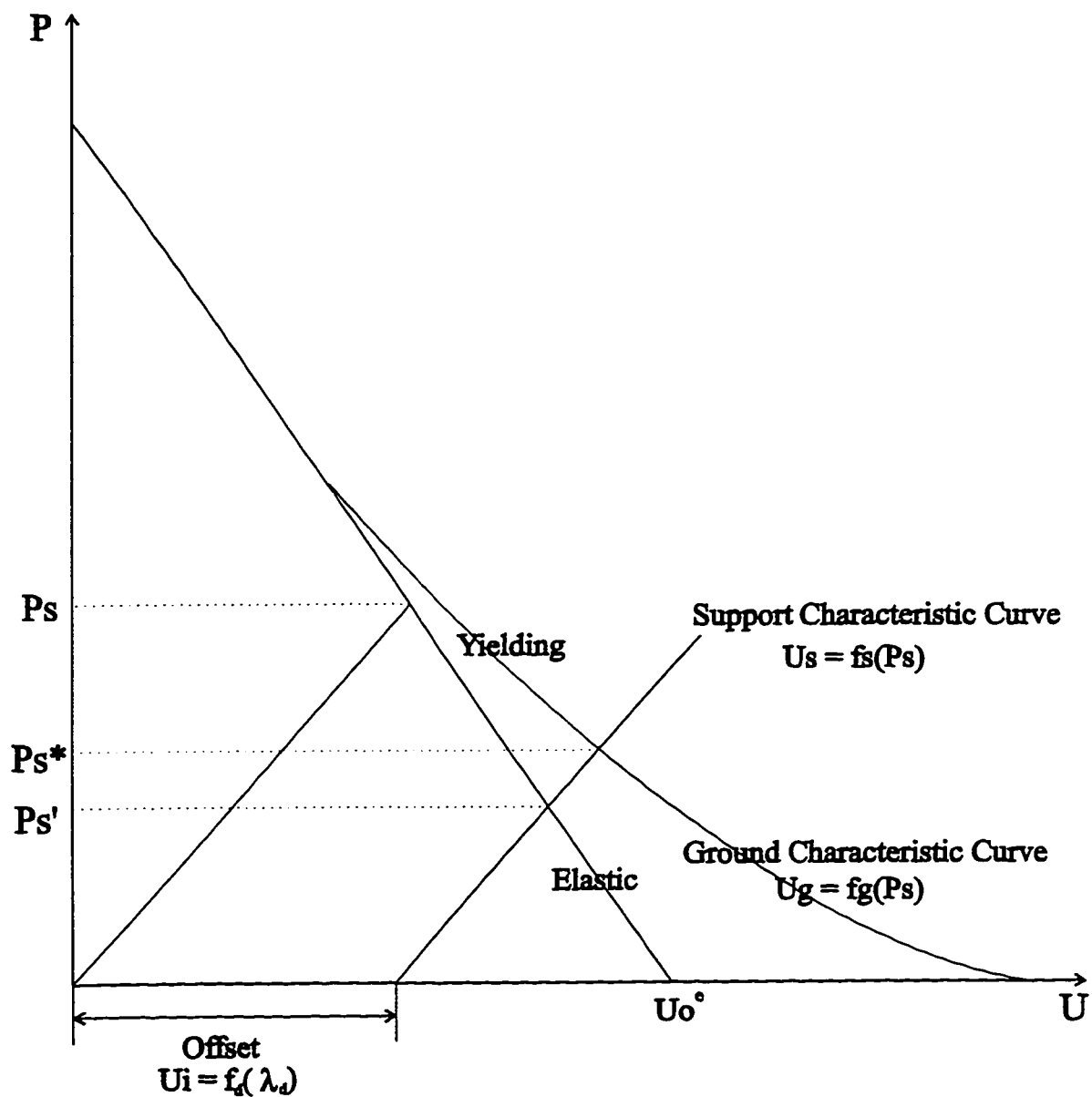


Figure 4.15 Tunnel Convergence as Function of Tunnel Face



**Figure 4.16 Convergence-Confinement Curves for Yielding Ground with Support Delay
(Modified after Schwartz and Einstein, 1980)**

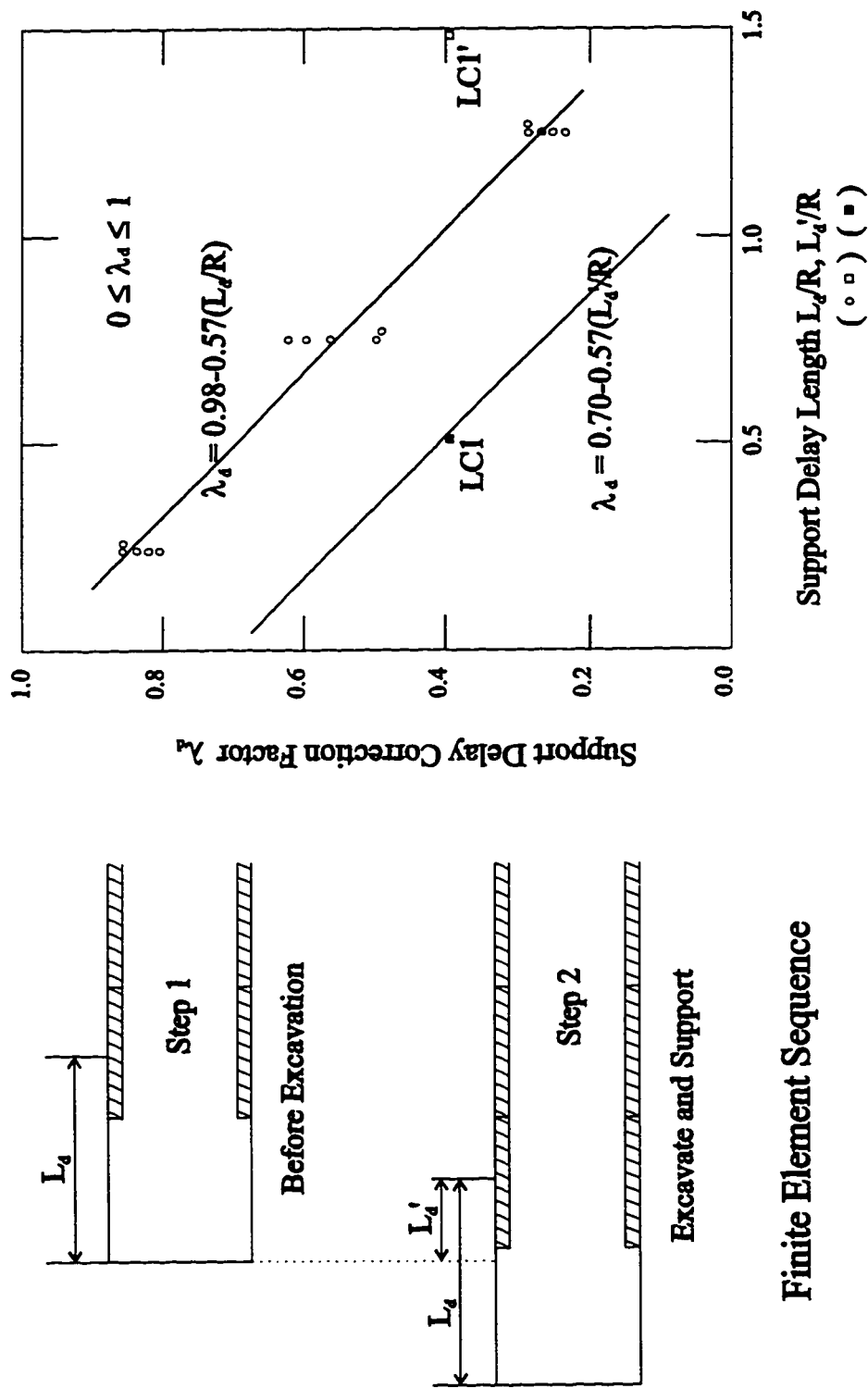
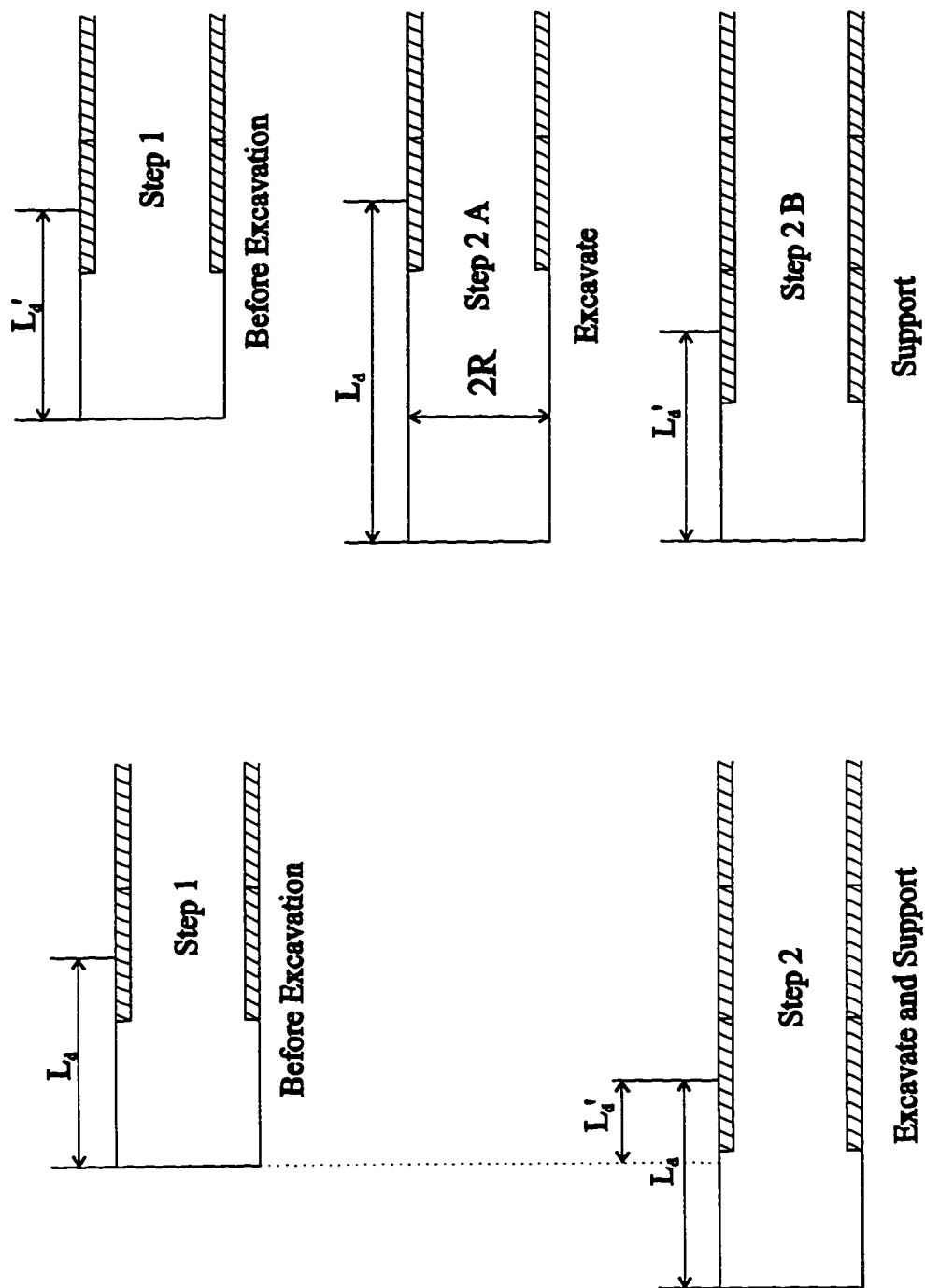
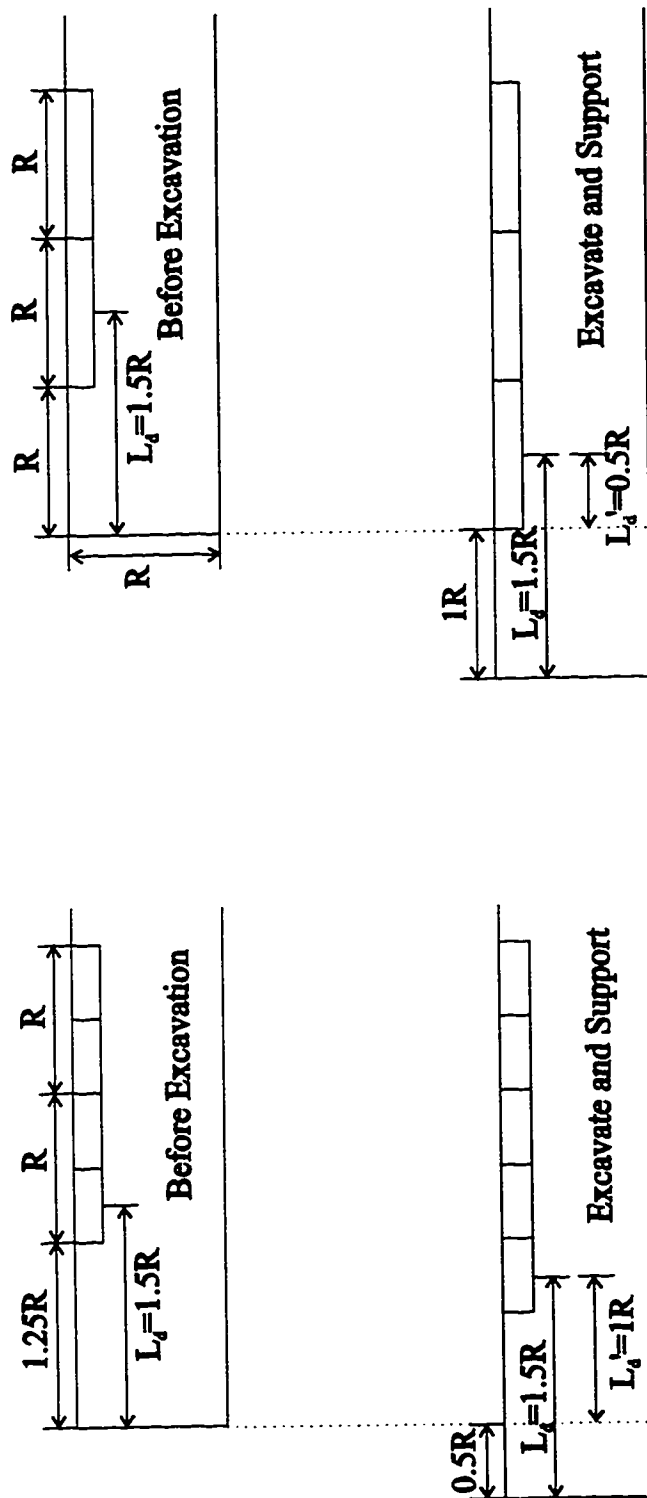


Figure 4.17 Support Delay Correction Factor
(Modified after Schwartz and Einstein, 1980 and Hutchinson, 1982)



(A) Finite Element Sequence (B) Actual Tunnelling Sequence

Figure 4.18 Definition of Support Delay Length



(A) Schwartz and Einstein (Round Length 0.5R) (B) Hutchinson (Round Length 1R)

Figure 4.19 Tunnelling Sequences used in the Finite Element Analyses

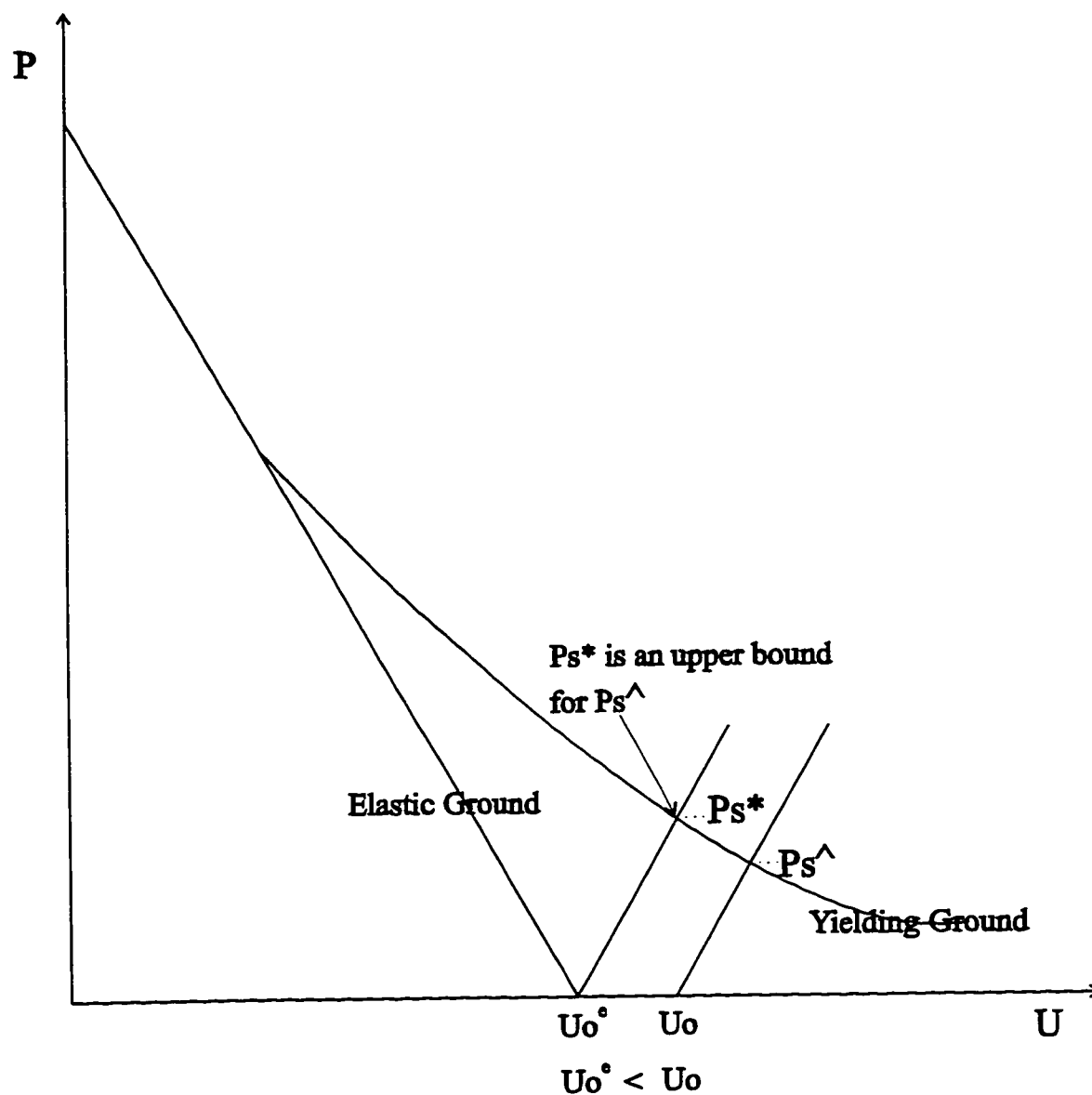


Figure 4.20 Upper Bound of Lining Load for Tunnels with Large Support Delay (Modified after Schwartz and Einstein, 1980)

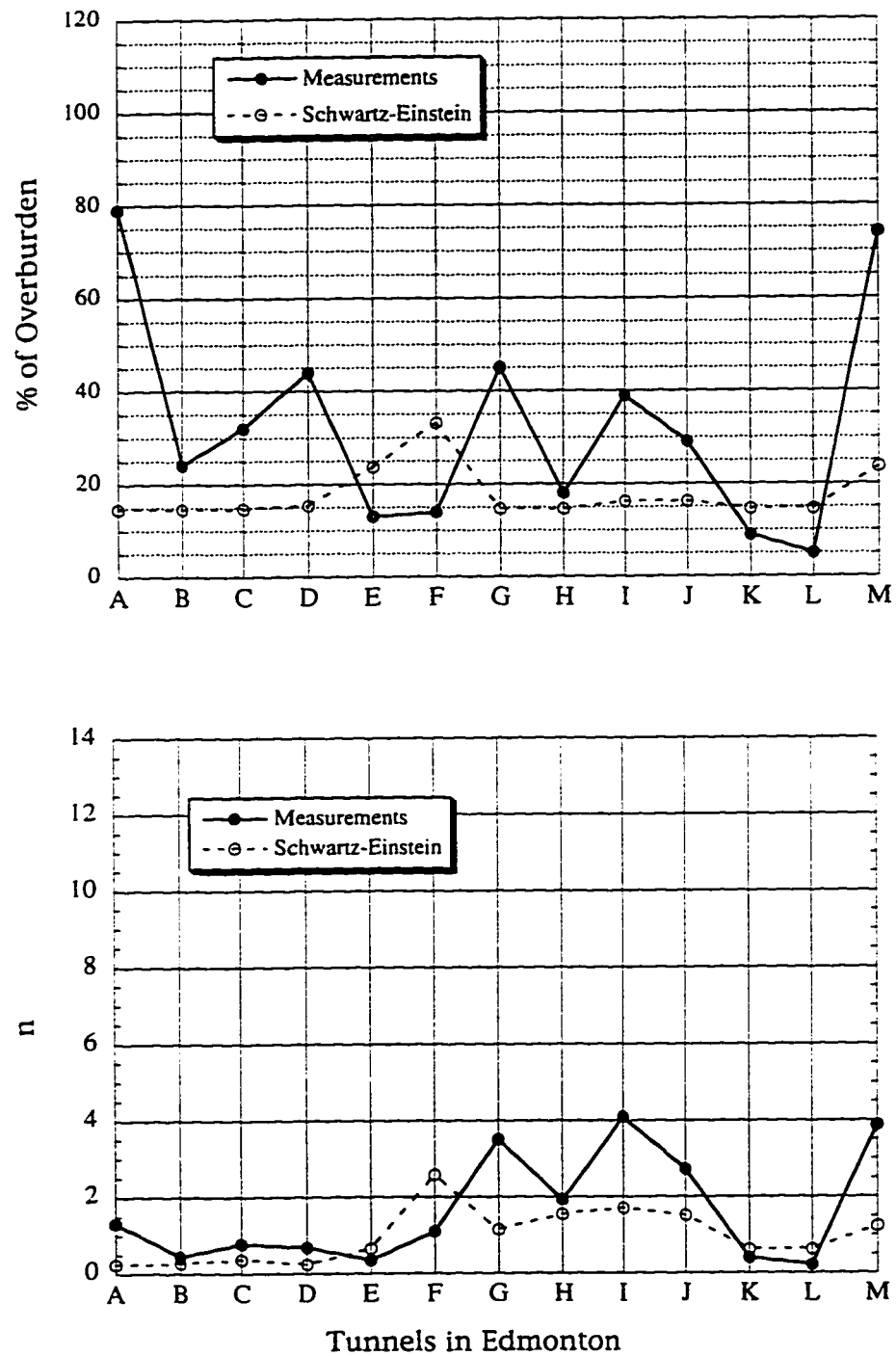


Figure 4.21 Measured and Calculated Lining Loads in Edmonton Tunnels Using Schwartz and Einstein's Method

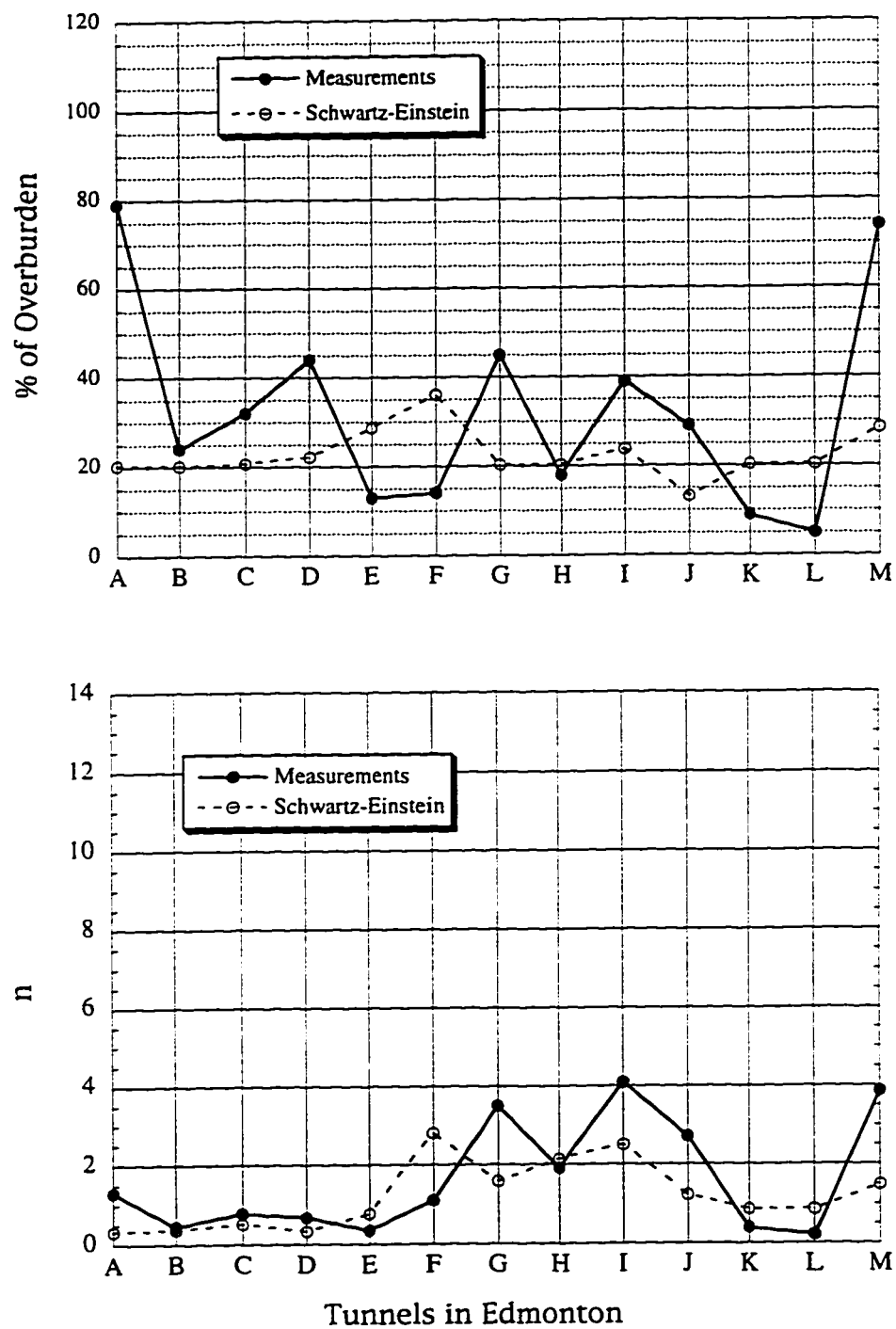


Figure 4.22 Measured and Calculated Lining Loads in Edmonton Tunnels Using Schwartz and Einstein's Method ($\lambda_d=0.2$)

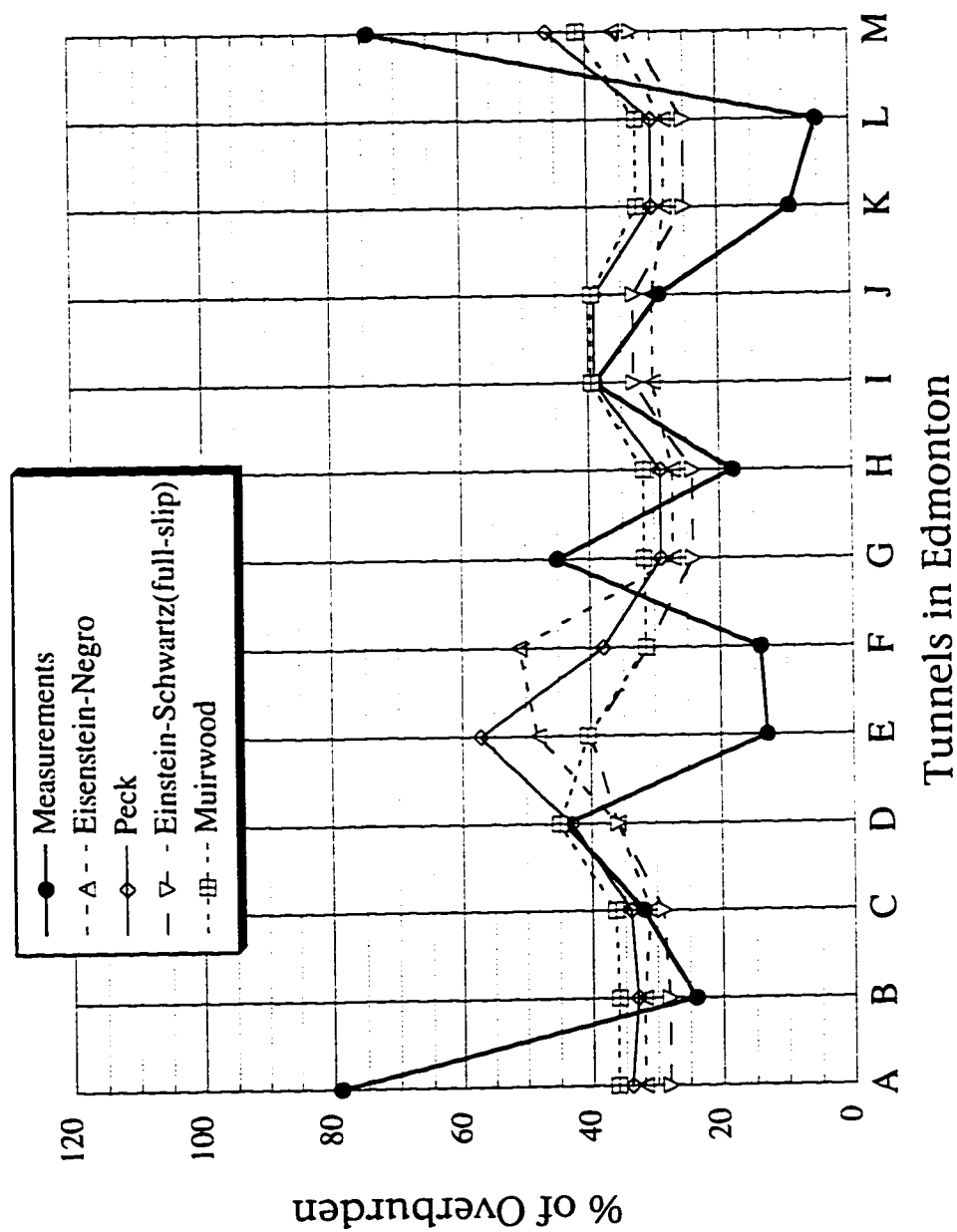


Figure 4.23 Measured and Calculated Percent of Overburden in Edmonton Tunnels Using Reduced Unit Weight

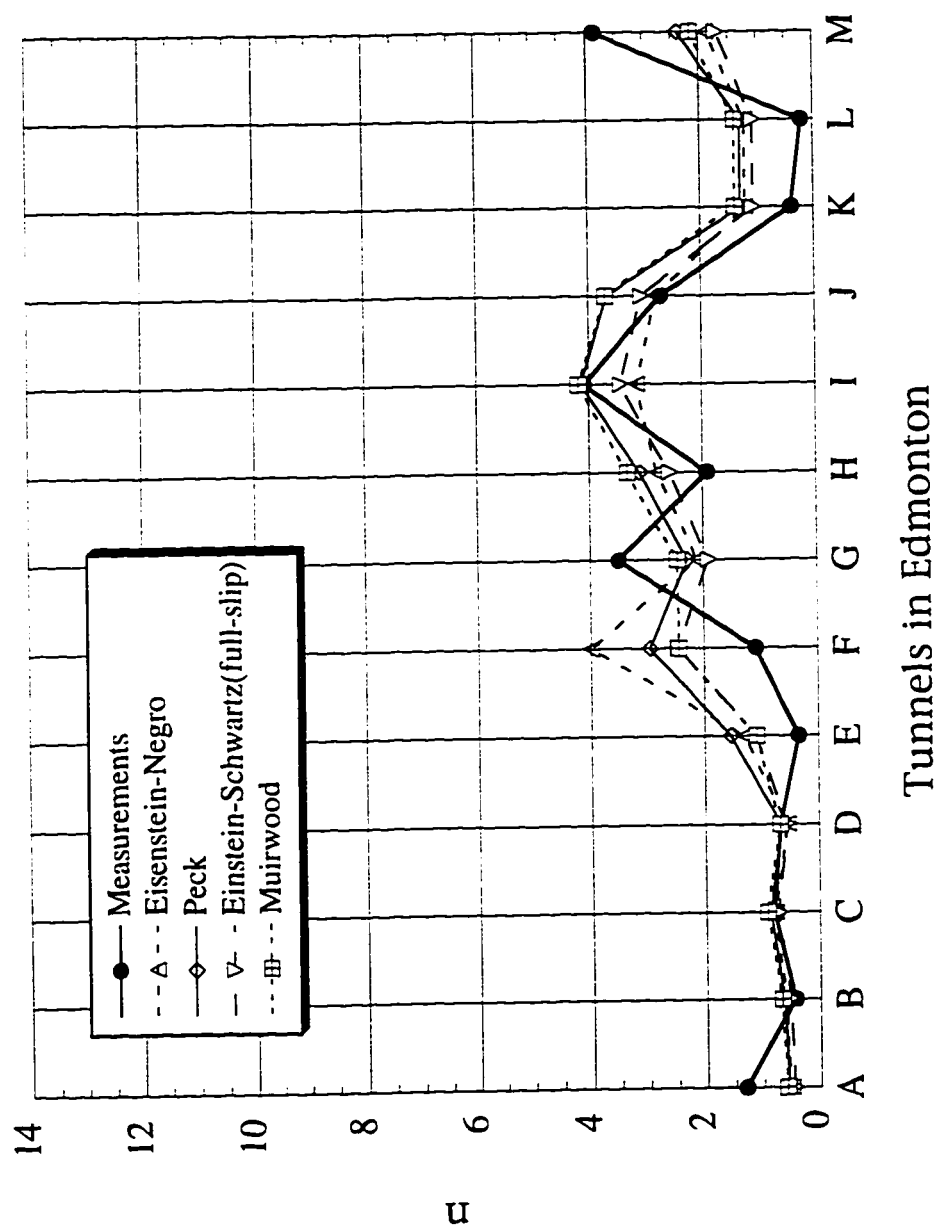


Figure 4.24 Measured and Calculated n for the Linings in Edmonton Tunnels Using Reduced Unit Weight

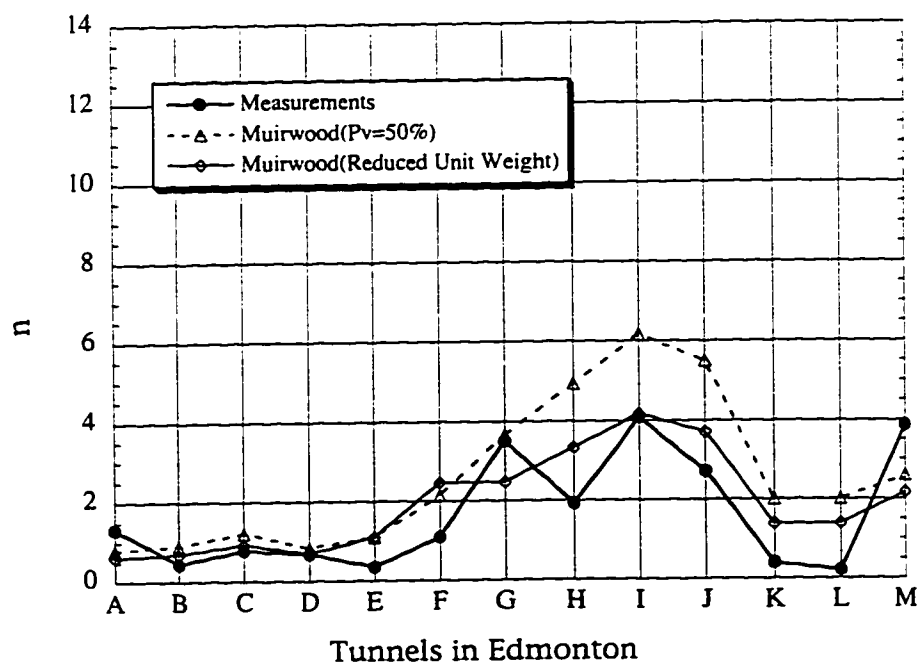
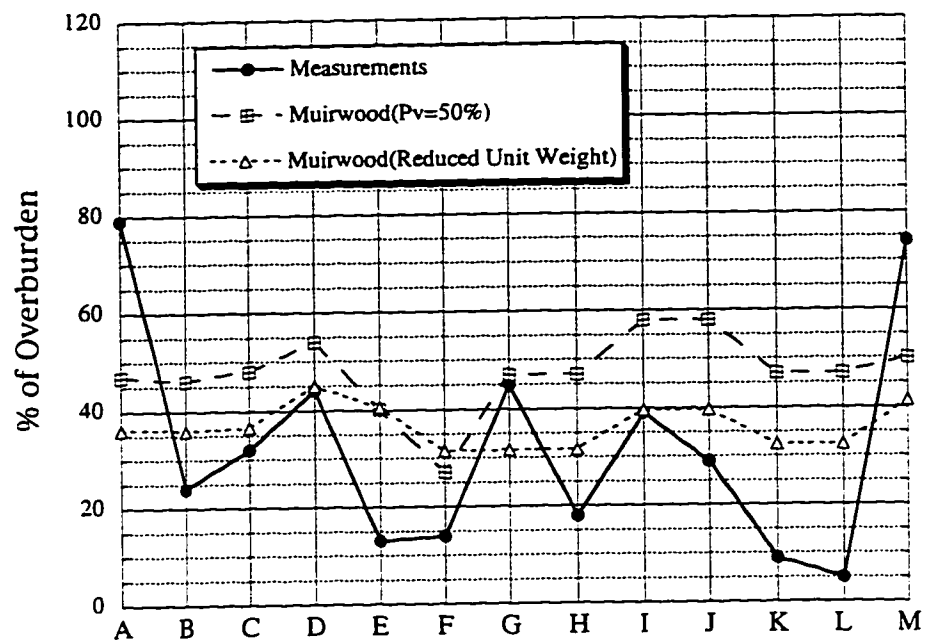


Figure 4.25 Measured and Calculated Lining Loads for Edmonton Tunnels Using Reduced Unit Weight and Arbitrary 50 % Stress Reduction for Muirwood's Method

5. Ground- Support Interaction During Excavation

5.1 Introduction

Tunnel excavation changes the state of stress and stiffness around the opening. The installation of a support system, which interacts with the soil, further alters the stress and stiffness of the ground. Ground-support interaction is a consequence of the resistance with which the liner reacts against the movement of the surrounding ground into the excavated opening. Kuesel (1987) stated that the design of a tunnel liner was not a structural problem but a ground and structural problem, with the emphasis on the ground because the loads acting on a liner are not well defined and its behaviour is controlled by the properties of the surrounding ground.

The transfer of loads from the excavated ground to the tunnel liner depends on the stress-strain-time properties of the ground, the relative stiffness between the liner and the ground, the initial stresses existing in the ground, the method of excavation, type and manner of placement of the liner and the distance between the tunnel face and the point of liner activation. The convergence-confinement method has played a major role in understanding the ground-liner interaction in advancing tunnels. In this chapter, the convergence-confinement method is reviewed and applied for a case history of a tunnel in Edmonton. The convergence curves are obtained from two-dimensional finite element analyses using three different material models and theoretical equations. These curves are compared with actual field measurements.

5.2 The Convergence-Confinement Method (CCM)

The current concepts for the design of tunnel supports recognize the behaviour of any system as a complex function of the ground-liner interaction rather than as a function of assumed loading diagrams. The convergence-confinement method (CCM) is one approach to the analysis of ground-liner interaction. The convergence curve for the ground shows the radial stress vs. radial displacement in response to the insertion of the excavated stress-free boundary in the original in-situ stress field. The confinement curve for the support represents the response of the liner installed to control these deformations which results in pressure build up within the liner until an equilibrium point is reached.

Therefore, the convergence-confinement method requires an understanding of the behaviour of the ground to determine the soil convergence related to the applied confining pressure and the liner behaviour to find the confining pressure acting on the lining in terms of deformation.

5.2.1 Review of Convergence-Confinement Method

In an early study, Rabcewicz(1969) presented the basic concept of the convergence curve from the work of Fenner(1938), which showed a release of 6 mm, equivalent to a shortening of the diameter of only 2%, a process which decreases the radial stresses to about 50%. The basic concept of the CCM was described by Deere et al.(1969) and Peck(1969). A hypothetical stress-displacement diagram is shown in Figure 5.1 (a). The instantaneous displacement that occurs before the liner can be installed is denoted by U_i . The radial stress is gradually increased on the liner due to ground displacements. If a perfectly incompressible liner is installed, the stress acting on a liner is P_i . In the case of a compressible liner, ground-liner interaction occurs, which results in the additional ground and liner displacements, U_l , and the reduction of the stress from the P_i to the P_l .

Lombardi (1970) used the CCM to discuss the effect of a weak rock core on tunnel face stability. Lombardi (1973) explained the plastic behaviour of ground, which is shown in Figure 5.1 (b). Point A is the initial state of the non-excavated section far ahead of the tunnel face, whereas point B corresponds to the excavated section behind the face. The initial stress, P_o , starts to reduce as the tunnel wall moves inward. Up to point A' the ground behaves elastically, so that a linear convergence curve develops. If the stresses near the tunnel exceed the ground strength at this point, the displacements increase more rapidly due to the addition of plastic deformation to the elastic deformation, and the convergence curve follows line A'D instead of line A'C. Lombardi also showed the effects of volume change due to the opening up of fissures, the strength of ground material, the location of the liner with respect to the face of the excavation and the time related to liner rigidity on final convergence-confinement curves.

Ladanyi (1974) presented a closed-form solution of convergence-confinement curves for a simple tunnel geometry and field stress conditions considering the strength decrease of the ground with time, linear or nonlinear failure envelope and the ground dilation due to breakage. In Figure 5.2 (a) the curve AB represents the instantaneous response of the excavation, while AB' shows the long term response due to the loss of strength of the ground with time. There is an infinity of similar lines (isochrones) between the lines AB and AB', each equivalent to a given time interval after the tunnel construction. The instantaneous displacement of the tunnel wall prior to the liner installation is denoted as U_i . Because of the time-dependent ground displacements, stress is gradually built up on the liner. The stresses on the liner and ground are in equilibrium at the pressure, P_i . If there is gap Δ between the liner and the ground, the ground will displace more and has a final stress, P_f . The convergence curves for long term cases are obtained by inserting reduced strength parameters into the equations. However, it is not an easy task to estimate the strength and deformation parameters of the ground with time. Ladanyi (1980) also showed that the CCM could be combined with the theory of non-linear visco-elasticity to determine the time-dependent pressure on a specific tunnel liner given certain assumptions.

The convergence curves which are shown so far intersect the horizontal axis, indicating that the excavation will be stable without liner. The ground should have enough strength in the form of cohesion in order to be self supporting, a condition which is not always possible. In practice the required support pressure could increase with displacements depending on the degree of strength loss in the yielded zone as shown in Figure 5.2 (b). According to Daemen (1975), this phenomenon is common in shallow tunnels when gravity effects dominate within the lower strength yield zone. Three different types of roof convergence curves are shown in the figure. Curve 1 shows that the support pressure increases dramatically with deeper failure propagation when the ground strength reduces very rapidly after the ultimate strength has been exceeded. The convergence curve for self supported ground is given by Curve 2. Curve 3 indicates that the support pressure required in the roof could be reduced during the initial stage of nonelastic deformation and only after some displacement begin to increase. This delayed

upward trend of the convergence curve is a result of a moderate strength reduction in a low field stress, an effect which can be seen in shallow tunnels. Daemen also presented confinement curve equations for shotcrete liners, blocked steel sets and rock bolts as well as a solution that allows consideration of the effect of a progressive, strain dependent strength decrease during rock failure. However, the equations are very long and complex.

Kaiser (1980) presented the derivation of a closed form solution that yields the convergence curve of a tunnel excavated in ground material that is assumed to be linear elastic, brittle-perfectly plastic with yield surfaces described by the Coulomb failure criterion. The derivation will be described in detail in a later section.

The limitations of the CCM were comprehensively discussed during the conference on "Analysis of Tunnel Stability by the Convergence-Confinement Method" held in Paris, 1978 and published in English in 1980. Gesta et al. (1980) showed how we can reduce the three dimensional problem due to the presence of the tunnel face to a problem of plane deformation using stress release factor λ , which was originally described by Panet (1976) and Panet and Guenot (1982). The authors defined the support pressure in the crown as the sum of the confinement pressure that decreases with the convergence and the confinement pressure due to gravity of the decompressed zone, which increases with the convergence. They also emphasized the importance of observational methods to ensure that the CCM gave reliable results.

Howells (1980) described the effect of gravity as shown in Figure 5.3 (a). The effect of gravity is more obvious for material that is weak in shear and loosely packed, such as jointed rock at shallow depth. Kerisel (1980) criticized the assumption behind of CCM, which suggests that the radial convergence is the same for all azimuths. The above assumption cannot be justified from field evidence due to the effect of gravity. He calculated the gravity load exerted on the sides, the face of the heading and the nearest support per unit length using theorems of limiting equilibrium and the results of centrifuge experiments. The author also compared the convergence among various support methods and concluded that the pre-splitting techniques gave the lowest convergence. Finally, he showed that the convergence curves for the face diverge

increasingly from the elastic curve if the safety factor suggested by Broms and Bennemark (1967) increases from 2 to 6.

Lombardi (1980) determined the convergence curves for the opening and for the unexcavated core in front of the face as shown in Figure 5.3 (b). Line 1 shows the convergence curve for the excavation that starts at point A. The characteristic curve for the core withdrawn from the tunnel in front of the face follows line 2 with radial expansion equal to OB. Line 3 represents the elastic convergence curve for the core after the core is relocated at the tunnel face. The convergence curve follows line 4 when the strength limit of the face is reached due to the plane state of stress at the face. The equilibrium position of the core would be either at C for elastic material behaviour or D for an elasto-plastic case. The length of OE represents the deformation, which takes place in the plane of the face of the heading. The author also showed the characteristic lines representing the excavation at various distances from the face at different times. The author finally concluded that the accuracy of CCM is limited by the assumptions on which it is based.

Duddeck (1980) illustrated more refined convergence-confinement curves as shown in Figure 5.4. The pressure on the liner is reduced by the amount ΔP_a due to the creep and shrink of the concrete liner in the upper diagram. The final equilibrium point moves from E_i to E_f . Therefore, the stiffness of the liner is reduced from D_i to D_f . The ground behaves rheologically in the lower sketch because the effect of arching within the ground reduces with time due to traffic vibrations or ground water. The liner pressure increases by ΔP_a due to the increase of the liner displacement of ΔU_a . In this case, the stiffness of the ground is decreased from S_i to S_f . The author described the assumptions for the CCM and pointed out the problems of the method, including the difficulties of finding the displacement before the liner installation. He concluded that the CCM may not be very good for direct design procedures, with some exceptions such as deep tunnels and highly pressurized rock. The author suggested the use of FEM for evaluation of the convergence curves and investigation of the parameter sensibility for future work. In other words, the FEM can be combined with the CCM for the direct evaluation of the curves, along with checking and adjustment by field measurement.

Egger (1980) suggested a method to consider the face effect assuming a state of spherical symmetry in the vicinity of the face, using an allowable value of the tunnel convergence to determine the necessary support pressure. Panet and Guenot (1982) derived a function that gave tunnel closure for a deep tunnel in terms of the distance to the face from the axi-symmetric finite element models using an elasto-plastic material. Final convergence and plastic radius are the major parameters for the equation, which can be provided by the in-situ convergence measurements. The authors also presented a method to include the convergence due to the time-dependent behaviour of excavated ground.

Brown et al. (1983) presented a closed-form solution of convergence curves using an elastic-brittle-plastic material model with dilation occurring at a constant rate with a major principal strain and the empirical strength criteria given by Hoek and Brown (1980). The authors also described a stepwise calculation sequence for an elastic-strain, softening-plastic material model with dilation occurring at different rates with major principal strain. A tunnel of circular cross section, plane strain conditions, and a hydrostatic in situ stress field were assumed. Experimental data are required to determine the parameters for the solution.

Eisenstein et al. (1984) recognized the difference between the behaviour of ground during excavation and the convergence curve provided by CCM due to three-dimensional arching around the cavity at the head of an advancing tunnel. The authors showed the three-dimensional nature of arching near the face of an advancing tunnel as given in Figure 5.5. The ground convergence was related only to the advance of the tunnel, i.e., without consideration of time dependency of the ground movement. The authors presented conceptual diagrams to relate radial stress to radial displacement for a point at the tunnel crown considering three dimensional effects as shown in Figure 5.5 (a). It shows the longitudinal distribution of vertical stress and vertical displacement at the tunnel crown. Points B and C respectively show a stress concentration ahead of the face and a rapid decrease of vertical stress to zero at the tunnel face. The radial stress along the unsupported cavity, points C-D, is zero. The vertical stress increases with the installation of lining and is stabilized at point F. Stress concentration could be expected

near the leading edge of the lining, point E, depending on the relative stiffness of the lining and the ground. The new convergence curve is presented conceptually in Figure 5.5 (b) from the stress and displacement distribution of Figure 5.5 (a), which has the merit of recognizing the actual load transfer mechanisms. The existing field measurements by Sauer and Jonuscheit (1976) supported the postulate of the mechanisms shown in the figure.

The authors carried out three-dimensional finite element analysis using a linear elastic material model. The displacements were obtained from the nodes on the excavation line along the crown. However, the stresses were used from the points located about 20 cm above the crown node to eliminate possible error which might have been introduced during the extrapolation of the stress data from a point inside an element to its boundary. The vertical displacement distribution was very similar to the conceptual diagram in Figure 5.5 (a). However, the vertical stress distributions did not show any significant stress concentration ahead or behind the unsupported cavity nor did they drop to zero along the unsupported span. The stresses even started to recover at some distance ahead of the leading edge of the lining. These slight discrepancies of stresses between the conceptual diagram and the results from the finite element analysis could be related to the fact that the stresses were not obtained at the excavation line as mentioned by the authors. The authors also observed that the lining position relative to the face had more pronounced effects on stress changes occurring ahead of the face than on displacements. Finally, it was concluded that the two-dimensional analysis represented an upper bound solution for equilibrium stresses and displacements as it laid above the final points of three-dimensional analyses.

Eisenstein and Branco (1990) examined the applicability of the CCM to the design of shallow tunnels by comparing the results of the method with field measurements for two tunnels in stiff clay. The authors pointed out that the CCM has a major limitation for shallow tunnels due to the proximity of a free surface above the tunnel, a non-hydrostatic stress field, and the effects of gravity around the tunnel. They showed that the completely different results between the loads and displacements predicted from the convergence-confinement formulation presented by Kaiser (1980) and

those from the field measurements were basically due to the inaccurate estimation of ground displacements before the lining installation. The authors suggested that an understanding of the ground behaviour before the lining activation would be a very important factor for the development of a design method for shallow tunnels.

5.2.2 Comments on the Convergence-Confinement Method

The limitations of CCM as a practical design tool have been described by many authors as mentioned above and can be summarized as follows:

- (1) The method can be used for circular tunnels with constant mechanical and geometric properties of supporting members.
- (2) The ground should be homogeneous, isotropic and continuous without fissures.
- (3) The closed form solutions of the method for the non-elastic ground are restricted to a stress field ratio equal to one.
- (4) The radial convergence is the same for all azimuths. Therefore, the bending of the liner is neglected.
- (5) The convergence curve is unknown and difficult to determine.
- (6) The time dependent behaviour of the ground on the convergence curve is difficult to estimate.
- (7) The effect of gravity can not be easily included for the method.
- (8) The radial displacement before the liner installation is unknown and a three dimensional approach is needed for its prediction.
- (9) The method does not well approximate the complex three dimensional load transfer mechanism occurring near the tunnel face and completely neglects the stress concentration that may occur at the leading edge of the liner.

The CCM has a great advantage in explaining the phenomena governing the ground-liner interaction. However, the method may not be appropriate as a direct design tool except for special cases such as deep tunnels and highly pressurized ground as mentioned by Duddeck (1980) due to the limitations mentioned above. To have a better

understanding of the method, especially the effect of a material model on the convergence curve, two-dimensional finite element analyses are performed in this study.

5.3 Two-Dimensional Finite Element Analyses

5.3.1 General

The Finite Element Method (FEM) has several advantages over simple closed form solutions, including the ability to allow any opening shapes, presence of the surface boundary, geologic discontinuities, non-linear material behaviour and variation of material properties in space and time. The criteria for modelling of underground openings using the FEM were presented by Kulhawy (1974) for the case of plane strain analyses of homogeneous, linear elastic rock masses. Mesh configuration, mesh size effects and boundary location effects were discussed. The author concluded that a minimum of 125-150 elements should be enough for analyses of simple structures where there is a plane of symmetry and only one-half of the system need to be analysed.

The boundaries of the finite element mesh also should be located at least 3 diameters away from the centre of the excavation to be the computed stresses and displacements within an error of less than 10 % of the theoretical. However, Heinz (1984) and Oteo and Sagaseta (1982) suggested that the lateral boundary should be more than 8 and 9 diameters away from the centre to have good results for the calculation of settlement. Kulhawy (1977) also showed that element aspect ratios, base to height, up to about 5 do not seriously affect the results and that aspect ratios of about 10 away from the main region of interest would be acceptable. It is also well known that a gradual increase in element size away from the zone, where rapid changes in stresses and strains are expected, is suitable to reduce the cost of analyses.

5.3.2 Simulation of Excavation

There are several different procedures to simulate the excavation for two-dimensional analyses. The methods were discussed in detail by Eisenstein (1982) and Heinz (1984) and will not be repeated here again. However, the gradual boundary stress reversal technique should be mentioned briefly. The analyses of the stress and

deformation on a certain length behind the face are a three-dimensional problem due to the presence of the tunnel front. Panet (1976), Gesta et al. (1980) and Panet and Guenot (1982) showed how the three-dimensional problem due to the presence of the tunnel face can be reduced to an equivalent plane strain problem using stress release factor λ .

Excavation and face advance are simulated by increasing λ from 0 for the section far ahead of the face to 1 for the unsupported section far behind the face as shown in Figure 5.6. In the elastic case λ can be expressed as follows:

$$\lambda = U_r / U_o^e$$

where U_r is the radial displacement at a certain distance behind the face and U_o^e is the final elastic displacement at infinity behind the face. The final elastic displacement, U_o^e , for an unlined circular opening in plane strain for an infinite ground mass under hydrostatic pressure P_o is given by:

$$U_o^e = P_o R(1+\nu) / E$$

where R is the tunnel radius, ν is the Poisson's ratio and E is the Young's modulus of the ground. Therefore λ can be expressed as follows:

$$\lambda = U_r E / P_o R(1+\nu).$$

The gradual boundary stress reversal technique basically follows the above procedures.

The method consists of excavation of the core elements and application of a gradual release of boundary stresses to simulate tunnel advance. The in-situ stresses along the excavated boundary are gradually reduced to a certain percentage of the original stresses to simulate the installation of a lining at a certain distance from the face. However, estimation of the percentage of boundary stress release, %SR, before the lining installation is not an easy task. Heinz(1984) compared the subsurface settlements of an ABV tunnel from field measurements presented by Negro and Eisenstein (1981) with those from the 2-D FEM using a hyperbolic soil model. The best fit results corresponded to the installation of lining after 40 % of stress release, which was found by trial and error. However, Heinz could not match the deformation of the lining. As the author pointed out, a good prediction of the actual behaviour of the excavation was relied on the assumed percentage of stress release before the lining installation. The author suggested using the displacements occurring ahead of the face instead of the displacements before

support installation due to its simplicity. The assumption is conservative for the calculation of load on the lining but unsafe for the estimation of displacements.

5.3.3 Material Model

Appropriate representation of the soil behaviour around an excavated tunnel is a very important issue for predicting the displacements and loads of the ground and liner. A review of the stress-strain behaviour of soil is beyond the scope of the present study. Desai and Siriwardane (1984) and Chen and Mizuno (1990) discussed the subject comprehensively. Some aspects of the models which have been used for tunnels in soil will be discussed briefly. The discussion will be limited to the time independent stress-strain relations.

Negro (1988) provided examples of various stress-strain relations for soils, which have been used in shallow tunnel modelling. Brown et al. (1983) reviewed the models of material behaviour used for the axisymmetric tunnel problem. The elastic and the elastoplastic or elastic-brittle-plastic models are the most commonly used. The simplest soil model is the linear elastic model for which stresses are directly proportional to the strains. The proportionality constants are Young's modulus, E , and Poisson's ratio, ν . The model is applicable only to stiff or dense soils in the case of limited development of plastic zones around the opening.

Panet and Guenot (1982) showed that the plastic behaviour of the ground increased as the stability number, which is the ratio of in-situ stress to undrained strength of the soil, increased. Kerisel (1980) compared the elastic convergence curve with convergence curves from the cases in which the stability numbers were high and concluded that local plasticity started to develop as soon as these numbers reached the value 2. As the stability number increased from 2 to 6, the convergence curves for the face diverged increasingly from the elastic curve as shown by Panet and Guenot (1982). In other words, the linear elastic model can be used when the stability number is less than 2. Negro et al. (1986) performed a three-dimensional finite element analysis using a linear elastic model to predict radial displacements at the face of shallow tunnels.

Kaiser (1981) introduced an equivalent stiffness concept to reduce the design of a tunnel in yielding or time-dependent ground to a tunnel in linear elastic ground using an equivalent modulus. A reduced modulus is used within the zone of yielding ground to have same deformation as the result from the non-elastic analysis. However, the parameters for the method should be determined from field observations of the actual tunnel or from exploratory tunnels. Negro and Eisenstein (1981) could match the surface settlement through using pseudo moduli for three Brazilian water tunnels from two-dimensional and linear elastic finite element analyses. However, the authors could not match the vertical displacements below the surface using the pseudo moduli due to the non-elastic behaviour of the ground. Heinz (1984) improved the matching of the vertical displacement at the same tunnels using a hyperbolic soil model.

Londe (1980) pointed out that the linear elastic model should be used carefully because the moduli might not be the same for the two directions and could be varied with stress change. The author suggested distinguishing between the modulus due to unloading and the modulus due to re-loading to better simulate the soil behaviour. Generally, the linear elastic model underestimates the displacements around a tunnel boundary because it is incapable of considering the plastic zones developed around the opening. It is relatively easy to correlate a limited number of parameters for the actual performance of a tunnel using the linear elastic model but extremely difficult to match completely elements such as vertical and horizontal displacements in the ground as well as lining deformations and loads for most soils.

The stress-strain behaviour of soil around the excavation is often non-linear. Ward and Pender (1981) suggested that there was no elastic ground, especially in soft ground tunnels. Duncan and Chang (1970) introduced a non-linear elastic, hyperbolic model based on the assumption that the stress-strain curves of triaxial compression tests for certain soils could be represented by a hyperbola in the $(\sigma_1 - \sigma_3)$ versus axial strain space. Kondner (1963) originally derived the model as a fitting function for the results of conventional triaxial tests. The hyperbolic model and main equations are shown in Figure 5.7. The soil modulus varies with the confining stresses and the shear stresses that the soil is experiencing. In non-linear incremental analysis of stresses and deformations, each

increment assumes the soil as being piecewise linear elastic with the tangent modulus, E_t , changing according to variations in the principal stresses. Variation of the stress-strain behaviour with confining stress depends on whether the soil is being loaded for the first time or is experiencing an unload or reload behaviour. The required soil properties can be obtained quite readily from the literature (e.g. Duncan et al., 1980) or from triaxial tests.

The model has been used extensively for the analysis of deformations of structures in a various soil types. Kawamoto and Okuzono (1977) analysed the surface settlement caused by a shallow tunnel operation using a 2-D FEM in relatively shallow diluvium deposits, which were mainly composed of sand, gravel and clay layers. The results from the hyperbolic model agreed well with the magnitude and pattern of the surface settlement, whereas those from the linear elastic model underestimated the settlement. Tan and Clough (1980) performed 2-D finite element analyses using the hyperbolic model for a silicate-stabilized sand zone and ungrouted sand to examine the surface settlement behaviour in stabilized shallow tunnels.

Katzenbach and Breth (1981) carried out a three-dimensional finite element analysis using the hyperbolic model for the surface settlement of a NATM tunnel in Frankfurt clay, which is heavily overconsolidated, laminated and fissured. The authors had a good correlation between measured and calculated surface settlements in cross section and longitudinal section. Using the same model, Negro (1988) and Eisenstein and Negro (1990) developed a new design method for shallow tunnels in soft ground.

Christian (1982) pointed out that the hyperbolic model gave good results at stress levels less than about 75 % of failure, which was the range in which most of the geotechnical problems occurred. In other words, the hyperbolic model cannot be used effectively when a significant non-linear response is to be anticipated. The author suggested using the model when the deviations from linear response under the working loads are small and when the stress paths are reasonably close to those that can be reproduced in the laboratory. It is also well known that the hyperbolic model has the limitation of all elastic models in that shear stresses do not cause volume change.

The elastic, perfectly-plastic model has also been widely used for various soil types. In the model, the stresses are directly proportional to strains until the yield point

and stresses are not affected by strains beyond the yield point. The Mohr-Coulomb yield criterion is used as the yield function. The material properties that must be defined for the elastic-plastic model are the initial linear elastic stiffness of the soil, E , Poisson's ratio, ν , cohesion, c , and the soil friction angle, ϕ . The formulation of the Mohr-Coulomb yield criterion was given by Chen and Zhang (1991).

Ladanyi (1974) presented a close-form solution for the determination of the true ground pressure on tunnel linings using the elastic, perfectly-plastic model combined with the Mohr-Coulomb failure theory. Rowe et al. (1981) analysed a shallow sewer tunnel in soft clay constructed in Thunder Bay, Canada using a linear elastic-plastic model with variations of the elastic modulus and a Mohr-Coulomb failure criterion.

5.3.4 Analysis of Experimental Tunnel

An experimental tunnel was chosen for the present analyses because of the availability of considerable field measurements of tunnel performance as well as soil parameters. The tunnel is described in detail in Sec. 4.2.6. SIGMA/W was used for the two dimensional finite element analysis. SIGMA/W, developed by GEO-SLOPE International Ltd, is a finite element program that can be used to conduct two-dimensional or axisymmetric stress and deformation analyses of earth structures.

The finite element meshes used for the analyses are shown in Figure 5.8. Originally, eight-noded elements were used with a total number of 329 elements and 1052 nodes. However, the number of elements and nodes was reduced to 122 and 411 respectively because of the memory limitation of the computer in 3-D analyses, which intended to use the same cross section as 2-D analyses. The results from the reduced meshes were in good agreement with those from the original meshes.

Initial in-situ stress before excavation was applied to the section assuming 21 KN/m³ of unit weight and a uniform in-situ stress ratio. The deformations and strains from the first step have no relevance and are considered to be zero. Two-dimensional load-deformation analyses were performed through excavation of a tunnel section using three different material models: linear-elastic, hyperbolic and elastic-plastic.

The elements in the tunnel section were deactivated in one step to simulate the excavation. The internal forces, which are equal to in-situ stresses but opposite direction, were applied to the nodes along the excavated tunnel boundary to prevent any soil movement due to excavation. The procedure to calculate the equivalent internal forces for initial stresses is shown in Figure 5.9. The upper diagram shows the contributing areas for planar two-dimensional elements with width equal to 1 unit. The forces, F_x and F_y , were reduced to zero in 11 different steps with a 10 % deduction of forces for each step.

For a linear elastic analysis, an elastic modulus of 30,000 KPa with Poisson's ratio of 0.4 were used based on the results of a pressuremeter test obtained by Thomson et al. (1982). The elastic modulus used is comparable with an elastic modulus of 35000 KPa obtained from the triaxial test by Negro (1988). The in-situ stress ratio of unity is assumed for the analysis as proposed by Eisenstein and Branco (1990). The assumption was validated from the field measurements, which showed that the horizontal soil displacements at the springline and vertical displacements at the crown were almost equal (El-Nahhas, 1980).

The results of the linear elastic analysis for the radial stresses and displacements of the crown, springline and floor are shown in Figure 5.10. The radial stresses are shown in a dimensionless form by dividing the radial stresses with the in-situ stresses. The ground reaction curves were straight lines due to the assumption that the ground exhibits linear elastic. The diagram shows three different lines for three different points of the tunnel perimeter due to the stress gradient across the tunnel profile generated by the action of gravitational body forces, which is disregarded in the convergence-confinement method.

Theoretically, the radial stresses should drop to zero when all of the internal stresses are reduced to zero but they did not. This is because the stresses at the nodal points were obtained from the values in the gauss points which were not located at the excavated tunnel boundary. Therefore, the smaller the element sizes along the excavated boundary are, the smaller are the radial stresses. For example, the radial stress at the crown decreased from 461.09 KPa of in-situ stress to 12.93 KPa after the excavation when a total number of 329 elements were used, whereas the radial stress decreased from

476.74 KPa of in-situ stress to 40.42 KPa when a total number of 122 elements were used. However, a total number of 122 elements were used for the analyses for the reason explained above and the accuracy of the analyses was good enough for the purpose of the present analyses. The final radial displacements at the crown, springline, and floor are 29.4 mm, 29.9 mm, and 30.7 mm respectively.

The material properties used for the hyperbolic model are obtained from the passive compression triaxial tests, σ_3 constant and σ_1 increasing, as determined by Negro (1988). The hyperbolic parameters are $K_L=83$, $n=0.92$, $\phi=16^\circ$, $c=45$ KPa, $\nu=0.47$, $K_{ur}=100$ and $R_f=0.95$. The results of the two-dimensional analysis, assuming a hyperbolic material model, are shown in Figure 5.11. The ground reaction curves show the elastic and plastic behaviour of the ground and do not intersect the horizontal axis, indicating that the excavation cannot be stable without a liner. The internal pressure can be released until step 7 which is equivalent to a 60 % stress release of the in-situ stress, with the displacements increasing drastically from step 8, indicating the collapse of the tunnel. The failure of ground around the opening takes place because the difference between the major stress and the minor stress increases at the tunnel boundary due to the increase of stress release, which causes the tangent modulus to be reduced to close to zero in step 8. Figure 5.11 shows the ground reaction curves from step 1 to step 7 only. The displacements from the analysis of step 7 at the crown, springline and floor are 54.4 mm, 48.6 mm and 40.4 mm respectively.

The parameters for an elastic-plastic model are $E=30000$ KPa, $\nu=0.4$, $c=50$ KPa and $\phi=16^\circ$. The ground reaction curves obtained from the two-dimensional finite element analysis, assuming an elastic-plastic model, are presented in Figure 5.12. The diagram shows the ground reaction curves up to step 10, which is equivalent to a 90 % stress release of the in-situ stress. The radial deformation increases rapidly in step 11, showing the collapse of the tunnel. The ground reaction curves show an elastic behaviour at the small displacement range up to about 17 mm and plastic behaviour after the limit. The curves also show that the excavation is unstable without a support system. The radial displacements from the analysis of step 10 at the crown, springline and floor are 175.6 mm, 164.2 mm and 148.9 mm respectively.

The ground reaction curves from the theoretical equations are presented in Figure 5.13 for comparison with the above results. These curves are derived from the formulation presented by Kaiser (1980) for a circular tunnel excavated in a material that is assumed to be linearly elastic, brittle-perfectly plastic, with yield surfaces described by the Coulomb failure criterion. The parameters for the equations are $E=30000$ KPa, $\nu=0.4$, $c=50$ KPa, $\phi=16^\circ$, strength ratio=0.9, and $\alpha=1$. The parameter α is a measure of the dilation occurring during plastic flow. The ground reaction curves show a linear elastic behaviour up to about 23 mm of radial deformation and begin to add plastic deformation after that. The ground reaction curves intersect the horizontal axis. The final radial deformation at the crown, springline, and floor are 175.4 mm, 203.9 mm, and 235.7 mm respectively.

5.3.5 Evaluation of 2-D FEM combined with CCM

The convergence curves of crown, springline, and floor from the numerical analyses and theoretical equations are plotted with the confinement curves from the field measurements in Figure 5.14, Figure 5.15, and Figure 5.16 respectively. El-Nahhas (1980) obtained the convergence-confinement curves of the tunnel from the combination of displacement measurements of the ground and displacement and load measurements of the liner.

The displacements of the ground were measured using multipoint and single point extensometers. The changes in the vertical and horizontal diameters of the liner were measured using a constant tension tape extensometer. The loads on the liner were obtained from the vibrating wire load cells, surface vibrating wire strain gauges, and embedded vibrating wire strain gauges.

A couple of problems occur when attempting to draw convergence-confinement curves from the field measurements even though the author presented the curves. First, the lining instruments were installed about 200 m away from the soil instruments. Ideally, the lining instruments should be installed in the same section as the soil instruments because the properties of the ground and the depth of the tunnel could vary along the tunnel sections. Second, the convergence curves should be drawn either assuming a linear

elastic soil model or using interpolation between the in-situ state point before excavation and the point obtained from the combination of measurements from the ground and liner because the pressure of the ground for each displacement before the installation of the liner is unknown. Therefore, only confinement curves at the crown are shown in the figures based on the measurements of soil displacements before liner installation, diameter changes of the liner, and loads on the liner. The confinement curves at the crown are also plotted with the confinement curves of springline and floor for comparison because the confinement curves for the springline and floor would be similar to those from the crown.

The convergence curves are almost linear up to 15 mm of radial displacement, which can be predicted well by a linear elastic model. The convergence curve from the hyperbolic model does not agree with other results including field measurements possibly due to the stress paths around the excavation, which are different from the laboratory tests used for obtaining related parameters. The radial stress around the opening decreases, whereas the tangential stress increases due to excavation. However, the material properties used for the hyperbolic model were obtained from the passive compression triaxial tests, σ_3 constant and σ_1 increasing.

The convergence curve from the linear elastic model underpredicts the radial displacements as expected because the plastic deformation was not considered. Furthermore, except for the linear portion of convergence curves ranging up to 15 mm of radial displacement, the curve from the linear elastic model underpredicts the radial stress for a certain amount of the radial displacement compared to those from other curves. The result from the theoretical equations shows good agreement with the lower bound field measurements but underpredicts the final load on the liner for the upper bound field measurements, which is on the unsafe side. The convergence curve from the elastic-plastic model matches pretty well with the final equilibrium point of the upper bound field measurements as shown in Figure 5.14.

5.4 Displacements before Liner Installation

The above results encourage the use of convergence curves to find the final load and displacement around a tunnel if the proper material model can be applied. However, the radial displacement before the liner installation, U_i , is a major unknown when using the method in practice as mentioned before. Daemen and Fairhurst (1972) recognized the importance of the effect of U_i on the support load and derived an approximate solution of lining load for the support delay effect. The displacement U_d , which is the difference between U_o^e and U_i , can be expressed as follows:

$$U_d = XU_o^e = X \frac{P_o R(1 + \nu)}{E}$$

$$X = \frac{U_o^e - U_i}{U_o^e}$$

The support pressure can be obtained as follows:

$$\frac{P_s}{P_o} = X \left[1 + \frac{E(1 + \nu_l) \left[(1 - 2\nu_l) + (1 - t/R)^2 \right]}{E_l(1 + \nu)(2 - t/R)(t/R)} \right]^{-1}$$

where P_o = in-situ stress

P_s = reduced lining load due to support delay

t = support thickness.

The authors suggested that only one finite element analysis with an axisymmetric elastic solution for an unlined tunnel was needed to determine U_i for the calculation of X .

Einstein and Schwartz (1980) compared the lining loads from Daemen and Fairhurst's approximate solution and from the elastic axisymmetric finite element analyses and concluded that the results were reasonably close for the fully supported cases, but the errors from the approximate solution become intolerable as the support delay was increased. Therefore, to use only one finite element analysis for calculating U_i and X is inadequate because the installation of a support changes the radial displacement distribution along the tunnel section.

Hocking (1976) presented solutions for the vertical displacement profile along the flat end of a cylindrical cavity in an infinite, homogeneous, isotropic and linear elastic

medium using the boundary integral equation method. The author concluded that 80 % of the vertical elastic displacement of the crown would occur within 0.75 radii from the face.

Ranken (1978) performed axisymmetric finite element analyses for advancing tunnels to determine the amount of displacement before installation of the liner for $K_0=1$ conditions in elastic and elastic-perfectly plastic ground. Only three cases were simulated with respect to the location of liner installation: at the advancing tunnel face, at a distance of one tunnel radius behind the face and at a point far behind the face. The results of analyses indicated that most of the displacements occurred ahead of the leading edge of the liner and for linings installed at more than one tunnel radius behind the face, the displacement taking place ahead of the face is independent of whether the tunnel is lined or unlined, results which were confirmed by Hutchinson (1982) from the axisymmetric finite element analyses. However, Ranken could not come to any general conclusions that could be used for actual tunnel design.

Panet and Guenot (1982) derived a function that gave tunnel closure for a deep tunnel in terms of the distance to the face from the axis-symmetric finite element analyses using an elasto-plastic material model. The results show that the radial displacement at the tunnel face, U_{fa} , is equal to 0.265 U_i in an elastic ground, where U_i is the radial displacement far behind the face. The displacement U_{fa} increases as the stability number increases in elasto-plastic material due to the development of plastic zones.

Heinz (1984) suggested taking the displacements occurring ahead of the face for the displacements U_i in NATM urban tunnels because the support should be placed as close as possible to the tunnel face to minimize ground displacements. However, the method could be too conservative for the estimation of lining loads and even unsafe for the estimation of displacements around tunnels especially when the shotcrete near the face is not hardened enough, as has been observed by many authors (Eisenstein and Negro, 1985; Wood et al., 1989; Eisenstein et al., 1991).

Negro et al. (1986) suggested a method to estimate the radial displacements at the face of shallow tunnels using a series of parametric three-dimensional finite element analyses. The radial displacement was expressed in the following dimensionless form:

$$U = U_{fa} E / (P_o D)$$

where D is a tunnel diameter with in-situ radial stress P_o . The method was supported by a large number of case histories. The authors showed that for soils exhibiting a limited plastic zone ahead of the advancing tunnel face such as in the case of stiff or dense soils, the dimensionless radial displacements at tunnel face could be estimated as follows:

$$U_c = 0.26 \text{ for the crown}$$

$$U_s = 0.17 \text{ for the springline}$$

$$U_f = 0.12 \text{ for the floor.}$$

Pelli (1987) carried out three dimensional finite element analyses using the program ADINA to study the near face behaviour of deep tunnels in linear elastic rock. The results will be discussed in detail in the next chapter. Negro (1988) performed three-dimensional finite element analyses to determine the effects of the delayed installation of the lining. The radial deformation of the crown at the lining activation is about 9 mm for the experimental tunnel based on the method presented by the author, which is much smaller than the actual measurement of about 33 mm because the method was mainly developed for shallow tunnels.

Eisenstein and Branco (1990) suggested obtaining the displacement U_i by using the addition of two ground displacements:

a) ground displacements that occur at the face: assumed to be one third of the final elastic displacement of the unlined tunnel based on the results of Ranken and Ghaboussi (1975)

b) ground displacements that occur along the length of the TBM are assumed to be one half of the difference between the excavated diameter and the diameter of the expanded primary lining.

Since the measured displacement at the face was about 15 mm, which is an elastic range according to Figure 12, the displacement at the face can be considered as one third of the final elastic displacement of the unlined tunnel. The above approximation is valid up to the stability ratio of 2 or 2.5 for the cohesive soil as shown in the study of Panet and Guenot (1982). However, to apply (b) is not easy because of the difficulties of finding the excavated diameter and the diameter of the expanded primary lining, both of which could

vary along the tunnel. The experimental tunnel was excavated using a shielded mole. The question is which length can be considered as an unsupported section along the tunnel.

Many field measurements showed that the ground moved into the gap left by the skin and tail of the shield (Ward, 1969; Muir Wood, 1969; Belshaw and Palmer, 1978). In the experimental tunnel, small gaps were observed between the lining and the soil just after expansion of the liner. Utilizing the inspection holes, their width was measured and found to be 2-3 mm. Therefore, expanding the segmented concrete lining could be considered to practically eliminate the annular space around the tunnel. The liner was activated about 2.4 diameters away from the face according to the field measurements and the shield could not prevent the soil displacement in the experimental tunnel either. In other words, the shield does not act as an extension of the liner.

Because the experimental tunnel can be considered a deep tunnel in cohesive soils with a stability number of about 1.7, which is less than 2 and the liner was activated far away from the face, the radial displacement before the liner installation could be approximated by an equation of the final elastic displacement of the unlined tunnel, U_o^e . The radial deformation of the crown from the equation is about 29 mm, which is quite close to actual measurement of 33 mm.

Even though linearly elastic ground is assumed for the radial displacement before the liner installation, the convergence curve from the linear elastic model cannot be used for the estimation of lining loads because a tunnel in a truly elastic ground mass does not need any support. Therefore, determining the convergence curve for a specific soil type is crucial for the method. The final loads on the liner obtained using the combination of convergence curves from the finite element method and the displacement U_o^e are generally on the safe side because the deformation from the equation is usually less than that from the actual measurement. However, the gap between the shield and soil should be bigger than U_o^e to use the U_o^e for U_i . As well, the ground should be stiff.

5.5 Limitations of 2-D FEM combined with CCM

The use of 2-D finite element methods combined with CCM gave reasonable results for the estimation of the final load and displacement around a tunnel if the proper

material model could be applied. However, the CCM has a major limitation because the face effects on the ground and lining behaviour are neglected. The radial displacement before the liner installation is a major unknown when using the method in practice. Determining the convergence curve for a specific soil type is also crucial for the method.

According to Negro (1988), with tunnel liner activation specified to take place at one diameter behind the face, most tunnels clearly show three-dimensional behaviour within the region bounded by one to two diameters ahead of the face to one diameter behind the location of liner activation. The extent of the three-dimensional zone is mainly a function of the distance between the face and the point of lining installation and the strength of the soil.

The ground displacements occurring ahead of the face cannot be considered even in the two-dimensional finite element analyses. In addition, two-dimensional analyses cannot model the fact that as the tunnel advances, the excavation is done in a zone ahead of the face in which the stress condition has already been changed by the approach of the face.

In summary, although the use of 2-D finite element methods combined with CCM could give reasonable results for the estimation of the final load and displacement around a tunnel, it is still difficult to draw any general conclusions that can be used for actual tunnel design from the results mainly due to the limitations of the ground and support properties applied for the analyses and the complexity of ground behaviour for different construction methods. Furthermore, the radial displacement before liner installation is very difficult to estimate.

5.6 Summary and Conclusions

The convergence-confinement method is one approach to the analysis of ground-support interaction. The method was reviewed in detail in this chapter. The CCM has a great advantage in explaining the phenomena governing the ground-liner interaction. However, the method may not be appropriate as a direct design tool except for special cases such as deep tunnels and highly pressurized ground due to the limitations mentioned in Sec. 5.2.2. To have a better understanding of the method, especially the

effect of a material model on the convergence curve, two-dimensional finite element analyses were performed.

The procedures to simulate the excavation for two-dimensional analyses were presented in Sec. 5.3.2. The convergence curves were obtained from two-dimensional finite element analyses using three different material models and theoretical equations. The limitation of the use of 2-D finite element methods combined with CCM for the estimation of the final load and displacement around a tunnel was discussed by comparing these curves with the actual field measurements obtained from a tunnel in Edmonton.

Most tunnels clearly show three-dimensional behaviour within the region bounded by one to two diameters ahead of the face to one diameter behind the location of liner activation. The ground displacements occurring ahead of the face could not be considered in the two-dimensional finite element analyses. In addition, two-dimensional analyses can not model the fact that as the tunnel advances, the excavation is done in a zone ahead of the face in which the stress condition has already been changed by the approach of the face.

To gain a better understanding of stress and displacement behaviour near the tunnel face, three-dimensional finite element analyses are performed in the following chapter. The influence of the construction sequences in ground-support interaction is investigated using the 3-D analyses. The possible causes of the differences in the final equilibrium stresses and displacements on the liner between the 2-D and 3-D analyses are also presented.

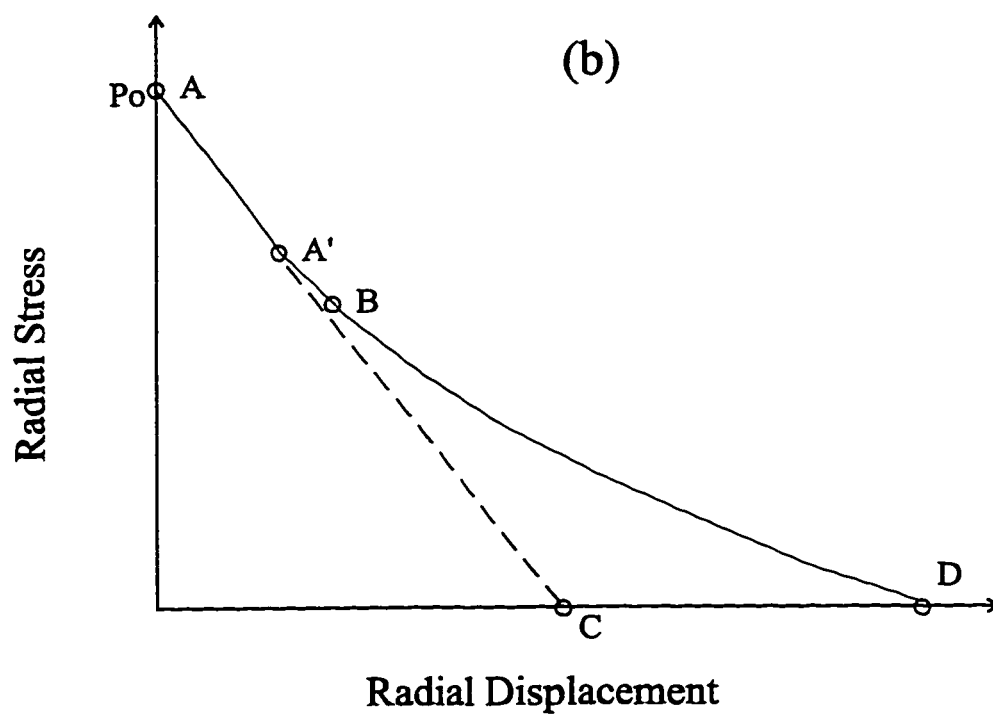
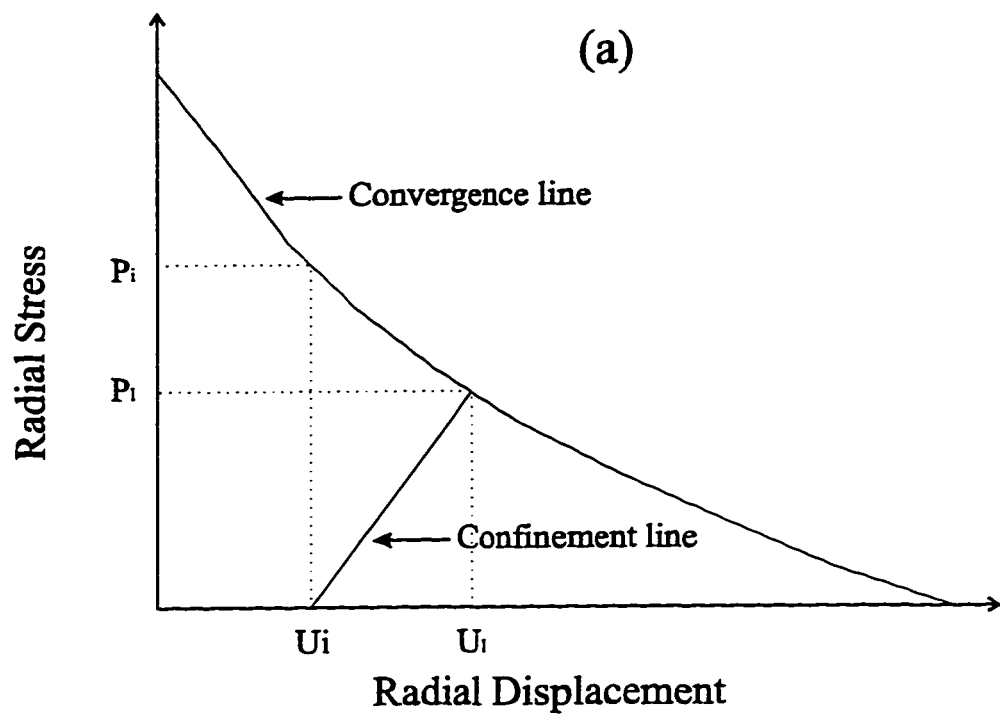


Fig. 5.1 a) Concept of Convergence-Confinement Method
b) Elastic and Plastic Material Behaviour

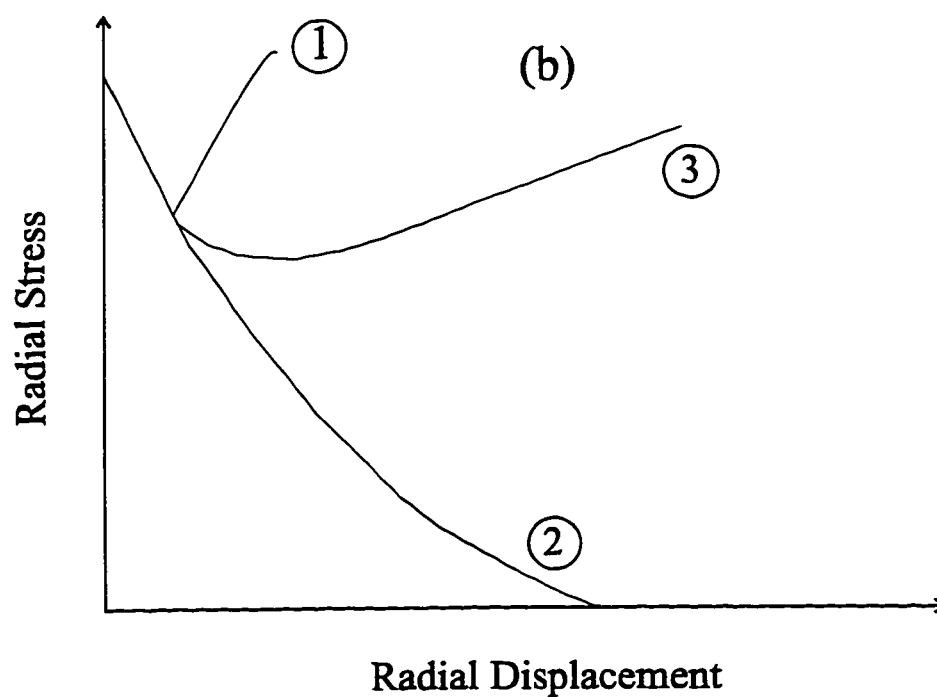
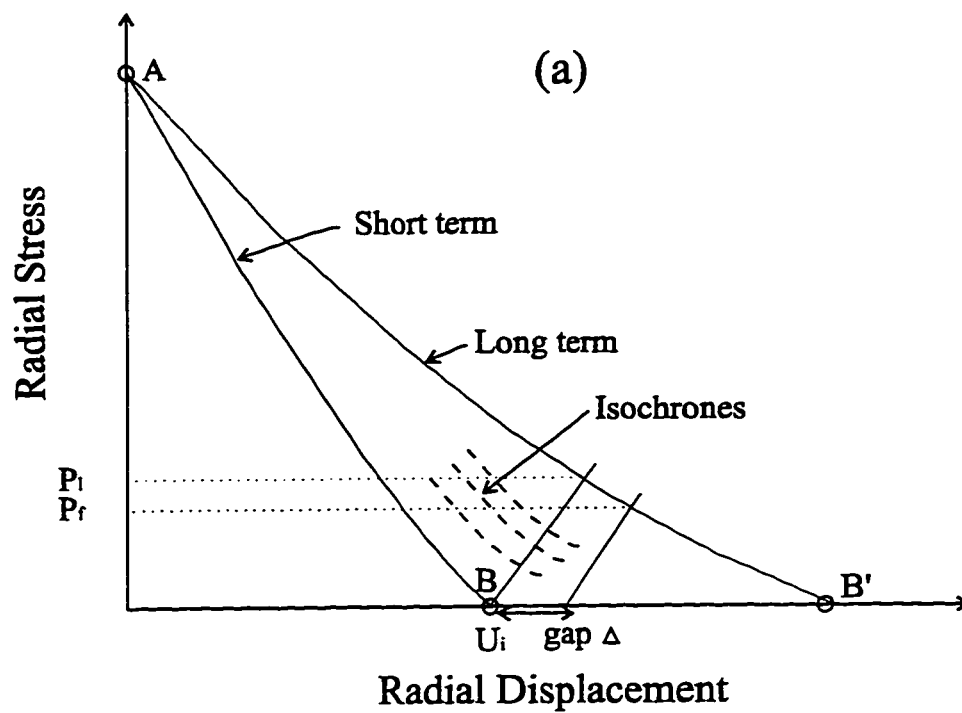


Fig. 5.2 a) Short Term and Long Term Convergence Curves
(Modified after Ladanyi, 1974)
b) Three Different Types of Convergence Curves

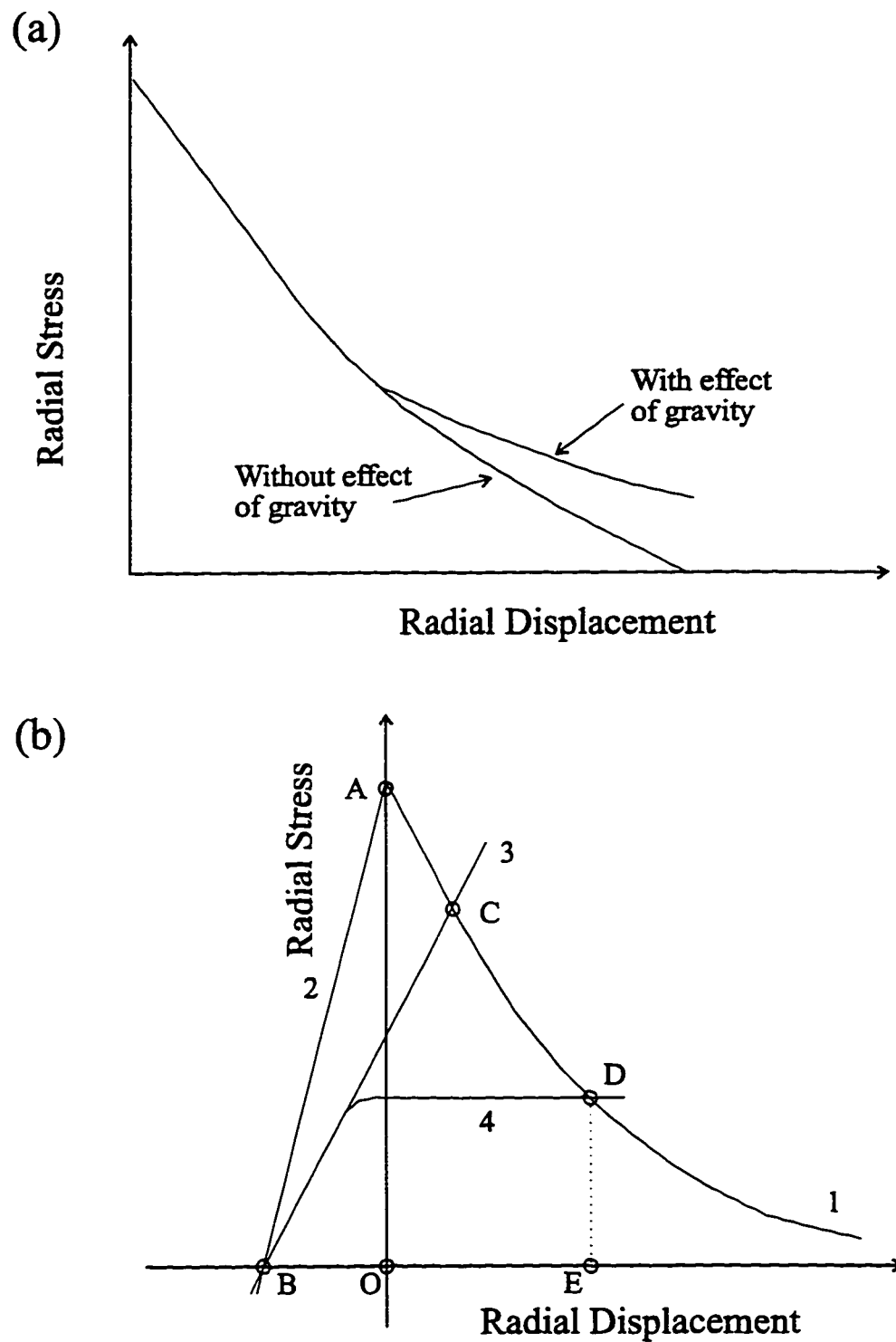


Figure 5.3 a) Effect of Gravity on the Convergence Curve
 b) Convergence Curves for the Excavation and Core
 (Modified after Lombardi, 1980)

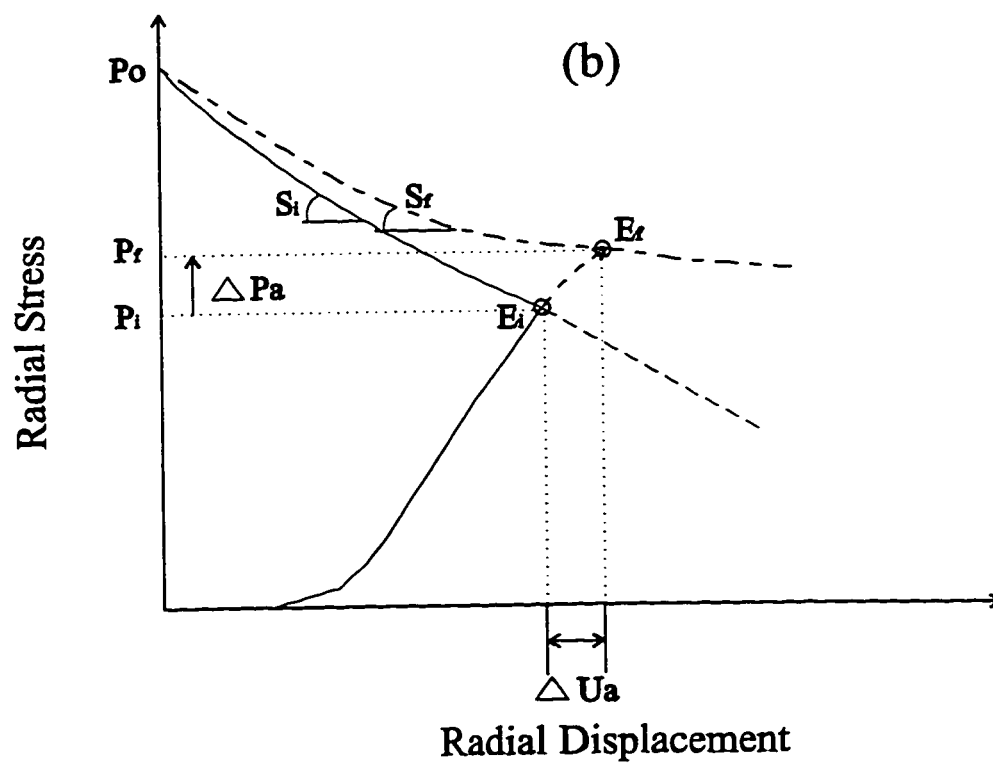
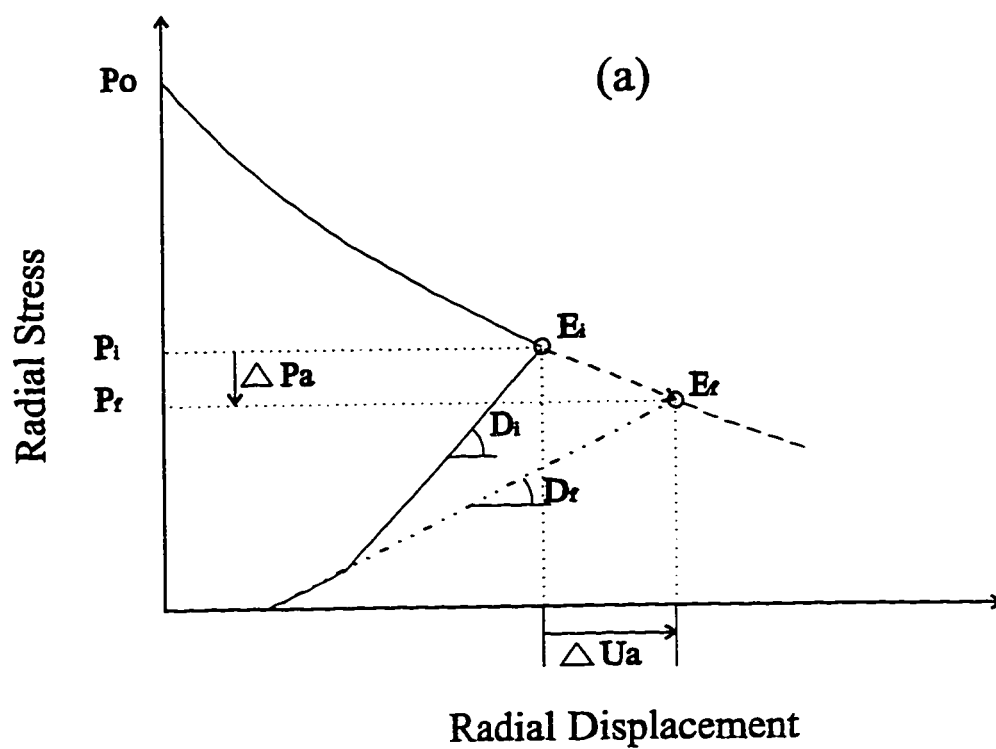


Fig. 5.4 a) Creep of Concrete Liner b) Creep of Ground
(Modified after Duddeck, 1980)

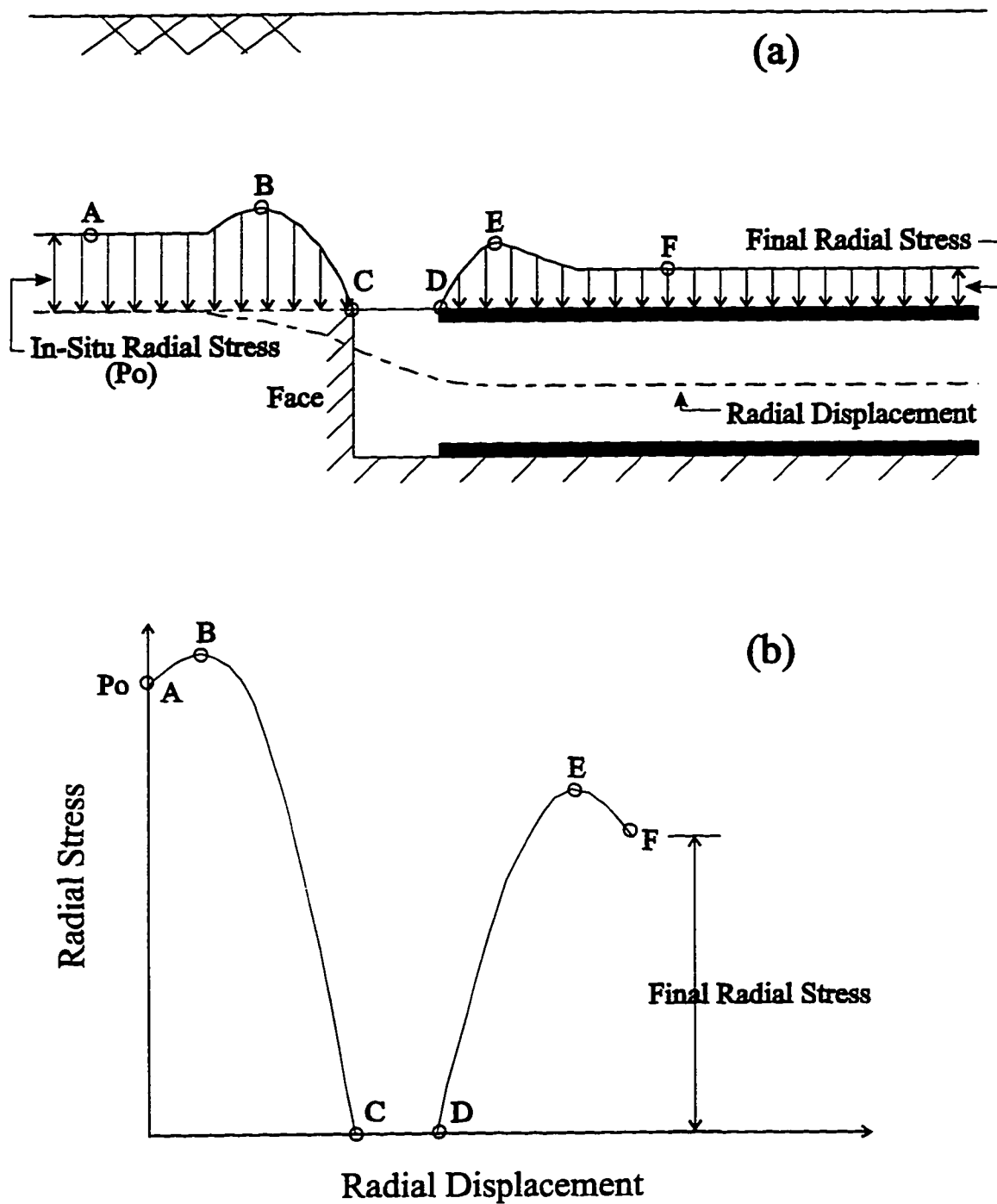


Figure 5.5 a) Radial Stress and Displacement Distribution along the Crown b) Ground Response at the Crown (Modified after Eisenstein et al., 1984)

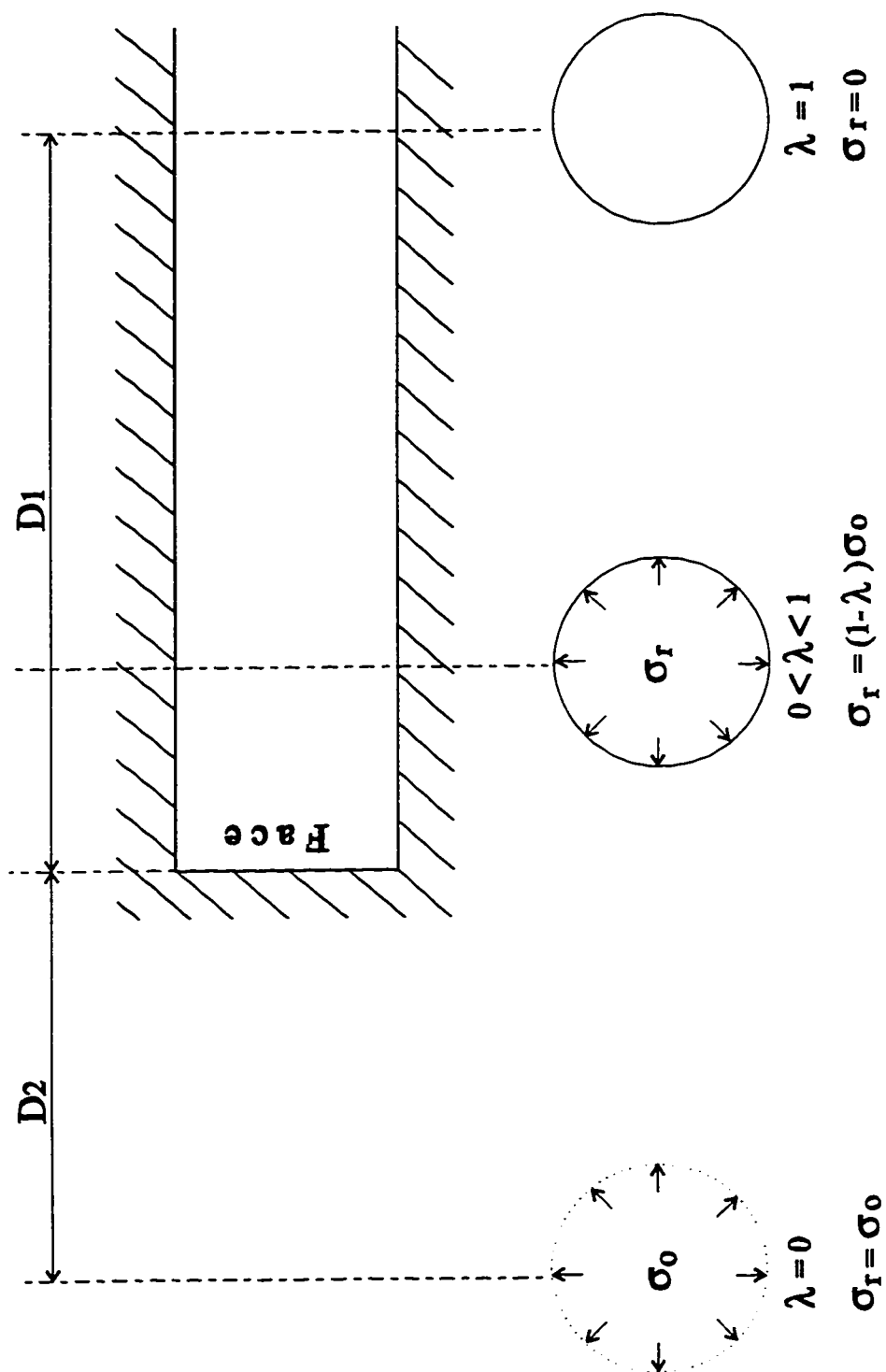
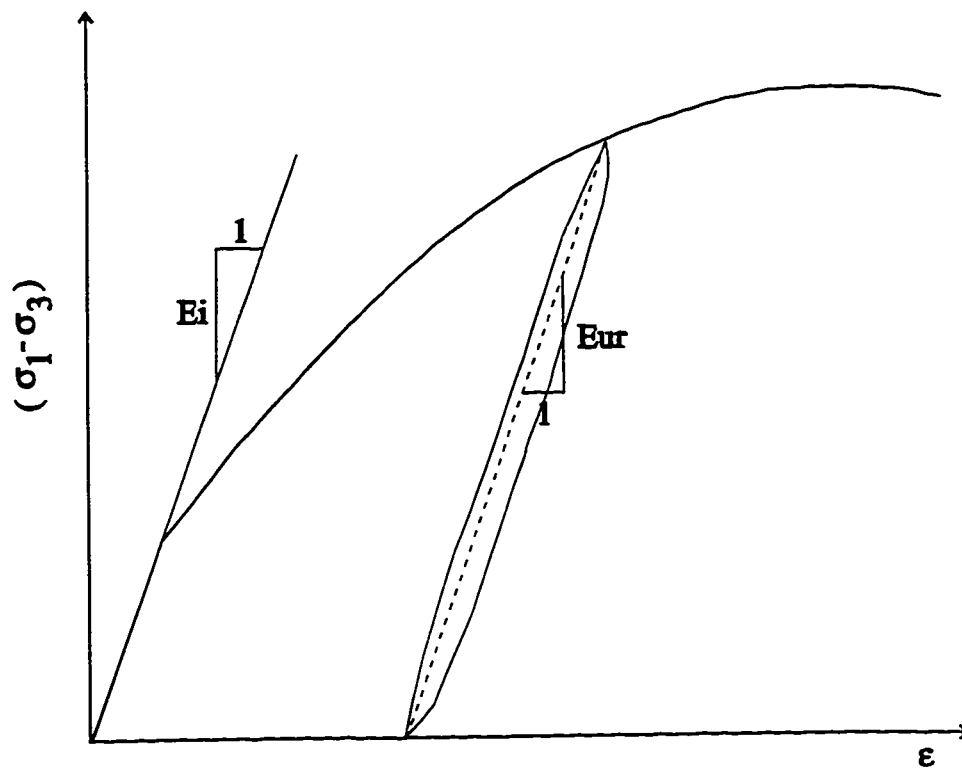


Figure 5.6 The Reduction of 3-D Problem Due to the Tunnel Face to a Problem of Plane Deformation (Modified after Panet, 1976)



$$E_i = K_L Pa (\sigma_3 / Pa)^n$$

$$E_t = E_i \{1 - [R_f (1 - \sin \Phi) (\sigma_1 - \sigma_3)] / [2c \cos \Phi + 2\sigma_3 \sin \Phi]\}^2$$

$$E_{ur} = K_{ur} Pa (\sigma_3 / Pa)^n$$

where

E_i = initial in-situ modulus as a function of confining stress σ_3

K_L = loading modulus number

Pa = atmospheric pressure

n = exponent for loading behaviour

E_t = tangent modulus

R_f = failure ratio

E_{ur} = unloading-reloading modulus

K_{ur} = unloading-reloading modulus number

Figure 5.7 Illustration of Hyperbolic Model

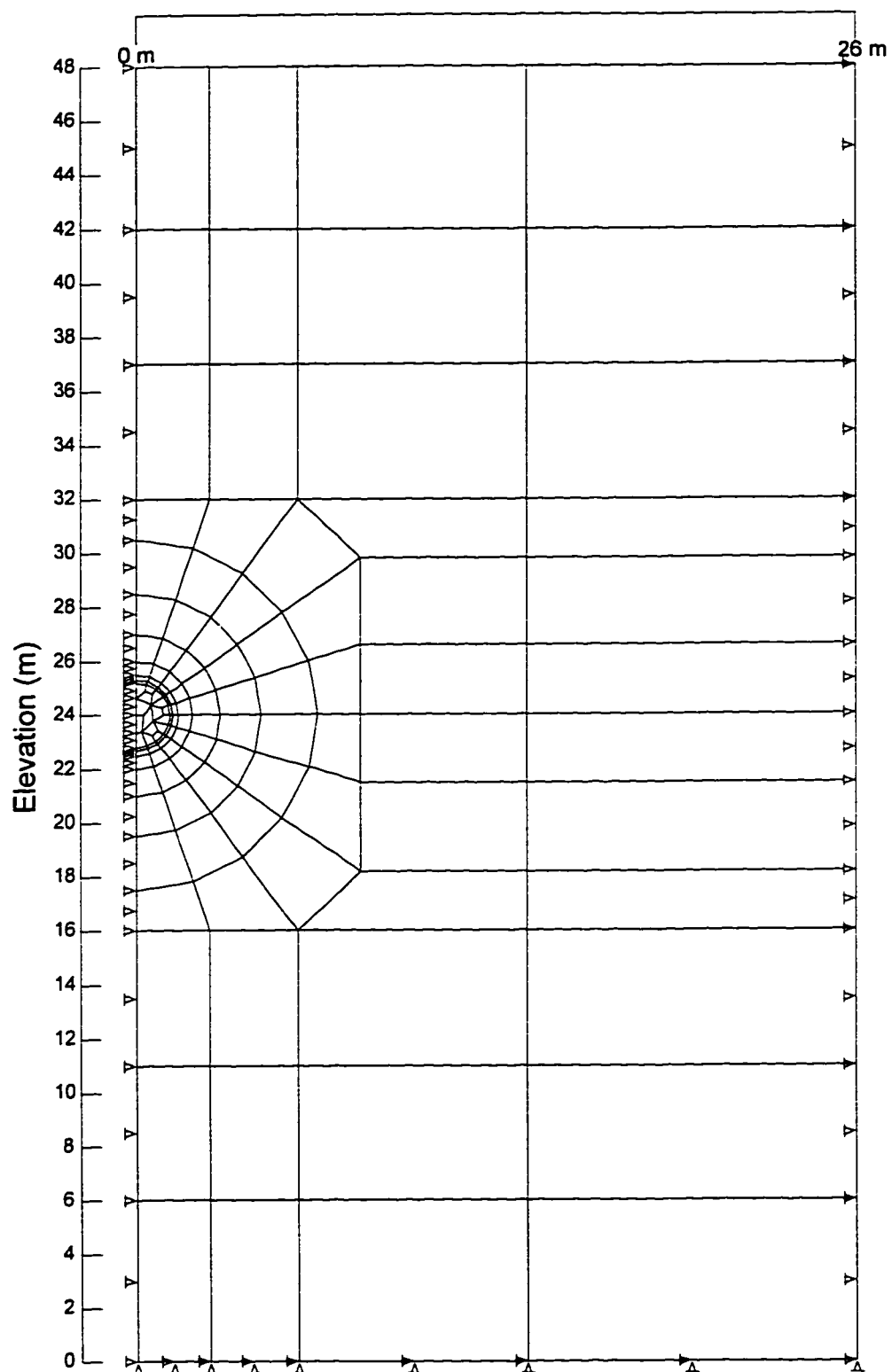
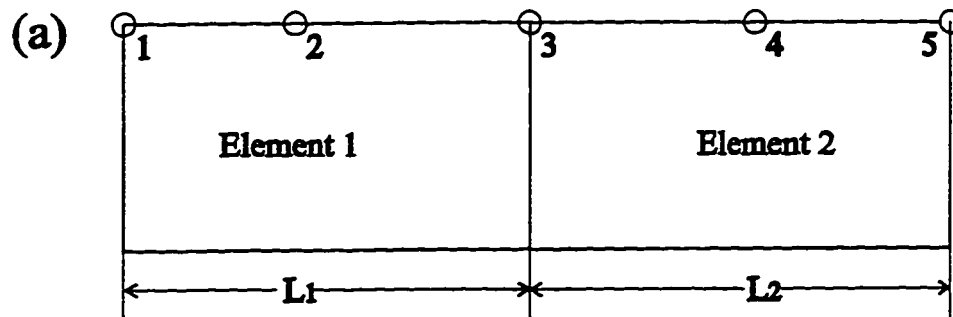


Fig. 5.8 Two-Dimensional Meshes of the Experimental Tunnel



$a_1 = L_1/6$ (Contributing Area for a node 1)

$a_2 = 4L_1/6$ $a_3 = L_1/6 + L_2/6$

$a_4 = 4L_2/6$ $a_5 = L_2/6$

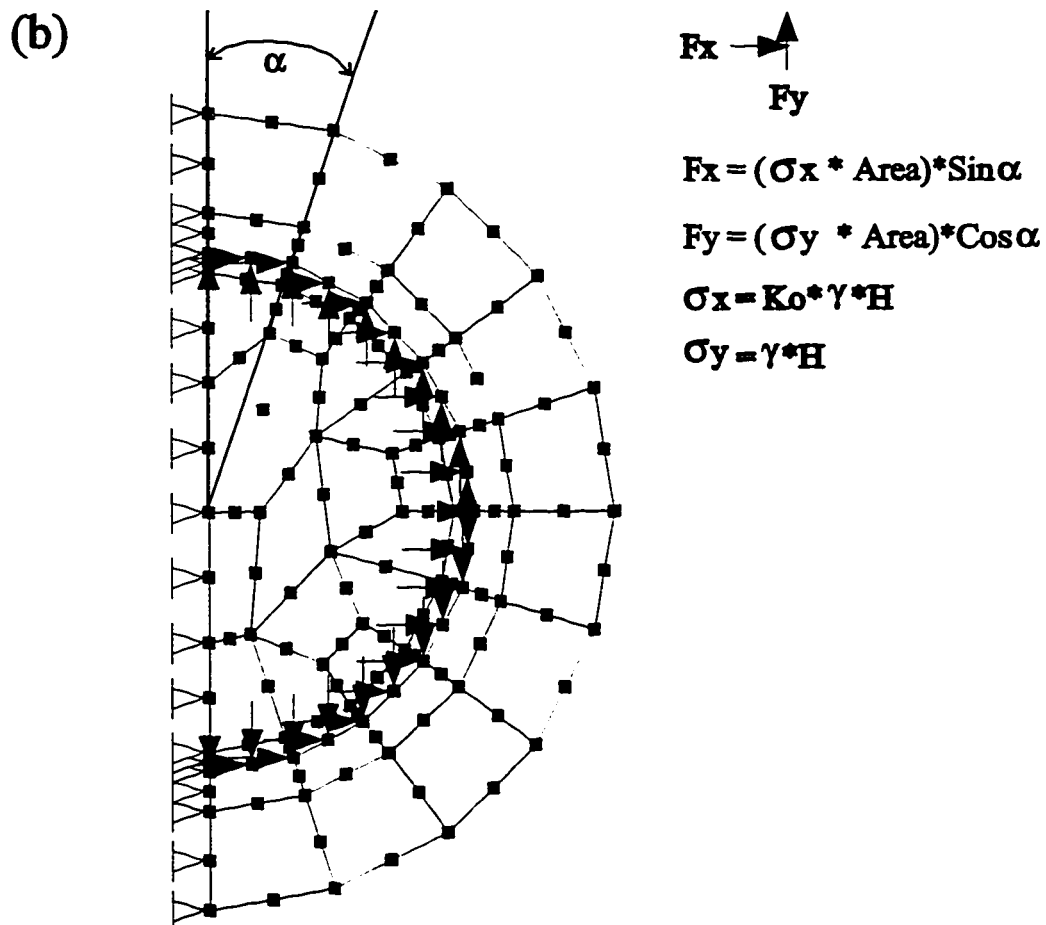


Figure 5.9 (a) Contributing Areas for Uniform Stresses
(b) Calculation of Equivalent Loads for Initial Stresses

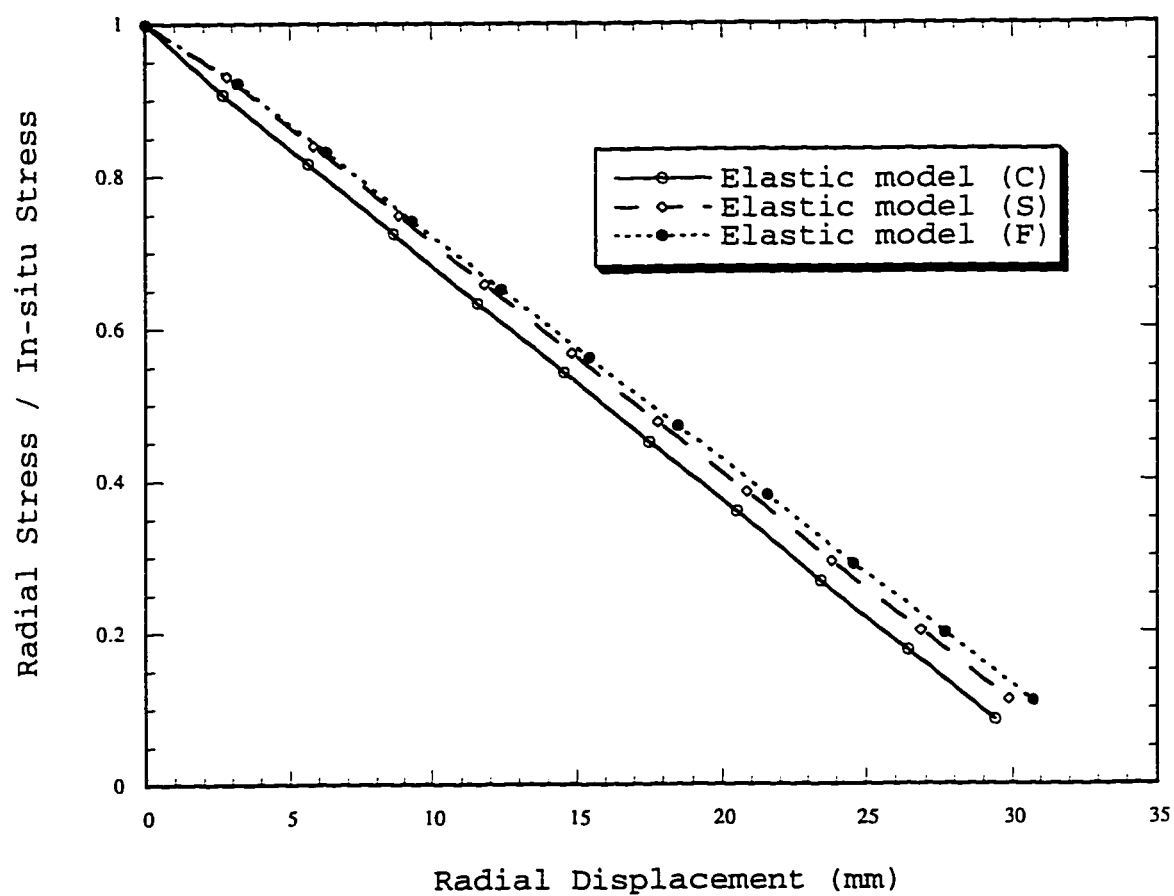


Figure 5.10 Ground Reaction Curves for the Experimental Tunnel in Section 3 (Elastic Model)

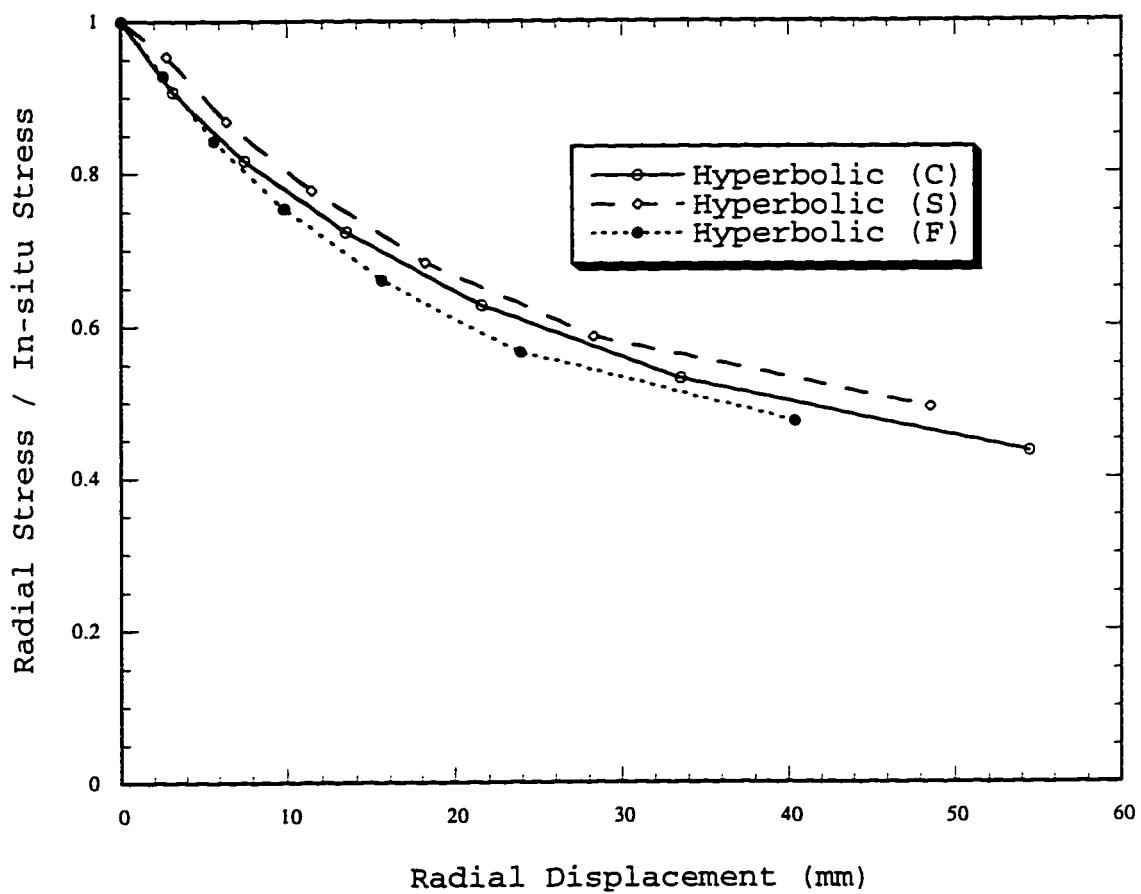


Figure 5.11 Ground Reaction Curves for the Experimental Tunnel in Section 3 (Hyperbolic Model)

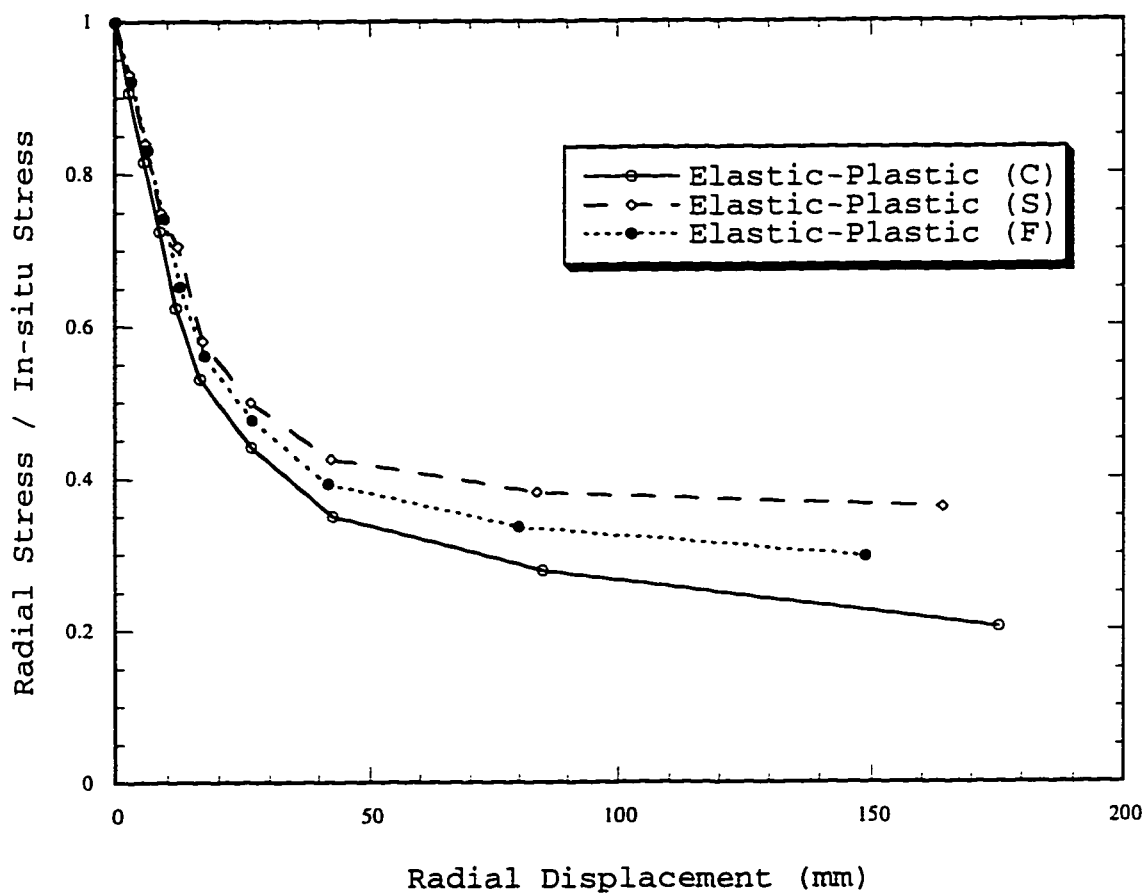


Figure 5.12 Ground Reaction Curves for the Experimental Tunnel in Section 3 (Elastic-Plastic Model)

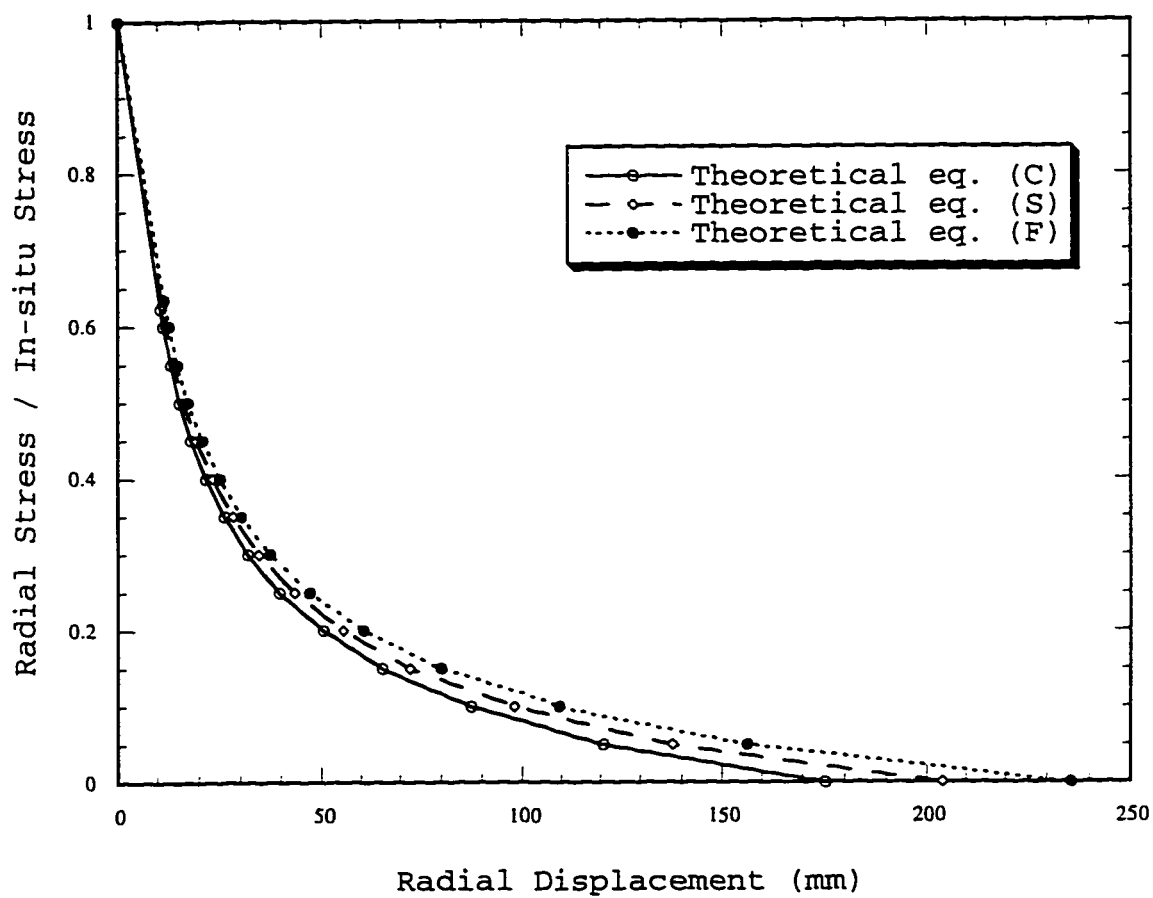


Figure 5.13 Ground Reaction Curves for the Experimental Tunnel in Section 3 (Theoretical Equation)

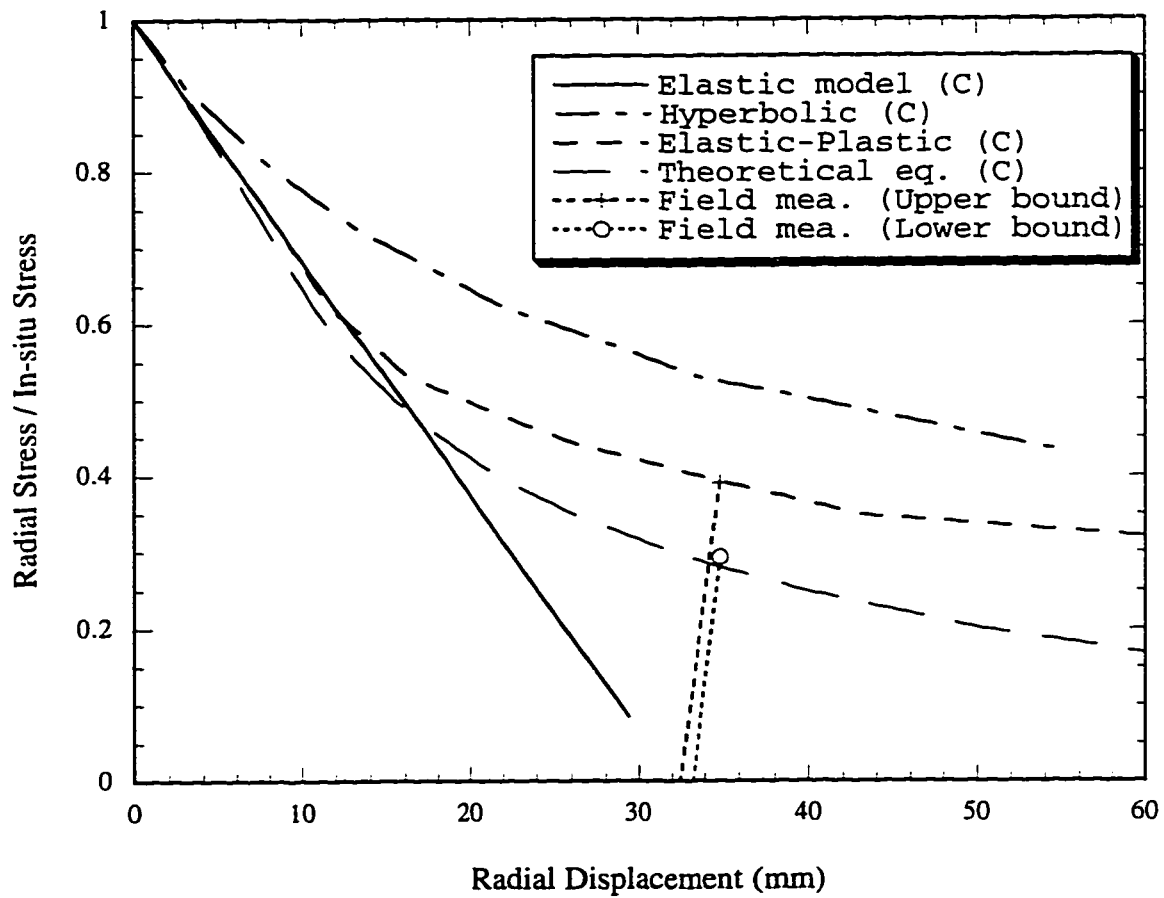


Figure 5.14 Ground Reaction Curves for the Crown of the Experimental Tunnel in Section 3

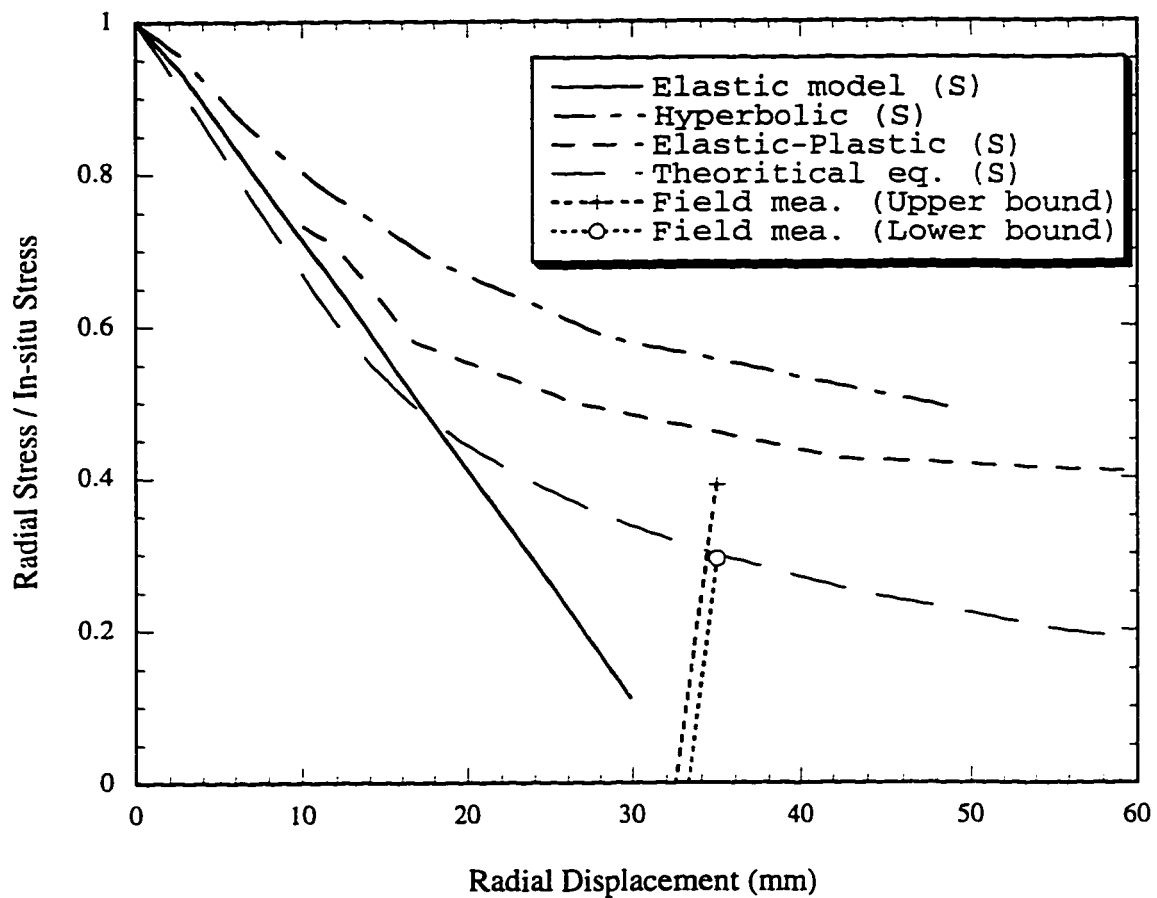


Figure 5.15 Ground Reaction Curves for the Springline of the Experimental Tunnel in Section 3

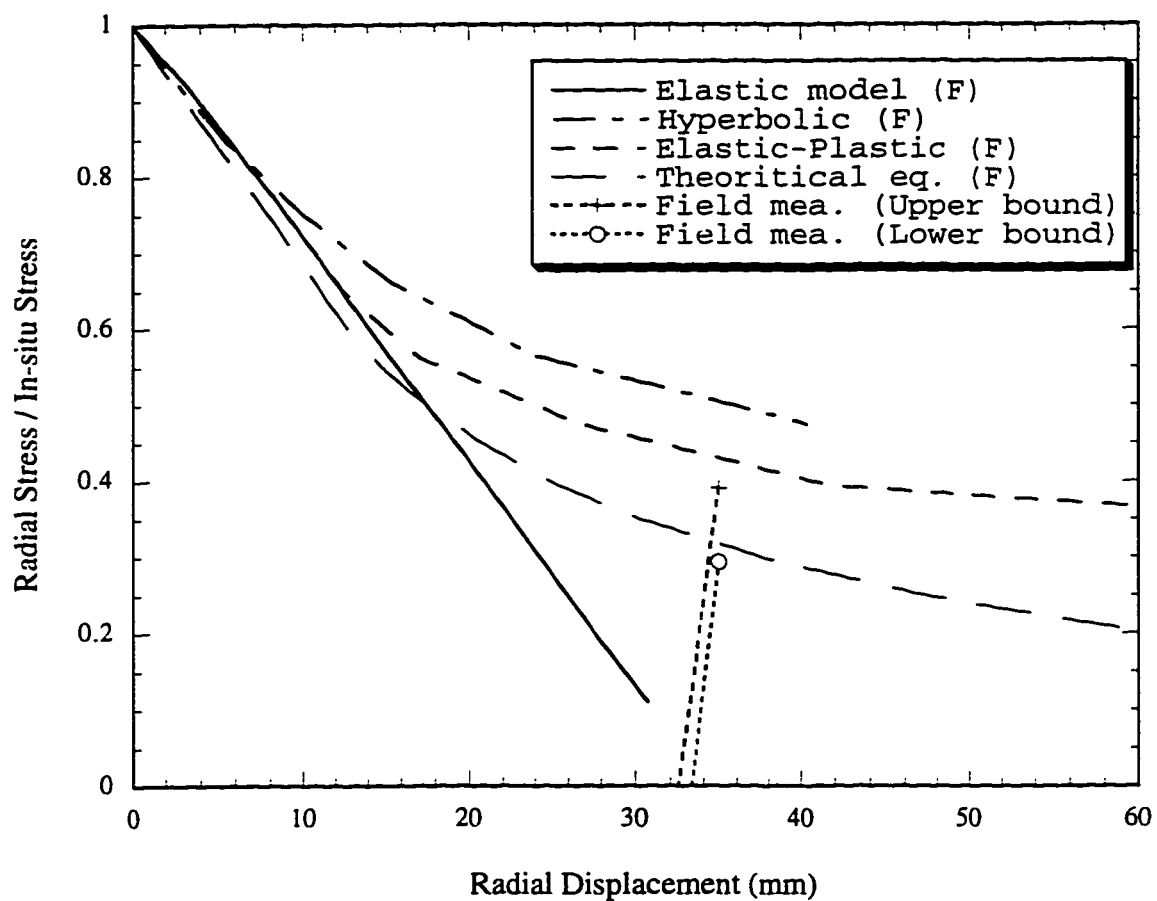


Figure 5.16 Ground Reaction Curves for the Floor of the Experimental Tunnel in Section 3

6. Three Dimensional Response of Ground

6.1 Introduction

The plane strain finite element analysis is still widely used for tunnel designs because of its simplicity and low cost compared to three-dimensional finite element analyses. However, in the vicinity of the advancing face, the longitudinal displacements are not zero. Field observations by El-Nahhas (1980) in the Edmonton experimental tunnel showed that the longitudinal strains reached their maximum values near the tunnel face and decreased to zero about 3.5 diameters ahead of the face and 4 diameters behind the face. The extent of this zone is a function of several parameters such as the position of liner installation relative to the face, the stiffness of the liner, the magnitude of the in-situ stresses and the shear strength of the ground.

Ranken (1978) showed that the zone extended with the increase of plastic yielding in the ground. The three-dimensional zone, particularly ahead of the advancing tunnel face, also increased as the distance between the face and the point of lining installation and the soil strength decreased according to the axisymmetric analyses performed by Ranken. Based on the literature reviews, Negro (1988) estimated the extent of the zone as one to two diameters ahead of the face to one diameter behind the location of liner activation for the tunnels with liner activation specified to occur at one diameter behind the face.

Eisenstein and Branco (1985) observed the longitudinal movement of the ground ahead of the advancing face towards the face using inclinometers. The soil moved back to its original position after the TBM passed by the points that initially moved towards the face. Therefore, the final differential longitudinal displacements from the field measurements were small close to a two dimensional plane strain condition. However, as Branco (1981) pointed out, the response of strain path dependent soil would not be completely described in a two dimensional plane strain representation because the strains were not zero during the tunnel advance.

In addition, as mentioned in the previous chapter, the plane strain analyses have difficulty determining the relationship between the position of liner installation and the amount of ground displacement occurring before installation of the liner. Furthermore,

two dimensional analyses cannot model the fact that as the tunnel advances, the excavation is done in a zone ahead of the face in which the stress condition has already been changed by the approach of the face. Therefore, in order to gain a better understanding of stress and displacement behaviour near the tunnel face, three-dimensional finite element analyses were performed and presented in this chapter.

6.2 Three Dimensional Arching around an Advancing Tunnel

The excavation of ground causes a load redistribution around the tunnel. Some of the redistributed load is transferred to the lining and some to the unexcavated ground ahead of the face. In the idealized two dimensional plane strain ground response, the face advance was represented by a gradual and continuous reduction of the in-situ stress as shown in Figure 5.6. Only the arching in the transverse plane has been considered in the two dimensional ground.

Eisenstein et al. (1984) presented the three dimensional arching near the face of an advancing tunnel caused by delayed lining installation as shown in Figure 6.1. The maximum principal stress trajectories were shown schematically using arrows in the figure. In addition to the transverse arching existing in the two dimensional ground, a similar stress transfer mechanism develops in the longitudinal direction of the tunnel over the unsupported section between the ground ahead of the tunnel face and the installed lining. The horizontal arching also exists in the longitudinal direction between the lining side walls and the ground ahead of the face. Therefore, the arching above the unsupported section is of a three-dimensional nature due to shear stress mobilization all around the opening, which can be modelled only in three-dimensional analyses.

6.3 Review of Three-Dimensional Modelling by the F.E.M.

Gartung et al. (1979) performed three dimensional finite element analyses for the 13 m wide section of a subway tunnel in Nuremberg to check the stability of the tunnel face. An elasto-brittle plastic material model was assumed for the sandstone, and the heading-bench excavation sequence was simulated. A total of 16 slices, with 51 elements for each slice, were used for the finite element mesh. The shotcrete was modelled using

shell elements with linearly elastic properties whereas internal pressure was applied at the wall of the tunnel to account for the action of the tensioned rock bolts. Several conclusions were obtained from the analyses. The initial state of stress showed obvious changes 2 m ahead of the tunnel face. The three dimensional arching effect could be shown from about 2 m ahead of the tunnel face to 6 m behind the face. The gradual transition from fully three dimensional to plane strain conditions was observed between 6 and 12 m behind the tunnel face.

Katzenbach and Breth (1981) investigated the critical zones of the ground around the opening and the safety of a 6.7 m diameter tunnel excavated by NATM in Frankfurt clay using three dimensional finite element analyses. The soil behaviour was approximated by a hyperbolic stress strain model. A total of 15 slices and 990 finite elements were used for the analyses. A full face excavation sequence was simulated for each step with a total of 15 steps. The final plots of horizontal, vertical and longitudinal strains clearly showed the three dimensional behaviour of arching around the opening. The authors also observed that the vertical stress started to increase from the in-situ stress three diameters ahead of the tunnel face and showed a vertical stress concentration 1.5 m ahead of the face. Beyond the stress concentration point, the vertical stress decreased rapidly because of the high longitudinal extension and the loss of horizontal support. Finally, the authors concluded that the safety of a tunnel depended on the depth of the tunnel beneath the surface, the tunnel diameter, the distance between the tunnel face and closed ring and the strength of the ground.

Pierau (1982) investigated the effects of the thickness of shotcrete and of the overburden depth on the ground surface settlements and on the stresses in the support using three dimensional finite element analyses. The excavation was simulated by reducing the modulus and the unit weight of the opening area to zero. A linear elastic material model was assumed for the ground with several E and ν values. Principal stresses plotted in a longitudinal section showed that the major principal stresses just ahead of the tunnel face were oriented roughly parallel to the face. The minor principal stresses oriented perpendicular to the face were approximately zero. The author also concluded that the settlements at the ground surface were highly dependent on the elastic

modulus of the soil but not on the thickness of the shotcrete. The loads on the lining increased considerably with increasing overburden but did not depend much on the thickness of the shotcrete, which varied between 10 and 30 cm.

Ghaboussi et al. (1983) performed finite element analyses to evaluate the influence of the sewer tunnel construction crossing over existing twin subway tunnels. First, two-dimensional plane strain analyses were carried out assuming a linear elastic soil model. The calculated stresses from the analyses showed conservative results due to the fact that ground displacements were not considered before liner installation in the subway tunnels and the limitation of the two-dimensional analyses for the shield jacking forces in the sewer tunnel. Even though the jacking forces were acting only along a section of subway tunnels where the sewer tunnel intersected, the forces were assumed to be acting along the whole length of the subway tunnels in the analyses. To obtain better results, a three-dimensional analysis of a single subway tunnel was performed with the proper location of jacking forces and compared with the results of the two-dimensional analyses. The authors showed that the computed stresses and displacements in the two-dimensional simulation of a sewer tunnel were conservative by at least a factor of two and five respectively compared to the results from the three-dimensional analysis due to the improper application of jacking forces. Therefore, the two-dimensional simulation of what is truly a three-dimensional geometry should be used with caution.

Heinz (1984) studied shallow tunnels excavated using the NATM with the three-dimensional finite element method. Selection of mesh size and appropriate simulation techniques were presented based on a literature review. According to an analysis of an ABV tunnel, the vertical displacements ahead of the face could be matched by the linear elastic model, which indicated that the behaviour ahead of the face did not depart much from the linear elastic assumption. The author also presented ground reaction curves by combining radial stress and displacement curves, which were obtained at the points approximately 0.2 m from the opening and at the excavation line respectively. The stress and displacement curves had to be smoothed out after superimposing the results from three consecutive steps of face advance because there was a considerable scatter of stresses and displacements behind the advancing face due to numerical inaccuracy. The

behaviour of the ground reaction curves was related to the advance of the tunnel including the three-dimensional nature of arching near the face, which caused the curves to be different from the convergence curve provided by CCM.

Pelli (1987) studied the distribution of stresses and displacements near the face of a deep unlined tunnel for the linear elastic, hyperbolic and elasto-plastic cases using three-dimensional finite element analyses. The in-situ stress ratio, $K_0=2$, was kept constant throughout the analyses. Only one quarter of a tunnel section was considered due to the assumption that the tunnel was deep. A total of 19 slices with 3145 nodal points and 988 finite elements were used for the analyses. Relatively low stress concentrations were observed ahead of the tunnel face in the non-linear cases due to more stress redistribution than for the linear elastic case. The radial displacements behind the tunnel face were larger for tunnels in non-linear cases than for tunnels in linear elastic cases, a condition which was not obvious ahead of the face. The effects of rock anisotropy on elastic stresses and displacements were also investigated for three different cases in terms of the orientation of Young's modulus. The author performed finite element analyses varying the relative stiffness of liner and rock, the delay of support installation and the excavation round length to investigate thrust forces and bending moments in the lining as well as stresses and deformations in the rock. The shorter excavation round lengths showed smaller displacements at the crown and at the springline, higher stresses on the liner and more homogeneous pressure distribution on the support. High thrust forces were obtained on the liner with low values of compressibility ratio as expected. Even though valuable results were obtained from the analyses, Pelli could not show any general conclusions that could be used for actual tunnel design.

Chaffois et al. (1988) carried out three-dimensional finite element analyses to study the behaviour of a shallow tunnel face excavated through granular soils using a bentonite slurry shield. A total of 8 slices and 272 finite elements were used for the analyses. The authors obtained a ground reaction curve of the face, which showed a linear relation between the displacement of a point on the face and the pressure applied to the face until the slurry pressure became less than a certain value. Beyond this level of horizontal stress, a plastic zone started to develop at the face. The ground reaction curve

allowed an estimation of the horizontal stress level to be applied to the face during the excavation to prevent the development of plastic areas and ensure safe works. The authors also clearly showed the effect of longitudinal and horizontal arching from the plot of principal stresses at the face in vertical and horizontal planes.

Negro et al. (1986) suggested a method estimating the radial displacements at the face of shallow tunnels from a series of parametric three-dimensional finite element analyses. Negro (1988) reviewed some of three-dimensional finite element modelling shown in the literature and performed three-dimensional finite element analyses to determine the effects of the delayed installation of the lining.

Ezzeldine (1995) carried out 3-D finite element analyses to study the face stability of tunnels constructed using pressurized shield methods. An elasto-plastic model based on the Mohr-Coulomb failure criterion with a non-associated flow rule was employed. The finite element mesh consisted of 17 slices with 711 elements and 3622 nodal points. The face pressure was gradually reduced from the initial ground pressure to find a yield pressure, which was defined by the rapid increase of face displacement.

Rossler (1995) investigated the extent and shape of the zones of discontinuity overstressing in linear elastic ground and an unlined ideally deep tunnel using 3-D parametric finite element analyses. Only one quarter of a tunnel section was considered due to the assumption that the tunnel was deep. A total of 17 slices with 1105 finite elements and 5180 nodal points were used for the analyses. The strike of clean and closely spaced joint planes was assumed to be located parallel or perpendicular to the tunnel axis. The mechanics of the ground response to the action of the grippers of a double-shield tunnel boring machine was also analysed to establish the conditions leading to an optimum gripper design. The influence of various ground parameters, gripper pressures and orientation of gripper pads and discontinuity planes on the development of tunnel wall overstressing was investigated assuming a linear elastic ground model.

6.4 Three-Dimensional Finite Element Analyses

6.4.1 Description of the Analyses

In order to understand the behaviour of stress and displacement near the tunnel face, three-dimensional finite element analyses were performed using the program SAGE developed by Chan (1985) at the University of Alberta. The extensive use of the program at the University of Alberta throughout the years has proven the reliability and accuracy of the program. Computational work was done on the RISC System/6000. The Experimental tunnel was chosen for the present analyses because of the availability of considerable field measurements of tunnel performance as well as soil parameters. The tunnel was bored through till and had an excavated diameter of 2.56 m. Each metre of the precast concrete lining consists of four segments with 0.11 m thickness. The tunnel is described in detail in Sec 4.2.6. A linear elastic model was used for the analyses with an uniform in-situ stress ratio. The use of an elastic model has been considered an oversimplification of soil behaviour. However, more attention was given to particular aspects of the 3D behaviour during tunnel excavation than to matching with field measurements using more complex constitutive laws.

The same cross section as for the 2-D analyses was used for the transversal section of the 3-D mesh as shown in Figure 6.2 in order to compare the results between them. Eight-noded elements were originally used with a total number of 329 elements and 1052 nodes. However, the number of elements in the transversal section was reduced to 122 with 411 total nodes because of the memory limitations of the computer. The results from the reduced meshes were in good agreement with those from the original meshes according to the 2-D analyses. The longitudinal cross section of the 3-D mesh is shown in Figure 6.3. A total of 10 slices with 1220 finite elements and 5101 nodal points were used for the analyses. The final mesh was finer than most of three-dimension meshes found in the literature.

The location of the boundaries in a 3-D analysis was suggested by the 'German recommendations for underground construction in rock' (DGEG, 1979; after Negro, 1988). According to the suggestion, for a symmetric mesh, the width should be greater than or equal to three times the tunnel diameter, and the length of the block along the

tunnel axis should be greater than or equal to four times the tunnel diameter. The location of the boundaries used for the experimental tunnel was 10 diameters wide and 8 diameters long, which was large enough for the 3-D analyses. Twenty nodes solid 3-D elements were used in the middle section, from slice number 4 to slice number 7, and sixteen nodes solid elements were used for the rest of the slices to maximize the refinement of mesh within the memory limits of the computer. In the case of the sixteen nodes solid elements, four mid-side nodes located parallel to the tunnel face did not exist. Even though the results of the whole tunnel section are presented in the following section, only the results from slice 3 to slice 8 can be considered reliable due to the large size of the excavation steps and the proximity of the mesh boundary for the rest of the slices.

A number of analyses were performed for unlined and lined tunnel cases. In the first case, the tunnel excavation without lining installation was simulated. Initial in-situ stress before excavation was applied to the section assuming 21 KN/m^3 of unit weight and $K_0=1$. The in-situ stresses were different across the tunnel profile due to the action of gravitational body forces. The elements in the tunnel section were deactivated in ten steps to simulate the excavation from slice 1 to slice 10. An elastic modulus of 30,000 KPa and a Poisson's ratio of 0.4 were used for the ground based on the results of pressuremeter test obtained by Thomson et al. (1982). The number of integration points used for the 3-D elements was twenty seven, $3 \times 3 \times 3$. The displacements were obtained for nodes at the excavation line. The stresses for the crown, springline and floor were obtained from the points located about 2 cm, 1.5 cm and 1 cm respectively from the excavated boundary, which were close enough from the nodal points used to get the displacements.

In the second case, lining installation was simulated with the advance of the tunnel. The lining had an elastic modulus of 25,100 MPa and a Poisson's ratio of 0.25. Therefore, the compressibility ratio, C , and the flexibility ratio, F , defined by Einstein and Schwartz (1979) were 0.0155 and 25.2 respectively. The tunnel construction was easily simulated with the birth and death option of the program. All the elements in the area to be excavated were initially active, and these elements were deactivated when excavation was to take place at a designated step. The lining elements were deactivated

initially as a soil material and later reactivated as support. The sequence of excavation was as follows:

Step 1: Initial in-situ stress before excavation was applied to the section assuming 21

KN/m³ of unit weight and $K_0=1$.

Step 2: Full face excavation of slice 1

Step 3: Full face excavation of slice 2 and installation of liner at slice 1

Step 4: Full face excavation of slice 3 and installation of liner at slice 2

Step 5: Full face excavation of slice 4

Step 6: Full face excavation of slice 5

Step 7: Full face excavation of slice 6 and installation of liner at slice 3

Step 8: Full face excavation of slice 7

Step 9: Full face excavation of slice 8 and installation of liner at slices 4 and 5

Step 10: Full face excavation of slice 9 and installation of liner at slices 6 and 7

Step 11: Full face excavation of slice 10 and installation of liner at slices 8 and 9.

6.4.2 Displacements

The radial displacement distribution of the tunnel wall along the longitudinal direction is shown in Figure 6.4. The radial displacement is expressed in a dimensionless form such as:

$$U = \frac{uE}{P_0 R(1 + \nu)}$$

where u is the radial displacement. The distance to the face, X , is normalized with respect to the tunnel diameter, $2R$. The figure shows that displacements were negligible, within 0.5 % of the plane strain value, at points more than about two tunnel diameters ahead of the face, while full displacement U_1 occurred at a distance of approximately two diameters behind the face. The dimensionless radial displacement U is 1 for the elastic displacement around a circular opening in a plane strain for an infinite ground mass under hydrostatic pressure P_0 . The U_1 far behind the tunnel face was not 1 in the 3-D analysis but about 0.97, probably due to the effect of the ground surface and stress gradient across the opening.

The U of the tunnel face for the crown and for the springline and floor were 0.28 and 0.27 respectively. Panet and Guenot (1982) obtained the same results from axisymmetric finite element analyses. Pelli (1987) performed 3-D elastic analyses for a deep tunnel with $K_0=2$ and obtained a U of 0.27 at the face, which indicates that the U at the face is not sensitive to the in-situ stress ratio. The U of the springline at A increased from 0.27 to 0.81 when the tunnel face was advanced to B, i.e. one tunnel radius, as shown in Figure 6.5. If the face is advanced more than two diameters away from the face A, the full displacement U_f will occur. In this case, the load that will act on the liner installed at the face A before the advance of face is directly proportional to the value $(U_f - U) / U_f$.

Figure 6.6 shows the distribution of radial displacements at the springline along the longitudinal direction with the location of the leading edge of liner. Only steps 6 and 8 are shown in the figure. The distributions of radial displacements at the crown and floor are not shown because of similarity to that of the springline. The displacement of point a, which is located 4 diameters behind the face A, showed an unrealistic result probably due to the effect of the mesh boundary. The irregular distribution of displacements behind the face clearly shows the influence of construction sequences. The U at point b was 0.30 after excavation of slice 1 in step 2. The additional displacement at point b after the excavation of slice 2 was only 0.8 mm due to the installation of liner at the same step and did not change with further advance of tunnel face. The dimensionless radial displacement U at point c was 0.08 in step 2 and increased to 0.37 in step 3. The U at point c in step 3 was slightly higher than that of point b in step 2 even though both of them were located at the face possibly because point c already had displacement due to the excavation of slice 1, whereas point b did not have any displacement in the previous step. The displacement at point c increased only 0.4 mm after the excavation of slice 3 in step 4 due to the installation of the liner, which was smaller than 0.8 mm for point b of equivalent steps because the distance from the face to point c in step 4 was closer than that of point b in step 3. The U at point d was 0.09 in step 3 when the face was located one radius behind of the point. The U increased to 0.35 in step 4, which was comparable to the displacement of point c in the equivalent step, i.e. step 3. The U at point d increased to 0.79 in step 6 due to the excavation of slices 4 and 5 without installation of

liner. The leading edge of the liner was located at point c in step 6. The U at point d for an unsupported tunnel was 0.82 in the same step, which is only 1.1 mm larger than that of a supported one. The U was almost unchanged after step 8 due to the installation of the liner. The displacements between points d and e clearly showed the effect of face advance from A to B because those sections were unsupported.

The following results were obtained for the radial displacements in the advancing tunnel from the present 3-D analyses.

(1) The radial displacements occur at points between more than about two tunnel diameters ahead of the face and about two diameters behind the face due to the advance of a tunnel.

(2) The dimensionless displacement U after the installation of the liner is very small and most of the displacement occurs ahead of the leading edge of the liner.

(3) The U at the face is almost unaffected by the distance to the leading edge of the liner.

(4) The U does not vary considerably with the change of an in-situ stress ratio.

(5) The unlined gap of only one diameter length can significantly increase the displacements even though the leading edge of the liner is located one radius away from the measured point, i.e. point d.

(6) The influence of delay length on the radial displacements is obvious in the section between the face and two tunnel diameters behind the face.

The above results are generally agreed with those published elsewhere (e.g. Ranken, 1978; Negro et al., 1986). Because of the enormity of the task of the preparation of input data and the interpretation of results for 3-D analyses, parametric analyses were not performed in this study. Some other findings can be added from the previous research shown in the literature.

(7) Kerisel (1980) stated that the displacement curves for the face diverged increasingly from the elastic curve as the stability number increased from 2 to 6. Panet and Guenot (1982) also showed that the U of the tunnel face increased as the stability number increased using a perfectly plastic von Mises criterion for the purely cohesive medium.

(8) The U behind the face decreases with decreasing compressibility ratio C but relatively insensitive to the change of flexibility ratio F according to the analyses performed by Pelli et al. (1986).

(9) Negro et al. (1986) showed that, even though the U was found to be about 0.27 in a relatively deep tunnel, the U could vary from 0.17 for the floor to 0.37 for the crown with an average of 0.26 in shallow tunnels due to the stress gradient across the tunnel.

6.4.3 Stresses

The longitudinal distributions of the normalized radial stress of the tunnel wall for the unlined tunnel are given in Figure 6.7. Only steps 6 and 8 are shown in the figure. The distributions of radial stresses at the crown and the floor are not shown because of similarity to that of the springline. The radial stresses of the excavated section behind the tunnel face decreased close to zero. The stresses did not drop to zero because they were not taken at the excavated boundary but taken about 1.5 cm inside of the boundary. The radial stresses at a point about one radius ahead of the face was yet almost equal to the in-situ stress. The stress increases were observed between the point about 0.72 m ($X/2R=0.281$) and 1.45 m ($X/2R=0.566$) ahead of the face due to stress redistribution caused by the excavation. The radial stress reduction just ahead of the face was probably caused by the longitudinal extension of the soil and the loss of horizontal support. A high stress concentration was found about 7 cm ($X/2R=0.027$) behind the tunnel face, which was about a 42 % increase of the in-situ stress. This high stress concentration was reduced to close to zero after the tunnel face advanced to B, which was only one length of tunnel radius.

Figure 6.8 shows the distribution of radial stresses at the springline for the steps 6 and 8 with the location of the leading edge of the liner. The weight of soil in the unsupported section was transmitted to both the ground ahead of the tunnel face and the leading edge of the liner by the action of arching. Therefore, the liner installed closest to the face carried the greatest load. The dimensionless radial stresses in slice 1 after excavation of slice 1 showed the highest load at the point located near the face, i.e. point a. The stress at point a was 0.73 in step 2 and decreased to 0.64 in step 3 due to more

displacement caused by the excavation of slice 2. The stress reduction was not large due to the installation of liner in slice 1.

The radial stress of point b, 0.82, was higher than that of point c, 0.60, in step 3 after installation of the liner in slice 1 due to stress concentration near the leading edge of the liner even though the stress of point b was lower than that of point c in step 2. The stress of point c was increased to 0.85 due to stress concentration at the leading edge of the liner after the excavation of slice 5 in step 6, whereas the stress of point b almost unchanged from step 3. The stresses in slice 2 had stabilized in step 6 and were no longer influenced by the further advance of tunnel face.

The stress increase was observed as about 13 % at point d after excavation of slice 1 but the stress at point e remained almost the same as the in-situ stress. The dimensionless stress at point d reduced to 0.23 but the stress at point e increased to 1.15 after the excavation of slice 2 and installation of the liner at slice 1 due to stress redistribution caused by excavation. The radial stress reduction just ahead of the face, at point d, was probably also related to the longitudinal extension of the soil and the loss of horizontal support as mentioned above. The stress at point d increased to 0.50 due to stress concentration near the leading edge of the liner installed in slice 2 and the stress at point e decreased to 0.48 due to the excavation of slice 3 in step 4. The dimensionless stresses at points d and e decreased to 0.47 and 0.00 respectively due to the excavation of slices 4 and 5. The stress at point d only increased to 0.49 after installation of the liner in slice 3 and excavation of slices 6 and 7, i.e. face at B, whereas the stress at point e increased to 0.17. However, the stress in the trailing edge of the liner, point d, was higher than that of the leading edge of the liner, point e, due to the stress concentration at point d in step 4.

The stress concentration just ahead of the leading edge of the liner was not observed at point f after the installation of liner in slice 3 because most of the stress at the point was already released in the previous steps 5 and 6. Tensile stress was developed at point f, which was also observed by Pelli (1987) at the trailing edge of liner. The tensile stress disappeared after further advance of the face as shown in Figure 6.8. The stress distributions ahead of the face for steps 6 and 8 were almost the same as those of

unsupported cases, which suggest that the installation of the liner about 1 diameter away from the face does not affect the stresses at the points ahead of the face. The uneven distribution of radial stress ahead of the face was also observed by Katzenbach and Breth (1981).

Figure 6.9 shows the changes of stress distribution after the further advance of the tunnel face. The face was located at B with the installation of the liner at B' in step 8 and moved to A with the liner at A' in step 11. The stresses between slice 1 and slice 3 remained almost constant because the supports were already installed in those slices with the excavation up to slice 7. This indicates that the liner stress is not influenced by what takes place one diameter ahead of the liner. The stresses between slice 4 and slice 7 increased with the advance of the face because the stresses in these points were close to zero due to the prior excavation of those slices and the installation of liner combined with the further advance of the face made the stresses increase.

The following results were obtained for the radial stresses in the advancing tunnel from the present 3-D analyses.

(1) The radial stress distributions ahead of the tunnel face are not influenced by the installation of the liner one diameter away from the face. The radial stress increase is observed between one radius and 0.6 radius ahead of the face due to stress redistribution caused by excavation. The radial stress reduction just ahead of the face is probably caused by the longitudinal extension of the soil and the loss of horizontal support.

(2) A high stress concentration is observed about 7 cm ($X/2R=0.027$) behind the tunnel face, which disappears immediately after the next step of tunnel advance.

(3) The radial stresses in the unsupported section drop close to zero just behind the face in an unlined tunnel but the stresses in the unsupported section of about one radius do not drop to zero due to the existence of the liner.

(4) The liner installed the closest to the face carries the greatest load.

(5) The stress increase is higher in the leading edge of the liner than that of the tailing edge after the advance of the tunnel face. However, the stress in the tailing edge can be higher than that of the leading edge depending on the construction sequences.

(6) After the face has advanced one diameter beyond a certain point, the liner stress at that point is no longer influenced by what takes place ahead of the liner.

(7) A stress concentration is observed just ahead of the leading edge of the liner if the excavation is done just ahead of the liner section at the same step as the installation of the liner such as in steps 3 and 4. The stress concentration is not found just ahead of liner in slice 3 because most of the stress at that point is released in the previous steps 5 and 6.

(8) The stress concentration does not disappear even after the further advance of the tunnel.

Some other findings can be added from previous research shown in the literature.

(9) Pelli (1987) showed that the thrust in the liner depended on the relative stiffness of the support. The high compressibility ratio C resulted in low stresses in the liner.

(10) Pelli (op. cit.) observed that smaller excavation round lengths allowed a more homogeneous pressure distribution on the liner with relatively moderate loads in the support.

6.4.4 Convergence Curves

The concept of convergence-confinement method was explained in detail in the previous chapter. However, the previous convergence curves do not include the actual load transfer mechanisms existing at the tunnel face. Heinz (1984) recognized the problem and presented ground reaction curves by combining the radial stress and the displacement curves from 3-D finite element analyses. Heinz experienced a considerable scatter of stresses and displacements behind the advancing face and considered it as numerical inaccuracy. Therefore, the stress and displacement curves had to be smoothed out after superimposing the stresses and displacements from three consecutive steps of face advance. This was done by making the face position in these three steps coincide. However, there may be several other reasons for the scatter of the results. First, the number of elements used was only 38 in the transversal section, which is relatively coarse to have accurate results around the excavation line according to 2-D test analysis done by the author for the present study. Second, the stress and displacement curves were

obtained at points approximately 20 cm from the opening and at the excavation line respectively, which might not be responsible for the scatter of results but could contribute the inaccuracy of the results. Third, the stress and displacement distributions for three different face positions could actually be different because the length of the element, i.e. construction sequences, used along the longitudinal direction, was not uniform.

The ground reaction curves or convergence curves are drawn for slices 5 and 6 by combining radial stresses and displacements obtained in the middle section of each element. The number of elements used in the transversal section is 122 as mentioned before, which is much finer than the mesh used by Heinz. The displacements are obtained for nodes at the excavation line. The stresses for the crown, springline and floor are obtained from the points located about 2 cm, 1.5 cm and 1 cm respectively from the excavated boundary, which are close enough from the nodal points used to get the displacements.

Figure 6.10 showed the convergence curves of the springline for slices 5 and 6 without the installation of the liner. The radial stresses are normalized to the in-situ stress. The convergence curves for the crown and the floor were not shown because of similarity to that of the springline. The convergence curves for slices 5 and 6 showed similar trends. The displacements started to occur ahead of the face with a slight increase of radial stresses from the in-situ stress due to the arching effect along the longitudinal direction of the tunnel. The dimensionless radial stresses decreased to about 0.91 when the face advanced 0.325 m behind the reference point A. The radial stresses dropped close to zero at point B after the face passed the points. The radial stresses of unsupported section between points B and C did not drop to zero because the stresses were obtained about 1.5 cm inside of the excavated boundary and the mesh was not fine enough to get zero stress in the boundary. The stresses at the excavated boundary would be closer to zero if more element were used according to the 2-D test analyses done by the author for the present study. However, the error induced by the use of the reduced mesh was very small according to the 2-D test analyses. The convergence curves between points B and C did not coincide because the excavation round length after the passage of reference points of slices 5 and 6 were slightly different. In case of the point of slice 5, more constant

stresses were observed than those of slice 6 probably due to the smaller round length, two consecutive round length of 0.5 radius, just after the passage of the reference point. However, the final stresses and displacements for those two points were exactly the same when the face advanced far away from those points as shown at point C.

Figure 6.11 presents the convergence curves obtained from two-dimensional linear elastic analyses with the results of 3-D analyses for slice 5 without liner. Two-dimensional analyses were performed using the program SIGMA/W developed by GEO-SLOPE International Ltd. The in-situ stresses were reduced to zero in 11 different steps as explained in the previous chapter. The same transversal cross section and material properties were used for the 2-D and 3-D analyses. The final equilibrium points are almost the same for the both analyses but the ground responses are completely different. The conventional plane strain convergence curve could not consider the 3-D arching effect occurring ahead of the face and the fast stress reduction in the unsupported section. Eisenstein et al. (1984) also recognized the non-linear nature of convergence curves even in linear elastic and time-independent ground because of the different rates of development of radial stress and displacement around an advancing tunnel.

The convergence curves of slice 5 with the installation of the liner are shown in Figure 6.12. The curves clearly show the influence of lining installation on the stress and displacement distributions at the crown, springline, and floor. There were increases of radial stresses without much displacement as the tunnel face advances further after the liner was installed at slice 5 in step 9. The stresses and displacements at those points were finally stabilized when the tunnel face advanced about 2 diameters away from the points. The final loads and displacements on the lining depend on the relative stiffness of the lining and the ground and the length of unsupported section at the time of lining installation. The convergence curves of the crown, springline and floor did not coincide due to the in-situ stress gradient across a tunnel. The floor had more displacement than those of the crown and springline because it had the highest in-situ stress among the points. However, the stresses and displacements ahead of the face were almost the same.

The convergence curves of slices 5 and 6 for the springline are shown in Figure 6.13 with the location of the liner installation. The convergence curves were almost

identical up to point A, which suggests that the radial stresses and displacements occurring ahead of the face were not sensitive to the excavation round length taking place behind the face. The stresses and displacements at points B and C were different even though the lengths of unsupported sections were the same because the distance from the face and the leading edge of the liner to the points were different from each other as shown in Figure 6.14 (a). Point C had more displacement and higher stress than those of point B due to the longer distance to the face and closer distance to the liner as observed in the previous section. The displacements at points B and C were close to the final displacements due to the installation of the liner in the next step. The final radial stress of slice 5 was higher than that of slice 6 because the liner of slice 5 was installed closer to the tunnel face than that of slice 6 as shown in Figure 6.14 (b).

The convergence curves of slice 5 with and without liner installation are shown in Figure 6.15 to check the influence of liner on the convergence curve. The two convergence curves did not coincide but the difference was not large at the points ahead of the tunnel face. As for the liner installation, the length of unsupported section was one diameter when the face just passed the reference point, which is plotted as point B in the figure. The reduction of displacements due to liner installation were obvious from point C when the liner was located only 0.375 diameter away from the reference point in slice 5. The convergence curves were completely different for both cases after the installation of the liner in slice 5. In case of the excavation with liner installation, the radial stresses started to increase with very small displacements as the tunnel face advanced and finally reached an equilibrium as the face moved 2 diameters away from the reference point. However, the radial stresses stayed fairly constant with the increase of the radial displacements to about 29 mm after the further advance of tunnel face for the case of the unlined tunnel.

6.4.5 Comparison of the Equilibrium Points from 2-D and 3-D analyses

The final equilibrium stresses and displacements on the liner from the 3-D analyses were compared with those obtained from the 2-D analyses. Support reaction curves or confinement curves were combined with the convergence curves from the 2-D

analyses to get the final equilibrium points. The confinement curve of a circular support loaded by a uniform radial stress, P_s , was defined by the relationship with the corresponding radial displacement, U_r , as shown in Figure 6.16.

Figures 6.17, 6.18 and 6.19 show the responses of the ground and the liner from the 2-D and 3-D analyses of the crown, the springline and the floor respectively. The response curve of the combined soil and liner system from slice 5 showed the actual three-dimensional stress transfer mechanisms as explained before. Two different confinement curves were plotted due to the difference in the displacement of the ground before the liner installation, U_i . The U_i for the confinement curves of A and B were obtained from the 3-D analyses with and without support simulation respectively. The final radial stresses from the 2-D analyses with the confinement curve A and from the 3-D analyses did not coincide as shown in the figures even though the final radial displacements were almost the same. The difference between the two was the largest at the crown. One of the possible reasons for the differences between the radial stresses of the two is due to the convergence curve of 2-D, which is obtained from the analyses without the liner installation. If the convergence curve is constructed with the liner installation, the curve should have a smaller final displacement, i.e. a steeper convergence curve. In this case, the final equilibrium points could be located closer to that of 3-D analyses. Negro (1988) carried out 2-D finite element analyses with four different uniform amounts of in-situ stress release at the excavation prior to the lining installation and also observed that the equilibrium points between the soil and the lining did not lie on the convergence curves, which were obtained from the analyses without liner installation. Another possible reason for the differences in the stresses could be related to the different nature of the two analyses. In 2-D analyses, the liner and the soil are stiffer than those of 3-D analyses because the liner and the soil are not free to move in longitudinal direction. Therefore, the stress from the 2-D analyses could be higher than that from the 3-D analyses. The final stresses obtained from the 2-D analyses combined with the confinement curve B showed closer results with those from the 3-D analyses. However, the displacements were overestimated due to the exclusion of the liner in 2-D analyses.

The convergence and the confinement curves were obtained by an independent study of the behaviour of the ground and the liner in the convergence-confinement method. Therefore, the convergence curves were determined without the consideration of the liner installation. The final equilibrium point from the 2-D analysis did not coincide with that from the 3-D analysis as shown above. The responses of the ground and the liner from the 2-D and 3-D analyses for the springline of slice 6 are shown in Figure 6.20. The response curves for the crown and the floor are not shown because of the similarities with those of the springline. The difference of radial stresses from the 2-D analyses with the confinement curves A and from the 3-D analyses was even larger than that of slice 5 probably due to the shorter length of the unsupported section. Negro (1988) also observed that the final equilibrium points plotted further to the convergence curves as the stress release allowed before lining installation decreased. Therefore, in addition to the difficulty of finding the U_i in CCM, the method could give more errors as the distance of the unsupported section is reduced in the sequence of tunnel construction. Furthermore, the final stresses and the displacements from both the 2-D and 3-D analyses underestimate the actual field measurements as expected due to the assumption of a linear elastic model for the ground.

6.5 Summary and Conclusions

In this chapter, 3-D finite element analyses have been reviewed and performed to gain a better understanding of stress and displacement behaviour near the tunnel face. A linear elastic model was used for the analyses because more attention was given to particular aspects of the 3-D behaviour during tunnel excavation than to matching analyses with field measurements using more complex constitutive material law. The radial displacements and the radial stresses of the ground have been obtained from the 3-D analyses with and without the liner. The results were summarized in the previous sections. The stress distribution along the tunnel clearly showed the influence of the construction sequences in ground-support interaction. The stresses on the liner may vary because of the length of the lining and the distance between the lining and the tunnel face

even though all the other material properties of the ground and the liner, the tunnel geometry and the in-situ stresses are the same.

The convergence curves were obtained by combining the radial stresses and the displacements. Because several results overlapped with those from the observation of the displacement and stress, only the following results were added for the convergence curves in the advancing tunnel.

(1) The radial displacements start to occur ahead of the face with a slight increase of radial stresses from the in-situ stress due to the arching effect along the longitudinal direction of the tunnel.

(2) The convergence curves obtained from 2-D and 3-D analyses without the installation of the liner have completely different ground responses even though the final equilibrium points are almost the same. The conventional plane strain convergence curve cannot consider the 3-D arching effect occurring ahead of the face and the face stress reduction in the unsupported section.

(3) The stresses and displacements at a certain point are stabilized when the tunnel face advances about 2 diameters away from the point.

(4) The convergence curves with and without liner installation do not coincide but the difference is not large at the points ahead of the tunnel face.

The final radial stresses from the 2-D analyses with the confinement curve and from the 3-D analyses did not coincide probably because the convergence curve of 2-D was obtained from the analysis without the liner installation. The difference was larger as the distance of the unsupported section was reduced in the sequence of tunnel construction. Therefore, the convergence-confinement method should be used carefully when the excavation has a shorter length of unsupported section throughout the construction.

The responses of the ground around an advancing tunnel certainly show three-dimensional nature and cannot be considered properly by a two-dimensional model. However, 3-D analysis is not an easy task to perform because of the difficulties involved in the preparation of the input data and the handling of the output data. Gartung et al. (1979) doubted that the three dimensional study might become a standard procedure for

the tunnel design in the future because of the very considerable effort in work, time and money required for the analyses. Ghaboussi et al. also (1983) stated that properly performed 2-D analyses combined with engineering assessment of the results could provide all the required information because of the enormity of the task preparing the input data and interpreting the results involved in the 3-D analyses. This is one of the reason that a simple design method should be available considering the three-dimensional nature of the ground around an advancing tunnel. In the following chapter, an improved design method is proposed to have better approximation for the behaviour of the tunnel without applying complex analyses.

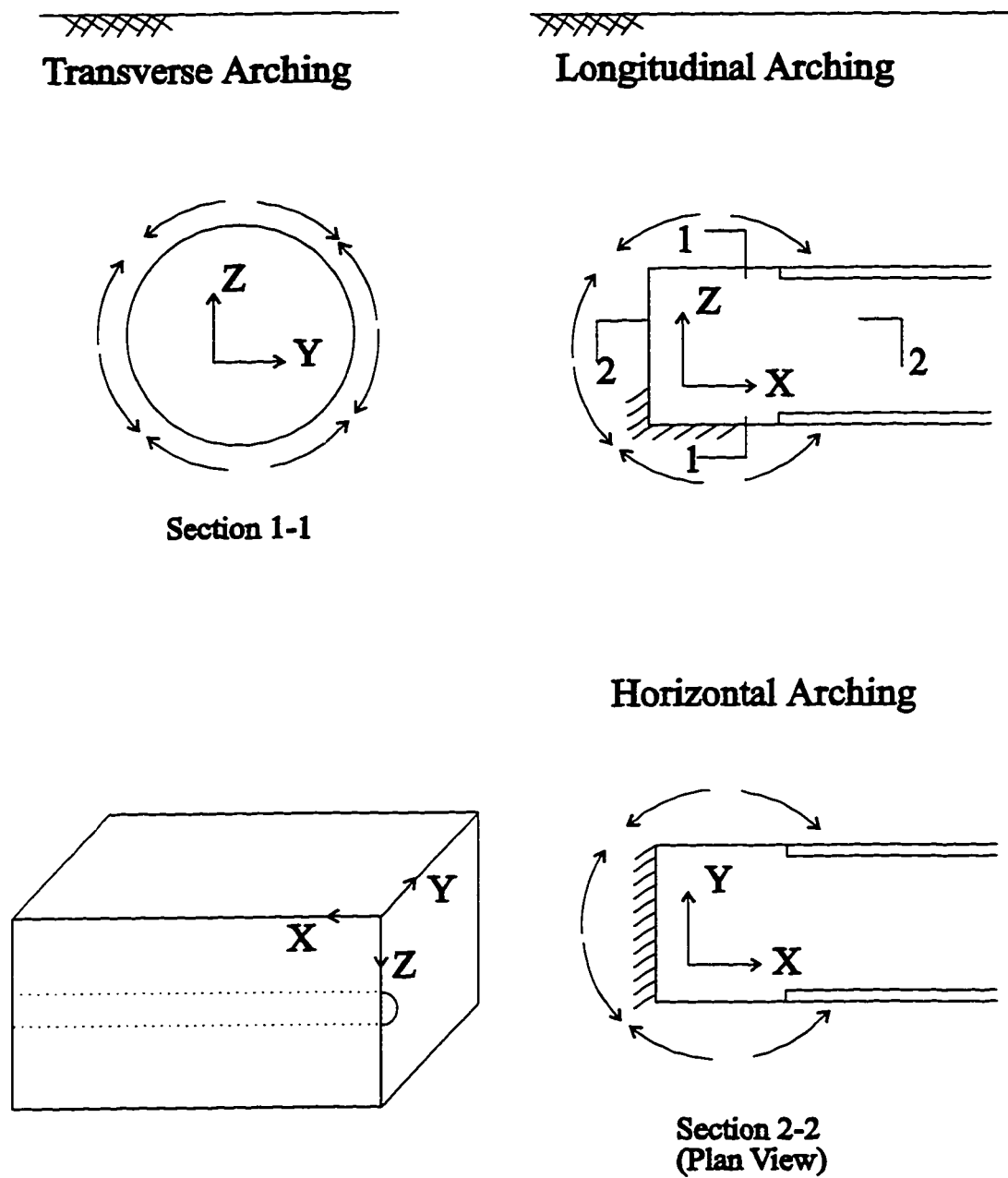


Fig. 6.1 Three-Dimensional Arching near the Face of an Advancing Tunnel (Modified after Eisenstein et al., 1984)

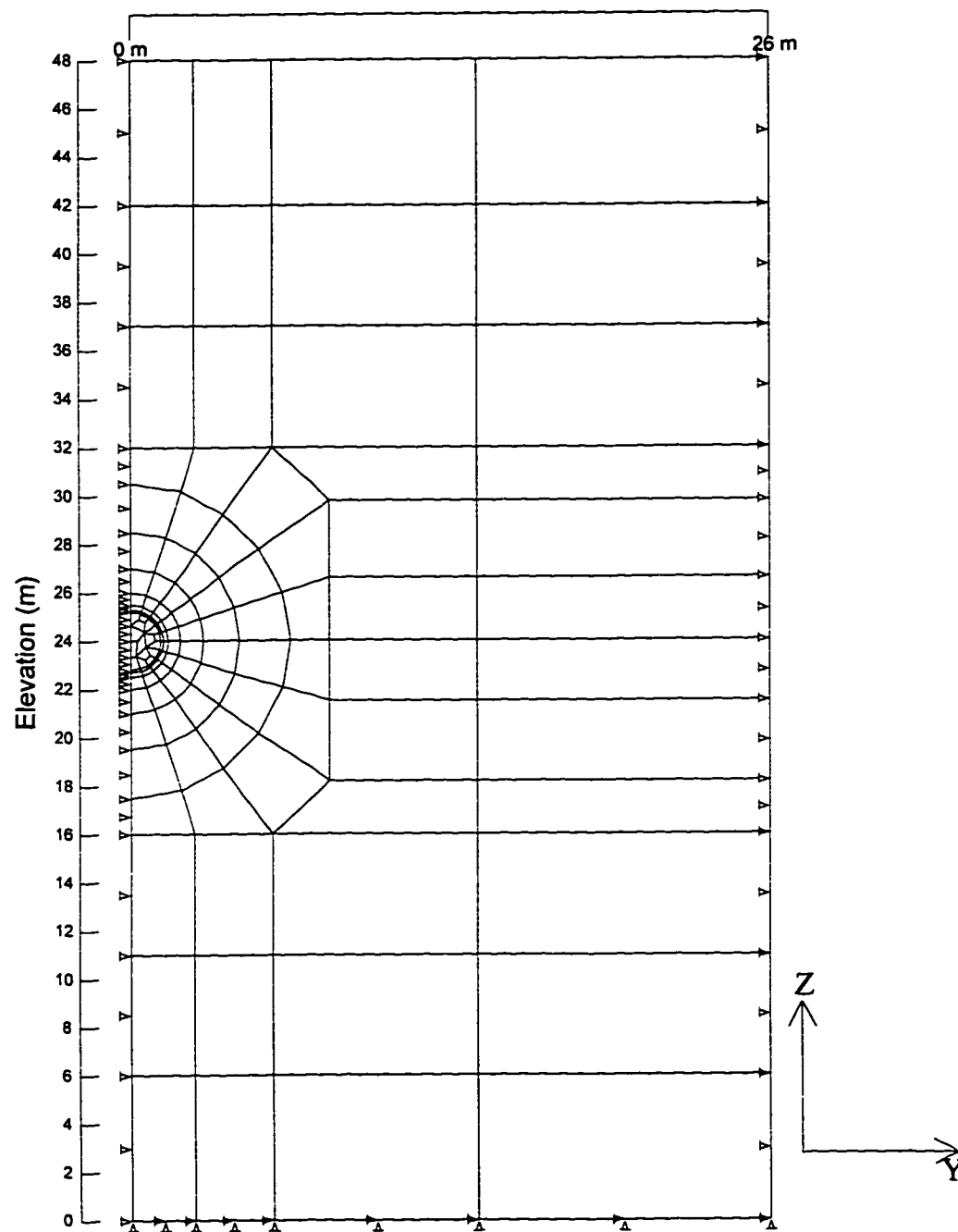


Fig. 6.2 Transversal Section of the 3-D Mesh of the Experimental Tunnel

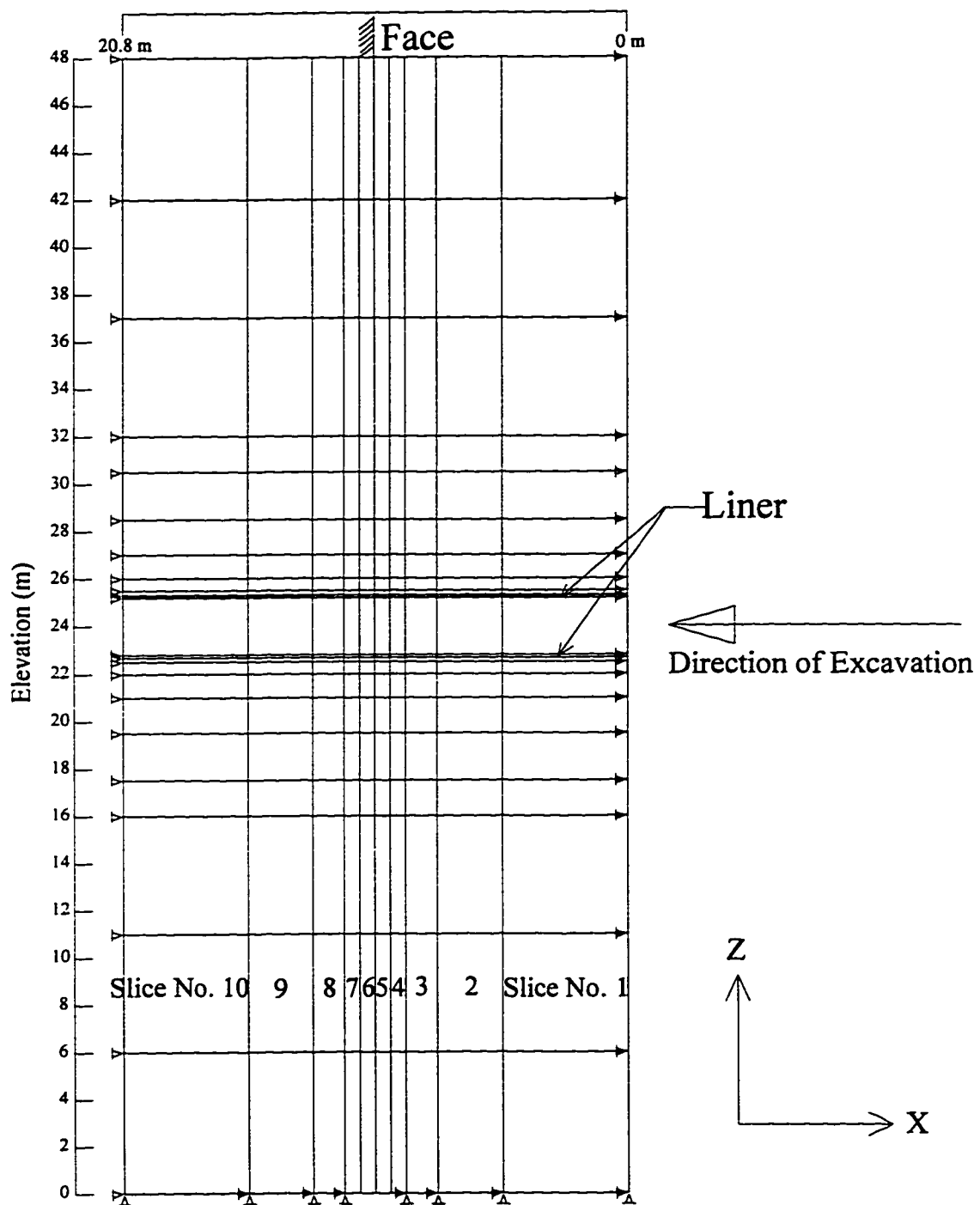


Fig. 6.3 Longitudinal Cross Section of the 3-D Mesh of the Experimental Tunnel

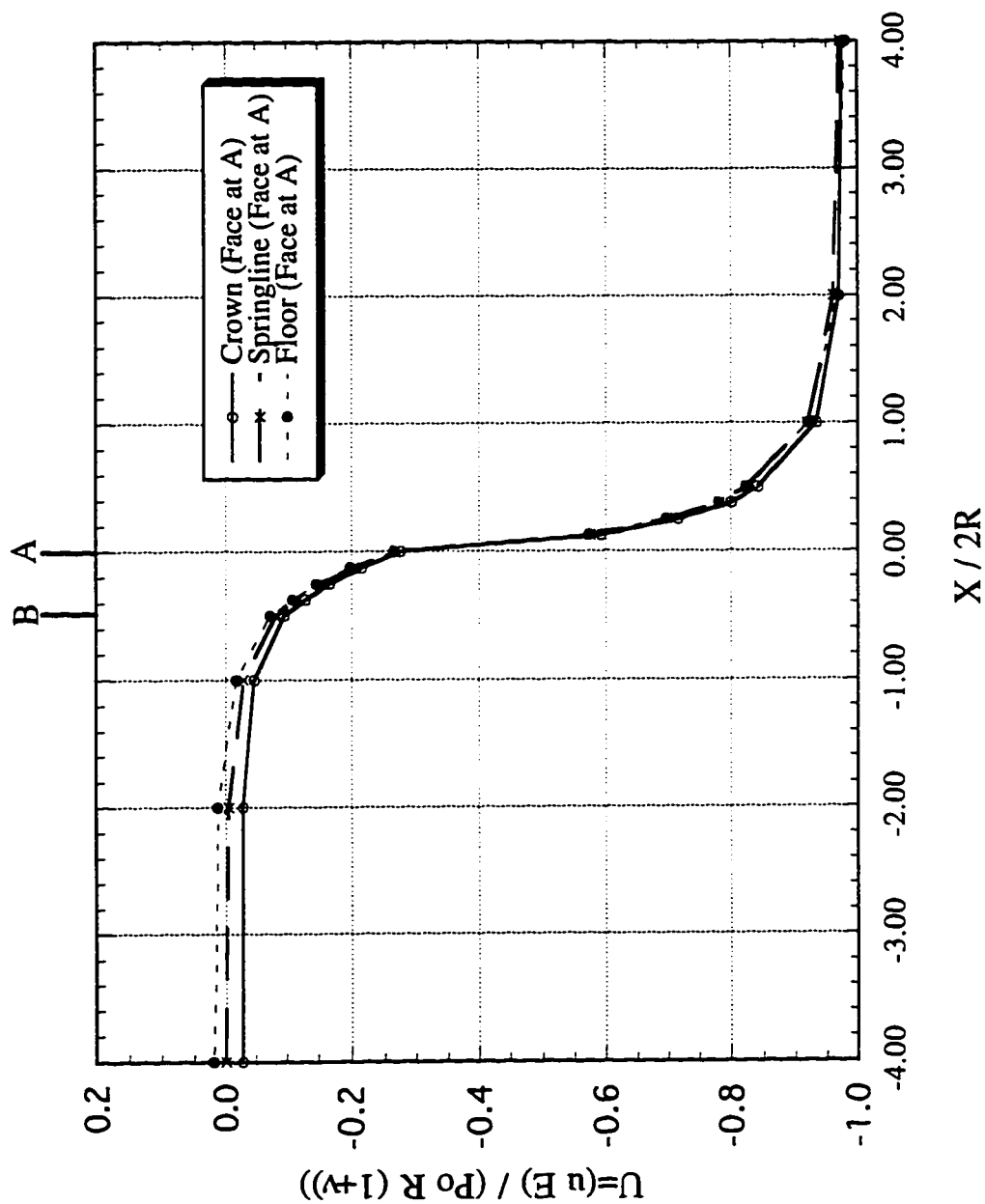


Figure 6.4 Radial Displacement Distribution at the Crown, Springline and Floor along the Longitudinal Direction (No Liner Installed)

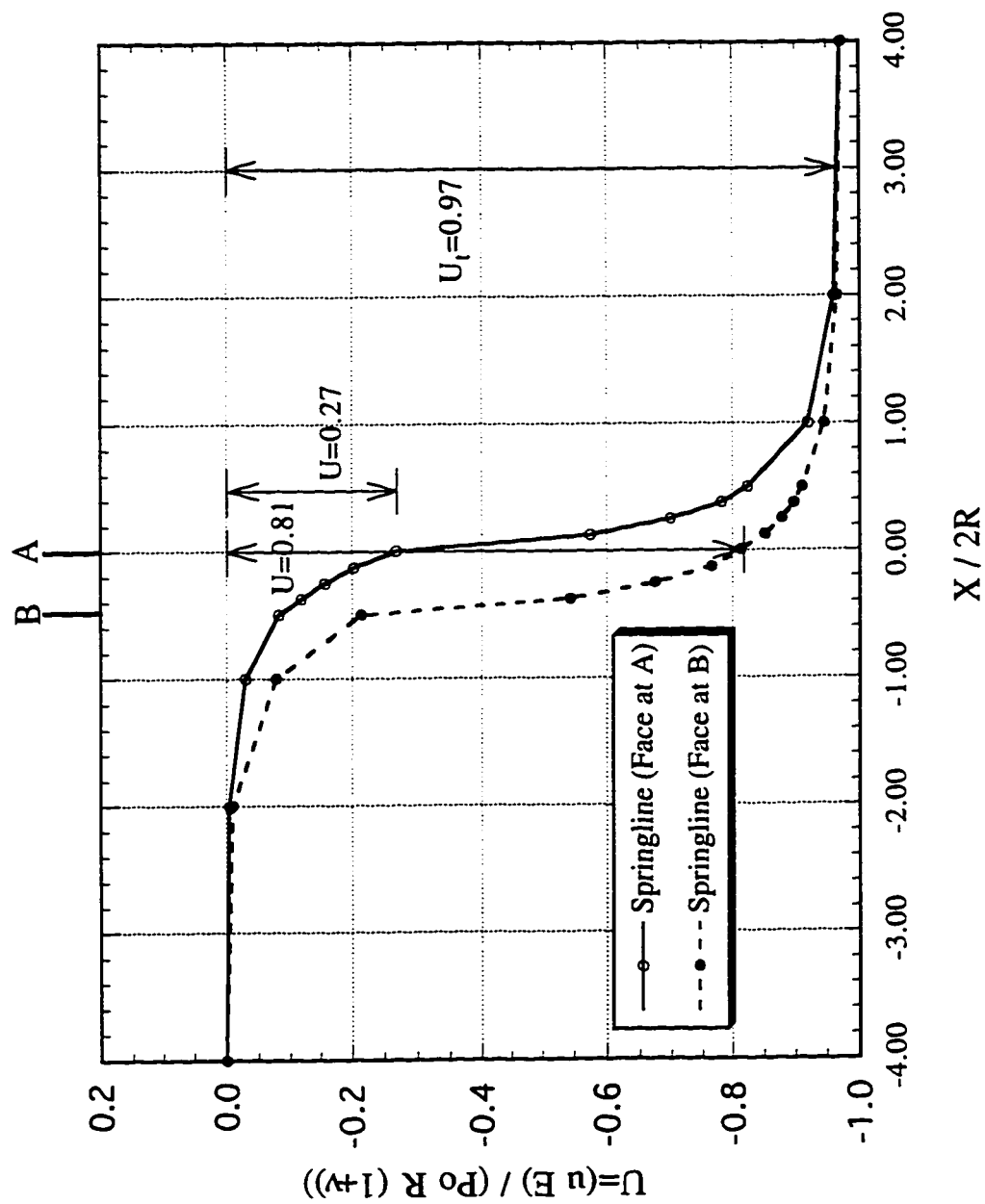


Figure 6.5 Radial Displacement Distribution at the Springline along the Longitudinal Direction (No Liner Installed)

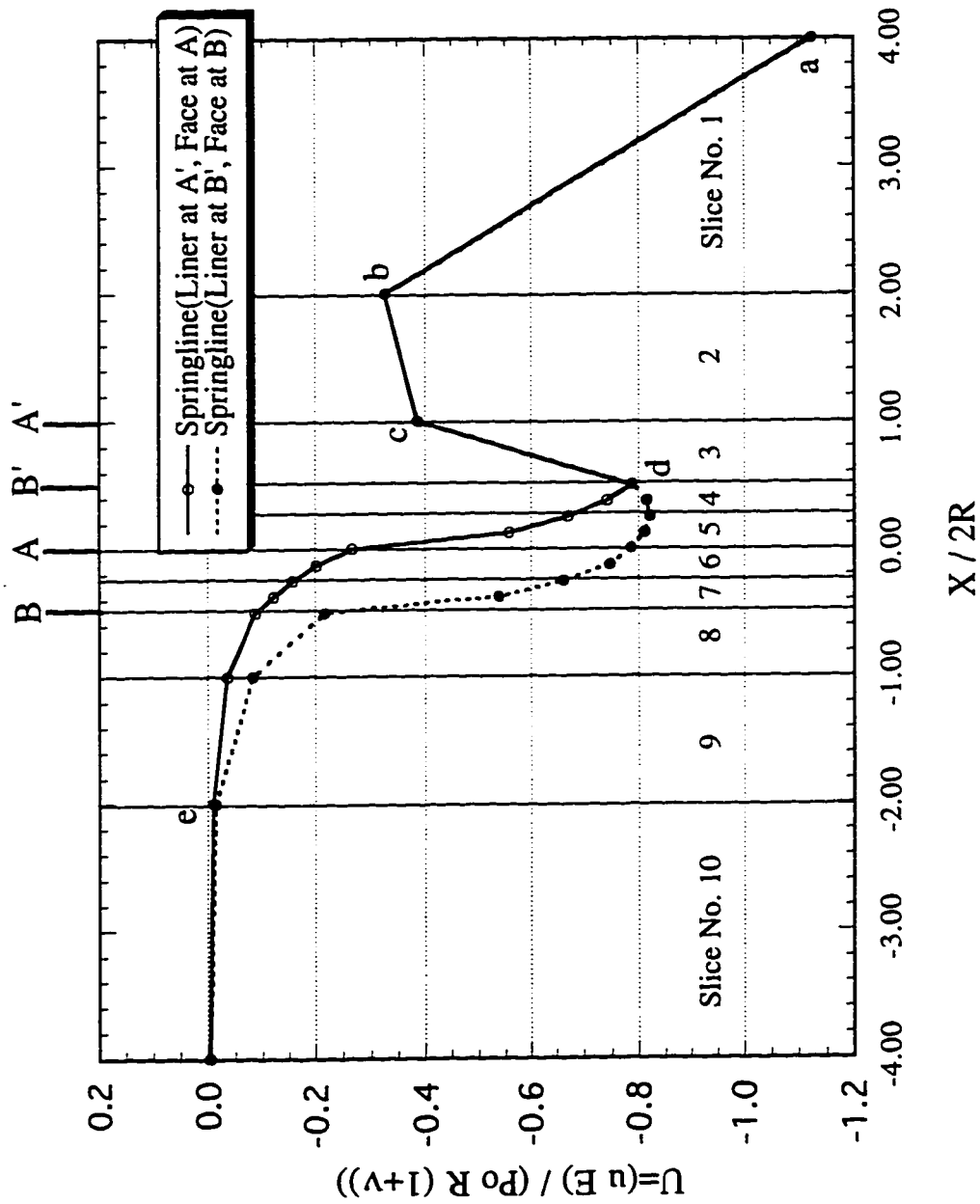


Figure 6.6 Radial Displacement Distribution at the Springline along the Longitudinal Direction (Liner Installed 1D away from the Face)

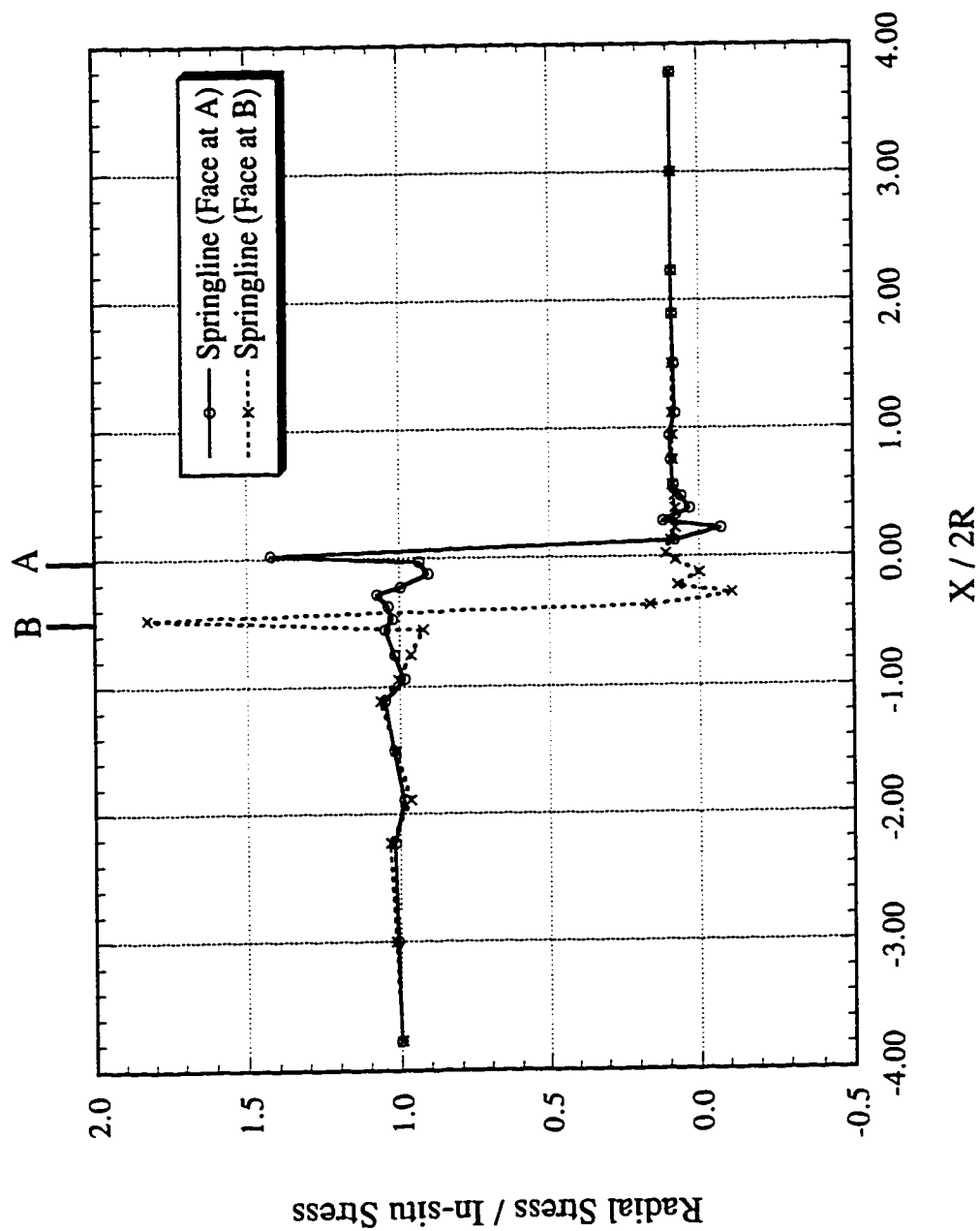


Figure 6.7 Radial Stress Distribution at the Springline along the Longitudinal Tunnel Direction (No Liner Installed)

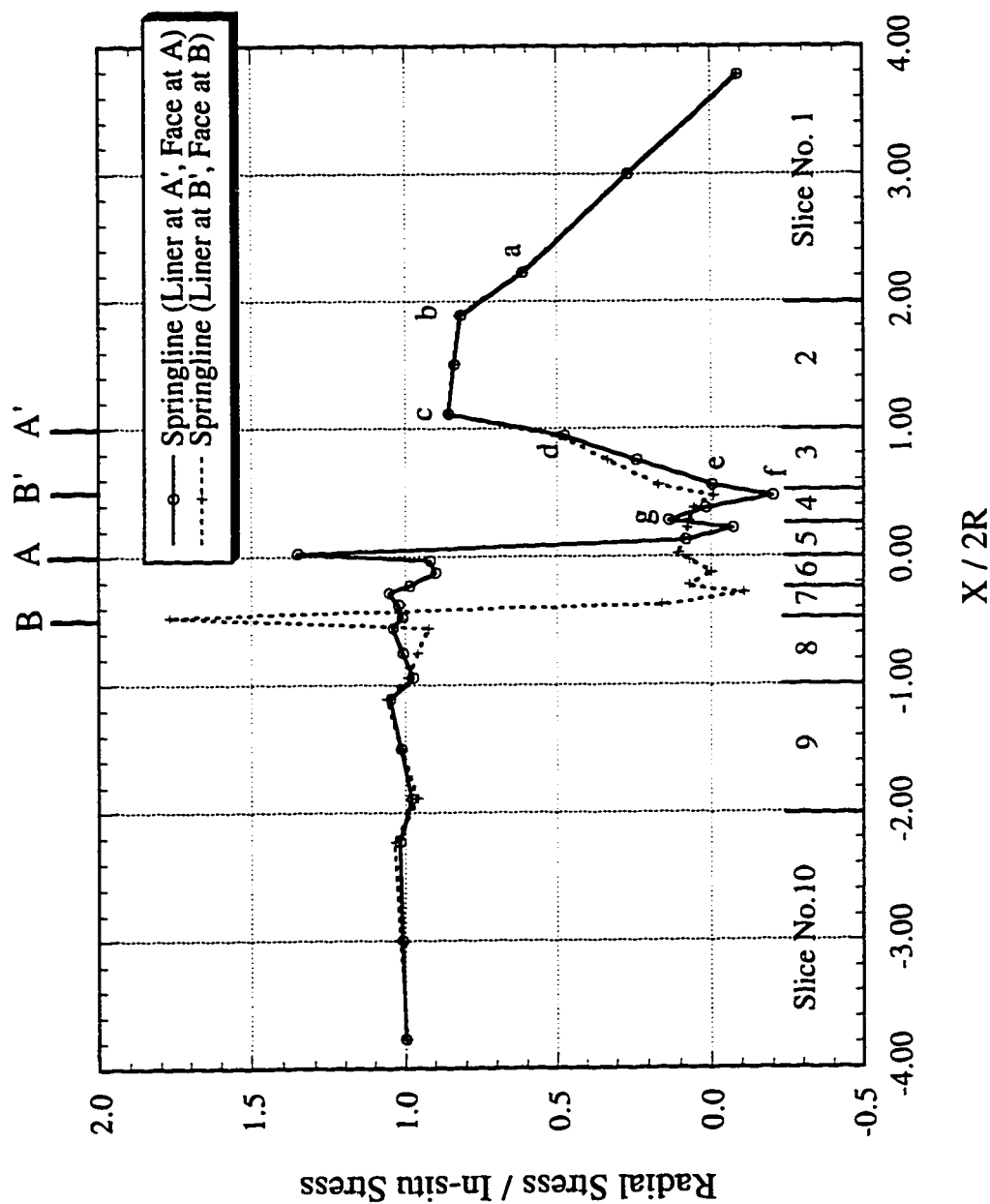


Figure 6.8 Radial Stress Distribution at the Springline along the Longitudinal Tunnel Direction (Liner Installed 1D away from the Tunnel Face)

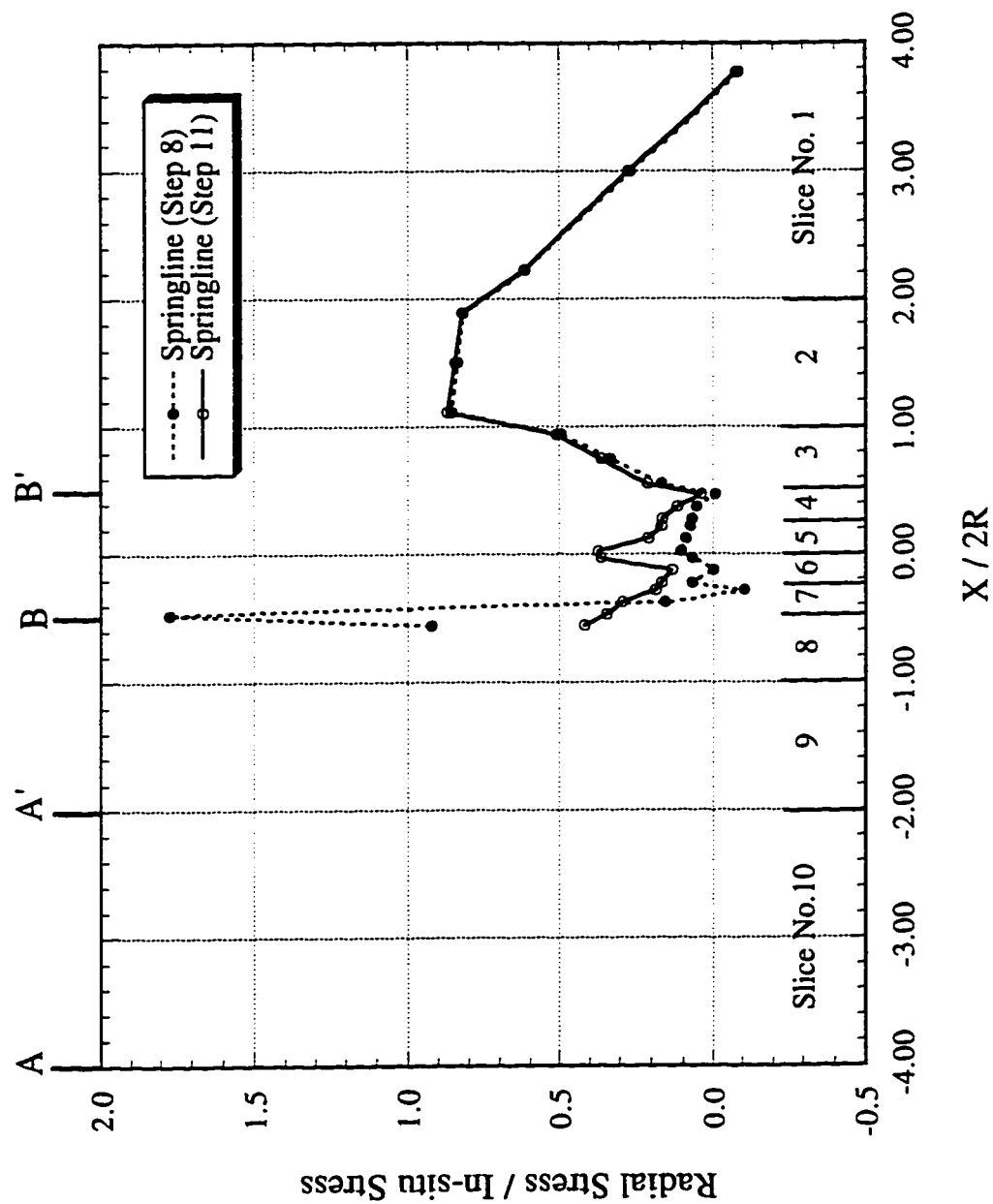


Figure 6.9 Radial Stress Distribution at the Springline along the Longitudinal Tunnel Direction for Step 8 and 11

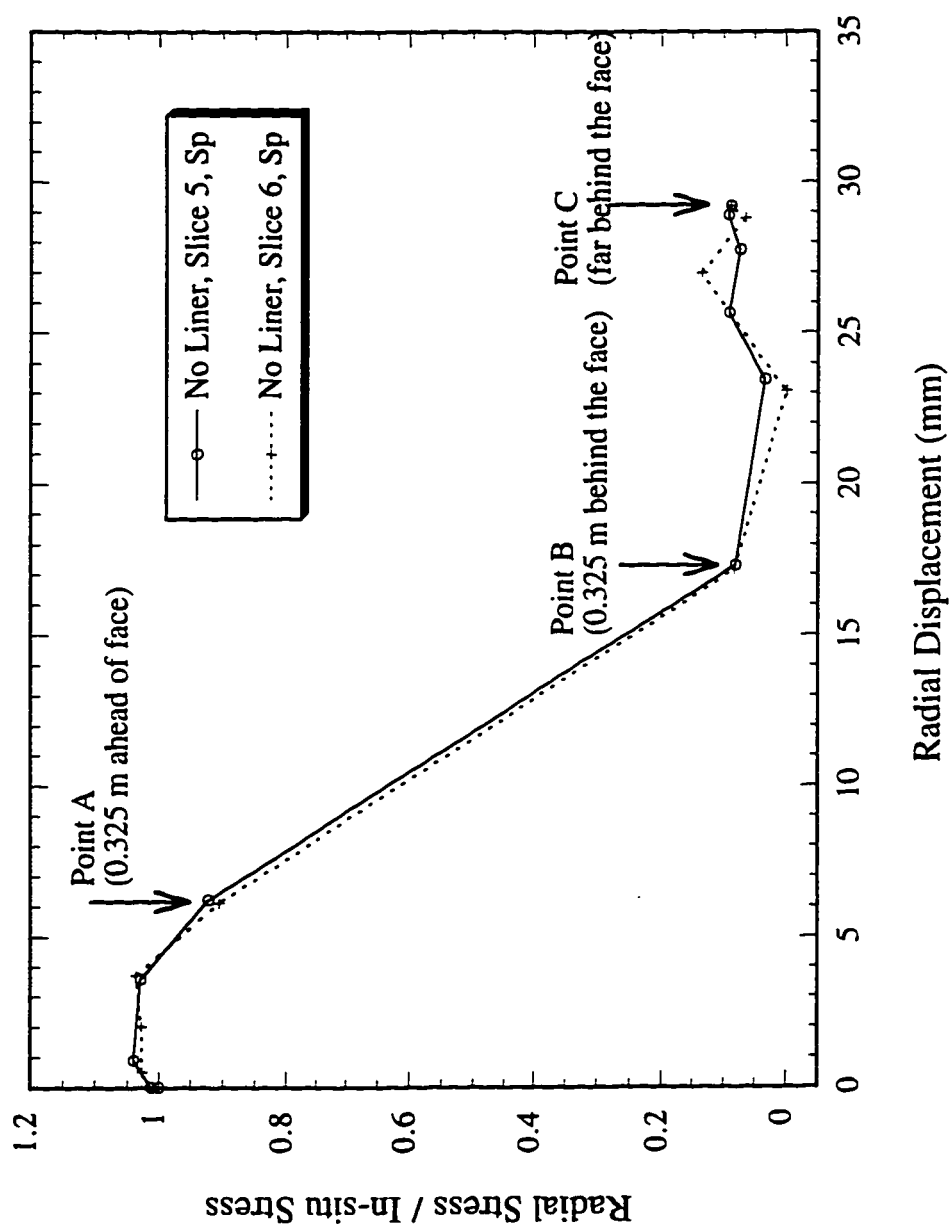


Figure 6.10 Comparison of Convergence Curves of Springline for Slices 5 and 6 without Liner

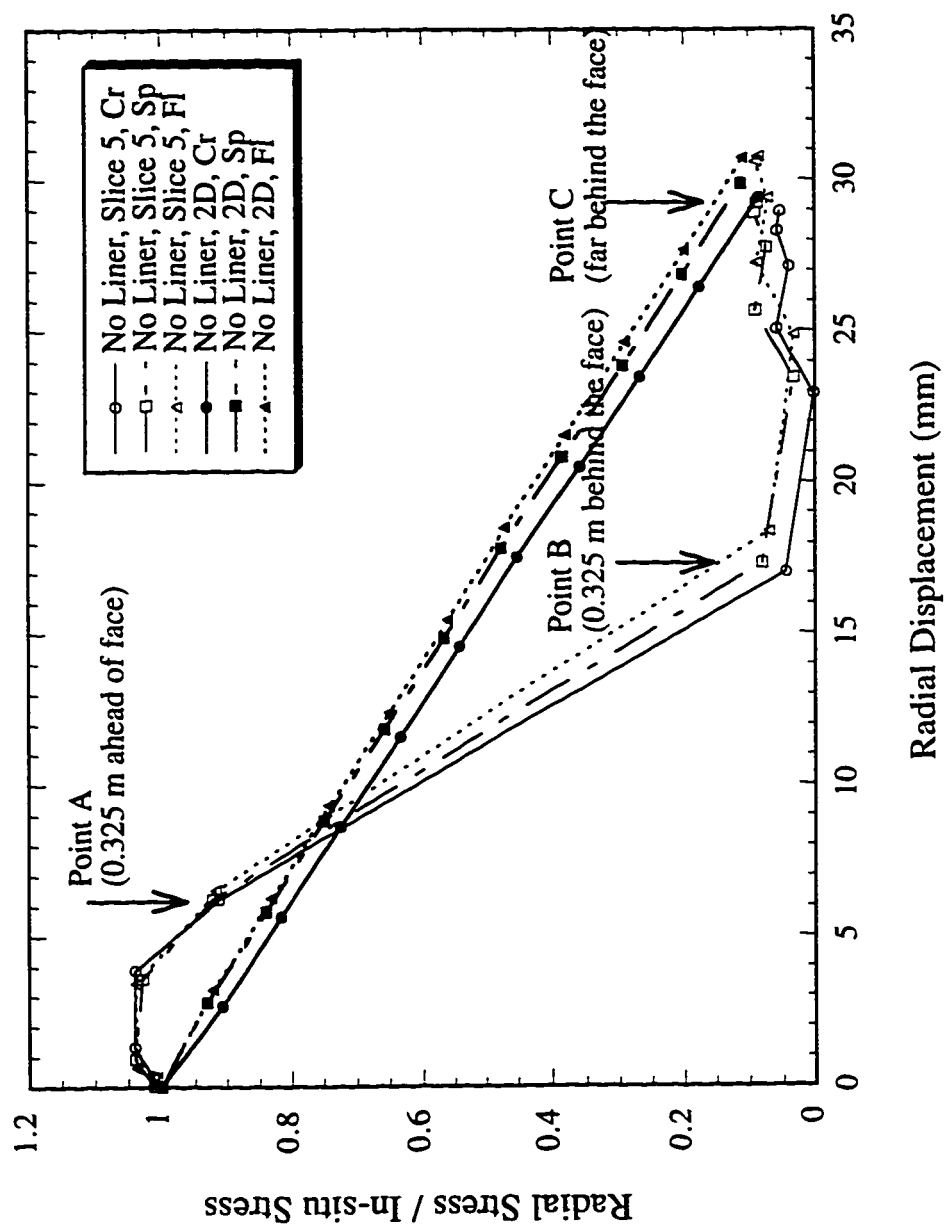


Figure 6.11 Comparison of Convergence Curves of Slice 5 for 2-D and 3-D Analyses

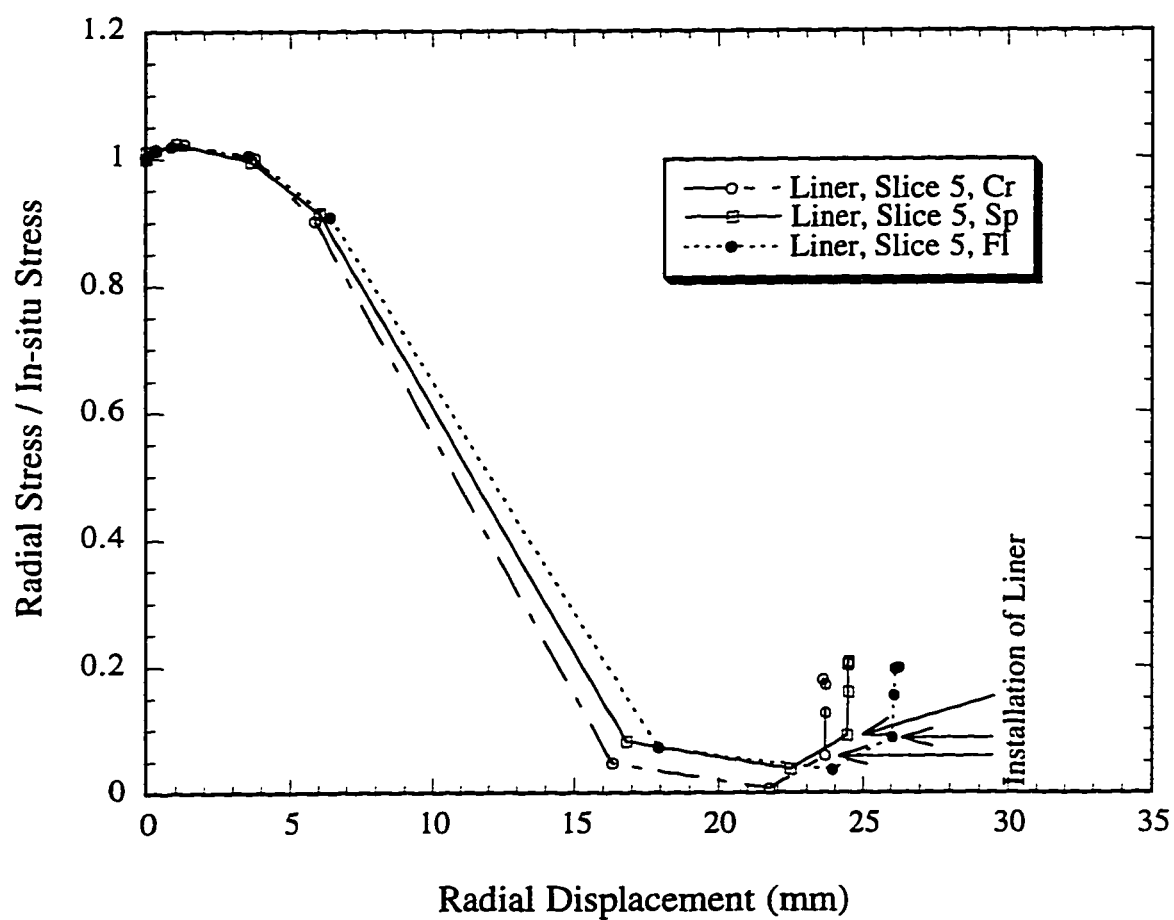


Figure 6.12 Convergence Curves for Slice 5 from 3-D Analyses with Liner Installation

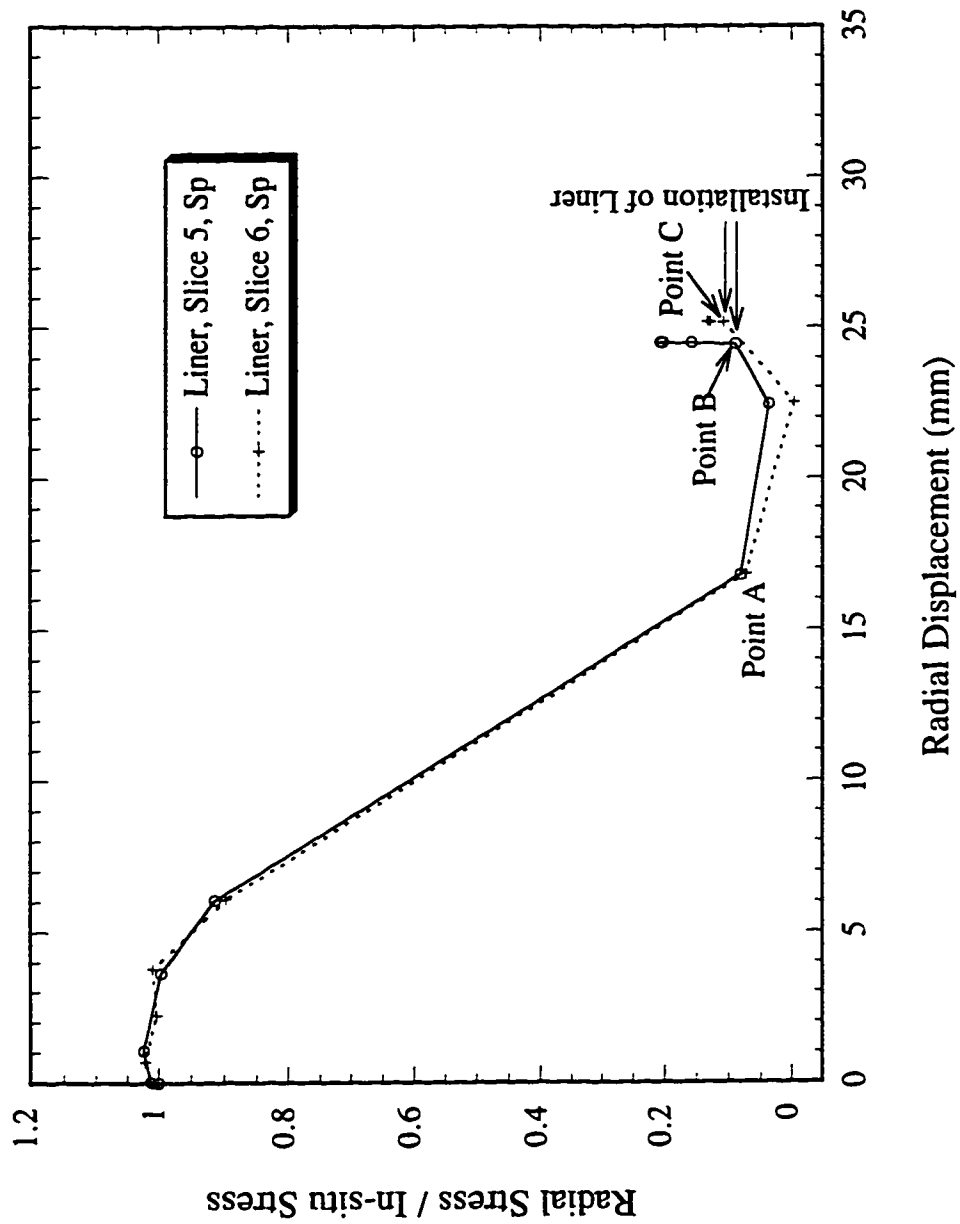


Figure 6.13 Comparison of Convergence Curves of Slices 5 and 6 with Liner Installation

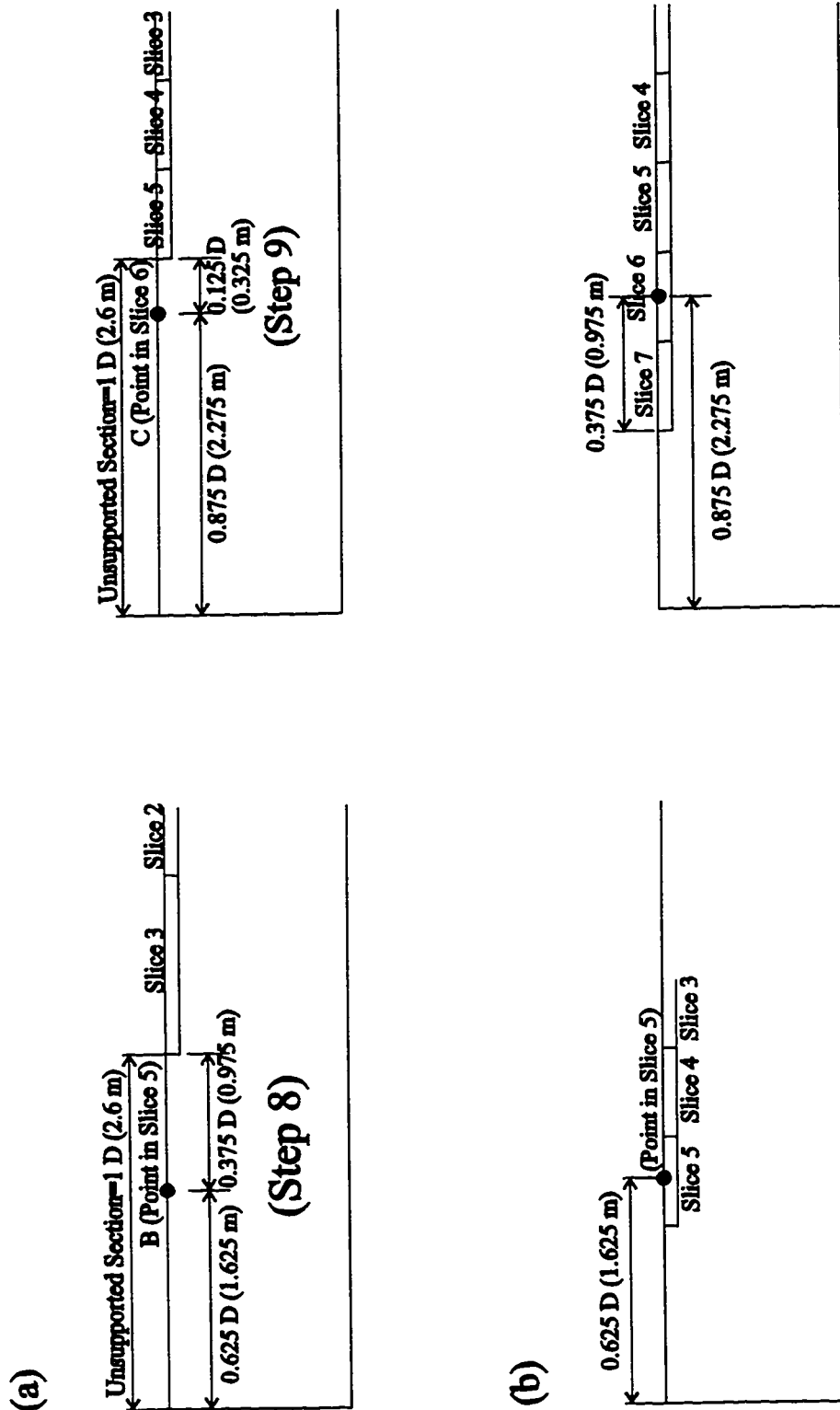


Figure 6.14 a) Location of Points B and C with respect to the Face and the Leading Edge of Liner
b) Location of Tunnel Face at the Time of Liner Installation in Slice 5 and Slice 6

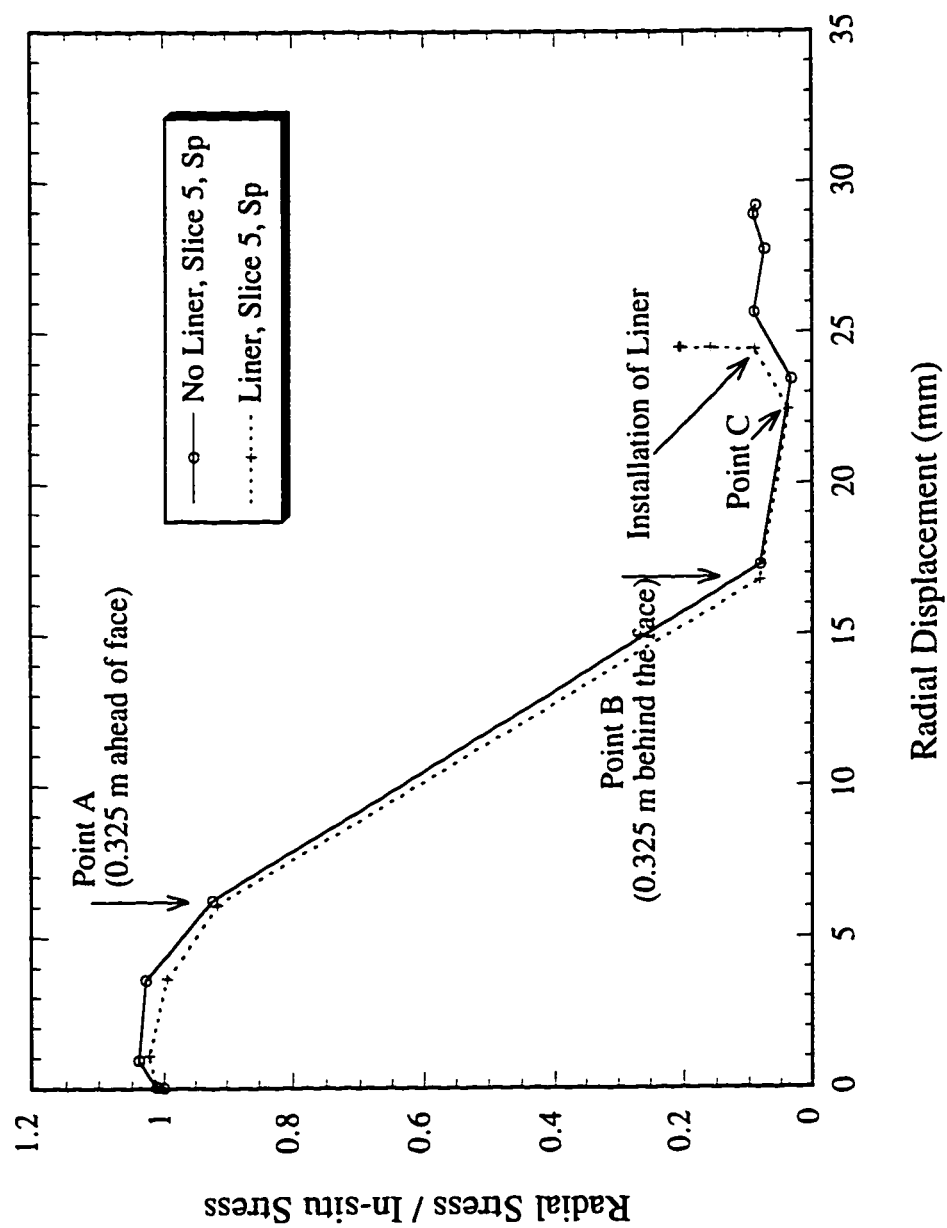
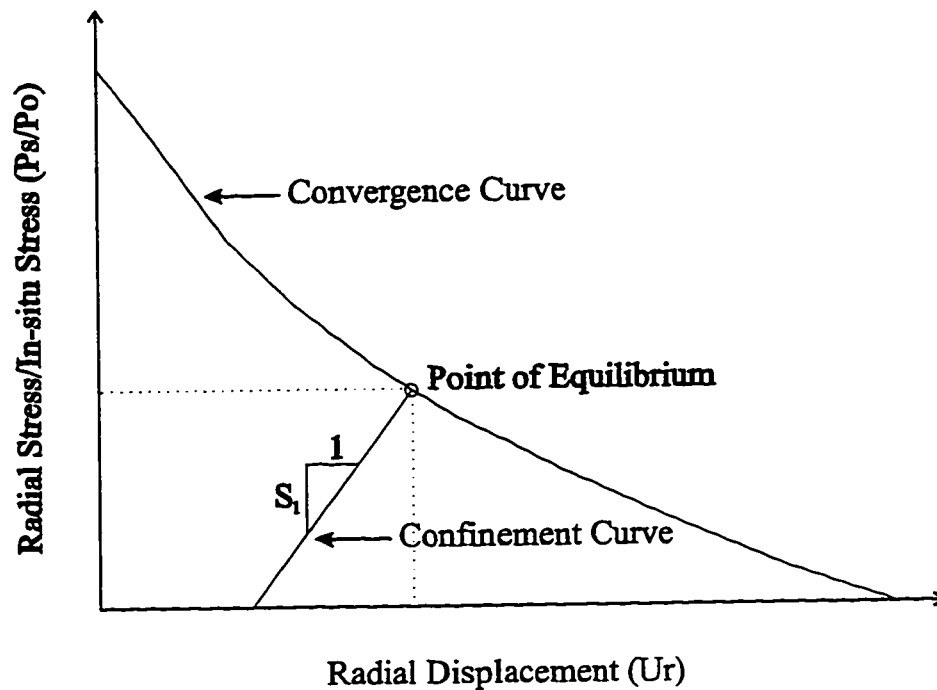


Figure 6.15 Comparison of Convergence Curves of Slice 5 with and without Liner



$$\text{Diametral Strain} = \Delta D/D = P_r r (1 - \nu_l^2) / (E_l t)$$

$$\Delta D = 2U_r$$

$$S_1 = (P_r/P_o) / U_r = E_l t / [R r (1 - \nu_l^2) P_o]$$

where:

S_1 ; Slope of Convergence Curve in P_s/P_o and U_r Plane

D & R ; Exterior Diameter and Radius

ν_l ; Poisson's Ratio of Lining

t ; Lining Thickness

U_r ; Radial Displacement

r ; ($=R-t/2$)

E_l ; Young's Modulus of Lining

Fig. 6.16 Calculation of Confinement Curve for Linear Elastic Support Properties

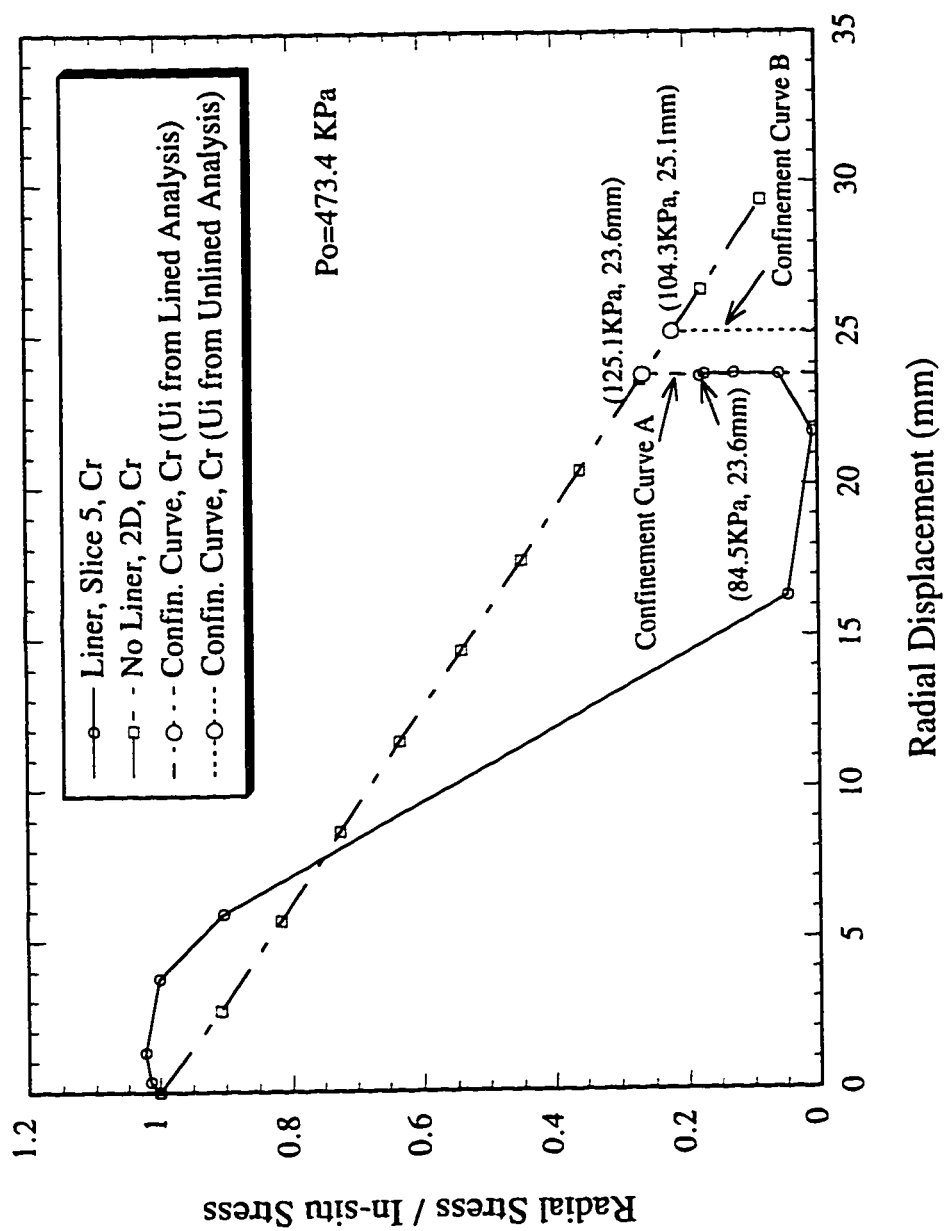


Figure 6.17 Final Equilibrium Stresses and Displacements on the Liner of Crown from the 2-D and 3-D Analyses

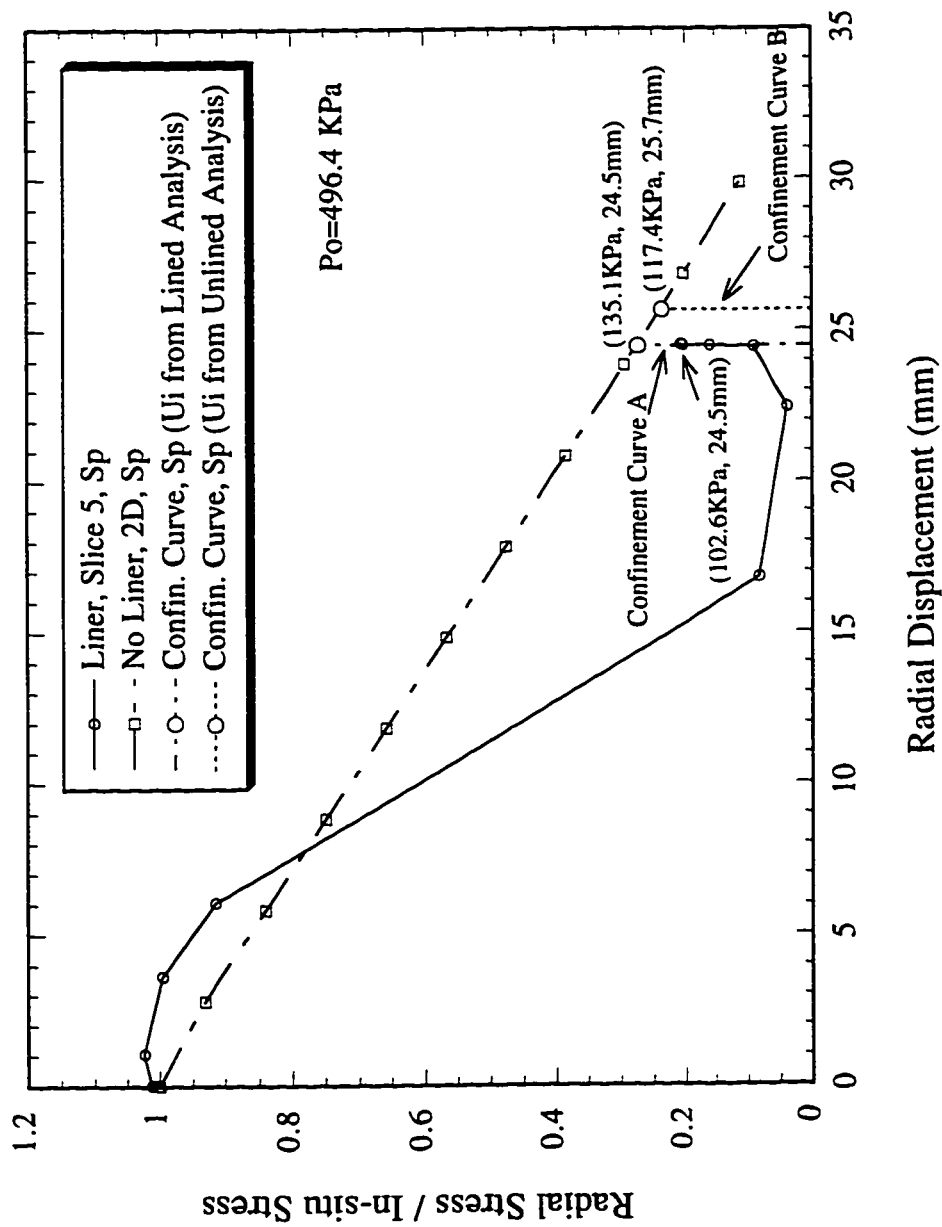


Figure 6.18 Final Equilibrium Stresses and Displacements on the Liner of Springline from the 2-D and 3-D Analyses (Slice 5)

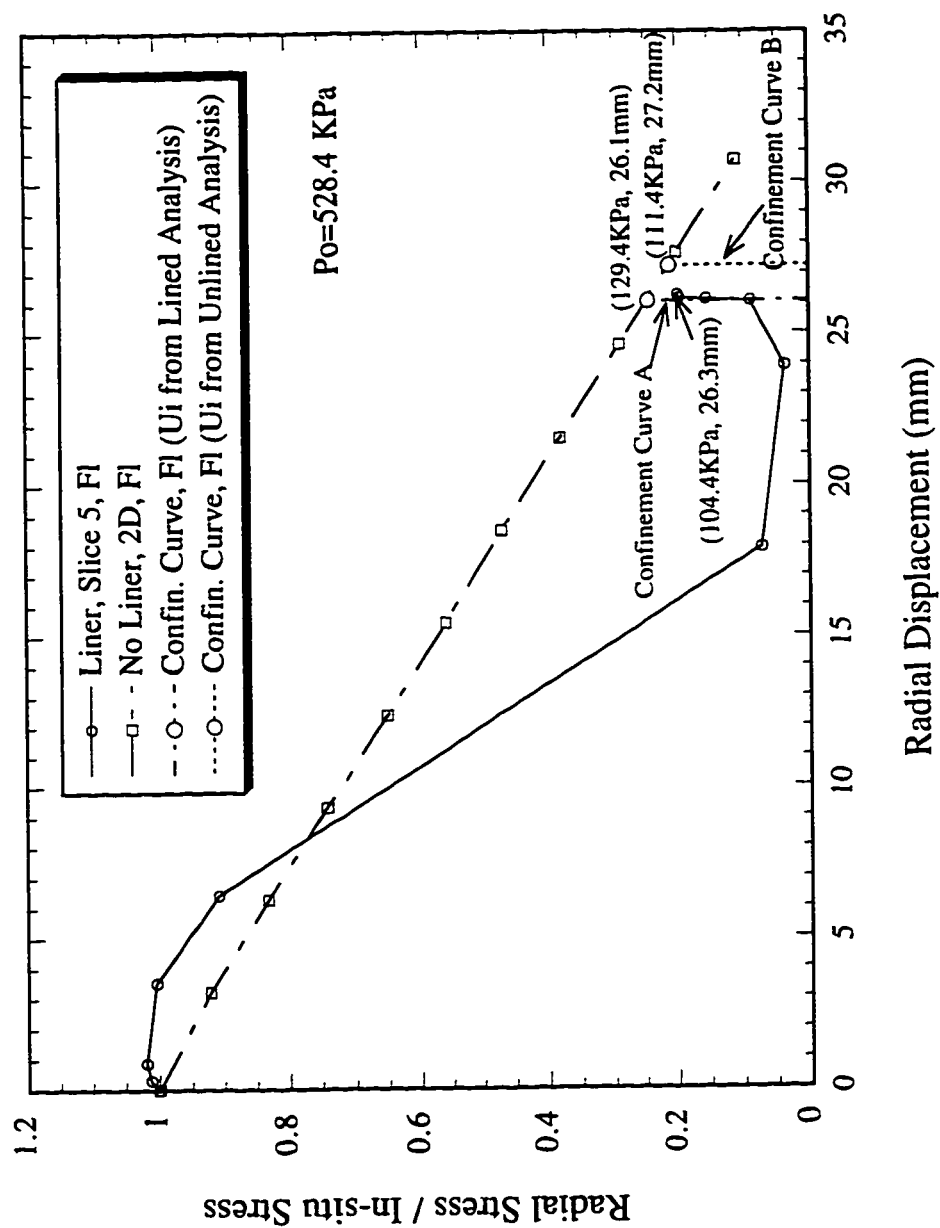


Figure 6.19 Final Equilibrium Stresses and Displacements on the Liner of Floor from the 2-D and 3-D Analyses

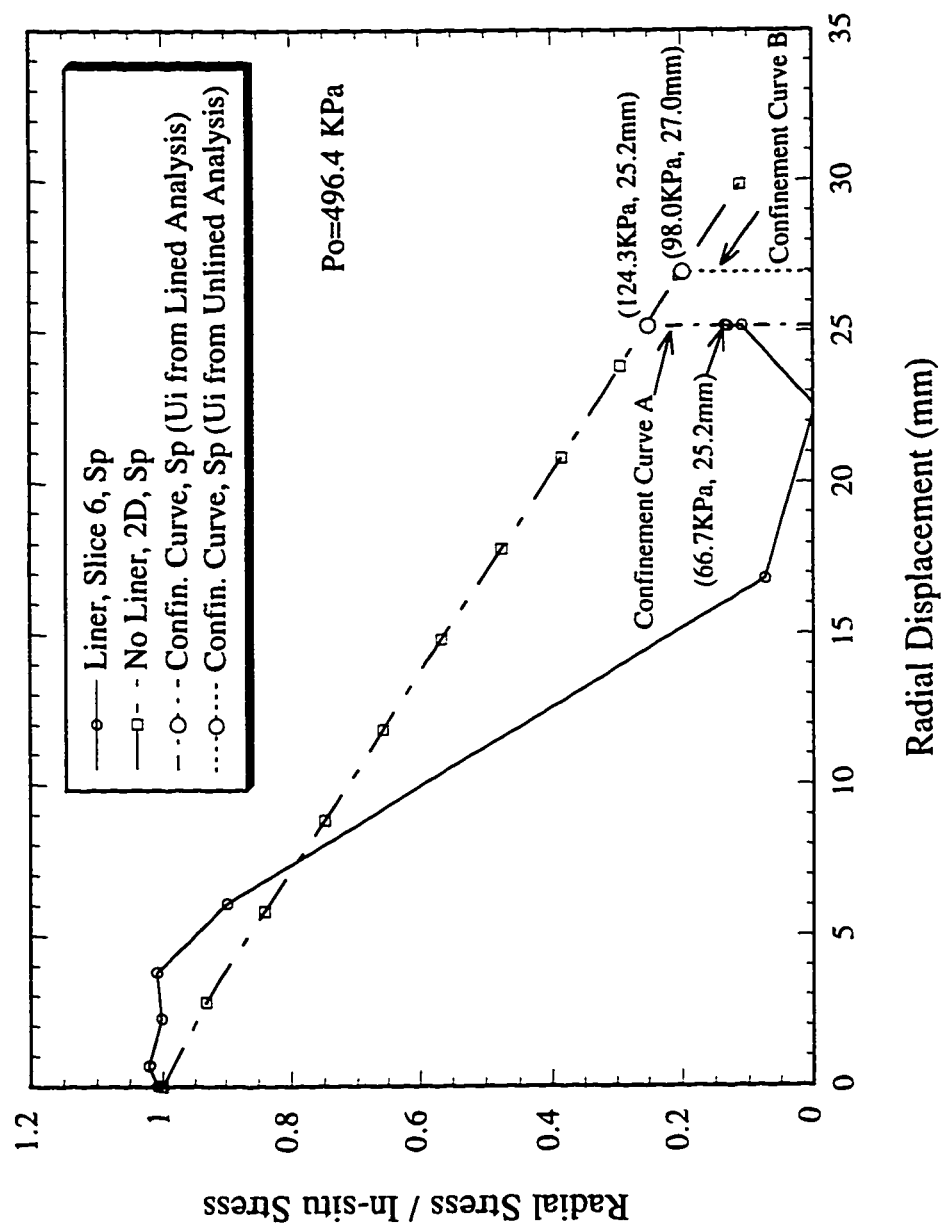


Figure 6.20 Final Equilibrium Stresses and Displacements on the Liner of Springline from the 2-D and 3-D Analyses (Slice 6)

7. Development and Validation of Suggested Methods

7.1 Introduction

The validity of the existing design methods was reviewed in Chapter 4 by comparing the loads calculated using the methods with the field measurements obtained from several tunnels in Edmonton and other areas. However, none of the existing methods were totally satisfactory for the estimation of lining loads because they could not consider all the factors affecting lining loads. Because certain methods could give reasonable results under specific conditions, an improved design method is proposed in this chapter using the existing design methods.

A design method for the prediction of lining loads should include the decrease of lining loads due to the stress release before lining installation as explained in the previous two chapters. The use of stress reduction factors, coupled with other analytical solutions, for the prediction of lining loads was discussed briefly in Sec. 4.7. The results encouraged the use of the reduced unit weight considering that the stress release occurred before lining installation. Therefore, a method to determine the stress reduction factors is described in detail in this chapter. In addition, a specific method or combination of two different methods is suggested for each type of tunnelling for the estimation of lining loads, especially on the primary linings. Finally, the proposed method is compared with field measurements from the case histories collected from many different areas to verify the method.

7.2 Estimates of Stress Reduction Factors

An estimate of the ground displacements can lead to an evaluation of the stress release because the stress release is closely related to the ground displacements. Negro (1988) presented several available solutions for the estimation of tunnel convergences based on comprehensive literature reviews. He observed that none of the existing methods could give generalized solutions for the radial displacements of the opening taking into account the presence of the lining due to the complexity of the problem. He also observed that the problem could be manageable if the presence of the lining and the non-linear stress-strain relationship of the ground were disregarded.

Neglecting the lining's presence will result in an overestimate of the stress release because the lining tends to inhibit the ground displacements around the heading. In other words, the lining loads can be underestimated because the lining was not considered. However, Barlow (1986) showed that the tunnel displacement at the leading edge of the lining was almost identical to that of an unlined tunnel for the same distance to the face for support delays equal to or greater than $5/8$ of the tunnel diameter. In most tunnels, the lining is usually activated at distances from the face greater than this value due to the clearance distance needed by the tunnelling crews for the operation of excavation or the existence of a gap between the soil and TBM or the soil and the lining. Therefore, errors involved in this simplifying assumption may be insignificant.

The assumption of linear elasticity is probably less restrictive regarding the behaviour of the good ground ahead of the tunnel face. However, the assumption can cause errors if a yielding zone starts to develop around an opening. Therefore, the assumption would be mainly applicable to stiff or dense soils, where good ground control construction is accomplished. It could also be applied to softer or weaker ground if an internal pressure, such as compressed air or slurry, is applied to the tunnel walls and face, a condition which will ensure a limited degree of yielding around the tunnel.

Negro performed three-dimensional finite element parametric analyses to estimate the radial displacement at the point of lining installation using the program ADINA (Bathe, 1978), disregarding the two factors mentioned above. Negro observed that an approximate linear relationship existed between the dimensionless radial displacements, U , of the tunnel wall and the in-situ stress ratio, K , at a given section of the tunnel. The dimensionless radial displacements, U , can be expressed as follows:

$$U = \frac{uE_t}{DP_o}$$

where

u = radial displacements

E_t = initial tangent modulus

D = tunnel diameter

P_o = in-situ radial stress.

Dimensionless radial displacements U as a function of K obtained from the analyses are shown in Table 7.1, which was expanded from the original table, Table 4.1, presented by Negro using an interpolation function between points. An estimation of the distance (X) from the face to the location of support activation enables the dimensionless radial displacements U for the crown, springline and floor to be established.

To predict the stress reduction factor at the time of the lining installation, both radial displacements before the lining installation and the convergence curve should be known. Therefore, convergence curves were obtained by parametric 2-D finite element analyses, assuming a hyperbolic elastic material model for distinct points around the tunnel perimeter and for varying ground and geometric conditions. The results of the generalization process for convergence curves were presented through equations and charts.

Stress reduction factors can be found combining the dimensionless radial displacements U calculated using Table 7.1 and a full range of diagrams in a variety of geometric and geotechnical conditions, as presented by Negro (op.cit.). However, obtaining stress reduction factors using the table and diagrams can be tedious and time consuming even though it is not difficult. Therefore, using the table and diagrams, the final stress reduction factors (α) were calculated and are presented in Table 7.2, Table 7.3, and Table 7.4 for $K_o=0.6$, $K_o=0.8$, and $K_o=1.0$ respectively by the current author. Calculation of equivalent friction angles is needed for soils with a non-zero cohesive strength component and with failure ratios different from unity using the following equations:

$$\phi_a = \arcsin \left[\frac{1 + \left(\frac{\sigma_3}{c}\right) \tan \phi}{1 + \left(\frac{\sigma_3}{c}\right) \sec \phi} \right]$$

$$\phi_e = \arcsin(1 - R_f + R_f \csc \phi_a)^{-1}$$

where

ϕ_a = adjusted friction angle

ϕ_e = equivalent friction angle

c = cohesion of soil

σ_3 = minor in-situ principal stress

R_f = failure ratio (generally from 0.7 to 1.0)

$$= \frac{(\sigma_1 - \sigma_3)_{\text{failure}}}{(\sigma_1 - \sigma_3)_{\text{ultimate}}}$$

As mentioned in the previous chapter, Muir Wood recommended a 50 % reduction of the full overburden pressures to account for face and heading effects occurring prior to lining installation. But the 50 % stress reduction was an arbitrary value, and various suggestions have been given by others, e.g. for about a 33 % stress reduction as suggested by Panet (1973). Einstein and Schwartz (1980) also suggested that the stress reduction factor could be between 15 % and 100 % according to simple analytical and numerical techniques and case study data. Stress reduction factors can be obtained easily and reliably if the above tables are used.

The tables clearly show several characteristics of stress reduction factors. More stress is released as X/D increases as expected. However, stress reduction factors (α) do not increase much from an X/D of 1 to an X/D of 2. Figure 7.1 shows a typical relationship between stress reduction factors and X/D . The tables also show that stress reduction factors increase as soil strength, ϕ , increases. However, stress reduction factors are not sensitive to the values of Z/D , especially with an Z/D between 3 and 6 even though slightly more stress is released as Z/D increases.

Negro defined X as the distance from the face to the leading edge of the lining. However, it is a well-known that the load distribution along one segment of lining is not uniform. The load at the leading edge of the lining is higher than that of the following edge because the stress near the excavation front is less released (See Figure 4.15). As a result, the load should be taken in the centre of the liner segment to get the average value. In other words, a support delay length L_d' , the distance from the face to the centre of the closest liner segment, should have been used rather than the distance X . The dimensionless displacement U might have been slightly underestimated. However, the errors are insignificant because the support delay length was normalized to a tunnel

diameter. Furthermore, the method was validated by Negro using X for a large number of case histories. Therefore, the distance X was used for the analyses of actual tunnels in this chapter.

Negro (op. cit.) showed that the dimensionless radial displacements were relatively insensitive for most tunnel depths encountered in practice even though the method was mainly developed for a shallow tunnel. The method is strictly valid, though, for stable ground due to the assumption of linear elastic ground and an unlined opening for the finding of the stress release factor. From a large number of case histories, Negro concluded that the method gave good results in NATM tunnels regardless of the soil type, provided the tunnel face was stable and in TBM tunnels constructed in firm ground or even in less stable ground if the lining was activated in full contact with the soil at a short distance from the face.

7.3 Suggested Methods for the Prediction of Lining Loads

Tunnels are divided into several types, depending on the soil behaviour around an excavation, a factor which is mainly controlled by construction methods, soil types, and tunnel depths. Tunnels are divided into two main groups depending on the tunnel depth. The classification is based on the fact that a certain minimum thickness is required for the construction of the lining up to a certain depth regardless of the soil loads. The deeper tunnels of the two, having a depth to centerline to diameter ratio greater than three, are further subdivided into three groups depending on whether the tunnels have positive face control or not.

A specific method or combination of two different methods is suggested for each type of tunnelling for the estimation of lining loads. The proposed method is strictly valid for tunnels in soil or soft rock with a ratio of tunnel depth to diameter up to 6 for tunnels constructed without face control and up to about 8 for tunnels with face control. However, the method may be used for slightly deeper tunnels than these as shown later in this chapter. The depth generally covers most urban tunnels. A point to be mentioned is that the calculated lining load is an average one. Therefore, to calculate lining loads for a

combined lining system, lining loads should be divided according to Young's modulus and the area of each of these linings as explained in Sec. 3.3.1.

7.3.1 A Depth to Centerline to Diameter Ratio Up to Three

Stress reduction factors cannot be used reliably in such shallow tunnels because arching may not be fully developed due to shallow soil covers. Furthermore, the whole soil section located above the tunnel crown can directly exert pressure on the tunnel lining because the plastic zone may be extended to the ground surface. Therefore, Peck's or Einstein and Schwartz's method without taking into account stress reduction factors is sufficient for the prediction of lining loads in a shallow tunnel.

In addition, the minimum thickness for cast-in-place concrete linings is generally controlled by the clearance between the initial support ribs and the interior form required for the concrete. The International Tunnelling Association (1988) recommended that the thickness of cast-in-place concrete linings may have a lower limit of 25-30 cm to avoid concrete placing problems such as undercompaction or honey-combing of concrete. For segment linings, special care should be taken to avoiding damage during transport and erection. O'Rourke (1984) observed that the minimum thickness for segment linings was usually governed by the requirements of the joints. He stated that the minimum practical thickness is usually enough for tunnels with a depth to centerline up to three diameters.

The predicted lining loads may be conservative if arching develops around an excavation. However, because the soil behaviour is uncertain due to the shallow soil cover, and the minimum practical thickness is usually enough for tunnels, the conservative estimate does not create problems.

Lining loads for tunnels constructed using the cut and cover method can also be estimated using Peck's method without taking into account stress reduction factors because the ground acts passively as a dead load, a loading condition which is similar to that of Peck's.

7.3.2 A Tunnel Depth to Diameter Ratio Greater than Three

7.3.2.1 No Face Control

Eisenstein and Negro (1985) suggested that the stress reduction factor (α) found using their method could be used, coupled with any analytical solution, for calculation of thrust forces and bending moments. The stress reduction factor can be accounted for through the use of a reduced unit weight of the soil. However, the method is strictly valid for stable ground due to the assumption of linear elastic ground and an unlined opening for the finding of the stress release factor as mentioned in Sec. 7.2.

A stability ratio, which was developed by Broms and Bennermark (1967), is an important criterion for determining whether the ground is stable or not. The stability ratio N_t was developed to estimate the stability of plastic clays and is expressed as follows:

$$N_t = (P_z - P_a) / C_u$$

where P_z = overburden pressure at the centerline of a tunnel

P_a = tunnel air pressure above atmospheric, if any and

C_u = undrained shear strength of the clay.

It was reported that tunnels in cohesive soils with stability ratios of up to 2 had quite small development of plastic zones according to axisymmetric finite element analyses (Panet and Guenot, 1982) and actual experience (Schmidt, 1984). Therefore, calculating the stress reduction factor using Tables 7.2 to 7.4 may be valid only for a tunnel with stability ratios up to 2.

According to Broms and Bennermark (op. cit.), tunnels may be constructed without any positive face controls with stability ratios of up to 6. They proposed that failure does not occur as a result of flow of soil into the opening if the stability ratio is less than six. However, Ward (1969) stated that shield tunnelling procedures might not be possible without air or other types of pressures if the stability ratio was more than 5 or 6. He further mentioned that he would expect ground movements of at least 10 times the present values if the stability ratio was in the order of 6.

Davis et al. (1980) also observed that the stability ratio of 6 was on the unsafe side for tunnels with small cover to diameter ratios. In other words, a tunnel should be constructed with stability ratios much smaller than 6, especially according to the modern

tunnelling philosophy in which displacements are controlled. Kuesel (1987) stated that the most important factor in lining construction is to maintain continuous contact between the lining and the ground, with the objective of the lining being to stabilize ground displacements and the most efficient lining being the one that mobilizes the strength of the ground by allowing controlled ground deformation. If excessive deformation is expected during the construction of a tunnel, compressed air or bentonite slurry under pressure is used. Therefore, the stress reduction factor can be estimated using Tables 7.2 to 7.4 for tunnels constructed with the modern tunnelling philosophy.

The actual stress reduction factor can be higher than that predicted if more displacements occur due to high stability ratios. However, the estimated lining loads will be on the safe side because radial stresses decrease as the tunnel wall deforms in a tunnel having controlled ground deformation according to the convergence-confinement concepts. Therefore, the stress reduction factor can be obtained from Tables 7.2 to 7.4 and combined with Einstein and Schwartz's method to calculate the lining loads for tunnels constructed according to the modern tunnelling philosophy and without the positive face control.

The average support thrust T_{av} can be expressed as follows according to Einstein and Schwartz's method:

$$T_{av} = \frac{1}{2} PoR(1 + Ko)(1 - a_o)$$

$$a_o = \frac{CF(1 - \nu)}{C + F + CF(1 - \nu)}$$

$$C = \frac{ER(1 - \nu_1^2)}{E_1 A_1 (1 - \nu^2)} \quad F = \frac{ER^3(1 - \nu_1^2)}{E_1 I_1 (1 - \nu^2)}$$

where

C = compressibility ratio

F = flexibility ratio

A_1 = average cross-sectional area of the support per unit tunnel length and

Po = vertical ground stress at the centre line of a tunnel.

It is customary to express soil loads on tunnels either in terms of the percentage of overburden pressure or in the form of:

$$P = n\gamma D$$

or
$$n = \frac{P}{\gamma D}$$

where

n = a dimensionless factor that depends on soil type and tunnelling method.

Then

$$\begin{aligned} n &= \frac{2T_{av}}{R(1 + K_o)\gamma D} \\ &= \frac{P_o(1 - a_o)}{\gamma D} \\ &= \frac{\gamma_{red}H(1 - a_o)}{\gamma D} \end{aligned}$$

where

γ_{red} = reduced unit weight of the soil caused by stress release around a tunnel

H = depth to tunnel centerline.

Since

$$\frac{\gamma_{red}}{\gamma} = (1 - \alpha)$$

therefore

$$n = \frac{H(1 - a_o)(1 - \alpha)}{D} \quad (7.1)$$

According to Eq. (7.1), the dimensionless factor n is a function of H , D , C , F , ν , and α . As shown in Figure 7.2, the flexibility ratio F was varied to investigate the effect of F on n . The dimensionless factor n is almost insensitive to F for a given compressibility of 0.4. For example, n decreases only 0.01 as F increases from 20 to 1000. Figure 7.3 shows the effect of compressibility ratio C on n for a given H/D of 3. The flexibility ratio was also varied as shown in the figure. The figure clearly shows that n decreases as C increases. In other words, n is a function of C . The factor n is also sensitive to F only when C is bigger than 1 and F is smaller than 50. Therefore, n is again

insensitive to F for most of practical tunnels. Because v of soil does not vary much, n is insensitive to v , too. Therefore, n is mainly a function of H , D , C , and α .

According to Terzaghi's theory, n should not be a function of the tunnel depth H . Terzaghi (1943) discussed the arching above a trap door covered with sand. According to his theory, the arching is approximated by the transfer of load by shear across imaginary vertical planes drawn from the sides of the trap door to the surface of the material. Terzaghi (1946) extended the arching concept to the determination of loads on tunnel liners in crushed rock and sand based on the loading configuration shown in Figure 7.4. He observed that the rock load in these materials did not exceed a small fraction of the weight of the rock located above the roof and was practically independent of depth if the depth of the tunnel was greater than about 1.5 times the combined width and height of the tunnel. In other words, lining loads are independent of the tunnel depth if the tunnel is 3 times or more deeper than its diameter.

Terzaghi (1943) derived equations for the horizontal and vertical components of pressure required by the support system to balance the strata loading generated from the loading condition as shown in Figure 7.4. The general formulae are shown below:

$$P_v = \gamma(B + 2H_t \tan(45 - \phi/2))/2 \tan \phi \quad (7.2)$$

$$P_h = 0.3(0.5H_t \gamma + P_v) \quad (7.3)$$

where P_v = support vertical loading pressure

P_h = support horizontal loading pressure

B = tunnel diameter.

Since

$$P = n\gamma B \text{ and } B = H_t \text{ for circular tunnels}$$

Therefore, the above equation can be rewritten as follows:

$$P_v = \gamma B(1 + 2 \tan(45 - \phi/2))/2 \tan \phi \quad (7.4)$$

$$n = (1 + 2 \tan(45 - \phi/2))/2 \tan \phi \quad (7.5)$$

Equations (7.2) and (7.3) have been used successfully in the design of tunnels in sand. Whittaker and Bonsall (1982) examined the use of these equations for Carboniferous rocks encountered in UK coal mines. They found that the support pressures calculated using the Terzaghi derived formulae were generally good when

compared to actual measurements for shallow tunnels located not deeper than 250 m. They stated that the support requirements were independent of depth in shallow tunnels. Their statement may be true from a certain depth up to 250 m. However, for most urban tunnels, the statement can be incorrect. Lining loads may often be a function of the tunnel depth as indicated in Eq. (7.1) for these tunnels. The validity of Eq. (7.1), (7.2), and (7.3) is reviewed in the following paragraphs for tunnels in Edmonton.

Eq. (7.2) is plotted in Figure 7.5 with the actual case histories in Edmonton using an average overburden unit weight of 21 KN/m^3 and a ϕ range of $30-40^\circ$, a range which is considered to cover the variety of geologic material as encountered in Edmonton tunnels. Terzaghi's formulae generally underestimated the vertical support pressure for the case of small diameter tunnels and overestimated the vertical pressure for large diameter tunnels as shown in Figure 7.5. The dimensionless factor, n , from Terzaghi's derived formulae, is plotted with the case histories in Figure 7.6. The figures clearly showed that Terzaghi's equation does not work for tunnels in Edmonton.

An interesting point is that only tunnels which are less than 3.2 m in diameter show higher n values than predicted values, except tunnel A. Terzaghi's equation also overestimates lining loads for tunnels having a H/D smaller than 4.3 and underestimates lining loads for tunnels having a H/D greater than 5.2, except tunnels A and F. To find out the effect of the tunnel diameter and tunnel depth on n , these parameters are plotted versus n as shown in Figure 7.7. The dimensionless factor n slightly increases as the tunnel depth increases. The factor n generally shows smaller values when the tunnel diameter is larger even though n varies in a similar diameter. The relationships between n and the tunnel depth and between n and the tunnel diameter are not obvious in the figure even though n is affected by these parameters.

The dimensionless factor n is plotted versus H/D in Figure 7.8 because n is a direct function of H/D according to Eq. (7.1). The figure clearly shows that n is a function of H/D . Therefore, even though it is expected that Terzaghi's equation may be valid from certain tunnel depths, Eq. (7.1) is valid for tunnels in Edmonton, which are not very deep.

Deere et al. (1969) and Cording et al. (1971) related the factor n and RQD for rock tunnels. It is convenient to find a similar relationship of n and other parameters for

tunnels in Edmonton using Eq. (7.1). Because n is a function of H , D , C , and α as discussed above, Eq. (7.1) is modified as follows to reduce variables:

$$\frac{nD}{H} = (1 - a_o)(1 - \alpha). \quad (7.6)$$

The calculation of nD/H for tunnels in Edmonton is done using the parameters shown in Table 7.5. Most typical values for Edmonton tunnels are selected for these parameters. The ratio of depth to springline to tunnel diameter (H/D) and tunnel radius were varied in exactly the same way for all of the different construction and support systems. For tunnels constructed using SEM, shorter support delay lengths were assumed because shotcrete is usually applied close to the tunnel face.

Parametric analyses were performed using Eq. (7.6) and values in Table 7.5. For supports, Young's modulus of 200000 MPa, 25100 MPa, and 10000 MPa were used for rib and lagging, segmented lining, and shotcrete respectively. For the ground, Young's modulus of 150 MPa, 100 MPa, and 250 MPa were used for till, sand, and claystone respectively. According to the analyses, the value of nD/H decreased as tunnel radius, rib spacing, and tunnel depth increased, whereas nD/H increased as the thickness of the lining increased. The effect of support delay length X/D on the factor n for each support system was insignificant because stress reduction factors do not change much for the ranges covered by the analyses as shown in Figure 7.1.

Typical values of nD/H for tunnels in Edmonton were calculated from the parametric analyses as shown in Table 7.6. Rib spacing of 1.22 m, lining thickness of 0.2 m, shotcrete thickness of 0.2 m, and shotcrete thickness of 0.2 m combined with 1.5 m rib spacing were considered as representative values for the calculation of nD/H for a rib and lagging system, segmented lining, shotcrete, and shotcrete and rib system respectively. For all of the groups, a H/D of 6 was used for the calculation of nD/H because tunnels shallower than a H/D of 3 can be treated as explained in Sec. 7.3.1. Furthermore, the table can still be used safely for tunnels located deeper than those with a H/D of 6 because nD/H decreases as the ratio of H/D increases. The value of nD/H was calculated using the two values of X/D for each group of tunnels as shown in Table 7.5, and an average value was taken for the final value.

Table 7.6 shows that steel rib and timber lagging of the conventional lining carries less loads than those of other lining systems due to high compressibility. The shotcrete lining in a SEM tunnel has a higher nD/H than those of linings in TBM tunnels, even though it has higher compressibility, because it has fewer stress reduction factors. The use of steel rib slightly increases the n of shotcrete lining in SEM tunnels.

Several recommendations have been given for the values of n for tunnels in Edmonton. For glacial till, the factor n was suggested to be about 1 for a rib and lagging system and 2.5 to 5 for a segmented lining (Eisenstein, 1992). For the conventional design of primary linings, Montgomery and Eisenstein (1995) recommended taking the dimensionless factor n as 2.5 for tunnelling in till and in claystone and as 3.5 for tunnelling in cohesionless soils. Montgomery and Eisenstein's recommendation did not include the effect of tunnel depth and construction method on the factor n . The recommended values are equivalent to H/D of 8.1, 7.8, and 5.3 for till, sand, and claystone respectively, when comparing the values with a rib and lagging system of a small diameter tunnel in Table 7.6. Because n is a function of H/D and construction method, using either Eq. (7.1) or Table 7.6 is recommended for estimating n values for tunnels in Edmonton.

The predicted values of n obtained using Eq. (7.1) and Table 7.6 are compared with the measured n for tunnels in Edmonton as shown in Figures 7.9 and 7.10 respectively. The calculated values of n from Table 7.6 are slightly more conservative than those from Eq. (7.1). However, the table can still be used for a quick estimation of lining loads for tunnels in Edmonton.

Actually, the proposed method is not suitable for tunnel A because the tunnel has a H/D of only 1.7. If Peck's method is applied without considering stress reduction factors for the calculation of n for tunnel A as suggested in Sec.7.3.1, tunnel A can be replotted as shown in the figures. The method is also not suitable for tunnel M due to the poor ground condition, combined with high water tables and construction of an embankment on the ground surface, as explained in Chapter 4. The average surface settlement for tunnel M was 0.3 m. Stress reduction factors cannot be applied to a tunnel which has such large displacements. Tunnel M can be replotted as shown in the figures if

stress reduction factors are not considered. The lining load of tunnel G is underestimated, probably due to the inaccuracy of the measurements because the lagging deflection is not a reliable way to measure lining loads as explained in Sec. 3.2.3. However, this assumption cannot be confirmed.

The proposed method has a tendency to give conservative results if these three tunnels are excluded. However, the proposed method gives a reasonable approximation of n , considering the accuracy of the load measurements, limited knowledge of ground and lining properties, and existence of possible gaps between the lining and ground.

7.3.2.2 Positive Face Control with Compressed Air or Fluids

Positive face control is necessary to maintain face stability and to prevent any excessive deformation at the face by allowing a limited amount of stress release to occur. Therefore, compressed air or slurry pressure is generally applied near the face. The pressure should be lower than the overburden pressure to prevent any possible blow-out. Eisenstein and Ezzeldine (1992) recommended applying about 40 % of the overburden pressure for a tunnel in Edmonton constructed using a hydroshield boring machine. Since less than overburden pressure is usually applied to the face, there should be a certain amount of stress release at the time of lining installation.

Deere et al. (1969) presented a ground reaction curve which showed the effect of air pressure. They assumed that the in-situ stress was reduced by the magnitude of the air pressure and that the lining load would increase again upon removal of the air pressure. However, they did not show how to evaluate the radial displacements of the tunnel wall at the time of lining installation. Negro (1988) suggested reducing the tunnel depth equivalent to the magnitude of the air pressure. However, he did not consider the stress increase on the lining after the removal of the air pressure.

It is obvious that the amount of stress release at the tunnel wall is reduced at the time of lining installation due to the positive face control compared to that of a tunnel constructed without face control. However, the amount of stress release is unknown. Deere et al. and Negro's concepts can be combined to evaluate the effect of positive face control on the lining loads. First, in-situ stresses are reduced by the magnitude of the air

or slurry pressure. The reduction of in-situ stresses is achieved by reducing the soil cover depth above a tunnel. The stress reduction factor can be found as explained in the previous section but using the reduced soil depth. The stress acting on the lining before the removal of the air or slurry pressure can be found by multiplying the reduced unit weight of the soil by the reduced soil depth. The air or slurry pressure should be added to the stress found above to obtain the final stress acting on the lining upon removal of the air or slurry pressure.

Eq. (7.1) should be modified to take into account all of these factors described above. It was shown that n can be expressed as follows:

$$n = \frac{P_o(1 - a_o)}{\gamma D}$$

Since

$$\frac{P_i}{\gamma} = H_{eq}$$

Therefore

$$\begin{aligned} n &= \frac{[\gamma_{red}(H - H_{eq}) + P_i](1 - a_o)}{\gamma D} \\ &= \frac{\gamma_{red}(H - H_{eq})(1 - a_o)}{\gamma D} + \frac{P_i(1 - a_o)}{\gamma D} \\ &= \frac{(1 - \alpha)(H - H_{eq})(1 - a_o)}{D} + \frac{P_i(1 - a_o)}{\gamma D} \end{aligned} \quad (7.7)$$

where

P_i = air or slurry pressure

H_{eq} = soil depth equivalent to P_i .

Therefore, the dimensionless factor n for a tunnel constructed using air or slurry pressure can be estimated using Eq. (7.7).

7.3.2.3 Positive Face Control using Jet-Grouted Piles

If a tunnel is driven through unstable material such as loose sand, jet-grouted piles should be used prior to tunnelling to enhance face stability during the tunnelling

operation. In this case, higher soil strength should be used, especially in terms of Young's modulus, for the calculation of the lining loads considering the use of jet-grouted piles. The low lining loads may be a result of the fillcreting operations used in the tunnel. Calculated lining loads will be lower than those measured if the increase of soil strength is not considered for the prediction of lining loads. In summary, Eq. (7.1) is applicable for tunnels belonging to this group to estimate the dimensionless factor n but with the increased Young's modulus considering the use of jet-grouted piles.

7.4 Verification of the Proposed Method Using Case Histories

There are several basic requirements of a good design method. First, the design method should be simple to use. Second, the design method should consider the stress release occurring before the installation of a liner in some way. Third, the method should take into account the plastic behaviour of the ground as well as that of elastic ground. The proposed method totally satisfies the first two conditions and partly satisfies the third conditions due to the assumption of stable ground used for the development of the stress reduction factors. However, the most important factor in a good design method should be the accuracy of the predicted lining loads. Therefore, the measured and calculated lining loads are compared in this section to check the validity of the proposed design method.

7.4.1 Tunnels in Edmonton

The South Tunnel section of the City of Edmonton's South Light Rail Transit Extension, Phase II involved excavation of 380 m long twin tunnels between the South Tunnel Portal in the North Saskatchewan River valley and the University Station. The twin tunnels which are named Southbound (SB) and Northbound (NB) were excavated from the South Portal to the University Station as shown in Figure 7.11.

A simplified geological section along the South Tunnel is shown in Figure 7.12. The stratigraphy consists of Upper Cretaceous claystone, overlain by a clay till, outwash sands and glacial lake clays. The tunnels were driven mainly in claystone. The undrained shear strength of the claystone is estimated to be about 350 to 450 KPa and its modulus of elasticity about 190 to 335 MPa, from self-boring pressuremeter tests (Thurber, 1986).

Recommended geotechnical design properties of the till, bedrock and sand were provided by EBA(1988), which are shown in Table 7.7.

The excavated diameters of both tunnels are approximately 6.3 m, and both tracks are parallel with approximately 10 m between centres in typical tunnel sections. The Sequential Excavation Method (SEM), also known as the New Austrian Tunnelling Method (NATM), was used for both tunnels. The tunnels were driven with a standard EL300 hydraulic excavator coupled with an electrically-driven Alpine roadheader boom. The tunnelling proceeded in two stages: heading and benching. The heading typically advanced 4 m ahead of the location where the invert was closed. Average monthly advance rates verified in typical portions were 2.5 to 3.5 m/day, with a peak of 4.2 m/day for the second NB tunnel(EBA, 1991). Excavation and primary lining of the SB tunnel were completed prior to placement of the NB tunnel excavation.

Steel ribs and two layers of shotcrete were used for a primary lining system for both tunnels, while permanent support is formed by cast-in-place concrete. A summary of the initial support for the tunnels is shown in Table 7.8. In claystone and hard clay till, the ribs were at 1.0 m or 1.5 m centres with 125 mm of shotcrete. However, where sand deposits were encountered ribs at 1 m centres, 170 mm of shotcrete and spiling were used.

Field measurements were carried out in order to verify the design methods and to provide an empirical evaluation of the behaviour of tunnels constructed in the Upper Cretaceous claystone and the clay till of the area. Five sets of electrical resistance load cells were installed in the ribs of the two tunnels: ribs No.137, No.138, and No.286 in the SB tunnel and No.144 and No.145 in the NB tunnel as shown in Figure 7.11 and Table 7.9. A cross-section in rib No. 138 is shown in Figure 7.13. In rib No.286, the tunnel was mainly driven through clay till except for the crown area which is composed of sand.

Load cells in ribs No.137, No.138, No.144, and No.145 were installed between rib segments at below elephant's foot, which is 1 m above springline, whereas load cells in rib No.286 were installed at springline. The leads from the load cells were brought through the final concrete liner and placed inside electrical boxes mounted on the concrete.

Table 7.10 shows measured loads on ribs No.137, No.138, and No.286 before and after the passage of the NB tunnel and loads on ribs No.144 and No.145 in the NB tunnel. For each rib, the total loads were obtained from the average of two load cells located in the left and right sides of the rib except rib No.138, which has a problem in a load cell located in the right side of the rib. The measured loads considered in this study were obtained before the final lining was placed. The NB tunnel excavation passed and the final linings were placed in the section of ribs No.137 and No.138 at 197 days and 266 days after the ribs were installed respectively. The NB tunnel passed the section of rib No.286 at 191 days after the rib was installed. In the NB tunnel, the final lining was placed in the section of ribs No.144 and No.145 at 161 days after the ribs were installed.

It has been suggested that the load share in terms of thrust between the shotcrete and steel ribs can be expressed as the ratio between the product of Young's modulus versus the area(EA) of each of these structural elements as explained in Sec 3.3.1. The equivalent shotcrete modulus 10 GPa was used for the calculation of the $(EA)_{\text{shotcrete}}$ as it agreed with the value suggested by Negro(1988), who successfully tested this value by backanalyzing many case histories. For the twin tunnels described above, the EA ratio between the rib and shotcrete was 18.4% for ribs No.137 and No.138, 78.2% for rib No.286, and 27.7% for ribs No.144 and No.145. Therefore, the estimates of the soil pressure on the primary liner were calculated based on load cell measurements and EA ratio between the rib and shotcrete shown as follows:

$$T_{\text{rib}} + T_{\text{shotcrete}} = \frac{\text{Rib}_{\text{load}} + \left(\frac{\text{Rib}_{\text{load}}}{EA_{\text{ratio}}}\right)}{\text{Spacing}} \quad [\text{KN/m}]$$

$$PL = \frac{T_{\text{rib}} + T_{\text{shotcrete}}}{R} \quad [\text{KPa}]$$

$$n = \frac{PL}{\gamma D}$$

where

Rib_{load} = Measured Load on the Steel Rib from the Load Cell

PL = Pressure on the Combined Lining

Spacing = Rib Spacing.

The average liner pressure for a typical tunnel section in the SB tunnel is approximately 50 % of the overburden soil pressure according to Table 7.10. However, the average liner pressure for the HUB Mall section in the SB tunnel is only 19 % of the overburden. The smaller lining load developed in the HUB Mall section as compared to a typical section is believed to be due to the use of spiling near the crown in the section. The average pressure on the lining of the NB tunnel is about 41 % of the overburden pressure.

Lining loads were predicted using Einstein and Schwartz's methods combined with Table 7.3, Table 7.4, and Eq. 7.1. Many authors have used coefficients of earth pressure of between 0.8 and 1.0 for Edmonton till and claystone (Phelps and Brandt, 1989; Branco and Eisenstein, 1985; Eisenstein et al., 1979; Negro, 1988). A K_o of 0.8 and 1.0 were used for till (rib No.286) and claystone (ribs No.137, 138, 144, and 145) respectively in this study. Young's modulus of 250 MPa and 10000 MPa were assumed for the soil and lining respectively. A support delay length of 4 m was used for all tunnels to find the stress reduction factors because the tunnel heading typically advanced 4 m ahead of the location where the invert was closed. Some interpolation was needed to obtain the stress reduction factor because the tables cannot cover the whole range of soil properties. The calculated stress reduction factors were 0.440 for ribs No.137 and No.138 and 0.402 for ribs No.144, No.145, and No.286. The predicted lining loads were compared with measured loads as shown in Table 7.10 and Figure 7.14.

The lining loads in rib No.286 were overestimated as shown in Figure 7.14 probably due to the use of steel spiling near the crown of the section which has the same effect as increasing soil strength in the area as explained in Sec. 7.3.2.3. In this case, a higher soil strength should be used, especially in terms of Young's modulus, for the prediction of the lining loads considering the use of spiling. However, the estimation of the soil strength increase due to the use of spiling is very difficult because the spiling was used only in the crown area. The increase of Young's modulus from 250 MPa up to 1600 MPa gave close agreement between the measured and predicted lining loads for rib No.286. However, the existence of spiling can be disregarded for the purpose of the tunnel lining design because it is a safe-side approximation.

The stress interaction effect is very small when the two tunnels' centres are two diameters apart according to the elastic stress distribution near single openings. However, the above theory can be applied when the ground is hard and regarded as entirely elastic. The liner pressures were higher than predicted in rib No.137 after the passage of the NB tunnel. The load cell measurements in rib No.137, which is about 1.6 diameters centre to centre from the NB tunnel, clearly show the interaction between the two tunnels. In the initially driven SB tunnel, the load measured on the pillar side increased rapidly for the first ten days and then stabilized at values around 165 KN. The passage of the second tunnel caused a load increase of about 10% for 80 days and then returned to the original values measured before the passage of the NB tunnel. The loads on the external side, i.e., the right side facing the direction of tunnel advancement, of rib No.137 stabilized at values of about 150 KN before the passage of the NB tunnel. The passage of the second tunnel caused a load increase of about 95%. Therefore, the amount of load increase on the lining due to the passage of a second tunnel should be considered separately for the estimation of lining loads, especially when the distance between two tunnels is closer than two diameters apart from centre to centre. Peck (1969), King et al. (1972), Ghaboussi and Ranken (1977), and Soliman et al. (1993) studied the interaction problem between two adjacent tunnels.

According to the elastic stress distribution theory, the pillar sides of both tunnels should have more loads than those of the external sides due to the superimposing of the two stress distributions surrounding the individual tunnels. Ghaboussi and Ranken (op.cit.) studied the behaviour and interaction on stresses and displacements between two parallel circular tunnels by performing a series of two-dimensional plane strain finite element analyses. The results generally showed that the stresses at the external side of each tunnel differed only slightly from those of a single tunnel, whereas higher stresses were observed on the pillar side of each tunnel. However, the load cell measurements in ribs No.137, No.144, and No.145 showed that the loads on the external side were higher than those of the pillar side in the long term period even though this phenomenon is not evident in ribs No.138 and 286 due to instrument malfunction. This situation can possibly be explained by arching theory. The loads measured on the pillar side for the short term

period were higher than those of the external side possibly due to the superimposing of stresses between the two tunnels (rib No.137) and disturbance of soil in the pillar side due to the first tunnel (ribs No.144 and No.145). However, as time went on the two tunnels possibly behaved like one tunnel because the distance between the two tunnels was only 1.6 diameters away from centre to centre. Therefore, more loads were acting on the external sides of both tunnels, and the pillar sides of the tunnels only carried the soil loads which were not arching to the external sides. This kind of load pattern was also observed on the lining of Edmonton SLRT tunnels by Tweedie et. al (1989). Therefore, more research should be done in the future to fully understand the interaction problem between two adjacent tunnels.

The load increase was not obvious in two other ribs in the SB tunnel. The loads on the external side of rib No.138 might have increased, similar to those of rib No.137. However, this could not be confirmed because the load cell was not functioning properly. The stable lining loads in rib No.286 after the passage of the NB tunnel could again be related to the use of spiling in the section.

In conclusion, the proposed method generally gives reasonable approximations of the lining loads for the tunnels in Edmonton, considering the accuracy of the load measurements, the limited knowledge of ground and lining properties, and the existence of possible gaps between the lining and ground. The stress interaction effect should be considered separately either using the existing methods or numerical analyses if the two tunnels are less than two diameters apart from centre to centre. One of the main reasons that the proposed method works reasonably well for the tunnels in Edmonton could be related to the stiff nature of the ground. To check the validity of the method for tunnels constructed in places other than Edmonton, the measured and predicted lining loads were compared as described in the following section.

7.4.2 Tunnels Located Other than Edmonton

Fourteen case histories were collected to verify the proposed method. These case histories are summarized in Appendix 1. Most of the soil and lining parameters used for the application of the method were obtained from the references shown in Appendix 1.

The properties of London clay were also available in a paper presented by Ward et al. (1959). If certain parameters were not available, the most probable values were assumed. The ratios of tunnel depth to tunnel diameter, H/D , considered were from 1.2 to 17.9, even though the method was not recommended for use in tunnels having a H/D greater than 6. The in-situ stress ratio, K_0 , of unity was used for tunnels having a ratio greater than 1, e.g., tunnels in London clay.

The support delay length is the most important parameter for estimating the lining loads reasonably well. For all of the tunnels except Tunnel No.1, the support delay length was taken from the face of the tunnel rather than from the tail of the shield due to the existence of gaps between the shield and soil. Ward (1969) also observed that the use of a shield did not prove to be effective to reduce ground movements in London. The support delay length was taken from the tail of the shield for Tunnel No.1 because the average diameter of the shield was only 0.5 cm larger than that of the lining.

The proposed lining loads were compared with measured loads as shown in Figure 7.15. The stress reduction factor was not considered for tunnels having a ratio of H/D of less than three as suggested in Sec.7.3.1. The predicted lining loads for these shallow tunnels, i.e., Tunnel Nos. 2, 8, 9, and 11, were conservative, as expected. However, the conservative estimates do not create problems because the minimum practical thickness of the linings usually governs the tunnel design. The figure also shows that the lining loads in Nipawin drainage tunnel No. 7 are very much underestimated. One of the possible reasons for this could be related to the fact that the space between the soil and lining was not fully filled. Matheson et al. (1986) stated that the volume of pea gravel injected into the gap between the soil and lining was about 80 % of the annular void. If the soil moved into the lining due to the existence of the gap behind the lining, the assumption of stable ground used for the development of the stress reduction factors could not be justified. However, the proposed method generally gives good approximations of the lining loads for most of the tunnels located in places other than Edmonton as shown in Figure 7.15.

7.5 Comments on the Estimates of the Stress Reduction Factors

A method to determine the stress reduction factors was described in detail in Sec. 7.2. Figure 7.1 shows that the stress reduction factors did not increase much from an X/D of 1 to an X/D of 2. As a result, the stress reduction factors obtained for an X/D of 1 can be used for an X/D of greater than 1 without much error. The stress reduction factors also were not sensitive to the values of Z/D , especially with a Z/D between 3 and 6, even though slightly more stress was released as Z/D increases. Therefore, the stress reduction factors for a Z/D of 3 can be used for a Z/D of 6. Furthermore, the stress reduction factors for an H/D of less than 3 do not have to be considered as explained in Sec. 7.3.1. Therefore, for simplicity, Table 7.11 can be used for the estimates of the stress reduction factors instead of Table 7.2, Table 7.3, and Table 7.4. According to the study of case histories, the table may be used for a Z/D of up to 9 or more. The study also showed that the in-situ stress ratio, K_0 , of unity could be used for tunnels having a ratio greater than 1. Again, the stress reduction factors should be considered only for tunnels constructed in stable ground.

7.6 Summary and Conclusions

An improved design method was proposed in this chapter using the existing design methods. A method for determining the stress reduction factors was also described. The values of the stress reduction factors for the different soil strengths, tunnel depths, and in-situ ratios were presented as tables. A specific method or combination of two different methods was suggested for the estimation of lining loads for various conditions of tunnelling.

Tunnels were divided into two main groups depending on the tunnel depth. For a shallow tunnel having a depth to centerline to diameter ratio up to three, Peck's or Einstein and Schwartz's method without taking into account stress reduction factor was suggested for the prediction of lining loads. Lining loads for tunnels constructed using the cut and cover method can also be estimated using Peck's method without taking into account stress reduction factors.

Deep tunnels, having a depth to centerline to diameter ratio greater than three, were further subdivided into three groups depending on whether the tunnels have positive face control or not. For a tunnel constructed without face control, the stress reduction factors could be used coupled with Einstein and Schwartz's method for the estimates of lining loads. The stress reduction factors can be easily obtained using Table 7.2, Table 7.3, and Table 7.4 or Table 7.11. Typical values of nD/H for tunnels in Edmonton were obtained from parametric analyses and presented in Table 7.6. The calculated values of n from the table were slightly more conservative than those from the suggested equation. However, the table can still be used for quick estimations of lining loads for tunnels in Edmonton.

For a tunnel constructed with compressed air, the reduced soil depth, considering the air pressure, was used for the calculation of the stress reduction factors. Einstein and Schwartz's method was also suggested for estimating the lining loads. The air pressure should be added to the stress found above to obtain the final stress acting on the lining upon removal of the air pressure. It was also observed that increased soil strength, especially in terms of Young's modulus, should be used for the calculation of the lining loads for a tunnel constructed with positive face control using jet-grouted piles.

Finally, the loads calculated using the proposed method were compared with field measurements collected from various tunnels in terms of soil types and construction methods to verify the method. The proposed method gave reasonable approximations of the lining loads for tunnels in Edmonton and other areas, considering the accuracy of the load measurements, limited knowledge of ground and lining properties, and the existence of possible gaps between the lining and ground. Therefore, the proposed method can be used reliably for the estimation of lining loads of a tunnel. The stress reduction factors can be included for the estimates of the lining loads if the tunnel has a stability ratio less than 2 or is constructed according to modern tunnelling philosophy in which displacements are controlled.

There have been no absolute methods which can be used for estimating lining loads for all the various conditions of tunnelling in terms of the ground and construction methods. No such method will be developed even in the future because the prediction of

lining loads requires accurate information on the ground and lining properties, which is not always possible to obtain and which often varies along the tunnel section. Furthermore, the lining loads are affected by construction procedures, which also vary from one project to another depending on the tunnelling practice of the region and the skill of the tunnel builders. In other words, tunnelling is really an art rather than a science due to the nature of the ground and construction procedures. Therefore, the proposed method is recommended as an approximate guideline for the design of tunnels, but the results should be confirmed by field measurements. This is the reason that in-situ monitoring should be an integral part of the design procedure described in this chapter.

Table 7.1 Coefficients of the Adopted U and K Relations
(Modified After Negro, 1988)

| X / D | Crown | | Springline | | Floor | |
|-------|-------|-------|------------|-------|-------|-------|
| | a | b | a | b | a | b |
| 0 | 0.375 | 0.147 | 0.210 | 0.033 | 0.226 | 0.137 |
| 0.1 | 0.538 | 0.240 | 0.282 | 0.025 | 0.366 | 0.222 |
| 0.2 | 0.701 | 0.334 | 0.354 | 0.018 | 0.505 | 0.307 |
| 0.25 | 0.783 | 0.380 | 0.390 | 0.014 | 0.575 | 0.350 |
| 0.3 | 0.811 | 0.395 | 0.404 | 0.014 | 0.596 | 0.367 |
| 0.4 | 0.867 | 0.424 | 0.432 | 0.015 | 0.639 | 0.400 |
| 0.5 | 0.923 | 0.453 | 0.460 | 0.016 | 0.681 | 0.433 |
| 0.6 | 0.950 | 0.470 | 0.480 | 0.022 | 0.700 | 0.450 |
| 0.7 | 0.977 | 0.487 | 0.500 | 0.029 | 0.718 | 0.468 |
| 0.8 | 1.005 | 0.503 | 0.520 | 0.035 | 0.737 | 0.485 |
| 0.9 | 1.032 | 0.520 | 0.540 | 0.042 | 0.755 | 0.503 |
| 1.0 | 1.059 | 0.537 | 0.560 | 0.048 | 0.774 | 0.520 |
| 1.1 | 1.068 | 0.542 | 0.563 | 0.049 | 0.775 | 0.521 |
| 1.2 | 1.076 | 0.548 | 0.566 | 0.049 | 0.777 | 0.522 |
| 1.3 | 1.085 | 0.553 | 0.569 | 0.050 | 0.778 | 0.523 |
| 1.4 | 1.093 | 0.558 | 0.572 | 0.050 | 0.780 | 0.524 |
| 1.5 | 1.102 | 0.564 | 0.575 | 0.051 | 0.781 | 0.525 |
| 1.6 | 1.110 | 0.569 | 0.578 | 0.052 | 0.782 | 0.526 |
| 1.7 | 1.119 | 0.574 | 0.581 | 0.052 | 0.784 | 0.527 |
| 1.8 | 1.127 | 0.579 | 0.584 | 0.053 | 0.785 | 0.528 |
| 1.9 | 1.136 | 0.585 | 0.587 | 0.053 | 0.787 | 0.529 |
| 2.0 | 1.144 | 0.590 | 0.590 | 0.054 | 0.788 | 0.530 |

Notes: (1) Crown and Floor: $U = a - bK$

(2) Springline: $U = a - b/K$

Table 7.2 Stress Reduction Factors Calculated Using Eisenstein and Negro's Method for $K_o=0.6$

| X/D | Z/D=1.5 | | | Z/D=3 | | | Z/D=6 | | |
|------|-----------|-----------|-----------|-----------|-----------|-----------|-----------|-----------|-----------|
| | $\phi=20$ | $\phi=30$ | $\phi=40$ | $\phi=20$ | $\phi=30$ | $\phi=40$ | $\phi=20$ | $\phi=30$ | $\phi=40$ |
| 0 | 0.215 | 0.261 | 0.268 | 0.225 | 0.268 | 0.275 | 0.229 | 0.272 | 0.278 |
| 0.1 | 0.281 | 0.368 | 0.399 | 0.296 | 0.379 | 0.409 | 0.300 | 0.384 | 0.414 |
| 0.2 | 0.333 | 0.453 | 0.514 | 0.351 | 0.466 | 0.527 | 0.354 | 0.473 | 0.533 |
| 0.25 | 0.356 | 0.489 | 0.565 | 0.375 | 0.504 | 0.579 | 0.377 | 0.510 | 0.586 |
| 0.3 | 0.362 | 0.499 | 0.579 | 0.381 | 0.514 | 0.594 | 0.383 | 0.521 | 0.601 |
| 0.4 | 0.373 | 0.518 | 0.607 | 0.394 | 0.535 | 0.622 | 0.395 | 0.541 | 0.630 |
| 0.5 | 0.384 | 0.536 | 0.633 | 0.405 | 0.554 | 0.650 | 0.407 | 0.560 | 0.658 |
| 0.6 | 0.388 | 0.542 | 0.642 | 0.410 | 0.561 | 0.660 | 0.411 | 0.567 | 0.668 |
| 0.7 | 0.392 | 0.549 | 0.652 | 0.414 | 0.568 | 0.670 | 0.415 | 0.575 | 0.678 |
| 0.8 | 0.395 | 0.555 | 0.661 | 0.418 | 0.575 | 0.680 | 0.419 | 0.582 | 0.688 |
| 0.9 | 0.399 | 0.561 | 0.670 | 0.423 | 0.582 | 0.689 | 0.423 | 0.588 | 0.698 |
| 1.0 | 0.403 | 0.567 | 0.679 | 0.427 | 0.589 | 0.699 | 0.427 | 0.595 | 0.708 |
| 1.1 | 0.403 | 0.568 | 0.681 | 0.428 | 0.590 | 0.701 | 0.428 | 0.597 | 0.710 |
| 1.2 | 0.404 | 0.569 | 0.682 | 0.428 | 0.591 | 0.702 | 0.429 | 0.598 | 0.712 |
| 1.3 | 0.405 | 0.571 | 0.684 | 0.429 | 0.593 | 0.704 | 0.429 | 0.599 | 0.714 |
| 1.4 | 0.405 | 0.572 | 0.686 | 0.430 | 0.594 | 0.706 | 0.430 | 0.601 | 0.716 |
| 1.5 | 0.406 | 0.573 | 0.687 | 0.430 | 0.595 | 0.708 | 0.431 | 0.602 | 0.718 |
| 1.6 | 0.406 | 0.574 | 0.689 | 0.431 | 0.596 | 0.710 | 0.432 | 0.604 | 0.720 |
| 1.7 | 0.407 | 0.575 | 0.691 | 0.432 | 0.598 | 0.712 | 0.432 | 0.605 | 0.722 |
| 1.8 | 0.407 | 0.576 | 0.692 | 0.432 | 0.599 | 0.714 | 0.433 | 0.606 | 0.724 |
| 1.9 | 0.408 | 0.577 | 0.694 | 0.433 | 0.600 | 0.716 | 0.434 | 0.608 | 0.726 |
| 2.0 | 0.408 | 0.578 | 0.696 | 0.434 | 0.602 | 0.717 | 0.435 | 0.609 | 0.728 |

Notes: Z = A Distance from the Surface to the Tunnel Crown; ϕ = An Equivalent Friction Angle

Table 7.3 Stress Reduction Factors Calculated Using Eisenstein and Negro's Method for $K_o=0.8$

| X/D | Z/D=1.5 | | | Z/D=3 | | | Z/D=6 | | |
|------|-----------|-----------|-----------|-----------|-----------|-----------|-----------|-----------|-----------|
| | $\phi=20$ | $\phi=30$ | $\phi=40$ | $\phi=20$ | $\phi=30$ | $\phi=40$ | $\phi=20$ | $\phi=30$ | $\phi=40$ |
| 0 | 0.236 | 0.250 | 0.253 | 0.241 | 0.255 | 0.259 | 0.244 | 0.258 | 0.263 |
| 0.1 | 0.319 | 0.353 | 0.367 | 0.325 | 0.361 | 0.375 | 0.330 | 0.365 | 0.380 |
| 0.2 | 0.383 | 0.439 | 0.468 | 0.391 | 0.448 | 0.478 | 0.396 | 0.454 | 0.484 |
| 0.25 | 0.409 | 0.476 | 0.514 | 0.418 | 0.487 | 0.525 | 0.424 | 0.492 | 0.530 |
| 0.3 | 0.416 | 0.487 | 0.527 | 0.426 | 0.497 | 0.538 | 0.432 | 0.503 | 0.544 |
| 0.4 | 0.430 | 0.506 | 0.552 | 0.440 | 0.518 | 0.564 | 0.446 | 0.524 | 0.570 |
| 0.5 | 0.442 | 0.525 | 0.576 | 0.453 | 0.537 | 0.589 | 0.459 | 0.544 | 0.596 |
| 0.6 | 0.447 | 0.532 | 0.585 | 0.458 | 0.544 | 0.598 | 0.464 | 0.551 | 0.605 |
| 0.7 | 0.451 | 0.539 | 0.594 | 0.462 | 0.551 | 0.608 | 0.469 | 0.558 | 0.615 |
| 0.8 | 0.455 | 0.545 | 0.603 | 0.467 | 0.558 | 0.617 | 0.474 | 0.566 | 0.624 |
| 0.9 | 0.460 | 0.552 | 0.612 | 0.471 | 0.565 | 0.626 | 0.478 | 0.572 | 0.634 |
| 1.0 | 0.464 | 0.558 | 0.620 | 0.475 | 0.572 | 0.635 | 0.482 | 0.579 | 0.643 |
| 1.1 | 0.464 | 0.559 | 0.622 | 0.476 | 0.573 | 0.637 | 0.483 | 0.581 | 0.645 |
| 1.2 | 0.465 | 0.561 | 0.624 | 0.477 | 0.574 | 0.639 | 0.484 | 0.582 | 0.647 |
| 1.3 | 0.466 | 0.562 | 0.626 | 0.478 | 0.576 | 0.641 | 0.485 | 0.583 | 0.648 |
| 1.4 | 0.467 | 0.563 | 0.627 | 0.479 | 0.577 | 0.643 | 0.486 | 0.585 | 0.650 |
| 1.5 | 0.468 | 0.564 | 0.629 | 0.480 | 0.579 | 0.644 | 0.487 | 0.586 | 0.652 |
| 1.6 | 0.468 | 0.566 | 0.631 | 0.480 | 0.580 | 0.646 | 0.488 | 0.588 | 0.654 |
| 1.7 | 0.469 | 0.567 | 0.633 | 0.481 | 0.581 | 0.648 | 0.489 | 0.589 | 0.656 |
| 1.8 | 0.470 | 0.568 | 0.634 | 0.482 | 0.583 | 0.650 | 0.490 | 0.590 | 0.658 |
| 1.9 | 0.471 | 0.569 | 0.636 | 0.483 | 0.584 | 0.652 | 0.490 | 0.592 | 0.660 |
| 2.0 | 0.472 | 0.570 | 0.638 | 0.484 | 0.585 | 0.653 | 0.491 | 0.593 | 0.661 |

Table 7.4 Stress Reduction Factors Calculated Using Eisenstein and Negro's Method for $K_0=1.0$

| X/D | Z/D=1.5 | | | Z/D=3 | | | Z/D=6 | | |
|------|-----------|-----------|-----------|-----------|-----------|-----------|-----------|-----------|-----------|
| | $\phi=20$ | $\phi=30$ | $\phi=40$ | $\phi=20$ | $\phi=30$ | $\phi=40$ | $\phi=20$ | $\phi=30$ | $\phi=40$ |
| 0 | 0.210 | 0.224 | 0.231 | 0.215 | 0.229 | 0.237 | 0.218 | 0.232 | 0.239 |
| 0.1 | 0.279 | 0.307 | 0.322 | 0.285 | 0.314 | 0.329 | 0.288 | 0.317 | 0.332 |
| 0.2 | 0.334 | 0.380 | 0.406 | 0.341 | 0.388 | 0.414 | 0.344 | 0.392 | 0.418 |
| 0.25 | 0.357 | 0.413 | 0.445 | 0.365 | 0.422 | 0.454 | 0.368 | 0.426 | 0.458 |
| 0.3 | 0.363 | 0.423 | 0.456 | 0.372 | 0.432 | 0.465 | 0.375 | 0.436 | 0.470 |
| 0.4 | 0.375 | 0.441 | 0.478 | 0.384 | 0.450 | 0.488 | 0.388 | 0.454 | 0.493 |
| 0.5 | 0.386 | 0.458 | 0.500 | 0.396 | 0.468 | 0.510 | 0.399 | 0.472 | 0.515 |
| 0.6 | 0.391 | 0.464 | 0.508 | 0.400 | 0.475 | 0.519 | 0.404 | 0.479 | 0.524 |
| 0.7 | 0.395 | 0.471 | 0.517 | 0.404 | 0.482 | 0.528 | 0.408 | 0.486 | 0.533 |
| 0.8 | 0.399 | 0.477 | 0.525 | 0.409 | 0.488 | 0.536 | 0.413 | 0.493 | 0.542 |
| 0.9 | 0.403 | 0.484 | 0.533 | 0.413 | 0.495 | 0.545 | 0.417 | 0.500 | 0.550 |
| 1.0 | 0.406 | 0.490 | 0.542 | 0.417 | 0.501 | 0.553 | 0.421 | 0.506 | 0.559 |
| 1.1 | 0.407 | 0.491 | 0.543 | 0.417 | 0.502 | 0.555 | 0.422 | 0.507 | 0.561 |
| 1.2 | 0.408 | 0.492 | 0.545 | 0.418 | 0.504 | 0.557 | 0.423 | 0.509 | 0.562 |
| 1.3 | 0.409 | 0.494 | 0.547 | 0.419 | 0.505 | 0.559 | 0.424 | 0.510 | 0.564 |
| 1.4 | 0.409 | 0.495 | 0.548 | 0.420 | 0.506 | 0.560 | 0.424 | 0.512 | 0.566 |
| 1.5 | 0.410 | 0.496 | 0.550 | 0.421 | 0.508 | 0.562 | 0.425 | 0.513 | 0.568 |
| 1.6 | 0.411 | 0.497 | 0.552 | 0.422 | 0.509 | 0.564 | 0.426 | 0.514 | 0.569 |
| 1.7 | 0.412 | 0.499 | 0.553 | 0.422 | 0.510 | 0.566 | 0.427 | 0.516 | 0.571 |
| 1.8 | 0.413 | 0.500 | 0.555 | 0.423 | 0.512 | 0.567 | 0.428 | 0.517 | 0.573 |
| 1.9 | 0.413 | 0.501 | 0.557 | 0.424 | 0.513 | 0.569 | 0.429 | 0.518 | 0.575 |
| 2.0 | 0.414 | 0.502 | 0.558 | 0.425 | 0.514 | 0.571 | 0.429 | 0.520 | 0.577 |

Table 7.5 Parameters used for the Estimation of nD/H for Tunnels in Edmonton

| Common | | TBM | | | | SEM | | | | |
|-----------|------|---------------|----------------|------------------|---------------------|-----------|------------------------|------------------------|------------------------|----------------|
| Variables | | Rib & Lagging | | Segmented Lining | | Shotcrets | | Shotcrets & Steel Ribs | | |
| H/D | R(m) | X/D | Rib Spacing(m) | X/D | Thick. of Lining(m) | X/D | Thick. of Shotcrets(m) | X/D | Thick. of Shotcrets(m) | Rib Spacing(m) |
| 3 | 1 | 1 | 1 | 1 | 0.11 | 0.6 | 0.1 | 0.6 | 0.1 | 1 |
| 6 | 2 | 2 | 1.22 | 2 | 0.15 | 1.0 | 0.2 | 1.0 | 0.2 | 1.5 |
| | 3 | | 1.5 | | 0.2 | | 0.3 | | | |

Table 7.6 Calculated Values of nD / H for Tunnels in Edmonton(a) Small Diameter Tunnel ($D < 4\text{m}$)

| | TBM | | Sequential Excavation | |
|-----------|---------------|------------------|-----------------------|-----------------|
| | Rib & Lagging | Segmented Lining | Shotcrets | Shotcrets & Rib |
| Till | 0.309 | 0.341 | 0.358 | 0.360 |
| Sand | 0.446 | 0.480 | 0.490 | 0.491 |
| Claystone | 0.474 | 0.557 | 0.542 | 0.546 |

(b) Large Diameter Tunnel ($D \geq 4\text{m}$)

| | TBM | | Sequential Excavation | |
|-----------|---------------|------------------|-----------------------|-----------------|
| | Rib & Lagging | Segmented Lining | Shotcrets | Shotcrets & Rib |
| Till | 0.251 | 0.328 | 0.327 | 0.331 |
| Sand | 0.381 | 0.467 | 0.458 | 0.462 |
| Claystone | 0.350 | 0.523 | 0.470 | 0.478 |

Table 7.7 Recommended Geotechnical Design Parameters (EBA, 1988)

| Stratum | Unit Weight (KN/m ³) | Cu (KPa) | E (MPa) | ν | ϕ' Deg. | c' (KPa) | K _o |
|-------------------|-------------------------------------|-------------|------------|-------|-----------------|-------------|----------------|
| Claystone Bedrock | 21 | 400 | 250 | 0.4 | 16 | 50 | 1.0-1.7 |
| Till | 21 | 300 | 250 | 0.4 | 40 | 0 | 0.8-1.2 |
| Sand | 21 | | 100 | 0.35 | 30 | 0 | 0.3-0.5 |

Cu = Undrained Shear Strength

E = Deformation Modulus

ν = Poisson's Ratio

ϕ' = Effective angle of shearing resistance

c' = Effective Cohesion

K_o = Coefficient of Earth Pressure at Rest

Table 7.8 Initial Support for the Edmonton SLRT-Phase II Tunnels

| TYPE | LOCATION | SPILING | ELEPHANT'S FOOT OR WALL PLATE | EXCAVATED TUNNEL RADIUS | STEEL RIBS | | SHOTCRETE THICKNESS | | |
|------|----------------|---------|-------------------------------------|-------------------------------|------------|---------|---------------------|-----------|-------|
| | | | | | SECTION | SPACING | 1st LAYER | 2nd LAYER | TOTAL |
| I | TYPICAL TUNNEL | NO | EF | 3125 | W150X14 | VARIES | 50 | 75 | 125 |
| V | HUB MALL | YES | WP | 3170 | W200X52 | 1000 | 40 | 130 | 170 |

ALL DIMENSIONS IN MILLIMETRES

Table 7.9 Summary of Instrumented Ribs for the SLRT-Phase II Tunnels

| RIB NO. | STEEL RIBS | | DATE | STATION | GEOLOGY |
|---------|------------|-------------|----------------------------|-----------|-----------|
| | SECTION | SPACING(mm) | | | |
| 137* | W150X14 | 1500 | H; 90/05/02 B; 90/05/03 | 302+036.4 | CLAYSTONE |
| 138* | W150X14 | 1500 | H; 90/05/02 B; 90/05/04 | 302+037.9 | CLAYSTONE |
| 286* | W200X52 | 1000 | H; 90/08/01 B; 90/08/03 | 302+222.1 | CLAY TILL |
| 144** | W150X14 | 1000 | H; 90/11/15 B; 90/11/16 | 402+023.2 | CLAYSTONE |
| 145** | W150X14 | 1000 | H; 90/11/15 B; 90/11/16 | 402+024.2 | CLAYSTONE |

* SOUTHBOUND TUNNEL

** NORTHBOUND TUNNEL

Table 7.10 Summary of Primary Liner Loads for the SLRT-Phase II Tunnels

| Rib No. | Depth (m) (H) | Diameter (m) (D) | H/D | Pv (KPa) | Measured Load (KN) | PL (KPa) | PL/Pv X100 (%) | h (m) | n (=h/D) | | Days |
|---------|------------------|---------------------|-----|-------------|-----------------------|------------------|-------------------|----------------|--------------|--------------|------------|
| | | | | | | | | | Measured | Predicted | |
| 137 | 25.69 | 6.25 | 4.1 | 539.49 | 157.3 237.9* | 215.87 326.58 | 40 61 | 10.28 15.55 | 1.64 2.49 | 1.71 1.71 | 124 257 |
| 138 | 25.64 | 6.25 | 4.1 | 538.44 | 191.3 184.1* | 262.61 252.72 | 49 47 | 12.51 12.03 | 2.00 1.93 | 1.70 1.70 | 91 220 |
| 286 | 20.2 | 6.34 | 3.2 | 424.2 | 110.9 111.4* | 79.72 80.08 | 19 19 | 3.80 3.81 | 0.60 0.60 | 1.09 1.09 | 179 193 |
| 144 | 25.98 | 6.25 | 4.2 | 545.58 | 145.2 | 214.20 | 39 | 10.20 | 1.63 | 1.87 | 155 |
| 145 | 26.1 | 6.25 | 4.2 | 548.1 | 158.5 | 233.75 | 43 | 11.13 | 1.78 | 1.88 | 155 |

* Measured Loads on the Rib after the Passage of the NB tunnel

H: Depth to Springline

Pv: Overburden Pressure

Measured Load: An Average Load of Two Load Cells Installed in a Steel Rib

PL: Pressure on the Combined Lining (Rib and Shotcrets)

h: Height of Soil Carried by Lining
(PL/Soil Unit Weight)

Days: Measured Days of Lining Loads after the Installation of a Steel Rib

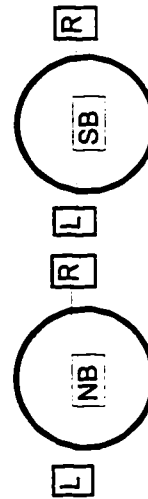


Table 7.11 Stress Reduction Factors Suggested for the Proposed Design Method
($3 \leq Z/D \leq 9$)

| Ko | ϕ_c | X/D | | | | | | | | | | | |
|-----|----------|-------|-------|-------|-------|-------|-------|-------|-------|-------|-------|-------|------------|
| | | 0 | 0.1 | 0.2 | 0.25 | 0.3 | 0.4 | 0.5 | 0.6 | 0.7 | 0.8 | 0.9 | 1.0 \leq |
| 0.6 | 20 | 0.225 | 0.296 | 0.351 | 0.375 | 0.381 | 0.394 | 0.405 | 0.410 | 0.414 | 0.418 | 0.423 | 0.427 |
| | 30 | 0.268 | 0.379 | 0.466 | 0.504 | 0.514 | 0.535 | 0.554 | 0.561 | 0.568 | 0.575 | 0.582 | 0.589 |
| | 40 | 0.275 | 0.409 | 0.527 | 0.579 | 0.594 | 0.622 | 0.650 | 0.660 | 0.670 | 0.680 | 0.689 | 0.699 |
| 0.8 | 20 | 0.241 | 0.325 | 0.391 | 0.418 | 0.426 | 0.440 | 0.453 | 0.458 | 0.462 | 0.467 | 0.471 | 0.475 |
| | 30 | 0.255 | 0.361 | 0.448 | 0.487 | 0.497 | 0.518 | 0.537 | 0.544 | 0.551 | 0.558 | 0.565 | 0.572 |
| | 40 | 0.259 | 0.375 | 0.478 | 0.525 | 0.538 | 0.564 | 0.589 | 0.598 | 0.608 | 0.617 | 0.626 | 0.635 |
| 1.0 | 20 | 0.215 | 0.285 | 0.341 | 0.365 | 0.372 | 0.384 | 0.396 | 0.400 | 0.404 | 0.409 | 0.413 | 0.417 |
| | 30 | 0.229 | 0.314 | 0.388 | 0.422 | 0.432 | 0.450 | 0.468 | 0.475 | 0.482 | 0.488 | 0.495 | 0.501 |
| | 40 | 0.237 | 0.329 | 0.414 | 0.454 | 0.465 | 0.488 | 0.510 | 0.519 | 0.528 | 0.536 | 0.545 | 0.553 |

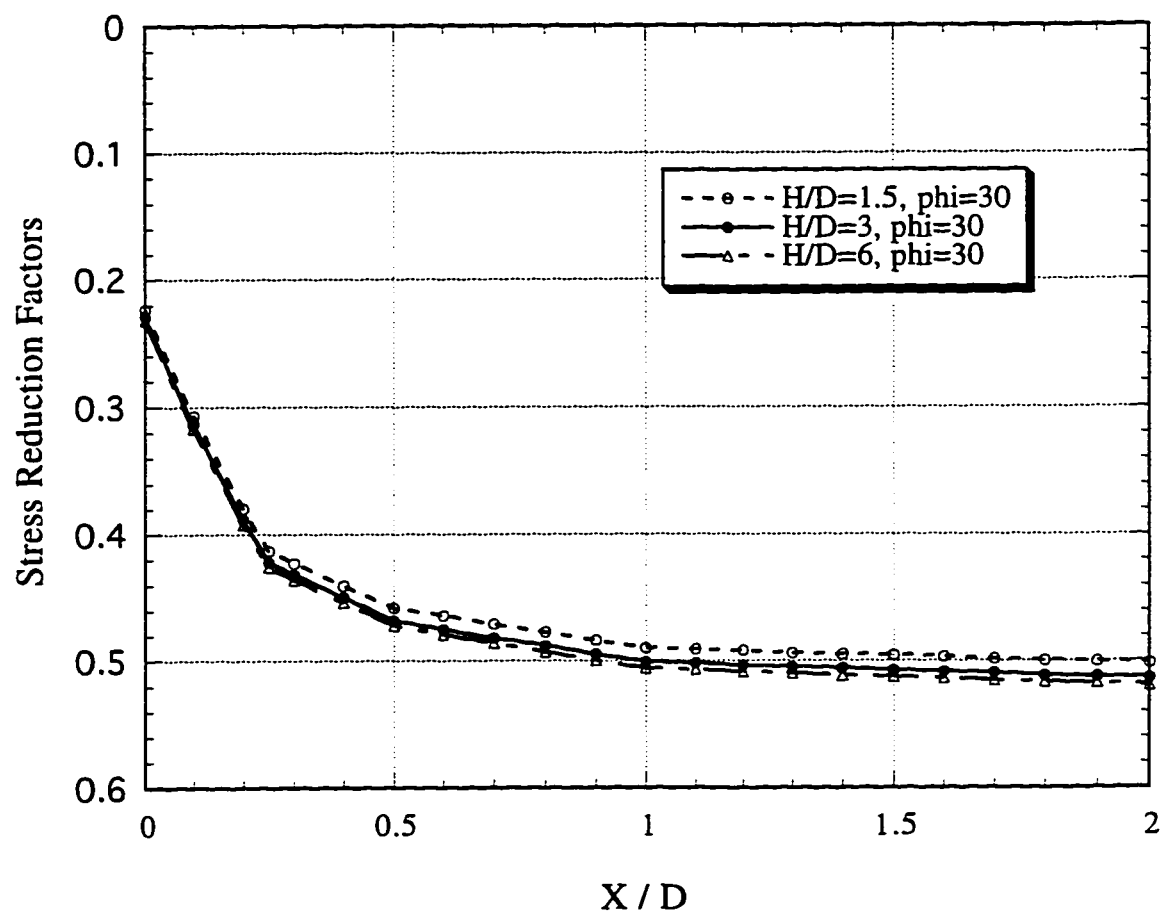


Figure 7.1 Stress Reduction Factors for Different Tunnel Depths
($\phi=30$, $K_o=1.0$)

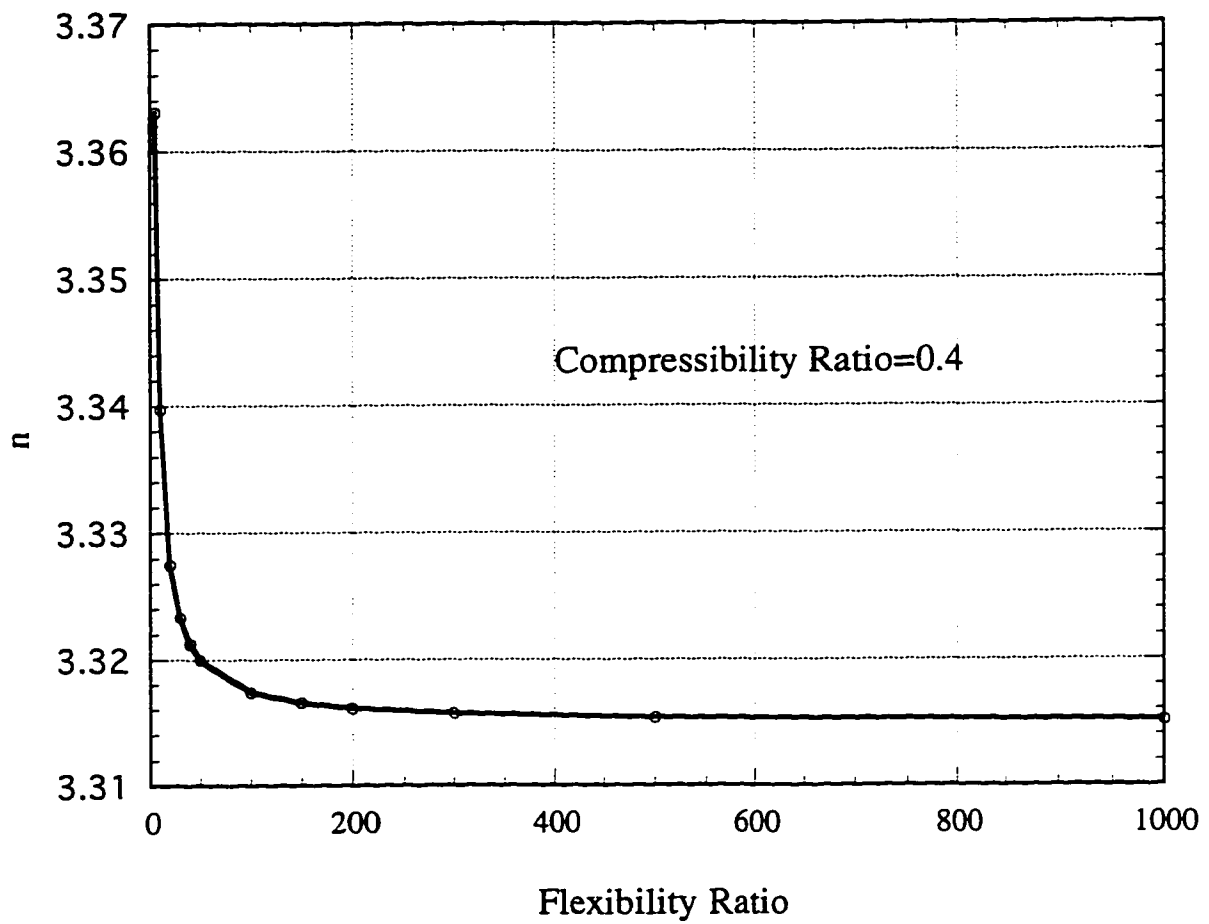


Figure 7.2 Variation of n with Flexibility Ratio ($K_o=1.0$)

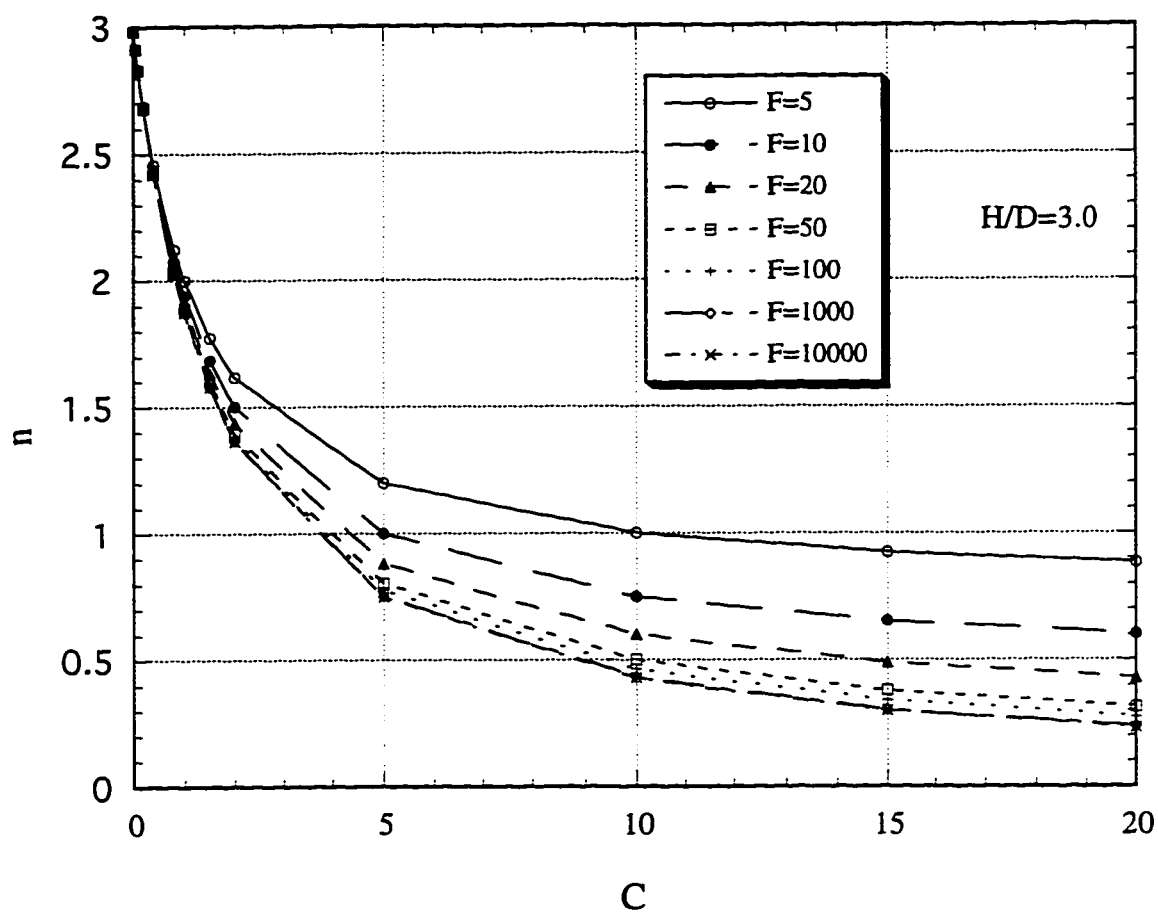


Figure 7.3 Variation of n with Compressibility Ratio ($Ko=1.0$)

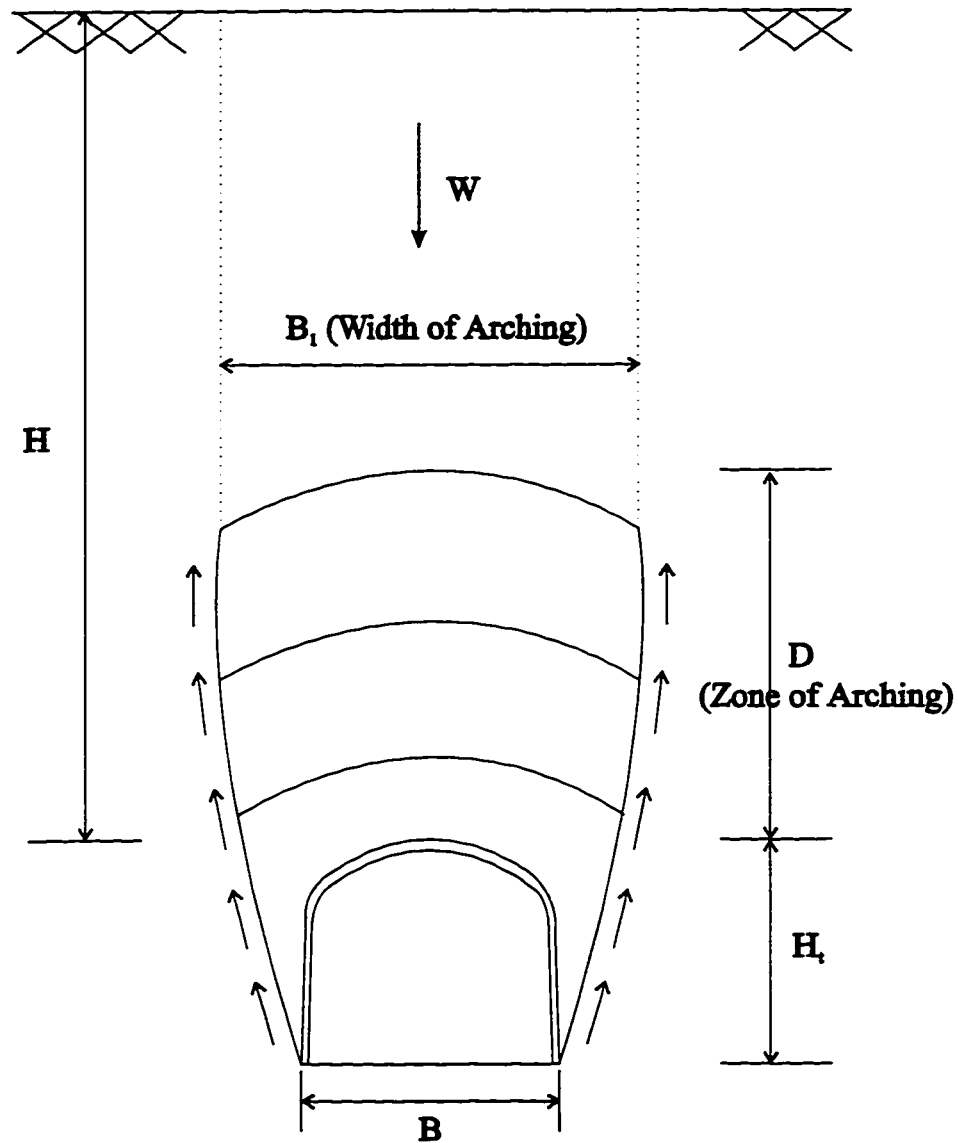


Figure 7.4 Simplified Representation of Rock Loading of Tunnel
(Modified after Terzaghi, 1946)

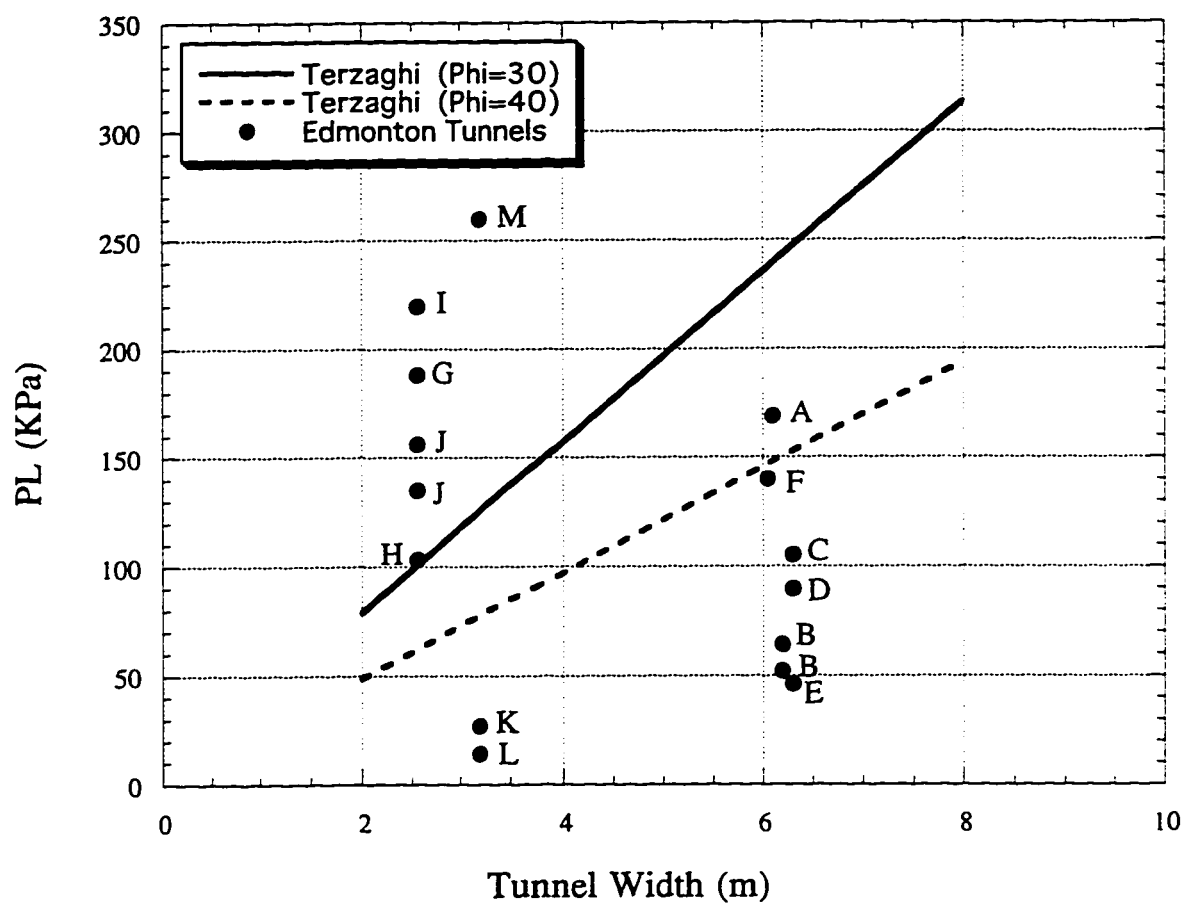


Figure 7.5 Comparison of Vertical Support Pressures in Relation to Tunnel Width according to Terzaghi Derived Formulae with Actual Case Histories in Edmonton

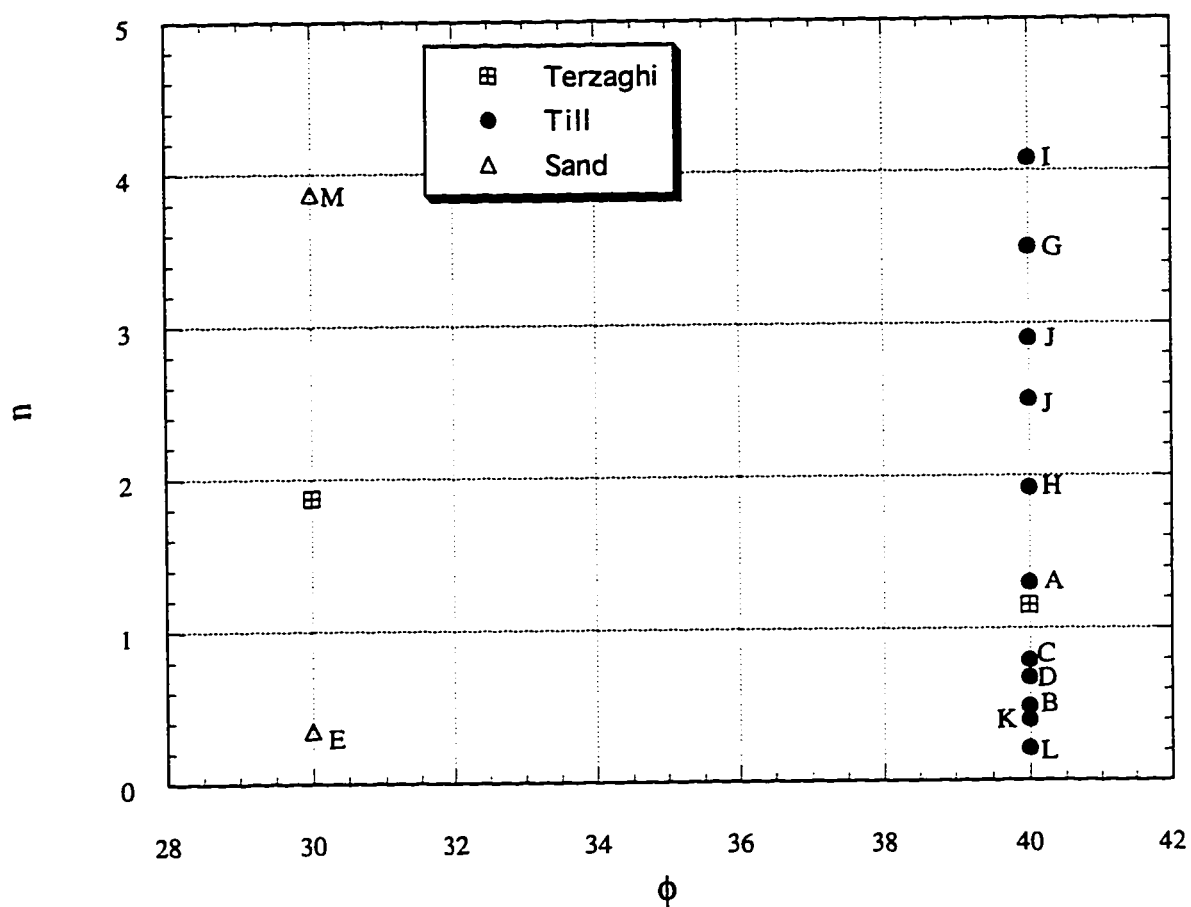


Figure 7.6 Comparison Between n Values according to Terzaghi Derived Formulae and Actual Case Histories in Edmonton

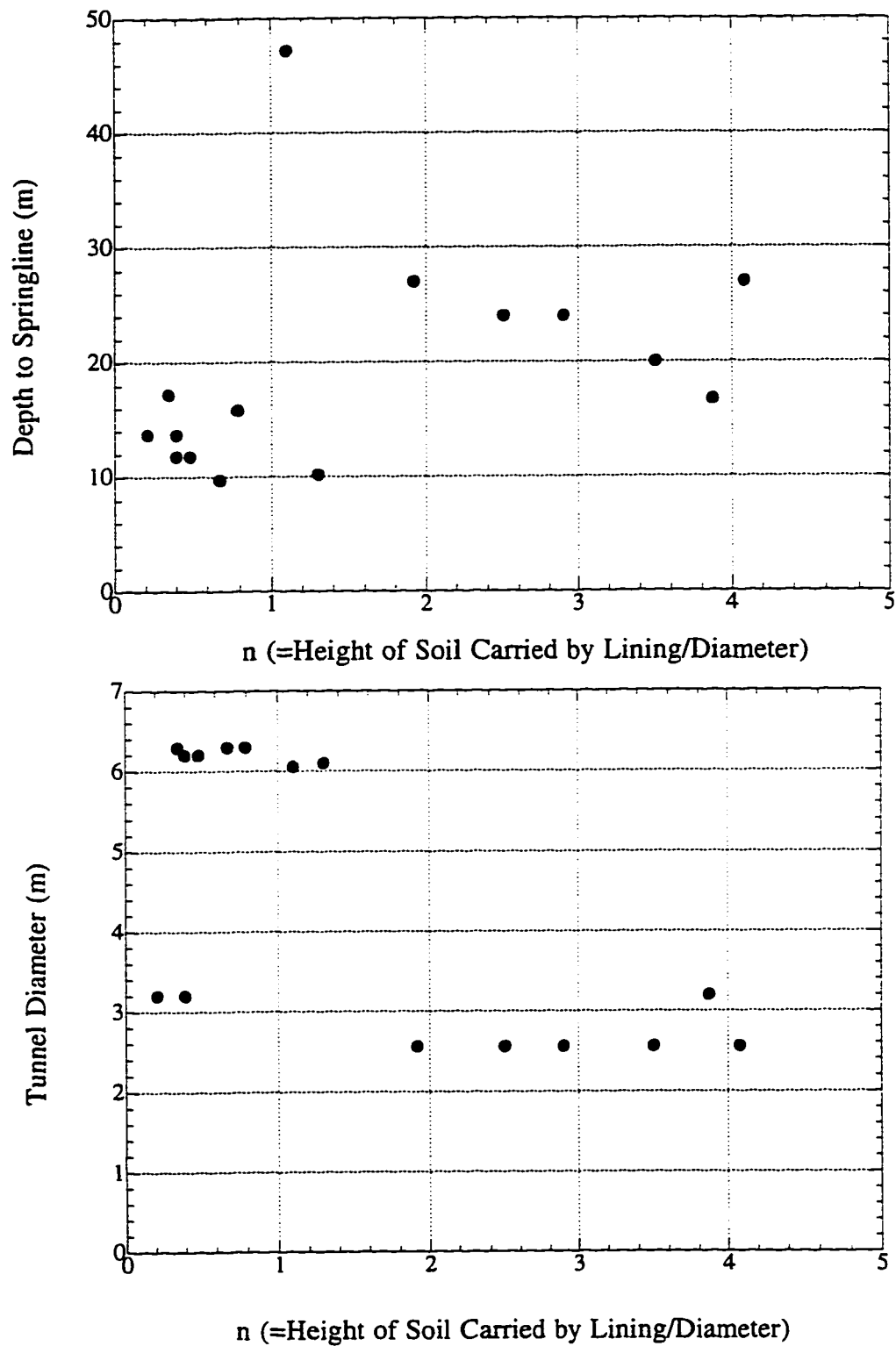


Figure 7.7 Comparison of the Dimensionless Factor (n) with Tunnel Depth and Diameter for Tunnels in Edmonton

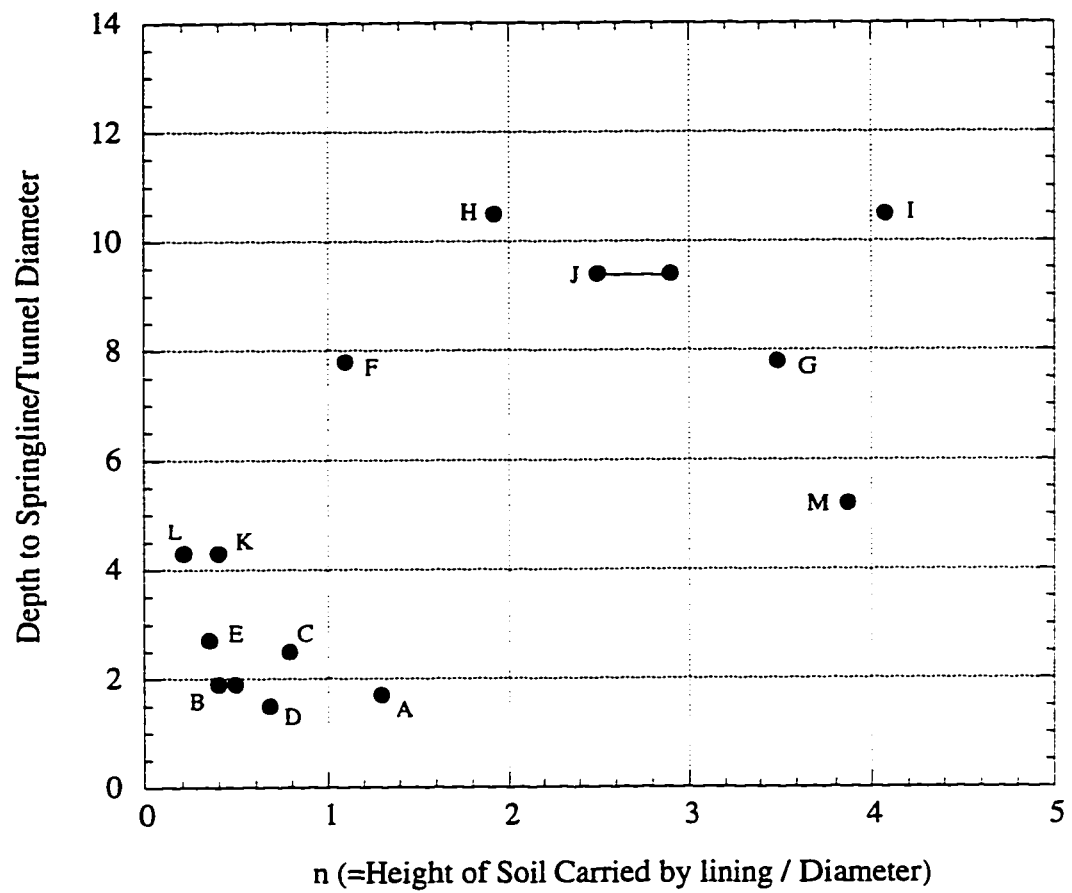


Figure 7.8 Comparison of the Dimensionless Factor (n) with H/D in Edmonton tunnels

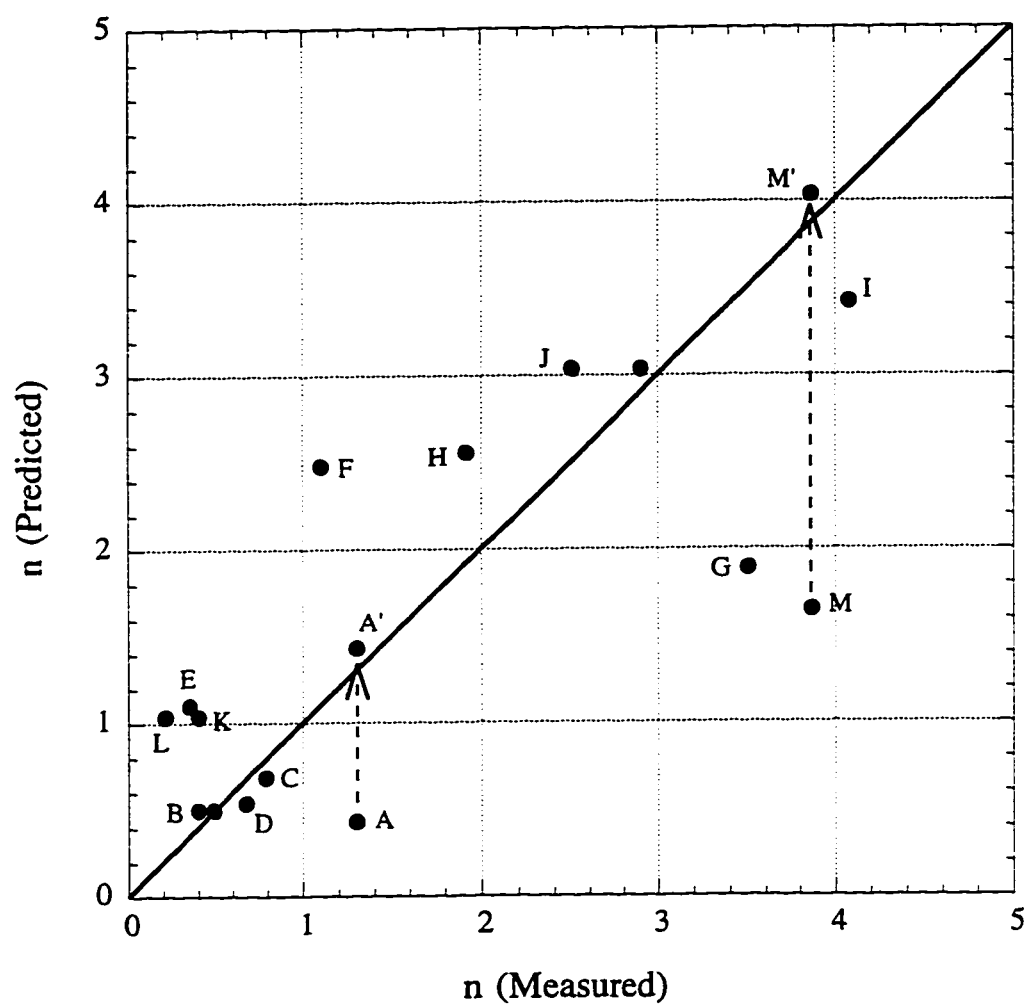


Figure 7.9 Comparison of Predicted n Calculated using the Proposed Method with Measured n for Tunnels in Edmonton (From Eq. 7.1)

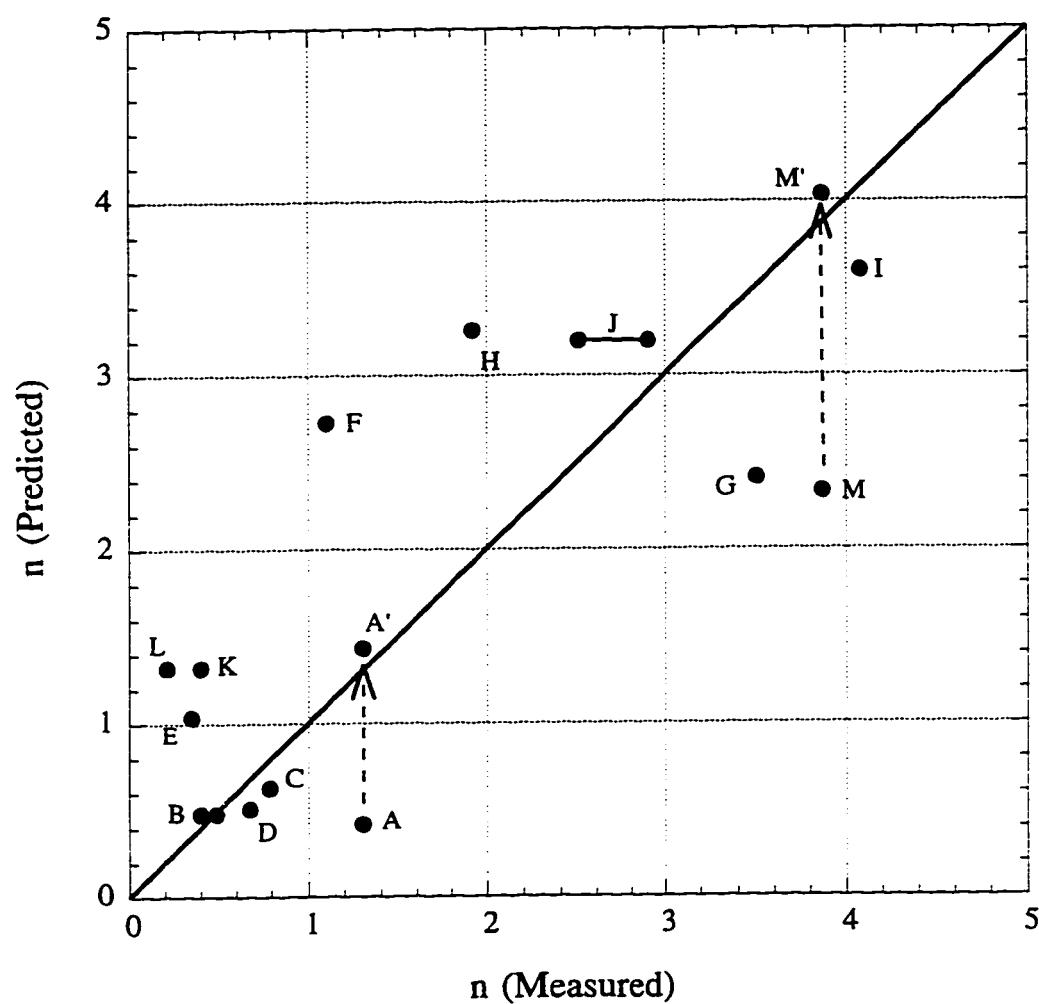


Figure 7.10 Comparison of Predicted n Calculated using the Proposed Method with Measured n for Tunnels in Edmonton (From Table 7.6)

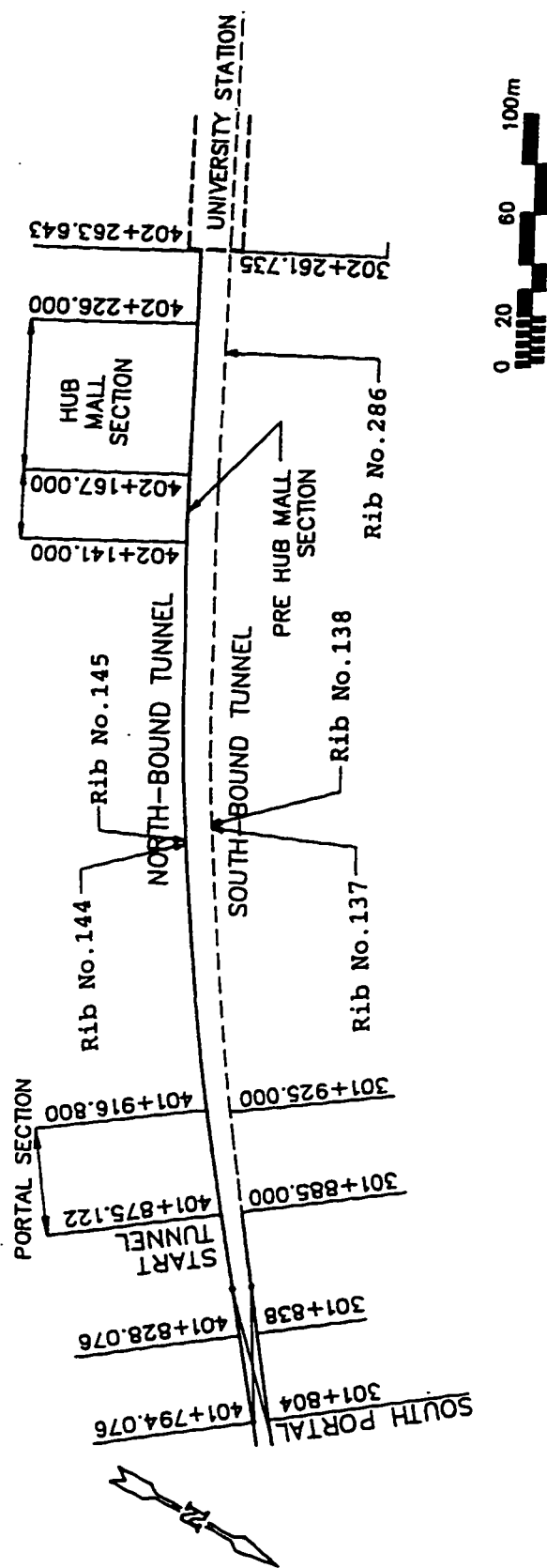


Figure 7.11 Plan View of Tunnel Sections with the Location of the Instrumented Ribs

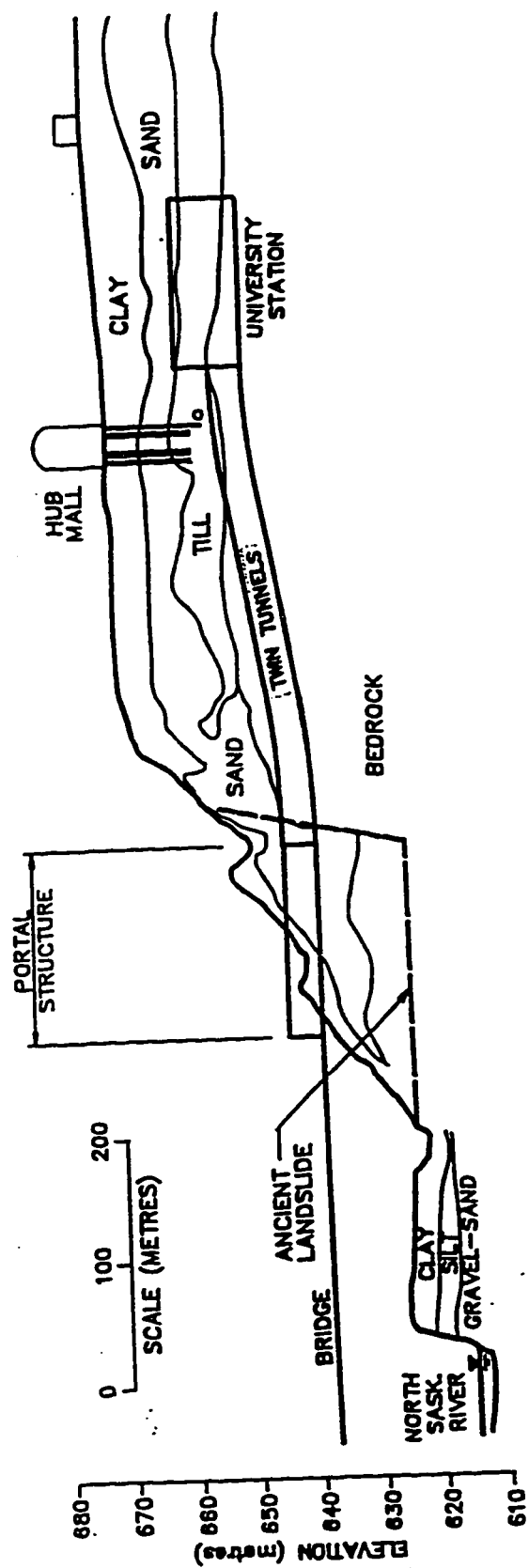


Figure 7.12 Simplified Geologic Cross Section (Modified after Cassie et al., 1991)

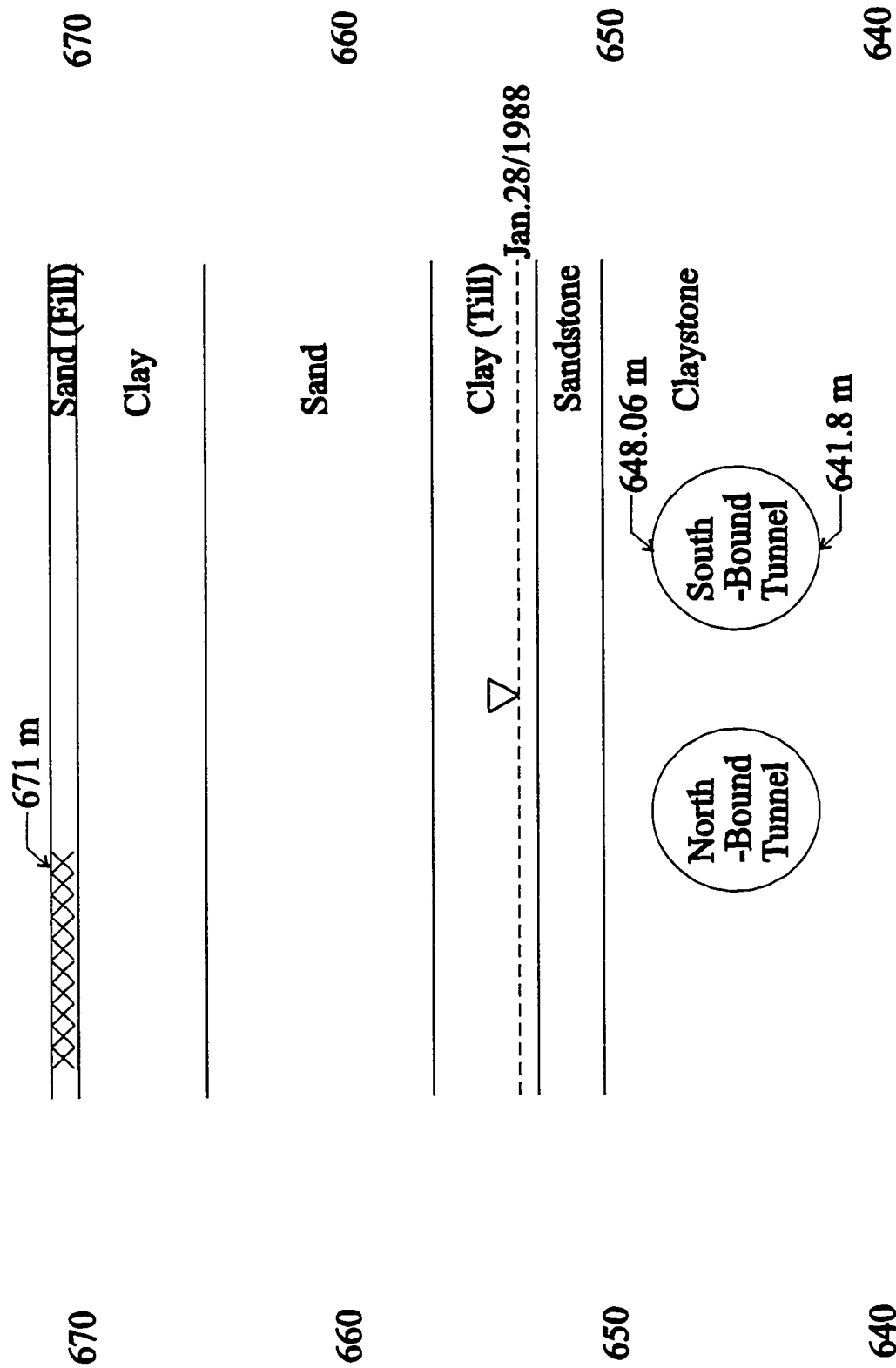


Figure 7.13 A Cross Section in Rib No. 138 of the SLRT-Phase II Tunnels

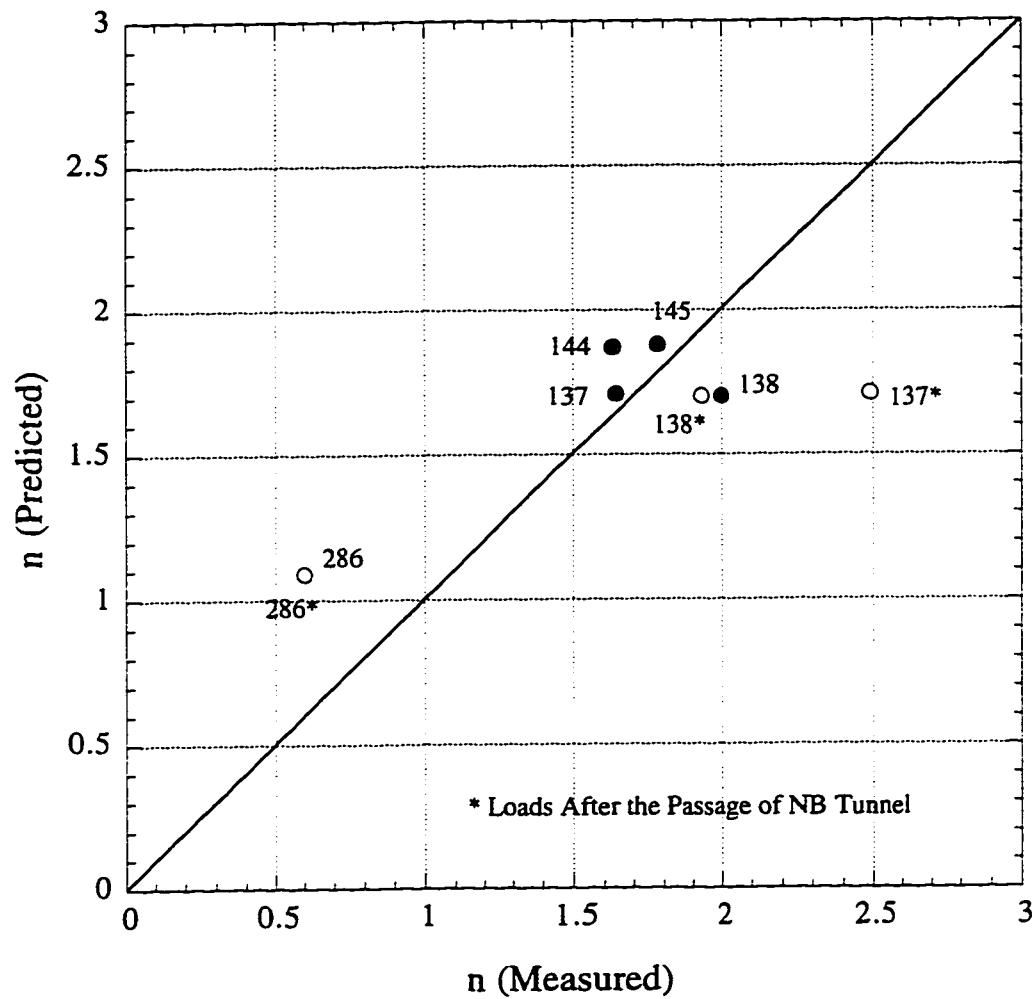


Figure 7.14 Comparison of Predicted n Calculated using the Proposed Method with Measured n for the SLRT-Phase II Tunnels

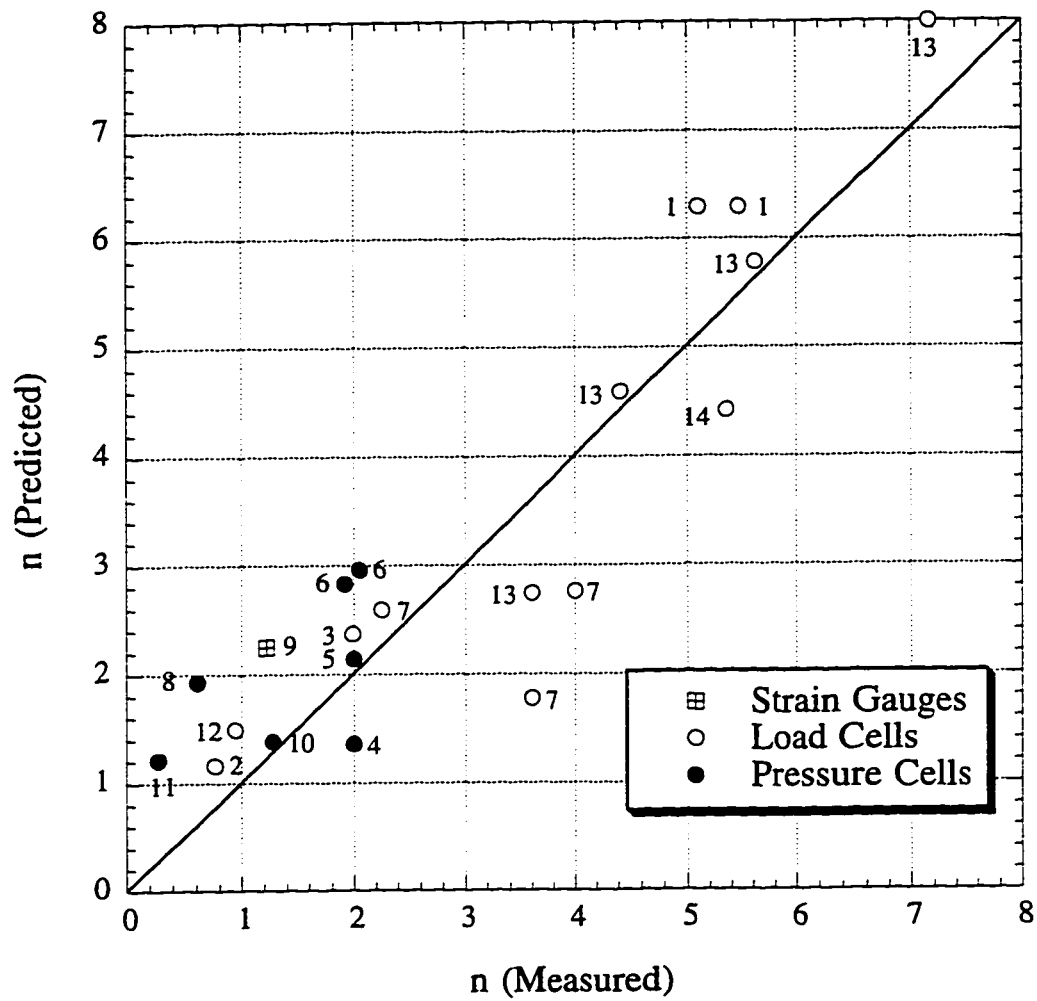


Figure 7.15 Comparison of Predicted n Calculated using the Proposed Method with Measured n for the Tunnels Located other than Edmonton

8. Conclusions

Prediction of lining loads due to tunnelling is one of the major issues to be addressed in the design of a tunnel. The objective of this study is to investigate rational and realistic design loads on tunnel linings, especially on the primary linings. Chapter 2 presented discussions on the soil response to tunnelling, factors influencing the load on the liner and available design methods to estimate the lining loads. The ground response to tunnelling was reviewed using the concept of the convergence-confinement method. Factors influencing the lining load were also summarized and discussed.

Available design methods were divided into four groups based on the calculation procedure by which a particular method was developed. The validity of the design methods was discussed briefly based on literature reviews. Prediction of the radial displacement before the liner installation was one of the major problems when using the existing design methods in practice.

The instruments for measuring the lining loads were reviewed and discussed in Chapter 3 because field measurements are often necessary to verify the design methods. It was shown that strain gauges and load cells were the most effective and reliable ways for measuring lining loads. Vibrating wire strain gauges or load cells were particularly recommended for the load measurements in a tunnel, considering the high humidity and dirty conditions. The methods for the processing of measurements were also presented for two different lining systems. The loads due to other than earth pressure were also discussed.

The geology and construction sequence, including the location of the tunnel face with respect to the instrumented lining, should be recorded in detail because they are closely related to the variation of the lining load. Several ribs in a row, usually three or four consecutive ones, should be instrumented to allow for variation in the load due to variations in geology and support installation details.

The validity of the existing design methods was reviewed in Chapter 4 by comparing the loads calculated using the methods with the field measurements obtained from several tunnels in Edmonton. A design method for the prediction of lining loads should include the decrease of lining loads due to the stress release before lining

installation and the increase of lining loads due to development of ground yielding. Only Muir Wood included a stress reduction factor, but the stress reduction of 50 % was rather arbitrary. Eisenstein and Negro's method considered the stress reduction factor more reliably. The yield factor was also considered in their method by using a hyperbolic elastic material model. Therefore, the method gave the closest estimates of actual lining loads. However, the method had some limitations for its full use. Furthermore, the method is valid only for stable ground due to its assumption of linear elastic ground and an unlined opening for the determination of the stress release factor.

The use of stress reduction factors, coupled with other analytical solutions, for the prediction of lining loads was discussed briefly in Sec. 4.7. The results encouraged the use of the reduced unit weight considering that the stress release occurred before lining installation. Schwartz and Einstein included both factors in their original closed form solutions in the form of a support delay factor λ_d and a yield factor λ_y respectively. Schwartz and Einstein's proposed method gave reasonable results for tunnels with short delay lengths. However, the method could not be used reliably for tunnels either with long delay lengths or with voids between the soil and TBM due to the difficulties finding U_o' and therefore λ_d . In conclusion, none of the above methods were totally satisfactory for the estimation of lining loads even though certain methods could give reasonable results under specific conditions. Therefore, there was some room for improvement in the prediction of lining loads.

The convergence-confinement method is one approach to the analysis of ground-support interaction. The method was reviewed in detail in Chapter 5. To have a better understanding of the method, especially the effect of a material model on the convergence curve, two-dimensional finite element analyses were performed. The procedures to simulate the excavation for two-dimensional analyses were presented in Sec. 5.3.2. The convergence curves were obtained from two-dimensional finite element analyses using three different material models and theoretical equations. The limitation of the use of 2-D finite element methods combined with CCM for the estimation of the final load and displacement around a tunnel was discussed by comparing these curves with the actual field measurements obtained from a tunnel in Edmonton.

Most tunnels clearly show three-dimensional behaviour within the region bounded by one to two diameters ahead of the face to one diameter behind the location of liner activation. The ground displacements occurring ahead of the face could not be considered in the two-dimensional finite element analyses. To have a better understanding of stress and displacement behaviour near the tunnel face, three-dimensional finite element analyses were performed in Chapter 6. More attention was given to particular aspects of the 3-D behaviour during tunnel excavation than to matching analyses with field measurements. The radial displacements and the radial stresses of the ground were obtained from the 3-D analyses with and without the liner. The stress distribution along the tunnel clearly showed the influence of the construction sequences in ground-support interaction. The stresses on the liner may vary because of the length of the lining and the distance between the lining and the tunnel face even though all the other material properties of the ground and the liner, the tunnel geometry, and the in-situ stresses were the same.

The convergence curves were obtained by combining the radial stresses and the displacements. The possible causes of the differences in the final equilibrium stresses and displacements on the liner between the 2-D and 3-D analyses were presented. The difference was larger as the distance of the unsupported section was reduced in the sequence of tunnel construction. Therefore, the convergence-confinement method should be used carefully when the excavation has a short length of unsupported section throughout the construction. The difficulties involved in the 3-D analyses were also discussed. This is one of the reasons that a simple design method should be available considering the three-dimensional nature of the ground around an advancing tunnel.

An improved design method was proposed in Chapter 7 based on the review of existing design methods and the performance of numerical analyses. A method for determining the stress reduction factors was also described. The values of the stress reduction factors for different soil strengths, tunnel depths, and in-situ stress ratios were presented as tables.

A specific method or combination of two different methods was suggested for the estimation of lining loads for different conditions of tunnelling. For a shallow tunnel,

having a depth to centerline to diameter ratio up to three, Peck's or Einstein and Schwartz's method, without taking into account the stress reduction factor, was suggested for the prediction of lining loads. Lining loads for tunnels constructed using the cut and cover method can also be estimated using Peck's method without taking into account stress reduction factors. Deep tunnels, having a depth to centerline to diameter ratio greater than three, were further subdivided into three groups depending on whether the tunnels have positive face control or not. For a tunnel constructed without face control, the stress reduction factors could be used coupled with Einstein and Schwartz's method for the estimates of lining loads. The method for the calculation of the lining loads for a tunnel constructed with compressed air or with positive face control using jet-grouted piles was also presented.

Typical values of nD/H for tunnels in Edmonton were obtained from parametric analyses and presented in a table. The calculated values of n from the table were slightly more conservative than those from the suggested equation. However, the table can still be used for quick estimations of lining loads for tunnels in Edmonton.

Finally, the loads calculated using the proposed method was compared with field measurements collected from various tunnels in terms of soil types and construction methods to verify the method. The proposed method gave reasonable approximations of the lining loads for tunnels in Edmonton and other areas, considering the accuracy of the load measurements, limited knowledge of ground and lining properties, and the existence of possible gaps between the lining and ground. Therefore, the proposed method can be used reliably for the estimation of lining loads of a tunnel. The stress reduction factors can be included for the estimates of the lining loads if the tunnel has a stability ratio less than 2 or is constructed according to the modern tunnelling philosophy in which displacements are controlled.

Tunnelling is really an art rather than a science due to the nature of the ground and construction procedures. The prediction of lining loads requires accurate information on the ground and lining properties, which is not always possible to obtain and often varies along the tunnel section. Furthermore, the lining loads are affected by construction procedures, which also vary from one project to another depending on the tunnelling

practice of the region and the skill of the tunnel builders. As a result, the proposed method is recommended as an approximate guideline for the design of tunnels, but the results should be confirmed by field measurements. This is the reason that in-situ monitoring should be an integral part of the design procedure.

REFERENCES

- Attewell, P. B. and El-Naga, N. M. A., 1977. Ground-Lining Pressure Distribution and Lining Distortion in Two Tunnels Driven Through Stiff, Stony/Laminated Clay. *Ground Engineering*, Vol. 10. No. 3, April, pp. 28-35.
- Attewell, P. B. and Farmer, I. W., 1974 (a). Ground Deformations Resulting from Shield Tunnelling in London Clay. *Canadian Geotechnical Journal*, Vol. 11, pp. 380-395.
- Attewell, P. B. and Farmer, I. W., 1974 (b). Ground Disturbance Caused by Shield Tunnelling in a Stiff, Overconsolidated Clay. *Engineering Geology*, Vol. 8, pp. 361-381.
- Barlow, J. P., 1986. Interpretation of Tunnel Convergence Measurements. M. Sc. Thesis, Department of Civil Engineering, University of Alberta, Edmonton, 235 p.
- Barratt, D. A. and Tyler, R. G., 1976. Measurements of Ground Movement and Lining Behaviour on the London Underground at Regents Park. TRRL Laboratory Report 684, Transport and Road Research Laboratory, Crowthorne, Berkshire.
- Barton, N, Lien, R., Lunde, J., 1974. Engineering Classification of Rock Masses for the Design of Tunnel Support. *Rock Mechanics*, Vol. 6, No. 4, pp. 189-236.
- Bathe, K. J., 1978. ADINA: A Finite Element Program for Automatic Dynamic Incremental Nonlinear Analysis. Report 82448-1, Massachusetts Institute of Technology, 385 p.
- Beaulieu, A. C., 1972. Tunnelling Experiences, City of Edmonton, Alberta, Canada. Proceedings, North American Rapid Excavation and Tunneling Conference. American Institute of Mining Engrs., Vol.2, pp.933-964.
- Belshaw, D. J. and Palmer J. H. L., 1978. Results of a Program of Instrumentation involving a Precast Segmented Concrete-Lined Tunnel in Clay. *Canadian Geotechnical Journal*, Vol. 15, pp. 573-583.
- Bieniawski, Z. T., 1976. Rock Mass Classifications in Rock Engineering. Proc. Symp. Exploration for Rock Engineering, pp. 97-106.
- Bieniawski, Z. T., 1984. Rock Mechanics Design in Mining and Tunnelling. A. A. Balkema, 272 p.

- Branco Jr., P., 1981. Behavior of a Shallow Tunnel in Till. M. Sc. Thesis, Department of Civil Engineering, University of Alberta, Edmonton, Alberta, 351 p.
- Branco, P. and Eisenstein, Z., 1985. Convergence-Confinement Method in Shallow Tunnels. Proceedings of 11th International Conf. on Soil Mech. and Found. Eng., San Francisco, Aug., Vol.4, pp.2067-2072.
- Broms, B. B. and Bennermark, H., 1967. Stability of Clay at Vertical Openings. Journal of the Soil Mechanics and Foundations Division, Proceedings of the American Society of Civil Engineers, pp. 71-94.
- Brown, E. T., Bray, J. W., Ladanyi, B. and Hoek, E., 1983. Ground Response Curves for Rock Tunnels. Journal of Geotechnical Engineering, Vol. 109, No. 1, pp. 15-39.
- Burke, H. H., 1960. Garrison Dam Test Tunnel, Investigation and Construction. Transactions, ASCE, Vol. 125, pp. 230-267.
- Chan, D., 1985. Finite Element Analysis of Strain Softening Materials. Ph. D. Thesis, Department of Civil Engineering, University of Alberta, Edmonton, Alberta, 355 p.
- Chen, W. F. and Mizuno, E., 1990. Nonlinear Analysis in Soil Mechanics, Theory and Implementation. Elsevier, 661 p.
- Chen, W. F. and Zhang, H., 1991. Structural Plasticity, Theory, Problems, and CAE Software. Springer-Verlag.
- Christian, J. T., 1980. The Application of Generalized Stress-Strain Relations, In: Application of Plasticity and Generalized Stress-Strain in Geotechnical Engineering. Proceedings of the Symposium on Limit Equilibrium, Plasticity and Generalized Stress Strain Applications in Geotechnical Engineering, Florida, ASCE, pp. 182-204.
- Cooley, P., 1982. Wedge-Block Tunnels in Water Supply. Journal of the Institution of Water Engineers and Scientists, Vol. 36, No. 1, pp. 9-26.
- Cooling, L. F. and Ward, W. H., 1953. Measurements of Loads and Strains in Earth Supporting Structures. Proceedings of the 3rd International Conference on Soil Mechanics and Foundation Engineering, Zurich, Vol. 2, pp. 162-166.
- Corbett, I., 1984. Load and Displacement Variations along a Soft Ground Tunnel. M. Sc. Thesis, Department of Civil Engineering, University of Alberta, Edmonton, Alberta, 246p.

Cording, E. J., Hendron, A. J., and Deere, D. U., 1971. Rock Engineering for Underground Caverns, Proceedings, Symposium on Underground Rock Chambers, ASCE National Meeting on Water Resources Engineering, Phoenix, Arizona, pp. 567-600.

Cording, E. J., Hendron, A. J., MacPherson, H. H., Hansmire, W. H., Jones, R. A., Mahar, J. W., and O'Rourke, T. D., 1975. Methods for Geotechnical Observations and Instrumentation in Tunneling. Report Prepared for U.S. National Science Foundation, Washington, D. C., Vol. 1, 2, 566 p.

Craig, R. N. and Muir Wood, A. M., 1978. A Review of Tunnel Lining Practice in the United Kingdom. Transport and Road Research Laboratory, Suppl. Report 335, 211 p.

Cronin et al., 1962. Discussion on the Thames-Lee Tunnel Water Main. Proceedings, Institution of Civil Engineers, Vol. 23, pp. 690-704.

Curtis, D. J., 1976. Discussion of: Muir Wood, A. M., The Circular Tunnel in Elastic Ground. Geotechnique, Vol. 26, No. 2, pp. 231-237.

Curtis, D. J., Lake, L. M., Lawton, W. T., and Crook, D. E., 1976. In-situ Ground and Lining Studies for the Channel Tunnel Project. Proceedings, Symposium, Tunnelling '76, London, pp. 231-242.

Cuthbert, E. W. and Wood, F., 1962. The Thames-Lee Tunnel Water Main. Proceedings, Institution of Civil Engineers, Vol. 21, pp. 257-276.

Daemen, J. J. K., 1975. Tunnel Support Loading Caused by Rock Failure. Ph. D. Thesis, University of Minnesota, Minneapolis.

Daemen, J. J. K. and Fairhurst, C., 1972. Rock Failure and Tunnel Support Loading. Proceedings, International Symposium on Underground Openings, Lucerne, pp. 356-369.

Dar, S. M. and Bates, R. C., 1974. Stress Analysis of Hollow Cylindrical Inclusions. Journal of the Geotechnical Engineering Division, ASCE, Vol. 100, No. GT2, pp. 123-138.

Davis, E. H., Gunn, M. J., Mair, R. J., and Seneviratne, H. N., 1980. The Stability of Shallow Tunnels and Underground Openings in Cohesive Material. Geotechnique, Vol. 30, No. 4, pp. 397-416.

- Deere, D. U., Peck, R. B., Monsees, J. E. and Schmidt, B., 1969. Design of Tunnel liners and support systems. Report for U. S. Department of Transportation, Office of High Speed Ground Transportation, Contract No. 3-0152, 287 p.
- DeLory, F. A., Crawford, A. M., and Gibson, M. E. M., 1979. Measurements on a Tunnel Lining in very Dense Till. *Canadian Geotechnical Journal*, Vol. 16, pp. 190-199.
- Desai, C. S. and Siriwardane, H. J., 1984. *Constitutive Laws for Engineering Materials with Emphasis on Geologic Materials*. Prentice-Hall, Inc., 468 p.
- Duddeck, H., 1980. On the Basic Requirements for Applying the Convergence-Confinement Method. *Underground Space*, Vol. 4, No. 4, pp. 241-247.
- Duddeck, H. and Erdmann, J., 1985. On Structural Design Models for Tunnels in Soft Soil. *Underground Space*, Vol. 9, pp. 246-259.
- Duddeck, H., Meister, D., Werner, E., Schlegel, R., and Theurer, M., 1979. Road Tunnel in very Soft Soil in Terrace Deposits in the Harz Mountains, Germany. *Tunnelling '79*, pp. 205-215.
- Duncan, J. M. and Chang, C. Y., 1970. Nonlinear Analysis of Stress and Strain in Soils. *Journal of the Soil Mechanics and Foundations Division, ASCE*, Vol. 96, No. SM 5, pp. 1629-1654.
- Duncan, J. M., Byrne, P., Wong, K. S. and Mabry, P., 1980. Strength, Stress-Strain and Bulk Modulus Parameters for Finite Element Analyses of Stresses and Movements in Soil Masses. Report No. UCB/GT/80-01, Department of Civil Engineering, University of California, Berkeley, 70 p.
- Dunnicliff, C. J., 1971. Equipment for Field Deformation Measurements. *Proceedings, Fourth Pan American Conference on Soil Mechanics and Foundation Engineering*, Vol. 2, pp. 319-332.
- Dunnicliff, J., 1988. *Geotechnical Instrumentation for Monitoring Field Performance*. John Wiley & Sons, 577 p.
- EBA Engineering Consultants Ltd., 1988. Preliminary Engineering Report-South Tunnel, SLRT Phase II. Submitted to The City of Edmonton and Stanley Associates Engineering Ltd.

EBA Engineering Consultants Ltd., 1991. Contract Completion Report-South Bank Tunnels, SLRT Phase II. Submitted to The City of Edmonton and Stanley Associates Engineering Ltd.

Egger, P., 1980. Deformations at the Face of the Heading and Determination of the Cohesion of the Rock Mass. *Underground Space*, Vol. 4, No. 5, pp. 313-318.

Einstein, H. H. and Schwartz, C. W., 1979. Simplified Analysis for Tunnel Supports. *Journal of the Geotechnical Engineering Division, ASCE*, Vol. 105, No. GT4, pp. 499-518.

Einstein, H. H. and Schwartz, C., 1980. Discussion on Simplified Analysis for Tunnel Supports. *Journal of the Geotechnical Engineering Division, ASCE*, No. GT7, pp.835-838.

Eisenstein, Z., 1982. The Contribution of Numerical Analysis to Design of Shallow Tunnels. *Proceedings, International Symposium on Numerical Models in Geomechanics, Zurich*.

Eisenstein, Z., 1992. Rock Engineering Class Notes. Department of Civil Engineering, University of Alberta.

Eisenstein, Z. and Branco, P., 1990. Convergence-Confinement Method in Shallow Tunnels. *Canadian Tunnelling, Tunnelling Association of Canada*, pp. 77-83.

Eisenstein, Z. and Kuwajima, F. M., 1990. Stress Measurements by Flat-Jack Method in the Shotcrete Lining of the SLRT South Tunnel. Report for the City of Edmonton and EBA Engineering Consultants Ltd., 18 p.

Eisenstein, Z. and Negro Jr., A., 1985. Comprehensive Design Method for Shallow Tunnels. *ITA/AITES International Conference, Underground Structures in Urban Areas, Prague*, pp. 3-20.

Eisenstein, Z. and Negro Jr., A., 1990. Integrated Design Method for Shallow Tunnels in Soft Ground. Presented at the JTA Tunnel Symposium in Tokyo, Japan, Vol. 2, pp.27-36.

Eisenstein, Z. and Thomson, S., 1978. Geotechnical Performance of a Tunnel in Till. *Canadian Geotechnical Journal*, Vol. 15, pp.332-345.

- Eisenstein, Z., El-Nahhas, F., and Thomson, S., 1979. Pressure-Displacement Relations in Two Systems of Tunnel Lining. Proceedings of 6th PanAmerican Conference on Soil Mechanics, Lima, pp. 85-94.
- Eisenstein, Z., El-Nahhas, F., and Thomson, S., 1981. Strain Field around a Tunnel in Stiff Soil. Presented for 10th International Conference on Soil Mechanics and Foundation Engineering, Session 2: Tunnelling in Soils, Stockholm.
- Eisenstein, Z., Heinz, H. and Negro, A., 1984. On Three-Dimensional Ground Response to Tunnelling. ASCE. Geotech III, Tunnelling in Soils and Rocks, Atlanta, pp. 107-127.
- Eisenstein, Z., Kulak, G. L., MacGregor, J. G., and Thomson, S., 1977. Report on Geotechnical and Construction Performance of the Twin Tunnels. Unpublished Report Prepared for The City of Edmonton Engineering Department, Edmonton, Alberta, 75 p.
- Eisenstein, Z., Kuwajima, F. M. and Heinz, H. K., 1991. Behaviour of Shotcrete Tunnel Linings. Proceedings, Rapid Excavation and Tunnelling Conference, Seattle, pp. 47-57.
- Eisenstein, Z., Thomson, S., and Branco Jr., P., 1982. South LRT Extension Jasper Avenue Twin Tunnel-Instrumentation test section at 102nd Street. Part I : Southbound Tunnel. Unpublished Report Submitted to The City of Edmonton, Edmonton, Alberta, 330 p.
- El-Nahhas, F., 1977. Field Measurements in Two Tunnels in the City of Edmonton. M. Sc. Thesis, Department of Civil Engineering, University of Alberta, Edmonton, Alberta, 85 p.
- El-Nahhas, F., 1980. The Behavior of Tunnels in Stiff Soils. Ph. D. Thesis, Department of Civil Engineering, University of Alberta, Edmonton, Alberta, 305 p.
- Fenner, R., 1938. Untersuchungen zur Erkenntnis des Gebirgsdruckes. Gluckauf, Vol. 74, Essen, pp. 681-695 and 705-715.
- GEO-SLOPE International Ltd., 1995. User's Guide for SIGMA/W Stress and Deformation Analyses. GEO-SLOPE International Ltd., Calgary, Alberta, Canada.
- Gesta, P., Kerisel, J., Londe, P., Louis, C., and Panet, M., 1980. Tunnel Stability by Convergence-Confinement Method. Underground Space, Vol. 4, No. 4, pp. 225-232.

- Ghaboussi, J. and Ranken, R. E., 1977. Interaction Between Two Parallel Tunnels. *International Journal for Numerical and Analytical Methods in Geomechanics*, Vol. 1, pp. 75-103.
- Ghaboussi, J., Hansmire, W. H., Parker, H. W., and Kim, K. J., 1983. Finite Element Simulation of Tunneling Over Subways. *Journal of Geotechnical Engineering, ASCE*, Vol. 109, No. 3, pp. 318-334.
- Harris, M. C. and Papanicolas, D., 1983. South LRT Extension Geotechnical Report No. 16, Corona Station Instrumentation Program. Report Submitted to Edmonton Transit-LRT Project, 39 p.
- Hartmann, F., 1970. Elastizitätstheorie des ausgekleideten Tunnelhohlraumes und des eingebohrten kreisförmigen Rohres. *Strasse Brücke Tunnel* 22 (1970), Heft 8, 209-215, Heft 9, 241-246, und Jg. 24 (1972), Heft 1, 13-20, Heft 2, 39-45.
- Heinz, H. K., 1984. Applications of the New Austrian Tunneling Method in Urban Areas. M.Sc. Thesis, Department of Civil Engineering, University of Alberta, 323 p.
- Hewett, B. H. M. and Johannesson, S., 1922. *Shield and Compressed Air Tunneling*. McGraw Hill, New York.
- Hoek, E., 1982. Geotechnical Considerations in Tunnel Design and Contract Preparation. *Tunnelling'82, Sir Julius Wernher Memorial Lecture, IMM, Transactions*, pp. A101-109
- Hoek, E. and Brown, E. T., 1980. Empirical Strength Criterion for Rock Masses. *Journal of the Geotechnical Engineering Division, ASCE*. Vol. 106, No. GT9, pp. 1013-1035.
- Hoek, E. and Brown, E. T., 1980. *Underground Excavations in Rock*. The Institution of Mining and Metallurgy, London, 527 p.
- Howells, M., 1980. Analysis of Tunnel Stability by the Convergence-Confinement Method. *Underground Space*, Vol. 4, No. 6, pp. 368-369.
- Hutchinson, D. E., 1982. Effects of Construction Procedure on Shaft and Tunnel Performance. M.Sc. Thesis, Department of Civil Engineering, University of Alberta, 267 p.
- International Tunneling Association Working Group on General Approaches to the Design of Tunnels, 1988. *Guidelines for the Design of Tunnels. Tunneling and Underground Space Technology*, Vol. 3, No. 3, pp. 237-249.

- Kaiser, P. K., 1980. Effect of Stress-history on the Deformation Behaviour of Underground Openings. 13th Canadian Rock Mechanics Symposium, CIM Special Volume 22, pp. 133-140.
- Katzenbach, R. and Breth, H., 1981. Nonlinear 3-D Analysis for NATM in Frankfurt Clay. Proceedings of the Tenth International Conference on Soil Mechanics and Foundation Engineering, Stockholm, Vol. 1, pp. 315-318.
- Kawamoto, T. and Okuzono, K., 1977. Analysis of Ground Surface Settlement Due to Shallow Shield Tunnels. International Journal For Numerical and Analytical Methods in Geomechanics, Vol. 1, pp. 271-281.
- Kerisel, J., 1980. Commentary on the General Report. Underground Space, Vol. 4, No. 4, pp. 233-239.
- King, H. J., Whittaker, B. N., and Batchelor, A. S., 1972. The Effects of Interaction in Mine Layouts. Fifth International Strata Control Conference, London, Paper 17, pp. 1-11.
- Kondner, R. L., 1963. Hyperbolic Stress-Strain Response: Cohesive Soils. Journal of the Soil Mechanics and Foundation Division, ASCE, Vol. 89, No. SM 1, pp. 115-143.
- Kuesel, T. R., 1987. Principles of Tunnel Lining Design. Tunnels and Tunnelling, pp. 25-28.
- Kulhawy, F. H., 1974. Finite Element Modeling Criteria for Underground Openings in Rock. Int. J. Rock Mech. Min. Sci. & Geomech. Abstr., Vol. 11, pp. 465-472.
- Kulhawy, F. H., 1977. Embankments and Excavations. In: Numerical Methods in Geotechnical Engineering (edited by Desai, C. S. and Christian, J. T.), McGraw Hill, pp. 528-555.
- Kuwajima, F. M., 1991. Behavior of Shotcrete in Shallow Tunnels. Ph. D. Thesis, Department of Civil Engineering, University of Alberta, Edmonton, 511 p.
- Ladanyi, B., 1974. Use of the Long-Term Strength Concept in the Determination of Ground Pressure on Tunnel Linings. Proceedings of the Third International Congress on Rock Mechanics, Denver, Vol. 2B, pp. 1150-1156.
- Ladanyi, B., 1980. Direct Determination of Ground Pressure on Tunnel Lining in a Non-Linear Viscoelastic Rock. Underground Rock Engineering, 13th Canadian Rock Mechanics Symposium, Toronto, CIM Special Vol. 22, pp. 126-132.

- Lane, K. S., 1960. Garrison Dam Test Tunnel, Evaluation of Test Results. Transactions, ASCE, Vol. 125, pp. 268-306.
- Lane, K. S., 1975. Field Test Sections-Save Cost in Tunnel Support. Report from Underground Construction Research Council, American Society of Civil Engineers, 59 p.
- Lombardi, G., 1970. The Influence of Rock Characteristics on the Stability of Rock Cavities. Tunnels and Tunnelling, Vol. 2, No. 1, pp. 19-22, and Vol. 2 No. 2, pp. 104-109.
- Lombardi, G., 1973. Dimensioning of Tunnel Linings with regard to Construction Procedure. Tunnels and Tunnelling, Vol. 5, pp. 340-351
- Lombardi, G., 1980. Some Comments on the Convergence-Confinement Method. Underground Space, Vol. 4, No. 4, pp. 249-258.
- Londe, M., 1980. Analysis of Tunnel Stability by the Convergence-Confinement Method. Underground Space, Vol. 4, No. 6, pp. 375-376.
- Matheson, D. S. and Rupprecht, H., 1985. The Nipawin Drainage Tunnel -Design and Construction. Presented at the CEA Hydraulic Power Section Meeting, Regina, Saskatchewan.
- Matheson, D. S., Macpherson, J. G., and Eisenstein, Z., 1986. Design and Construction Aspects of the Nipawin Drainage Tunnel. Canadian Tunnelling, pp. 59-73.
- Meister, D. and Wallner, M., 1977. Instrumentation of a Tunnel in Extremely Bad Ground and Interpretation of the Measurements. International Symposium on Field Measurements in Rock Mechanics, Zurich, pp. 919-933.
- Montgomery, C. J. and Eisenstein, Z., 1995. Soft Ground Tunnel Design in Edmonton. Unpublished Report Submitted to The City of Edmonton, Edmonton, Alberta, 198 p.
- Morton, J. D., Dunbar, D. D., Palmer, J. H. L., Use of a Precast Segmented Concrete Lining for a Tunnel in Soft Clay. International Symposium on Soft Clay, Bangkok, pp. 587-598.
- Muir Wood, A. M., 1969. Discussion of: Peck, R. B., Deep Excavations and Tunneling in Soft Ground. Proceedings, 7th International Conference on Soil Mechanics and Foundation Engineering, Vol. 3, pp. 363-367.

- Muir Wood, A. M., 1975. The Circular Tunnel in Elastic Ground. *Geotechnique* 25, No. 1, pp.115-127.
- Muir Wood, A. M. and Gibb, F. R., 1971. Design and Construction of the Cargo Tunnel at Heathrow Airport, London. *Proceedings, Institution of Civil Engineers*, Vol. 48, Jan., pp. 11-34.
- Negro, A. Jr., 1988. Design of Shallow Tunnels in Soft Ground. Ph. D. Thesis, Department of Civil Engineering, University of Alberta, Edmonton, 1480 p.
- Negro, A. and Eisenstein, Z., 1981. Ground Control Techniques Compared in Three Brazilian Water Tunnels. *Tunnels and Tunnelling*, Oct. pp. 11-14, Nov. pp. 52-54, Dec. pp. 48-50.
- O'Rourke, T. D., 1984. Guidelines for Tunnel Lining Design. *American Society of Civil Engineers*, 82 p.
- Oteo, C. S. and Sagaseta, C., 1982. Prediction of Settlements due to Underground Openings. *Proceedings, International Symposium on Numerical Models in Geomechanics*, Zurich, September, pp. 653-659.
- Panet, H., 1973. La stabilite des ouvrages souterrains-soutenement et revetement. *Rapport de recherche No. 28*. Paris:Laboratoires des Ponts et Chaussees.
- Panet, M., 1976. Stability Analysis of a Tunnel Driven in a Rock Mass Taking Account of the Post-Failure Behaviour. *Rock Mechanics*. Vol. 8, pp. 209-223.
- Panet, M. and Guenot, A., 1982. Analysis of Convergence Behind the Face of a Tunnel. *Tunnelling '82*, The Institution of Mining and Metallurgy, pp. 197-204.
- Paterson, M. S., 1978. *Experimental Rock Deformation -The Brittle Field*. Springer-Verlag, 254 p.
- Peck, R. B., 1969. Deep excavation and Tunneling in soft ground. *Proceedings, 7th International Conference on Soil Mechanics and Foundation Engineering*, Mexico, State-of-the-Art Volume, pp. 225-290.
- Peck, R. B., Hendron, A. J., and Mohraz, B., 1972. State of the Art of Soft-Ground Tunneling. *RETIC Proceedings*, Vol. 1, pp.259-286.
- Pelli, F., 1987. Near Face Behavior of Deep Tunnels in Rock. Ph.D Thesis, Department of Civil Engineering, University of Alberta, 406 p.

- Pelli, F., Kaiser, P. K., and Morgenstern, N. R., 1986. Three-Dimensional Simulation of Rock-Liner Interaction Near Tunnel Face. Symposium on Numerical Models in Geomechanics, Ghent, pp. 359-368.
- Phelps, D. J. and Brandt, J. R., 1989. Design and Construction of Tunnels for the Edmonton LRT. Canadian Tunnelling, Tunnelling Association of Canada, pp.45-59.
- Plichon, J. N., 1980. Analysis of Tunnel Stability by the Convergence-Confinement Method. Underground Space, Vol. 4, No. 6, pp.384-388.
- Rabcewicz, L. V., 1969. Stability of tunnels under rock load. Water Power, June, pp.225-229; July, pp. 266-273; Aug, pp. 297-302.
- Ranken, R. E., 1978. Analysis of Ground-Liner Interaction for Tunnels. Ph.D. Thesis, Department of Civil Engineering, University of Illinois, 427p.
- Ranken, R. E. and Ghaboussi, J., 1975. Tunnel Design Considerations: Analysis of Stresses and Deformations around Advancing Tunnels. U.S. Department of Commerce, Springfield, Report UILU-ENG75-2016.
- Rocha, M., 1968. New Techniques for the Determination of the Deformability and State of Stress in Rock Masses. Proceedings, International Symposium on Rock Mechanics, Madrid, pp. 289-302.
- Rocha, M., Lopes, J. J. B., and da Silva, J. N., 1966. A New Technique for Applying the Method of the Flat Jack in the Determination of Stresses inside Rock Masses. Proceedings, First Congress of the International Society of Rock Mechanics, Lisbon, Vol. 2, pp. 57-65.
- Rowe, R. K., Lo, K. Y. and Kack, G. J., 1981. The Prediction of Subsidence above Shallow Tunnels in Soft Soil. Implementation of Computer Procedures and Stress-Strain Laws in Geotechnical Engineering, Vol. 1, pp. 266-280.
- Sauer, G. and Jonuscheit, P., 1976. Stress Redistribution in the Middle Wall Between Tubes of a Twin-Tunnel During Synchronous Excavation. Rock Mechanics. Vol. 8, pp. 1-22.
- Schmidt, B., 1984. Tunnel lining design - Do the theories work?. Fourth Australia - New Zealand Conference on Geomechanics, Perth, pp. 682-693.

- Schwartz, C. W. and Einstein, H. H., 1980 (a). Improved Design of Tunnel Supports: Vol. 1 - Simplified Analysis for Ground-Structure Interaction in Tunneling. Report No. UMTA-MA-06-0100-80-4, U.S. Department of Transportation, 427 p.
- Schwartz, C. W. and Einstein, H. H., 1980 (b). Simplified Analysis for Ground-Structure Interaction in Tunneling. The State of the Art in Rock Mechanics, Proceedings of the Twenty-First U. S. Symposium on Rock Mechanics, pp. 787-796.
- Soliman, E., Duddeck, H., and Ahrens, H., 1993. Two- and Three-dimensional Analysis of Closely Spaced Double-tube Tunnels, Tunnelling and Underground Space Technology, Vol. 8, No. 1, pp. 13-18.
- Sorensen, K. L., 1986. Tunnelling for the South LRT Extension in Edmonton, Alberta. 6th annual Canadian Tunnelling Conference, Niagara Falls, Ontario.
- Srivastava, R. K., Sharma K. G., and Varadarajan, A., 1988. Analysis of Stresses in the Pillar Zone of Twin Circular Interacting Tunnels. Numerical Methods in Geomechanics, pp. 1597-1606.
- Szechy, K., 1966. The Art of Tunnelling. Akademiai Kiado, Budapest, 891 p.
- Tan, D. Y. and Clough, G. W., 1980. Ground Control For Shallow Tunnels by Soil Grouting. Journal of the Geotechnical Engineering Division, Proceedings of the American Society of Civil Engineers, Vol. 106, No. GT.9, pp. 1037-1057.
- Tattersall, F., Wakeling, T. R. M., and Ward, W. H., 1955. Investigations into the Design of Pressure Tunnels in London Clay. Institution of Civil Engineers Proceedings, London, Vol. 4, Part 1, pp. 400-471.
- Terzaghi, K., 1943. Theoretical Soil Mechanics, Wiley, New York, pp. 194-197.
- Terzaghi, K., 1946. Rock Defects and Loads on Tunnel Supports; In: Rock Tunneling with Steel Supports by Proctor, R. V. and White, T. L., Commercial Shearing Co., Ohio, pp. 17-99.
- Thomas, H. S. H. and Ward, W. H., 1969. The Design, Construction and Performance of a Vibrating-Wire Earth Pressure Cell. Geotechnique, Vol. 19, No. 1, pp. 39-51.
- Thomson, S. and El-Nahhas, F., 1980. Field Measurements in Two Tunnels in Edmonton, Alberta. Canadian Geotechnical Journal, Vol. 17, pp. 20-33.

- Thomson, S., Martin, R. L. and Eisenstein, Z., 1982. Soft Zones in the Glacial Till in Downtown Edmonton. *Canadian Geotechnical Journal*, Vol. 19, pp. 175-180.
- Thurber Consultants Ltd., 1986. SLRT Extension-Phase II, Insitu Testing at the Proposed University Station Site. Geotechnical Report No.3, Submitted to The City of Edmonton.
- Tweedie, R. W., Harris, M. C., Gerber, G. E., and Eisenstein, Z., 1989. Ground and - Structure Monitoring for the Edmonton SLRT-Phase II Tunnels. *Canadian Tunnelling*, pp.61-72.
- Uff, J. F., 1970. In Situ Measurements of Earth Pressure for a Quay Wall at Seaforth, Liverpool. *Proceedings of the Conference on In situ Investigations in Soil & Rock*, British Geotechnical Society, London, pp. 229-239.
- Ward, W. H., 1969. Discussion of: Peck, R. B., Deep Excavations and Tunneling in Soft Ground. *Proceedings, 7th International Conference on Soil Mechanics and Foundation Engineering*, Vol. 3, pp. 320-325.
- Ward, W. H., 1978. Ground Supports for Tunnels in Weak Rocks. *Geotechnique*, Vol. 28, No. 2, pp. 133-171.
- Ward, W. H. and Chaplin, T. K., 1957. Existing Stresses in Several Old London Underground Tunnels. *Proceedings, Fourth International Conference on Soil Mechanics and Foundation Engineering*, Vol. 2, pp. 256-259.
- Ward, W. H. and Pender, M. J., 1981. Tunnelling in Soft Ground - General Report. *Proceedings of the Tenth International Conference on Soil Mechanics and Foundation Engineering*, Stockholm, Vol. 4, pp. 261-275.
- Ward, W. H. and Thomas, H. S. H., 1965. The Development of Earth Loading and Deformation in Tunnel Linings in London Clay. *Proceedings, Sixth International Conference on Soil Mechanics and Foundation Engineering*, Vol. 2, pp. 432-436.
- Ward, W. H., Coats, D. J. and Tedd, P., 1976. Performance of Tunnel Support Systems in the Four Fathom Mudstone. *Tunneling '76*, London, pp. 329-340, disc. pp. 348-367.
- Ward, W. H., Samuels, S. G., and Muriel, E. B., 1959. Further Studies of the Properties of London Clay. *Geotechnique*, Vol. 9, No. 2, pp. 33-58.

Weber, J., 1984. Experience using Compressed-Air Drivage and Shotcreting. Tunnel 1/84, pp. 16-27.

Whittaker, B. N. and Bonsall, C. J., 1982. Design Aspects Relating to the Stability of Coal Mining Tunnels. First International Conf. on Stability in Underground Mining, SME Symp., Vancouver, pp. 519-534.

Whittaker, B. N. and Frith, R. C., 1990. Tunnelling -Design, Stability and Construction. The Institution of Mining and Metallurgy, London, 460 p.

Wong, R. C. K. and Kaiser, P. K., 1986. Interpretation of Performance of a Small Tunnel in Clayshale. Presented at the 39th Canadian Geotechnical Conference, Ottawa.

Wood, D. F., Nickel, G. B. and Borch, N. G., 1989. Developments in the use of shotcrete for tunnel support. Proceedings of International Congress on Progress and Innovation in Tunnelling, ITA, Toronto, pp. 439-447.

Table A.1 Data from Case History No.1

| |
|---|
| Case : Ashford Common Hydro Pressure Tunnel |
| References: Tattersall et al. (1955) |
| Year of Completion: 1952 |
| Purpose: Conveying Water |
| External Diameter (m): 2.84 |
| Ground Type: London Clay ($E=255$ MPa) |
| Depth to the springline (m): 27.4 |
| Excavation Method: Shield |
| Support Type: Precast Concrete (10 Seg./ring) ($E_c=9653$ MPa) |
| Support Delay Length X (m): 0 * |
| Thickness (and Length) of Lining (m): 0.15 (0.53) |
| Backfill of Lining: Expansion of Lining (UngROUTED) |
| Instrumentation: Pressure Cells (Vibrating-Wire Type) Load Cells (Vibrating-Wire Type) |
| Period of Measurements: 1 year |
| PL/Pv x 100 (%): Pressure Cells - 38, 57, 79 (rings 179, 180, 352) Load Cells - 53, 57 (rings 756, 755) |
| n: Pressure Cells - 3.64, 5.47, 7.65 Load Cells - 5.10, 5.47 |
| Remarks: Considerable scatter in the measurements of pressure cells (Not compared with predicted values) Two load cells per a segment of lining (Considered more reliable than the pressure cell results by the authors) * Average diameter of the shield was only 0.5 cm larger than that of the lining |

Table A.2 Data from Case History No.2

| |
|--|
| Case : Heathrow Airport Cargo Tunnel |
| References: Muir Wood (1969) Muir Wood and Gibb (1971) |
| Year of Completion: 1968 |
| Purpose: Road Tunnel |
| External Diameter (m): 10.9 |
| Ground Type: London Clay ($E=27$ MPa) |
| Depth to the springline (m): 12.77 |
| Excavation Method: Hand Excavation using Pneumatic tools and Shield |
| Support Type: Precast Concrete Liner without Bolts (27 Seg./ring) |
| Support Delay Length X (m): 3.2 (Approx. Length of Shield) |
| Thickness (and Length) of Lining (m): 0.3 (0.6) |
| Backfill of Lining: None |
| Instrumentation: Four photoelastic Load Cells in one ring |
| Period of Measurements: 600 days |
| PL/Pv x 100 (%): 65 at axis |
| n: 0.76 |
| Remarks: Face was supported at all times using face rams to minimize surface settlement. |

Table A.3 Data from Case History No.3

| |
|--|
| Case : Fleet Line at Regents Park |
| References: Attewell and Farmer (1974 a, 1974 b) Barratt and Tyler (1976) |
| Year of Completion: 1974 |
| Purpose: |
| External Diameter (m): 4.15 |
| Ground Type: London Clay ($E=128 \text{ MPa}^*$) |
| Depth to the springline (m): 20 |
| Excavation Method: Hand Excavated with a Shield |
| Support Type: Expanded Precast Concrete Lining (22 Seg./ring) |
| Support Delay Length X (m): 3.35 m |
| Thickness (and Length) of Lining (m): 0.168 (0.6) |
| Backfill of Lining: None |
| Instrumentation: Four Load Cells (Vibrating Wire Type) and Four Earth Pressure Cells (Vibrating Wire Gauge) in One Ring |
| Period of Measurements: Six Months |
| PL/Pv x 100 (%): 41 (Avg.) |
| n: 1.99 ** |
| Remarks: One load cell in the invert and one pressure cell in the springline were malfunctioned. Twin tunnels (Measurements from a second tunnel) * Estimated from the results of Ward et al. (1959) ** From load cells |

Table A.4 Data from Case History No.4

| |
|---|
| Case : Ontario Sewer Tunnel |
| References: DeLory et al. (1979) |
| Year of Completion: 1973 |
| Purpose: Sewer Tunnel |
| External Diameter (m): 4.3 |
| Ground Type: Dense Till ($E=170$ MPa) |
| Depth to the springline (m): 13.15 |
| Excavation Method: Shield (Alpine Miner Road Header) |
| Support Type: Primary - Steel H Rings in 4 Seg. and Concrete Planks |
| Support Delay Length X (m): 12-18 * |
| Thickness (and Length) of Lining (m): 0.1x0.1 and 0.075x0.2 x1.2 (1.22) |
| Backfill of Lining: Filled with Pea Size Gravel and Grout |
| Instrumentation: Pressure Cells (Bourdon-Type) Resistance Strain Gauges Welded to the Steel Ribs |
| Period of Measurements: 2.5 yrs |
| PL/Pv x 100 (%): 65 |
| n: 2.0 (From Pressure Cells) |
| Remarks: Four pressure cells out of 12 gave unrealistic results. Strain gauges showed poor performance due to high humidity and dirt conditions. Groundwater level was about 6 m below the surface before construction started. * Filling the space between the lining and soil with pea size gravel at the distance 12-18 m from the tunnel face. |

Table A.5 Data from Case History No.5

| |
|--|
| Case : Thunder Bay Tunnel (Ontario) |
| References: Morton et al. (1977) Belshaw and Palmer (1978) |
| Year of Completion: 1976 |
| Purpose: Sewer Tunnel |
| External Diameter (m): 2.38 |
| Ground Type: Soft to Firm Clay (E=170 MPa assumed) |
| Depth to the springline (m): 11 |
| Excavation Method: Full-Face Tunnel Boring Machine |
| Support Type: Unbolted Precast Segmented Concrete Lining (4 Seg./ring, unreinforced) |
| Support Delay Length X (m): 5.6 (Length of TBM) |
| Thickness (and Length) of Lining (m): 0.11 (1) |
| Backfill of Lining: Clay Grout |
| Instrumentation: Twelve Total Pressure Cells (Vibrating Wire Pressure Transducer) in one Ring of the Lining |
| Period of Measurements: 1 yr. |
| PL/Pv x 100 (%): 43 |
| n: 2.00 |
| Remarks: Grout was injected into the space between the lining and soil immediately after the TBM advanced. Mined diameter of the tunnel was 2.47 m and the outside diameter of the completed lining was 2.38 m. Surface settlement was observed above the TBM. |

Table A.6 Data from Case History No.6

| |
|--|
| Case : Tyneside Sewer Tunnel I, II |
| References: Attewell and El-Naga (1977) |
| Year of Completion: |
| Purpose: Sewer Tunnel |
| External Diameter (m): 3.20 |
| Ground Type: Stiff Stony Clay and Laminated Clay ($E=150 \text{ MPa}^*$) |
| Depth to the springline (m): 13.37 (I), 13.99 (II) |
| Excavation Method: Hand Excavation without Shield |
| Support Type: Bolted Segmental Concrete Lining (6 Seg. plus a Key in a Ring) |
| Support Delay Length X (m): 0 |
| Thickness (and Length) of Lining (m): 0.05 (0.61) |
| Backfill of Lining: Cementitious Grout Soon After Erection |
| Instrumentation: Six Pressure Cells (Hybrid Electro-Hydraulic Type) for each Test Location |
| Period of Measurements: 50 days |
| PL/Pv x 100 (%): 52 * (I), 53 * (II) |
| n: 1.92, 2.05 |
| Remarks: The absence of a shield in the drives allowed both instrumented rings to be erected tight up to the tunnel face. The radial pressure reached a constant maximum after a period of 7-8 days. * Maximum recorded pressure near to the tunnel crown. |

Table A.7 Data from Case History No.7

| |
|---|
| Case : Nipawin Drainage Tunnel |
| References: Matheson and Rupprecht (1984) Matheson et al. (1986) |
| Year of Completion: 1983 |
| Purpose: Drainage Tunnel in Hydroelectric Project |
| External Diameter (m): 3.45 |
| Ground Type: Till ($E=150$ MPa assumed) |
| Depth to the springline (m): 14.5 (Ring 2), 13.5 (Ring 3), 36 (Ring 4) |
| Excavation Method: Full face TBM |
| Support Type: Bolted Precast Concrete Lining (4 Seg./ring) |
| Support Delay Length X (m): 6 (Length of TBM) |
| Thickness (and Length) of Lining (m): 0.15 (1.25) |
| Backfill of Lining: Pea Gravel without Grout |
| Instrumentation: Four Load Cells per a Ring |
| Period of Measurements: 2.5 yrs. |
| PL/P _v x 100 (%): 23.8 (Ring2), 55.3 (Ring 3), 38.3 (Ring 4) |
| n: 2.25 (Ring 2), 3.60 (Ring 3), 4.00 (Ring 4) |
| Remarks: The space between the liner and soil was backfilled with pea gravel immediately after the ring was clear of the shield. Overburden pressure in rings 2 and 3 are 720 KPa and 496 KPa respectively due to loading on the ground surface. |

Table A.8 Data from Case History No.8

| |
|---|
| Case : Alto da Boa Vista (ABV) Tunnel |
| References: Negro and Eisenstein (1981) Negro (1988) |
| Year of Completion: 1978 |
| Purpose: To Connect Two Water Treatment Plants |
| External Diameter (m): 4 |
| Ground Type: Variegated Silty Sand ($E=40$ MPa) |
| Depth to the springline (m): 8.15 |
| Excavation Method: NATM |
| Support Type: Shotcrete with a Light Wire Mesh |
| Support Delay Length X (m): 2.6 |
| Thickness (and Length) of Lining (m): 0.1 |
| Backfill of Lining: N.A. |
| Instrumentation: Hydraulic Pressure Cells (Interfels Type HPG077) |
| Period of Measurements: |
| PL/Pv x 100 (%): 30 (Avg.) |
| n: 0.61 |
| Remarks: |

Table A.9 Data from Case History No.9

| |
|--|
| Case : Frankfurt Baulos 23, Damplatz Tunnel |
| References: Negro (1988) |
| Year of Completion: 1971 |
| Purpose: Subway Tunnel |
| External Diameter (m): 6.7 |
| Ground Type: Frankfurt Clay * ($E=21.79$ MPa) |
| Depth to the springline (m): 15.15 |
| Excavation Method: Open Face Shield |
| Support Type: Segment Precast Concrete Ring (5 Seg./ring) |
| Support Delay Length X (m): 7.35 |
| Thickness (and Length) of Lining (m): 0.35 (0.9) |
| Backfill of Lining: Grout |
| Instrumentation: Mechanical Strain Gauge (DEMEC Type) |
| Period of Measurements: |
| PL/Pv x 100 (%): 54 |
| n: 1.22 |
| Remarks: A twin tunnel system (13.2 m centre to centre) Measurements in the second tunnel * Overconsolidated fissured soil |

Table A.10 Data from Case History No.10

| |
|--|
| Case : Munich U-Bahn-Line 8/1, Baulos 18.2 |
| References: Negro (1988) |
| Year of Completion: 1976 |
| Purpose: Subway Tunnel |
| External Diameter (m): 6.98 h x 6.32 w (6.91 equi. diameter) |
| Ground Type: Stiff to Hard Calcareous Clay Marl (200 MPa) |
| Depth to the springline (m): 25.49 |
| Excavation Method: NATM |
| Support Type: Shotcretes and Horseshoe Shaped Segmented Steel Ribs at 1 m Spacing |
| Support Delay Length X (m): 7.0 |
| Thickness (and Length) of Lining (m): 0.16 |
| Backfill of Lining: N.A. |
| Instrumentation: Glotzl Contact Pressure Cells |
| Period of Measurements: 7 months |
| PL/Pv x 100 (%): 35 (Avg.) |
| n: 1.28 |
| Remarks: A twin tunnel system (19 m centre to centre) Steel ribs neglected for calculation of lining loads. A substantial scatter was observed in the pressure cell data |

Table A.11 Data from Case History No.11

| |
|---|
| Case : Butterberg Tunnel, Germany |
| References: Meister and Wallner (1977) Duddeck et al. (1979) |
| Year of Completion: 1979 |
| Purpose: Road Tunnel |
| External Diameter (m): 10.11 h x 11.70 w (11.5 m equi. diameter) |
| Ground Type: Sandy-Silty Gravel ($E=245$ MPa) |
| Depth to the springline (m): 18.66 |
| Excavation Method: NATM |
| Support Type: Shotcrete with Steel Wire Mesh (Light Steel Ribs at 1 m Spacing) |
| Support Delay Length X (m): 9.5 |
| Thickness (and Length) of Lining (m): 0.3 |
| Backfill of Lining: N.A. |
| Instrumentation: Seven Earth Pressure Cells (Maihak Pressure Gauges) in a Ring |
| Period of Measurements: 6 months |
| PL/Pv x 100 (%): 17 |
| n: 0.28 |
| Remarks: Excavation at the crown was carried out under the protection of short forepoling (1.3 m long) |

Table A.12 Data from Case History No.12

| |
|---|
| Case : Munich U-Bahn-Line 5/9, Baulos 7 |
| References: Weber (1984) Negro (1988) |
| Year of Completion: |
| Purpose: Subway Tunnel |
| External Diameter (m): 7.0 h x 6.5 w (6.95 equiv. diameter) |
| Ground Type: Stiff to Hard Clay Marl * (with Sand Layer above Tunnel) |
| Depth to the springline (m): 23.5 |
| Excavation Method: NATM |
| Support Type: Shotcrete Ring and Lattice Girder at 1.0 m Spacing |
| Support Delay Length X (m): 5.5 |
| Thickness (and Length) of Lining (m): 0.15-0.18 |
| Backfill of Lining: N.A. |
| Instrumentation: Load Cells |
| Period of Measurements: 140 days |
| PL/P _v x 100 (%): 28 ** |
| n: 0.94 |
| Remarks: A twin tunnel system (13 m centre to centre) A compressed air pressure of 60 KPa was used for the section containing sand layer with a perched water table. * E=200 MPa ** Measurements in the first tunnel before the second tunnel. |

Table A.13 Data from Case History No.13

| |
|--|
| Case : Thames-Lee Tunnel (Donseg Ring) |
| References: Cuthbert and Wood (1962) Cronin et al. (1962) Cooley (1982) |
| Year of Completion: 1959 |
| Purpose: Conveying Water |
| External Diameter (m): 3.01 |
| Ground Type: London Clay ($E=255$ MPa) |
| Depth to the springline (m): 18.5, 39, 31, 54 |
| Excavation Method: Shield |
| Support Type: Precast Unreinforced Concrete (Don-Seg System) (12 Seg./ring) |
| Support Delay Length X (m): 1.80 (Length of Shield *) |
| Thickness (and Length) of Lining (m): 0.152 (0.53) |
| Backfill of Lining: None |
| Instrumentation: Load Cells (Vibrating Wire Type) |
| Period of Measurements: 1 yr. |
| PL/Pv x 100 (%): 60, 53, 45, 49 |
| n: 3.60, 5.62, 4.42, 7.16 |
| Remarks: Overburden Pressures were given by Cooley (1982) * Assumed from Thames-Lee Experimental Tunnel |

Table A.14 Data from Case History No.14

| |
|--|
| Case : Thames-Lee Tunnel (Wedge-Block Rings) |
| References: Cuthbert and Wood (1962) Cronin et al. (1962) Cooley (1982) |
| Year of Completion: 1959 |
| Purpose: Conveying Water |
| External Diameter (m): 3.01 |
| Ground Type: London Clay ($E=255$ MPa) |
| Depth to the springline (m): 30 |
| Excavation Method: Shield (Hand) |
| Support Type: Precast Concrete (Wedge-Block Lining) (12 Seg./ring) |
| Support Delay Length X (m): 1.80 (Length of Shield *) |
| Thickness (and Length) of Lining (m): 0.14 (0.61) |
| Backfill of Lining: None |
| Instrumentation: Load Cells (Vibrating Wire Type) |
| Period of Measurements: 1 yr. |
| PL/Pv x 100 (%): 57 ** |
| n: 5.35 |
| Remarks: * Assumed from Thames-Lee Experimental Tunnel ** An average load of three sections |